UNIVERSITÀ DI PARMA

UNIVERSITA' DEGLI STUDI DI PARMA

DOTTORATO DI RICERCA IN

"SCIENZE DEL FARMACO, DELLE BIOMOLECOLE E DEI PRODOTTI PER LA SALUTE"

CICLO XXXIII

NEW INTEGRIN-TARGETED SMALL MOLECULE PEPTIDOMIMETICS AND THEIR COVALENT CONJUGATES AS POTENTIAL BIOMEDICAL TOOLS IN ONCOLOGY- AND FIBROSIS-RELATED DISEASES

Coordinatore:
Chiar.mo Prof. Marco Mor

Tutore:
Chiar.ma Prof.ssa Lucia Battistini

Dottoranda: Kelly Bugatti

Anni Accademici 2017/2018 – 2019/2020

Alle mie sorelle

Scientific contributions

- **Scientific publications**

  - Bugatti, K.; Bruno, A.; Arosio, D.; Sartori A.; Curti, C.; Augustijn, L.; Zanardi F. and Battistini L. "Shifting Towards $\alpha_V\beta_6$ Integrin Ligands Using Novel Aminoproline-Based Cyclic Peptidomimetics", *Chemistry A European Journal,* **2020***, 59(*26); 13468-13475. - IF (2019) 4.857
  - Battistini, L.; Bugatti, K.; Sartori, A.; Curti, C. and Zanardi, F. "RGD Peptide-Drug Conjugates as Effective Dual Targeting Platforms: Recent Advances", *European Journal of Organic Chemistry*, Submitted - IF (2019) 2.889

- **Flash communications**

  - "Towards new small-molecule peptidomimetics as selective $\alpha_V\beta_6$ integrin ligands", Merck & Elsevier Young Chemists Symposium - MEYCS2019, 25-27 November 2019, Rimini (Italy), p.143
  - "Synthesis of new small-molecule peptidomimetics as selective $\alpha_V\beta_6$ integrin ligands", Merck & Elsevier Young Chemists Symposium - MEYCS 2018, 19-21 November 2018, Rimini, Italy, p.126

- **Poster presentations**

  - Towards new small-molecule peptidomimetics as potent and selective $\alpha_V\beta_6$ integrin ligands, ULLA Summer School, 29 June-6 July 2019, Helsinki, Finland
  - $\alpha_V\beta_6$ integrins: towards new small molecules peptidomimetics as selective ligands, XVIII Giornata della Chimica Emilia-Romagna, 17 December 2018, Parma, Italy, P11
  - Synthesis of new cyclic peptidomimetics as selective ligands for $\alpha_V\beta_6$ integrins, XXII International Conference on Organic Synthesis - XXII ICOS, 16-21 September 2018, Firenze, Italy
  - Towards new small-molecule peptidomimetics as selective $\alpha_V\beta_6$ integrin ligands, Peptides and conjugates for tumor targeting, therapy and diagnosis - RiminiPeptides2018, 16-19 June 2018, Rimini, Italy, p.65

- **Scientific Awards**

  - *Best Flash Communication Award,* Società Chimica Italiana Giovani, "Towards new small-molecule peptidomimetics as selective $\alpha_V\beta_6$ integrin ligands", Merck & Elsevier Young Chemists Symposium - MEYCS2019, 25-27 November 2019, Rimini (Italy), p.143

Table of Contents

Abstract 1

Abbreviations 3

Chapter 1. Introduction 4

1.1. Integrin receptors 5

1.2. Peptidomimetics as RGD-recognizing integrin ligands 7

1.3. Small Molecule-Drug Conjugates 9

1.3.1. SMDCs: design and structure 10

1.3.2. Uncleavable RGD integrin-targeted SMDCs 12

1.3.3. Cleavable RGD integrin-targeted SMDCs 15

1.4. References 18

Chapter 2. Targeting $\alpha_v\beta_6$ integrin 21

2.1. Introduction 22

2.1.1. $\alpha_v\beta_6$ integrin 22

2.1.2. Epithelial-To-Mesenchymal Transition (EMT) 23

2.1.3. $\alpha_v\beta_6$ integrin ligands: state of the art 24

2.2. Aim of the project 27

2.3. Results and discussion 28

2.3.1. Design of novel $\alpha_v\beta_6$ integrin ligands 28

2.3.2. Synthesis of the $\alpha_v\beta_6$ ligands 30

2.3.3. Solid phase receptor binding assay 32

2.3.4. Docking studies of hit compounds 34

2.4. Conclusions and perspectives 36

2.5. Experimental section 37

2.5.1. Docking studies 37

2.5.2. Chemistry 37

2.5.2.1. General methods and materials 37
2.5.2.2. HPLC chromatograms 60
2.5.3. Biology 65
2.6. References 66
Chapter 3. Targeting PAR2 68
3.1. Introduction 69
3.1.1. PAR2: structure and generalities 69
3.1.2. Ligands targeting PAR2 receptors: state of the art 71
3.2. Aim of the project 75
3.3. Results and discussion 76
3.3.1. Design of potential PAR2 agonists 76
3.3.2. Synthesis of the designed PAR2 agonists 77
3.3.2.1. Protocol based on the Rink-Amide resin 77
3.3.2.2. Protocol based on the 2-Chlorotrityl resin 78
3.3.2.3. Post-SPPS modifications 79
3.3.3. The library of PAR2-targeting peptidomimetics: a SAR study 79
3.4. Conclusions and perspectives 82
3.5. Experimental section 83
3.5.1. General methods and materials 83
3.5.2. HPLC chromatograms 99
3.6. References 109
Chapter 4. Dual conjugates targeting $\alpha_V\beta_6/\alpha_V\beta_3$ and TK 111
4.1. Introduction 112
4.2. Aim of the project 116
4.3. Results and discussion 117
4.3.1. Design and retrosynthesis 117
4.3.2. Synthesis of the cyclic peptidomimetics 118
4.3.3. Synthesis of the linker-piperazinyl nuclei 119

4.3.4. Synthesis of the oxindole nucleus and Claisen-type reaction 122
4.3.5. Final click reaction and deprotection 123
4.3.6. Preliminary biological evaluation 124
4.4. Conclusions and perspectives 127
4.5. Experimental section 128
4.5.1. General methods and materials 128
4.5.2. HPLC chromatograms 144
4.6. References 147
Chapter 5. Dual conjugates targeting $\alpha_V\beta_6$ and PAR1 149
5.1. Introduction 150
5.2. Aim of the project 152
5.3. Results and discussion 153
5.3.1. Design of a novel MMP2/9-sensitive covalent PAR1/$\alpha_V\beta_6$ integrin targeted conjugate 153
5.3.2. Synthesis of functionalized cyclopeptide 2 154
5.3.3. Synthesis of compound 3, the functionalized version of RWJ-58259 155
5.4. Conclusions and perspectives 159
5.5. Experimental section 160
5.5.1. General methods and materials 160
5.6. References 168
Final Remarks 170
Acknowledgments 171

Abstract

The work described in this PhD dissertation concerns the design and the synthesis of new small molecule cyclic peptidomimetics to be used as potent and selective integrin ligands, as both refined $\alpha_V\beta_3$ binders and novel $\alpha_V\beta_6$-targeting ligands. In addition, their covalent integration with active components, be they chemotherapeutics, antiangiogenic or antinflammatory agents, would result in the fabrication of novel conjugates to be evaluated for their potential as biomedical tools in oncology-, fibrosis- or inflammation-related diseases.

After an opening general introduction, Chapter 2 is focused on the design and the synthesis of a panel of novel cyclic peptidomimetics targeting the $\alpha_V\beta_6$ integrin, which is overexpressed in many epithelial tumors, as well as in liver and pulmonary fibrotic tissues, and has emerged as a biomarker of the Epithelial-to-Mesenchymal Transition (EMT).
Inspired by previously established aminoproline (Amp)-RGD based cyclopeptidomimetics with attracting $\alpha_V\beta_3$ integrin affinity and selectivity, the design and synthesis of eighteen new AmpRGD chemotypes bearing additional structural variants were implemented, to shift toward peptide-like $\alpha_V\beta_6$ integrin targeted binders. All the newly synthesized peptidomimetics were tested for their $\alpha_V\beta_6$ binding affinity by competitive solid phase binding receptor assays and the most potent candidates were also tested towards $\alpha_V\beta_3$ receptors. Four of the synthesized compounds gave promising results, with $IC_{50(\alpha V\beta 6)}$ values in the low nanomolar range (4.6-58.5 nM) and selectivity indexes (reported as the ratio between $IC_{50(\alpha V\beta 3)}$ and $IC_{50(\alpha V\beta 6)}$) in the range 243-628.

In Chapter 3 the work done during my period abroad is described. The project carried out at the University of Erlangen-Nürnberg, in the research group of Prof. Dr. Gmeiner, was focused on the development of novel peptidomimetics as ligands of Proteinases-Activated Receptor 2 (PAR2), which it is implicated in the progression of different pathological events including cancers, arthritis and inflammation, but also exerts protective effects in certain other diseases (e.g. ischemia, wound healing and colitis).
Starting from preliminary results by the Prof. Gmeiner's research group, a panel of twenty novel compounds was designed, synthesized and characterized. All the final compounds were tested by IP-One-HEK assay and the most promising ones were also subjected to the arrestin-HEK-PS1K assay. The best performing PAR2 agonist among the twenty new synthesized compounds showed IC_{50} (tested by IP-One-HEK assay) in the nanomolar range, confirming that the proposed structural modifications can drive the research towards a full understanding of the receptor binding/activation properties of new ligands targeting PAR2.

Chapter 4 is focused on the synthesis of nine different covalent conjugates as potential antitumor and antifibrotic agents, based on the substantial evidence of the cross-talk between integrins and Growth Factor Receptors (GFRs), which seems to determine drug resistance and sustain the EMT. The projected conjugates are constituted by an analogue of the kinase inhibitor nintedanib, which is linked to an RGD-based cyclopeptidomimetic as the targeting unit by means of a robust linker moiety. The panel of nine compounds was realized by conjugating the same kinase inhibitor to one out of three different integrin ligands, two of them targeting $\alpha_v\beta_6$ integrin and bearing the sequence *c*(AmpLRGDL), and one targeting $\alpha_v\beta_3$ integrin and possessing the *c*(AmpRGD) cyclopeptide. Another point of variability was the linker, which was selected among three possible structures

differing in length, polarity and valency. Preliminary results towards TGFβ-treated melanoma tumor cells seemed to confirm that antagonizing both kinase receptor and $\alpha_V\beta_6$ integrin could be a good strategy to address cancer related diseases.

Finally, Chapter 5 concerns the design of MMP2/MMP9-cleavable conjugates addressing both PAR1 and $\alpha_V\beta_6$ receptors, since it is well known that these receptors are spatially and functionally related and their cross-talk has emerged as a possible target for the treatment of Idiopathic Pulmonary Fibrosis (IPF).
The designed conjugates comprise the $\alpha_V\beta_6$-targeting ligand *c*(AmpLRGDL), the properly modified PAR1 antagonist RWJ-58259 and the MMP2/9-sensitive peptide sequence PLG-LAG, which is supposed to be cleaved at the disease site, thus releasing the two independent active units. The opening move of this project was the parallel synthesis of the two separated active modules, intended to be evaluated first in *in-vitro* assays towards the corresponding receptors, with the aim to prove that the independent moieties maintain their biological activity upon the proteolytic release.

For clarity's sake, this thesis is organized into four main chapters following the opening introduction with self-consistent numbering of compound formulas, figures, schemes and references.

Abbreviations

ACN, acetonitrile; Ac_2O, acetic anhydride; AcOH, acetic acid; Amp, 4-amino-L-proline; Boc, tert-butoxycarbonyl; CLB, Chlorambucil; Collidine, 2,4,6-trimethylpiridine; CPT, Camptothecin; $Cu(OAc)_2$, copper(II) acetate; DCE, 1,2-dichloroethane; DCM, dichloromethane; DIBAL-H, diisobutylaluminium hydride; DIPEA, diisopropylethylamine; DiPhe, β-phenyl-Phenylalanine; DMAP, 4-(dimethylamino)pyridine; DMF, *N,N*-dimethylformamide; DMP, Dess-Martin periodinane; ECL, extracellular loop; ECM, Extracellular Matrix; EMT, Epithelial-to-Mesenchymal Transition; EtOAc, ethyl acetate; FGFR; Fibroblast Growth Factor Receptor; FMDV, Food-and-Mouth Disease Virus; Fmoc, 9-fluorenylmethoxycarbonyl; Fmoc-OSu, N-(9-Fluorenylmethoxycarbonyloxy) succinimide; FN, fibronectin; GFR, Growth Factor Receptor; GPCR, G Protein-Coupled Receptor; HATU, *O*-(7-azabenzotriazol-1-yl)-*N,N,N′,N′*- tetramethyluronium hexafluorophosphate; HOAt, 1-hydroxy-7-azabenzotriazole; IPF, Idiopathic Pulmonary Fibrosis; LAP, Latency Associated Peptide; LLC, Large Latency Complex; LTBP, Latency TGFβ Binding Protein; MeOH, methanol; MIDAS, Metal Ion-Dependent Adhesion site; MMAE, monomethyl auristatin E; MMP, Metal Matrix Proteases; MTBE, Methyl tert-butyl ether; $NaBH(OAc)_3$, sodium triacetoxyborohydride; NaOAc, acetic acid sodium salt; NSCLC, Nonsmall-Cell Lung Carcinoma; PAB, *p*-aminobenzyl; PABC, *p*-aminobenzyl carbamate; PABE, *p*-aminobenzyl ether; PABQ, *p*-aminobenzyl quaternary ammonium salt; PAR, proteinases-activated receptor; PDGFR, Platelet-Derived Growth Factor Receptor; Pmc, 2,2,5,7,8-pentamethylchroman-6-sulfonyl; *p*-TsCl, *p*-toluenesulfonyl chloride; *p*-TsOH, *p*-toluenesulfonic acid; PTX, paclitaxel; PyBoP, (benzotriazol-1-yl-oxytripyrrolidino phosphonium hexafluoro-phosphate); RAFT, Regioselectivity Addressable Functionalized Template; SLC, Small Latency Complex; SMDC, Small Molecule-Drug Conjugate; SPPS, solid phase peptide synthesis; *t*BuOK, Potassium tert-butoxide; TEA, triethylene amine; TFA, trifluoroacetic acid; TFE, 2,2,2-trifluoroethanol; TGFβ, Transforming Growth Factor β; TIS, triisopropylsilane; TK, Tyrosine Kinases; TKI, Tyrosine Kinases Inhibitor; TL, tethered ligand; TMSCl, trimethylsilyl chloride; Triphosgene, bis(trichloromethyl) carbonate; VEGFR, Vascular Endothelial Growth Factor Receptor; VN, vitronectin.

Chapter 1. Introduction

1.1. Integrin receptors

Integrins are heterodimeric cell surface receptors involved in the delicate communication between cells and between cells and the extracellular matrix (ECM). They mediate several biological processes, such as the control of the balance cell proliferation/apoptosis, but they also contribute in maintaining the tissue integrity by arbitrating cell adhesion. Integrins are structurally comprised of a non-covalent association between α and β subunits.[1,2] In mammals there are 24 different integrin heterodimers, derived from the association of distinct 18 α subunits and 8 β subunits, which are distributed in different tissues and have specific roles and functions. Each subunit has an extracellular portion, the so-called "head", which is connected to the transmembrane domain, in turn linked to a small intracellular portion. Integrins perform their cell-anchoring function to the ECM components through their extracellular domain, and they transmit their "outside information" to the cytoskeleton through the intracellular domains (Figure 1).

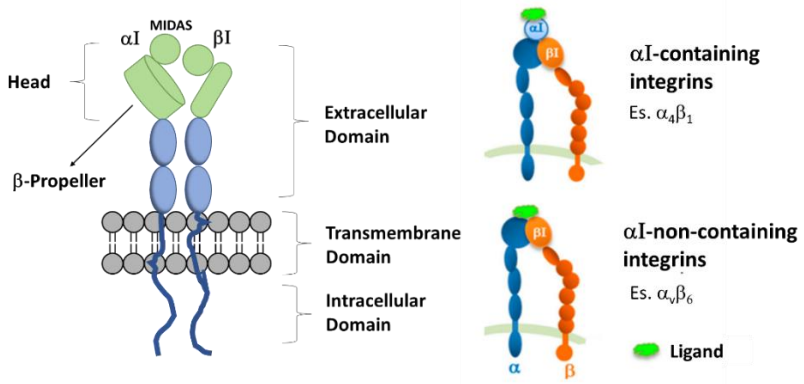

***Figure 1**. General structure of integrin receptors (on the left) and ligand biding-site for integrin containing αI domain or not (on the right). Adapted from Ref. 2.*

In particular, the head of the α subunit is called β-propeller, as it is constituted by seven domains, which form a cylindric helix: in some integrins this portion contains the αI domain. When this specific domain is present, the receptor binds the ligand at this level, while, in αI-non-containing integrins, the ligand binds to the receptor at the interface between the α and β subunits, in its βI domain (Figure 1).[2] The αI and βI regions are structurally homologous and contain the Metal Ion-Dependent Adhesion Site (MIDAS), which binds bivalent metal ions, such as Ca^{2+} or Mg^{2+}.

Integrins are not only systematically classified based on the different α/β subunit association (Figure 2), but they are also divided into four different families, based on the natural ligands they recognize:[3] *(i)* Arg-Gly-Asp (RGD)-recognizing integrins, which are the most populated family; *(ii)* collagen-recognizing receptors, which bind the sequence Gly-Phe-Hyp-Gly-Glu-Arg; *(iii)* leukocyte-recognizing integrins; and *(iv)* laminin-binding integrins.

Integrins are transmembrane receptors and they consequently can activate several intracellular pathways. Their structure and mechanism of action were initially hypothesized thanks to the $\alpha_{IIb}\beta_3$ and $\alpha_V\beta_3$ receptors, using dynamic simulations and NMR conformational analysis,[4,5] but the pioneering work of Xiong[6,7] revealed the receptor-ligand structure with an X-ray crystallographic analysis. In particular, in this study they solved the structure of the extracellular domain of $\alpha_V\beta_3$ in the presence or absence of cilengitide, a selective peptidomimetic integrin ligand which will be described later. Based on all these studies, integrin receptors have been detailed to have three main different conformations (Figure 3):[8] *(i) bent conformation*, where both heads of each subunit

are close to the cellular membrane, while the transmembrane domains are deeply associated; *(ii) extended conformation*; where both heads are directed to the ECM, but the transmembrane domains are still associated; and *(iii) open conformation,* both with heads being directed to the ECM, and transmembrane domains are finally separated.

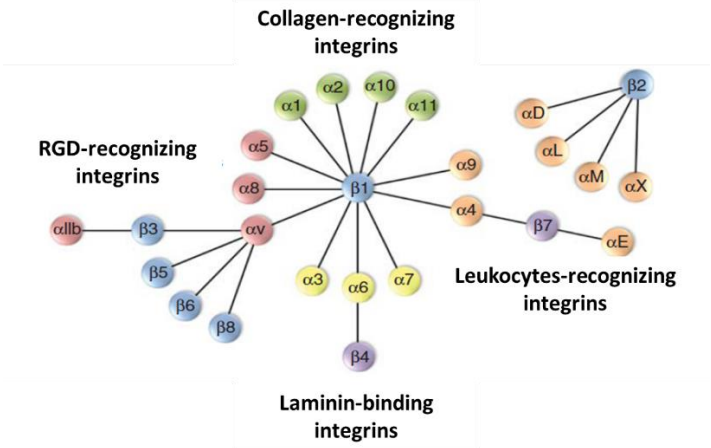

Figure 2. *Classification of the integrin receptors family. Adapted from Ref. 3.*

It has been shown that the bent conformation has low affinity for the external endogenous ligand, while the open one has the highest affinity. However, the ligand can bind the integrin also when it is in its bent conformation, thus triggering several rearrangements ultimately forcing the receptor to assume the open conformation; this particular process has been described as "switchable mechanism".[9] Modulation of the mechanism of activation can be mediated not only by ECM proteins, but also by elements present in the intracellular environment. This bidirectional system of activation has been defined as "inside-out/outside-in signalling" and it refers to the exquisite integrin capacity of mediating communication from the outside to the inside environment and *viceversa*. During the "inside-out" signalling, the cytoskeleton proteins interact with the intracellular portion of integrins, causing a distension of the extracellular domains and separation of the transmembrane domains. In this way, the receptor moves from the low-affinity state to the high-affinity conformation and it can interact with its extracellular ligands. On the other hand, during the "outside-in" signalling, the extended extracellular domains bind the ligand in the ECM, thus triggering the intracellular cascade. Usually, such activated intracellular pathways regulate cell migration, morphology and survival. In particular, cell migration is a consequence of a process described as "integrin cluster", an association of a big number of integrin receptors in a specific point, called "focal adhesion point". In fact, after receptor activation, FAK (focal adhesion kinase) is activated and it starts a phosphorylation cascade, which is concluded with the lamellipodia and filopodia formation; the focal adhesion points are formed on these receptors. These proteins accumulated on this region bind the ECM and work as anchoring points for the cell, which can migrate accordingly. Subsequently, the focal adhesion point is destroyed and a new one is formed in another side, allowing continuous migration of the cell.[10]

Among the integrin family, the RGD-recognizing integrins represent the most populated sub-group. The RGD sequence (the Arg-Gly-Asp tripeptide) was discovered in 1984 as a recognition site in fibronectin, an ECM protein.[11] Subsequently, the RGD sequence was identified in several other ECM proteins, including vitronectin, osteopontin, laminin and so on,[12] and nowadays eight out of 24 human integrin heterodimers are known to bind this sequence. However, integrins recognize this tripeptide with a specificity which goes beyond this small motif, as the specificity depends on

additional recognition regions and on distinct conformational and spatial presentation of the various ECM ligands.[1,13] Hence, despite their apparent similarity, the RGD-recognizing integrins can finely distinguish among different RGD-containing ECM proteins and respond differently upon interaction with each of them.[14]

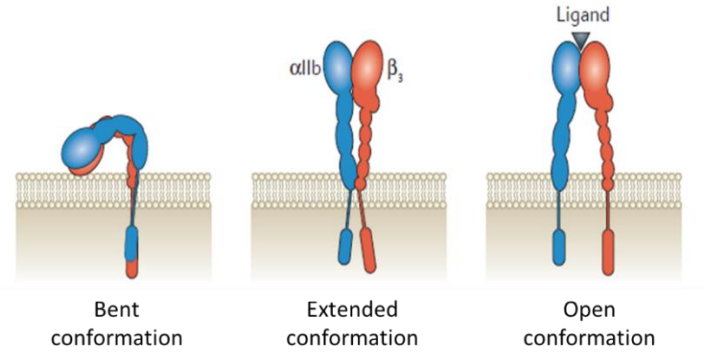

Figure 3. *Different conformation states of integrin receptors, as exemplified by $\alpha_{IIb}\beta_3$ integrin. Adapted from Ref. 8.*

Several RGD-recognizing integrins have been associated to different disease genesis and progression.[3] For instance, $\alpha_V\beta_3$ and $\alpha_V\beta_5$ are highly expressed on osteoclasts, endothelial cells, as well as on solid tumor cells and are claimed to play a role in angiogenesis; $\alpha_V\beta_6$ is significantly upregulated during inflammation, wound healing, fibrotic diseases and in cancers of epithelial origin, while it is expressed in healthy epithelial cells at very low level;[12,15] $\alpha_{IIb}\beta_3$ is uniquely expressed on the surface of platelets and megakaryocytes (a type of platelet-producing cells in the bone marrow) and it is involved in platelet aggregation during primary hemostasis that is mediated mainly by the fibrinogen. It has been demonstrated that inactivation of $\alpha_{IIb}\beta_3$ integrin on platelets is a successful clinical approach for anti-thrombotic therapy.[3,16]

Given the involvement of integrins in several physio-pathological processes,[1] the development of ligands which can selectively distinguish and target specific RGD-recognizing integrins is a highly valuable goal.

1.2. Peptidomimetics as RGD-recognizing integrin ligands

Peptides, historically defined as small-medium sequence of amino acids (2-50 units),[17] play important roles in several physio-pathological mechanisms and represent an interesting class of drugs, as they usually exhibit high specificity and affinity for their pharmacological targets and are extremely well tolerated by living organisms. In addition, peptides generally possess small-medium molecular weight in comparison to proteins and, for this reason, the synthesis of such compounds has been implemented successfully at commercially useful scale.[18] Despite this interesting drug-like quality, peptides suffer from several drawbacks, such as limited stability towards proteolysis, poor absorption and transport properties, possible interactions with multiple targets and antibodies. For this reason, natural peptides can be interesting starting points for the discovery of lead compounds, by introducing suitable structural modifications to obtain new peptidomimetics, that is peptide-resembling compounds designed to overcome peptide limitations, improve their metabolic stability and bioavailability, while retaining both high specificity and affinity towards their receptors.[17,19]

Vagner et al. defined peptidomimetics as "compounds whose essential elements (pharmacophore) mimic a natural peptide or protein in 3D space and which retain the ability to interact with the biological target and produce the same biological effect".[20] However, during the last decades, different definitions and classifications of peptidomimetics have been suggested,[21] and the most recent one divides these compounds into four different classes:[22] *(i) Class A mimetics*, which are the most similar to the parent peptides and have only local modifications that stabilize structure, conformation and modify metabolic stability; *(ii) Class B mimetics*, which still have large peptidic characteristics, but contain more important modifications both in the backbone and side chains; *(iii) Class C mimetics*, characterized by increasing small-molecule properties and usually endowed with a non-peptidic fragment; and *(iv) Class D mimetics*, which are the most dissimilar to the parent peptides, but able to mimic the mode of action of the parent bioactive molecule.

Nowadays, different RGD-integrin peptidomimetic ligands have been developed and some of them are commercially available drugs. In particular, in the field of antiplatelet drugs, two peptidomimetic inhibitors of $\alpha_{IIb}\beta_3$ integrin (also known as the glycoprotein GPIIb/IIIa complex) are used in clinics, namely eptifibatide and tirofiban.[16] The first one is a cyclic heptapeptide based on the structure of the snake venom disintegrin called barbourin (Figure 4a), which could be classified as Class B/Class C peptidomimetic. Indeed, it has an RGD-mimicking sequence in which arginine is replaced by homo-arginine, similarly to the KGD sequence present in the disintegrin proteins which inspired this drug; moreover, eptifibatide possesses a disulphide bridge between two non peptidic portions, a terminal modified-cysteine and an aminopropanethiol motif. On the contrary, tirofiban (Figure 4b) is an L-tyrosine derivate which mimics the RGD sequence and it could be classified as Class D peptidomimetic, since it essentially does not contain any peptidic residue. In fact, it comprises a piperidine portion mimicking the arginine residue and a free carboxylic acid which replaces the aspartic acid motif. However, despite their high potency, both eptifibatide and tirofiban are not orally active and therefore are only useful to treat acute conditions, such as acute myocardial infarction.[23]

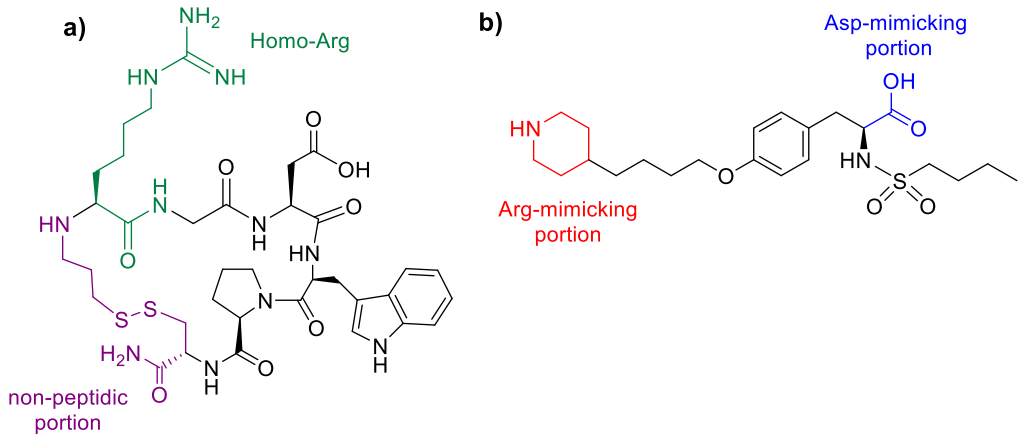

Figure 4. *Structures of the $\alpha_{IIb}\beta_3$ inhibitors eptifibatide (**a**) and tirofiban (**b**).*

Among the developed peptidomimetic integrin ligands, cilengitide was the most promising concerning cancer therapy (Figure 5a). This molecule is a cyclic RGD-containing peptide which binds $\alpha_V\beta_3$ (with sub-nanomolar affinity), $\alpha_V\beta_5$ and $\alpha_5\beta_1$ (with low nanomolar affinity) integrins and it was proposed as the first possible anti-angiogenic integrin-targeting drug.[24] Cilengitide could be classified as a Class B peptidomimetic, since it basically maintains peptidic characteristics but *(i)* it

is cyclic, *(ii)* it contains the non-natural amino acid D-phenylalanine and *(iii)* the amide nitrogen between valine and D-phenylalanine residues is methylated. Despite its promising results in several Phase II studies, cilengitide failed in advanced Phase III study for the peculiar pro-angiogenic effects it exerts at low concentrations.[23] However, the promising results obtained by cilengitide inspired scientists in developing similar structures, which are currently investigated both in preclinical and clinical studies.[1,24]

In recent past years, much attentions in the field of RGD-recognizing integrins have been devoted to the previously mentioned $\alpha_V\beta_6$ integrin, to which a specific following chapter will be dedicated. Recently, a peptidomimetic $\alpha_V\beta_6$ inhibitor developed by GSK (GSK3008348, Figure 5b) has successfully passed Phase II studies for the treatment of Idiopathic Pulmonary Fibrosis;[25] this compound can be classified as Class D peptidomimetic, since the structure is basically non peptidic but it possesses both an arginine and an aspartic acid mimicking groups (the naphthyridine motif and the carboxylic acid group, respectively).

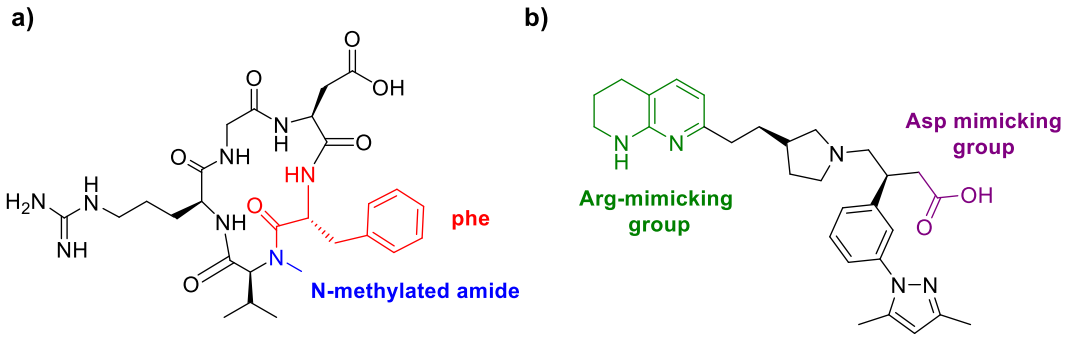

Figure 5. *Structures of the $\alpha_V\beta_3$ and $\alpha_V\beta_5$ integrin ligand cilengitide (**a**) and of GSK $\alpha_V\beta_6$ integrin inhibitor (**b**).*

Other interesting integrin-targeted peptidomimetics have been studied worldwide, reaching promising results;[23,26] moreover, these compound classes have raised interest not only as ligands *per se*, but also as directing components of more sophisticated structures called Small Molecule-Drug Conjugates (SMDCs).

1.3. Small Molecule-Drug Conjugates

The lack of selectivity of several commercially available drugs is the typical cause of drawbacks of several chemotherapeutics. Specific target delivery of drugs is an important and ambitious goal in the treatment of different pathologies, such as cancer- or fibrotic-related diseases. In order to achieve the maximal therapeutic effect and the minimum off-target reactions, several strategies have been applied in the last decades aiming to improve drug delivery, encompassing supramolecular, nanoparticle systems[27] and the so-called Ligand-Targeted Drug delivery systems (LTDs).[28] Among LTDs compounds, Antibody-Drug Conjugates (ADCs)[29] and Small Molecule-Drug Conjugates (SMDCs) have become important tools in the treatment of cancer and other pathologies.[30,31] In particular, SMDCs are covalent conjugates typically constituted by three key components: a targeting unit, a linker and a payload drug (see infra). SMDCs have recently emerged as an alternative approach to ADCs, which instead are biopharmaceutical drugs which combine specific surface-antigen monoclonal antibodies with a therapeutic agent by chemical linkages. Indeed, the high molecular weight and possible immunogenicity are important drawbacks of ADCs, still limiting the use of these systems as truly druggable pharmacological agents. SMDCs could pose

remedy to some of ADCs disadvantages, since they have *(i)* lower molecular weights, leading to better cellular permeability and stability, *(ii)* improved accuracy of the drug loading and *(iii)* lower immunogenicity in comparison to ADCs. However, most of the developed SMDCs have to be administrated intravenously, maintaining this drawback in common with ADCs.

1.3.1. SMDCs: design and structure

Typically, a SMDC is constituted by three different units (Figure 6): *(i)* a *payload*, the drug which exerts the therapeutic activity; *(ii)* a *targeting unit*, the element which "drives" the system at the diseased site possibly helping the payload internalisation; in addition to this targeting task, this unit may have a supplementary therapeutic activity synergistically working with the payload; *(iii)* a *linker* (also called *spacer*), which makes possible connecting the targeting unit to the payload. The linkers are classified in "uncleavable" connections, which maintain their integrity during the SMDC life, and "cleavable" units, which ideally would allow the payload to be specifically released at the diseased site thanks to specific microenvironment inducing-cutting (for instance, by *in situ* variation of pH or by specific enzymatic cleavage, as describe later).

Figure 6. *Schematic structure of a general SMDC. Adapted from Ref. 32.*

The development of novel SMDCs needs a rational design, considering the different features of each unit within the system. First of all, the potency of the payload should be high enough to achieve a therapeutic effect when the targeted receptors are largely saturated with SMDCs. If receptor numbers and/or recycling rates are inadequate to deliver therapeutic concentrations of the payload, increasing the number of drug units attached to each targeting ligand should be considered, creating the so-called multimeric conjugates. Furthermore, the chemical structure of the payload should have an adjustable portion to be used as anchoring unit without affecting its pharmacological activity. Frequently, the payload is a cytotoxic or, more generally, a non-specific drug which can improve its selectivity profile thanks to the conjugation to the targeting unit.[29]

Concerning the targeting unit, this element should be a highly potent and selective molecular portion addressed towards a specific receptor expressed exclusively (or quite exclusively) on cells of the diseased district, to minimize the off-target delivery of the payload. In case no low-nanomolar targeting units are available, or if the affinity of the designed system has to be implemented, the use of multivalent ligands can be a good option, with multiple copies of targeting units attached to the same therapeutic payload.[33]

The targeted receptor should be preferably exposed at the cell surface, due to three main reasons: first, to allow minimization of the cell-permeability of the small-molecule targeting unit, and consequently reducing the problem of non-specific cellular internalisation; second, to avoid the risk that the demonstrated high cellular permeability of the targeting unit is compromised by the conjugation to the payload; third, SMDCs directed to cell surface-exposed receptors be engineered to be membrane-impermeable to receptor-negative cells.[33] Another important criterion in the selection of the targeting unit concerns the absolute level of targeted-receptor expression in the

diseased cell type. In fact, if the positive therapeutic outcome can only be achieved with the intracellular drug concentration exceeding a minimum value, sufficient receptor numbers must be present on the targeted cell to enable sufficient drug delivery. For instance, if the in vitro binding affinity IC_{50} values of the targeting ligand were found to be 10 nM and the pathologic cell was assumed to have a volume of 4 000 μm^3, the cell would have to express >72000 receptors for sufficient drug internalization and inhibition of the receptor activity.[28] In many cases the choice of a "wrong" targeted receptor can be directly correlated to the failure of the activity of the designed SMDCs.

Besides the payload and the targeting moieties, the linker is the third fundamental element, being responsible for both the stability of the intact construct in the blood circulation and the possible drug release at the diseased site. In particular, structural weaknesses of the linker moiety can be responsible for the low stability of the construct in blood circulation, resulting in premature drug release from the vehicle and the consequent failure of the therapy. Additionally, this element allows the creation of a novel chemical entity and, consequently, it may influence not only the biological profile of both payload and targeting unit, but also the physical-chemical proprieties of the whole SMDC structure. Minimal steric interference among the payload and the targeting unit is necessary for not compromising the ligand affinity towards its receptor. Moreover, the linker can be chosen to improve the pharmacokinetic proprieties of the SMDCs; for instance, a peptidic or polyethylene glycol linker can enhance the system solubility or kidney excretion. The mechanism by which the linker released the payload at the diseased site is based on its "cleavability", and both cleavable and uncleavable linkers have been largely reported in literature.[29] Uncleavable linkers are generally stable all along the life of SMDCs, which consequently reach the target site in an intact state and exert their activity as unique chemical entities; on the contrary, cleavable linkers must remain intact during the transit through the vasculature but must rapidly release the payload *in situ* in the diseased site.[34]

Examples of both cleavable and uncleavable SMDCs will be described in the following paragraphs, focusing on those RGD integrin-targeted SMDCs, which have recently attracted attention in the field of targeted drug delivery and are nowadays intensively investigated.[35] Particular emphasis will be also placed on the linker moieties and chemistry of conjugation, with peculiar characteristics for each of the chosen SMDC examples. These delivery systems exploit the expression specificity of the RGD-recognizing integrin receptors, since they are overexpressed on cancer, fibrotic and inflammatory cell surface and influence the onset and progression of several diseases.[1] For this reason, using RGD integrin-targeting ligands has the additional advantage of combining the targeting function of such compounds with their intrinsic pharmacological activity; this leads to particular SMDCs possibly possessing synergic biological effects with consequent enhancement of the pharmacologic effect. Moreover, integrin receptors and their ligands have been shown to be efficiently internalized via receptor-mediated endocytosis,[36] and this may lead to an active drug release in the intracellular environment. All these characteristics render RGD integrin-targeting peptidomimetics good candidates to be used as targeting units in the development of highly potent and selective SMDCs. The choice of using peptidomimetic compounds has the additional advantage of combining the physical-, chemical- and pharmacokinetic properties of such components to the high potency of the payload, possibly leading to enhanced safety and efficacy of the chosen drug.[37]

On these grounds, the development of novel RGD integrin-targeted peptidomimetic SMDCs represent an interesting therapeutic option for several diseases as evidenced by the several

promising compounds of this type that have been reported in literature till now,[35] both as cleavable and uncleavable systems.

1.3.2. Uncleavable RGD integrin-targeted SMDCs

As mentioned before, the payload and the targeting unit can be conveniently connected by an uncleavable linker, and the whole SMDC can consequently reach the diseased site as an intact dual construct. Several types of linkers can be used,[37] and the most commonly utilized spacers include polyethylene glycol or alkyl chains of different length, stable peptide, amide or carbamate bonds.

The covalent conjugation chemistry that makes connection between the two units possible obviously depends upon the functional groups present on the linker, the payload and the targeting unit. "Click reactions" are commonly used in the field of bioconjugation, as they occur in one-pot very efficiently, they generally tolerate water and generate minimal and inoffensive by-products.[38] These reactions can be performed between several functional groups,[39] and the most common reactions in the field of bioconjugation are: *(i)* the copper-catalyzed reaction of an azide with a terminal alkyne to form a 5-membered triazole ring and, *(ii)* the reaction between an aldehyde/ketone and hydroxylamine/hydrazine to give oxime/hydrazone products. Additionally, and importantly, maleimide is used in bioconjugation and usually it is involved as an electrophile in a Michael addition with a nucleophile, such as a thiol terminal group (Figure 7).

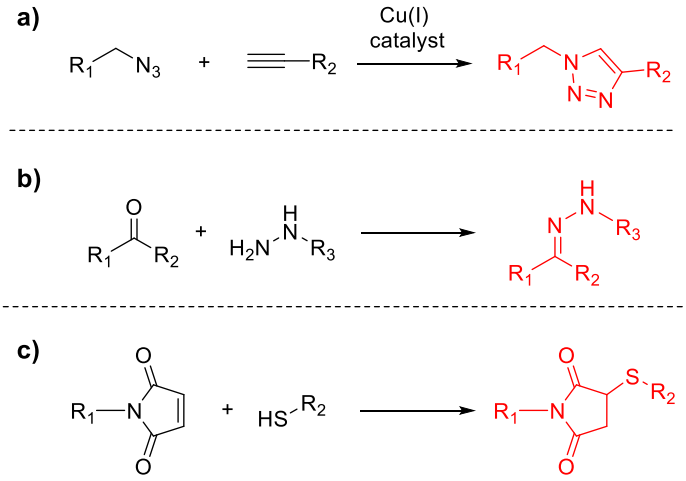

***Figure 7**. General examples of the most commonly utilized reactions for the covalent bioconjugation: **a**) "click" reaction between azide and alkyne providing a triazole; **b**) "click" reaction between ketone and hydrazine giving hydrazone; **c**) Michael addition of a thiol nucleophile on maleimide acceptor.*

Nowadays, different uncleavable RGD integrin-targeted SMDCs have been described, with some prototypes reaching promising results.[37] Paralleling the general philosophy of all SMCDs, the most commonly pursued goal of RGD integrin-targeted SMDCs is to direct the non-specific action of the cytotoxic drug to the diseased district by exploiting the targeting capabilities of the RGD integrin ligand moiety, thus minimizing off-target effects.

For instance, Marchán et al. synthesized two conjugates, in both monomeric and tetrameric versions, where a Pt(IV) derivative of picoplatin was linked to the dual $\alpha_v\beta_3/\alpha_v\beta_5$ integrin ligand c(RGDfK) (Figure 8); the selectivity and high affinity of these ligands were exploited for the targeted delivery of the anticancer metallodrug to SK-MEL-28 melanoma cells overexpressing these integrin receptors.[40] For the synthesis of the monovalent conjugate, they used a PEG2 linker connected to both the drug and the peptidomimetic through amide bonds; on the other hand, for the tetrameric

conjugate, they exploited the known "Regioselectively Addressable Functionalized Template" (RAFT) cyclodecapeptide scaffold, which was decorated with four copies of c(RGDfK) by triazole rings, derived from four-fold click reactions between azide and alkyne terminals. The authors demonstrated the effective drug delivery of the Pt(IV) complex: both cell internalization and cytotoxic performance in vitro proved good for both the conjugates; in particular, for the multimeric conjugate, the cytotoxic activity increased by 20-fold in melanoma tumor cells expressing $\alpha_V\beta_3/\alpha_V\beta_5$ integrin; by contrast, the cytotoxicity of the conjugates was inhibited in control cells lacking $\alpha_V\beta_3$ and $\alpha_V\beta_5$ integrin expression.

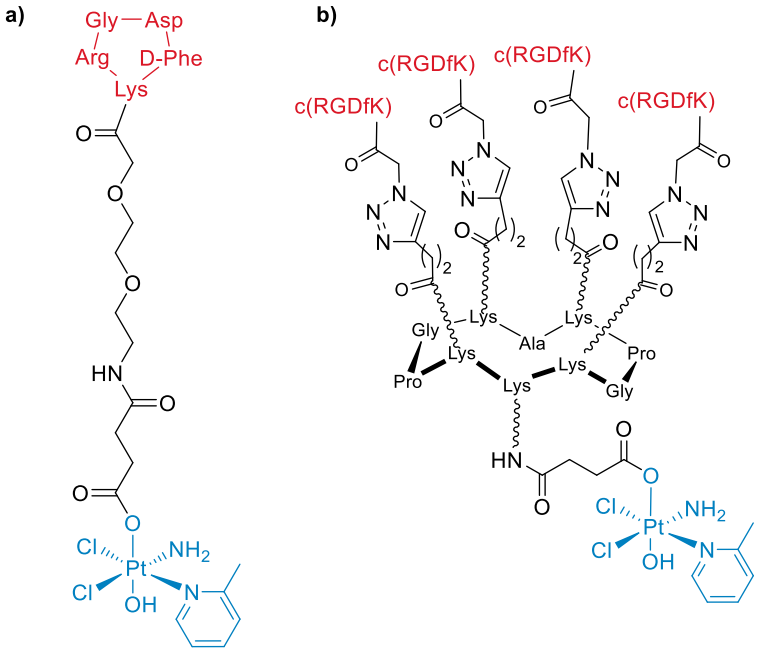

Figure 8. *Monomeric (**a**) and tetrameric (**b**) covalent conjugates synthesized by Marchán et al.*

In 2012, Manzoni et al.[41] synthesized nine novel molecular conjugates containing paclitaxel (PTX) covalently attached to either cyclic peptidomimetic c(AbaRGD) (alias the azabicycloalkane-RGD cyclopeptide), or c(AmpRGD) (alias aminoproline-based RGD cyclotetrapeptide), which had previously been described as dual $\alpha_V\beta_3/\alpha_V\beta_5$ integrin ligands. Among the nine conjugates, the one which showed the best growth inhibitory results is displayed in Figure 9a, bearing a robust triazole ring connected to ethylene glycol units by an amide function. This compound was selected for in vivo studies in an ovarian carcinoma model xenografted in immunodeficient mice: interestingly, remarkable antitumor activity was attained, superior to that of PTX itself. Therefore, this conjugate represents a perfect example of how an RGD-dual conjugate combines minimization of the toxic effect of a cytotoxic drug by targeted delivery, with overall antitumor activity enhancement, possibly due to a synergistic effect between the payload and the RGD-targeting unit.

Other examples of PTX conjugates were successfully reported by the same group[42] and others; for instance, in 2019 Zanda et al.[43] synthesized a novel dual covalent conjugate, where a 1,2,3-triazole-based $\alpha_V\beta_3$-targeting RGD peptidomimetic ligand is conjugated to PTX via an oxime heterobifunctional linker (Figure 9b); the design of this conjugated was driven by previous molecular modelling studies, which suggested the possibility of functionalization at the 5th position of the triazole ring. This compound showed highly selective toxicity towards $\alpha_V\beta_3$ integrin expressing cells (U87MG) in contrast to free paclitaxel, which was indiscriminately toxic towards both U87MG

and non-expressing $\alpha_V\beta_3$ cells (MCF7). This result is consistent with the hypothesis that the conjugate can address cancer cells via $\alpha_V\beta_3$ integrin selective targeting.

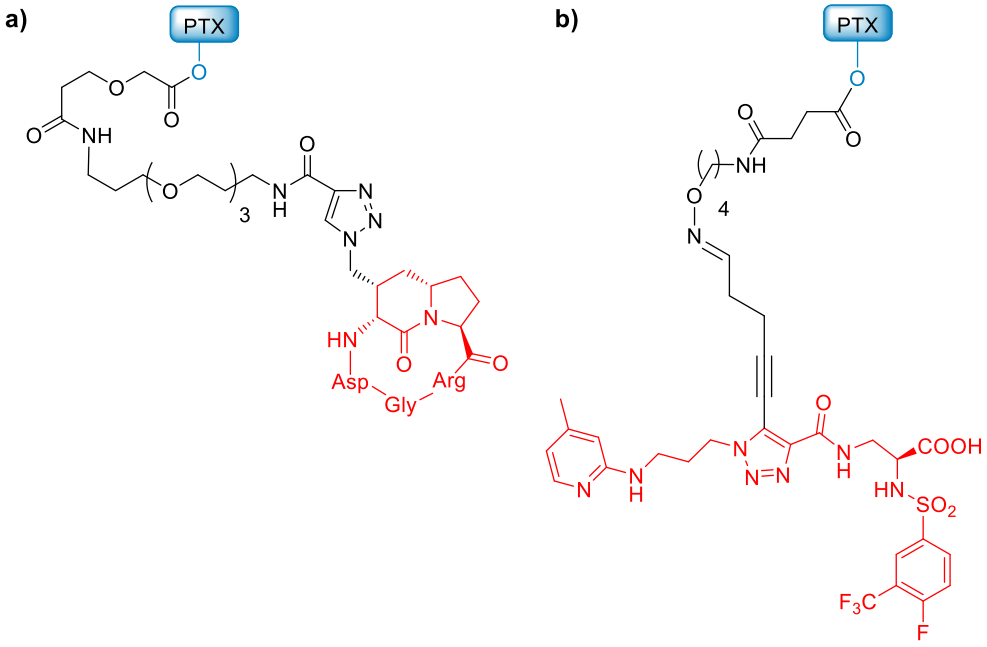

Figure 9. *Structures of the PTX covalent conjugates synthesized by Manzoni et al. (**a**) and Zanda et al. (**b**).*

As a further example, Zanardi et al. have recently published the synthesis and characterization of three different covalent conjugates, two monomers and one dimeric system, where the previously mentioned peptidomimetic cAmp(RGD) is covalently connected to the anti-tumor and anti-angiogenic RTK inhibitor sunitinib.[44-46] The two active moieties are linked either by an alkyl or a PEG linker through the triazole ring derived from a copper-catalyzed click reaction. Among the three conjugates, the dimeric one (Figure 10) showed promising results both *in vitro* towards melanoma cells and *in vivo*, towards ovarian carcinoma- and melanoma-implanted mice, paving the way for the use of these selective conjugates as drugs able to counteract the compensatory escape mechanisms that tumor cells establish against conventional sunitinib-based pharmacological treatments. Additionally, the authors demonstrated the complete $\alpha_V\beta_3$ integrin-dependent internalization of these compounds in A375 melanoma cells within 25 min exposure, underlying the importance of the role of cAmp(RGD) not only as targeting unit *per se*, but also as an active element for the integrin-mediated sunitinib internalization.

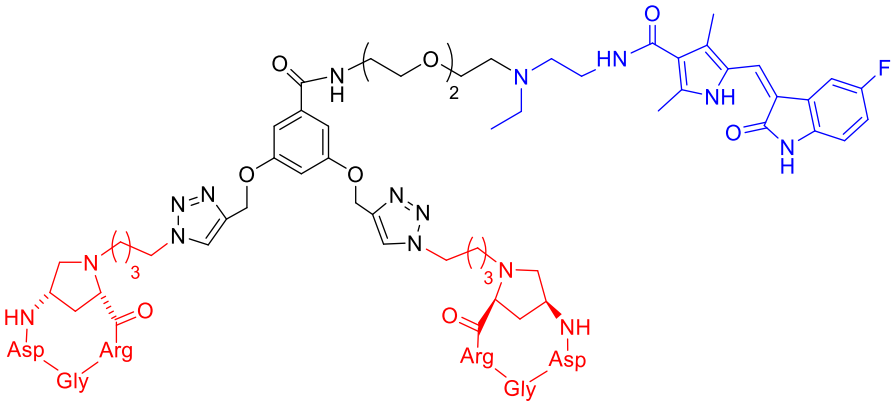

Figure 10. *Structure of the dimeric covalent conjugate developed by Zanardi et al.*

To conclude, in 2016 Gellerman et al. developed three novel peptide-drug conjugates based on the cyclic peptidomimetic cilengitide, in which the methylated valine was replaced by either Lys or Ser.[47] Two chemotherapeutic agents namely, Chlorambucil (CLB) and Camptothecin (CPT), were alternatively linked to the core carrier peptides using either amide/ester bonds for CLB, or carbamate bond for CPT (Figure 11). The synthesized conjugates were tested in different cell lines (both expressing α_V integrin or not) and their chemo-stability and drug release were demonstrated in several systems. Functional versatility of the conjugates was reflected in the variability of their drug release profiles, while the conserved RGD sequence ensured selective binding to the α_V integrin family. Additionally, they demonstrated the ability of the cyclic RGD–CLB conjugates to overcome drug resistance; also, this type of assembly could represent a "second chance" for those cytotoxic agents like CPT, which are poorly bioavailable and display high off-target toxicity when administered alone. Based on these promising results, the authors are continuing studies on these systems, with the idea of developing versatile and "all-purpose" RGD-based targeting unit to be used for the drug-delivery of distinct cytotoxic agents.[48,49]

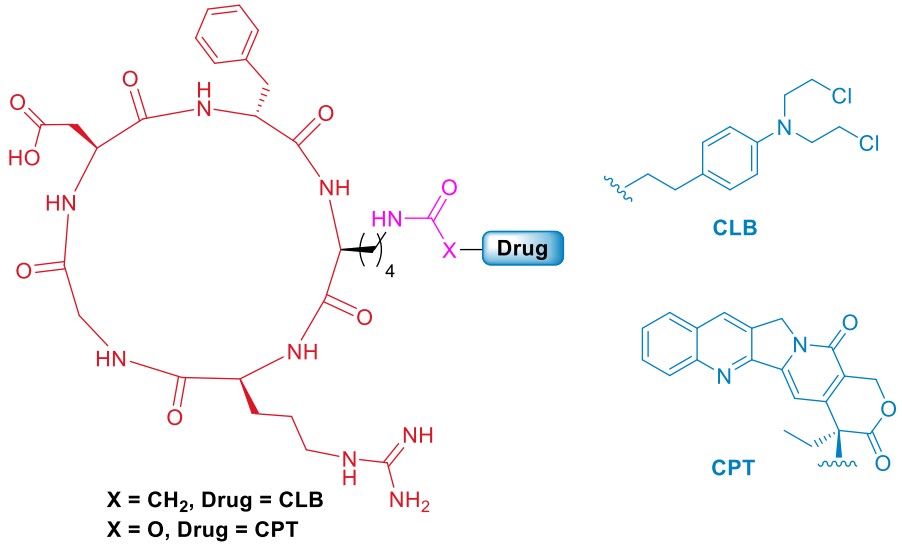

Figure 11. *Cleavable dual conjugates loaded with CLB and CPT developed by Gellerman et al.*

Several other examples of promising RGD-based dual covalent conjugates have been reported in literature so far, not only in the field of cancer therapy, but also addressed to other pathologies, such as inflammation,[50] showing the high potential of these systems in the development of innovative drugs.

1.3.3. Cleavable RGD integrin-targeted SMDCs

Beside uncleavable linkers, the strategy of using cleavable linkers for punctual drug delivery in the diseased site has been extensively studied and reviewed.[28,29,34] Several linkers have been developed to release payloads in the presence of specific hallmarks of the diseased site, including acidic pH, proteolytic enzyme overexpression, hypoxic and reducing conditions. Cleavable linkers can be represented by rather simple structures or more sophisticated systems; for instance, ordinary functional groups, such as esters, carbamates or disulphide bonds can be exploited in drug delivery as they are cleaved by specific enzymes or hydrolyzed in acidic environment. On the other hand, cleavable linkers can be represented by specific peptide sequences, which are recognized by

disease-related enzymes (e.g. metalloproteases,[37] cathepsins[34] or β-gluconoridases[28]), either as single elements or flanked by ancillary units called "self-immolative spacers", chemical entities which undergo spontaneous degradation upon linker cleavage.

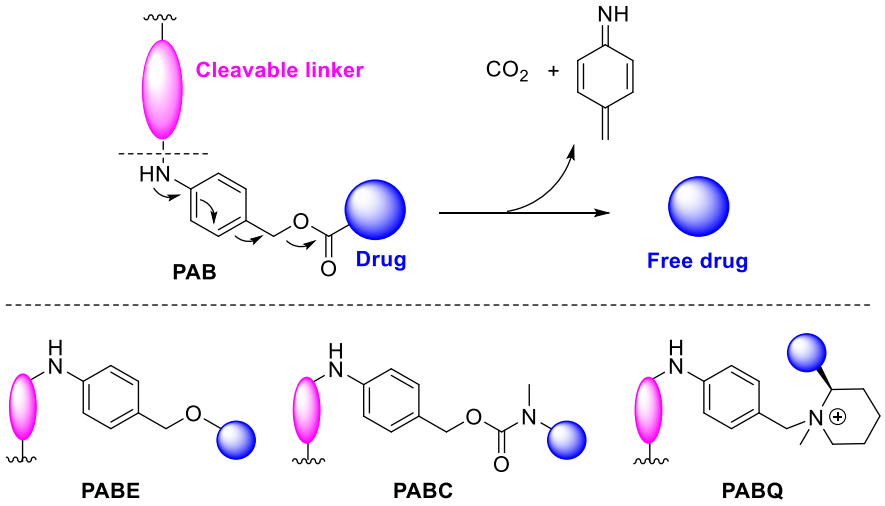

Figure 12. *Release mechanism of PAB self-immolative spacer and structures of commonly used spacers PABE, PABC and PABQ.*

In this context, aromatic moieties or conjugated π-systems represent ideal structures; for instance, the *p*-aminobenzyl (PAB) scaffold is the most used and versatile structure (Figure 12). When disconnected from the linker upon cleavage, the free aniline moiety of PAB rapidly undergoes 1,6-elimination, affording an azaquinone methide metabolite, carbonic anhydride, and releasing the drug. Other similar self-immolative spacers, such as *p*-aminobenzyl ether (PABE), *p*-aminobenzyl quaternary ammonium salt (PABQ), and dicarbamate coupled with PAB (PABC) have been reported and successfully exploited.[34]

In this regard, the research group of Gennari et al. have long focused on the development of cleavable SMDCs. For instance, in 2019 they synthesized two new integrin-targeted cleavable conjugates, constituted by four components: the diketopiperazine-based targeting unit c(DKP-RGD), a glucuronide linker, a self-immolative spacer, and the potent microtubule-disruptor monomethyl auristatin E (MMAE).[51] Since the spacer between the ligand and the linker moieties may be crucial for different aspects, such as the conjugate flexibility, solubility, ligand binding affinity, the two SMDCs featured two different additional spacer units, a glutaric acid derivative in the first conjugate and a triazole-PEG4 spacer in the second one (Figure 13a). β-glucuronidase is a well-known tumour-associated enzyme and cleaves the SMDC in situ at the glucuronide moiety; after cleavage, the self-immolative spacer is free to undergo spontaneous degradation and to release the MMAE. Interestingly, the PEG4-conjugate inhibited the proliferation of $\alpha_v\beta_3$ integrin-expressing human glioblastoma U87MG and renal carcinoma 786-O cells at low-nanomolar concentrations, and the cytotoxic activity was shown to be more pronounced in the presence of β-glucuronidase. These promising data suggest that this conjugate may be therapeutically active *in vivo* against solid tumours concomitantly expressing both integrin $\alpha_v\beta_3$ and β-glucuronidase.

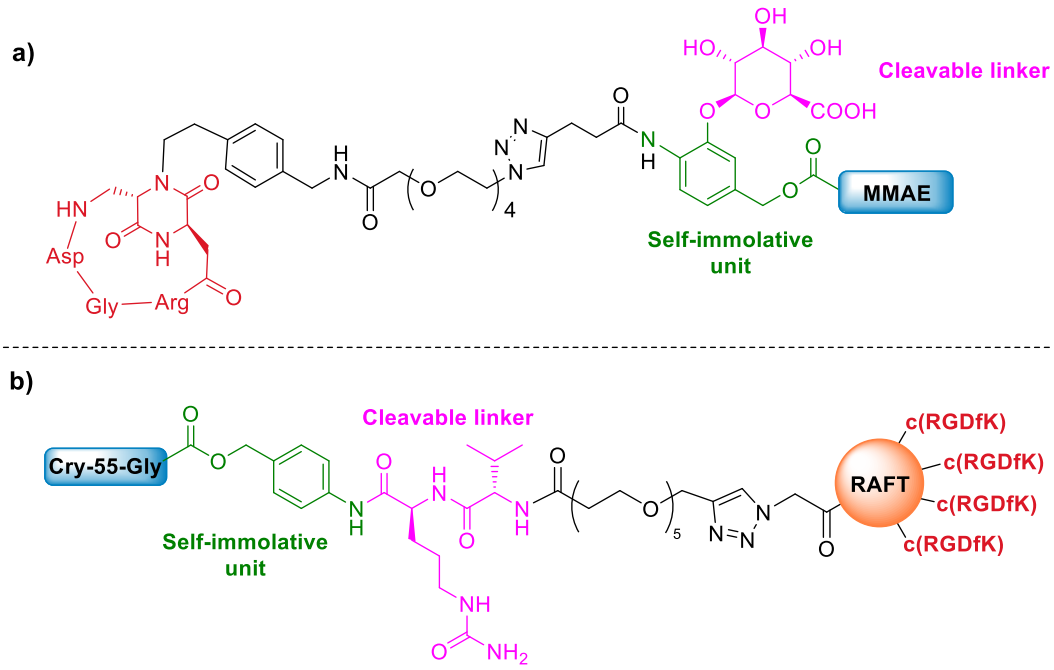

Figure 13. *Molecular structure of the cleavable SMDC developed by Gennari et al. (**a**) and structure of the multimeric SMDC synthesized by Sewald et al. (**b**).*

The same self-immolative spacer has been recently used by Sewald et al. in a novel multivalent $\alpha_V\beta_3$ integrin ligand SMDC.[52] They synthesized a multifunctional tetrameric conjugate containing four copies of c(RGDfK), the RAFT template, the Val-Cit linker, which is enzymatically cleaved in lysosomes, the self immolative spacer PABC, and glycinate cryptophycin-55, a potent inhibitor of tubulin polymerization (Figure 13b). The conjugate was tested towards several cell lines expressing different levels of $\alpha_V\beta_3$ integrin and the results suggested that the RGD-containing scaffold is highly effective for the delivery of cryptophycin, as the tetrameric RGD-cryptophycin conjugate displays impressive potency in vitro, especially in M21 melanoma cells. They also confirmed that the multimeric RAFT-c(RGDfK)$_4$ presentation enhances the selectivity of and improves tumor-targeted drug delivery, providing a rationale for possible future therapeutic applications in combination with cytotoxic agents.

Based on these promising studies and results, we may conclude that peptidomimetics can play crucial roles in pharmaceutical and medicinal chemistry as both ligands *per se* and targeting units in SMDCs. In particular, RGD-recognizing integrin peptidomimetics have attracted much attention in recent past years, due to the direct involvement of diverse integrin subclasses in several cancer- and fibrosis-related diseases. Despite the promising results these compounds have reached, nowadays few RGD integrin-targeted peptidomimetics have been approved for clinical treatments (vide supra), and there are not RGD-based SMDCs commercially available to date.

While the reasons responsible for this void have to be carefully analyzed (relatively still “young” research field, spatio-temporal release of drugs not completely elucidated, difficulties connected to multi-step synthesis, …), we retain that the implementation of novel high-affinity and selective ligands and versatile SMDCs are urgently needed, with the ultimate goal of developing novel chemotherapeutic treatments addressing cancer and fibrosis-related diseases.

1.4. References

(**1**) Nieberler, M.; Reuning, U.; Reichart, F.; Notni, J.; Wester, H.-J.; Schwaiger, M.; Weinmüller, M.; Räder, A.; Steiger, K.; Kessler, H. Exploring the Role of RGD-Recognizing Integrins in Cancer. *Cancers* **2017**, *9*, 116.

(**2**) Tolomelli, A.; Galletti, P.; Baiula, M.; Giacomini, D. Can Integrin Agonists Have Cards to Play against Cancer? A Literature Survey of Small Molecules Integrin Activators. *Cancers* **2017**, *9*, 78.

(**3**) Kapp, T. G.; Rechenmacher, F.; Sobahi, T. R.; Kessler, H. Integrin Modulators: A Patent Review. *Expert Opin. Ther. Pat.* **2013**, *23*, 1273–1295.

(**4**) Auzzas, L.; Zanardi, F.; Battistini, L.; Burreddu, P.; Carta, P.; Rassu, G.; Curti, C.; Casiraghi, G. Targeting $\alpha_v\beta_3$ Integrin: Design and Applications of Mono- and Multifunctional RGD-Based Peptides and Semipeptides. *Curr. Med. Chem.* **2010**, *17*, 1255–1299.

(**5**) Morino, N.; Mimura, T.; Hamasaki, K.; Tobe, K.; Ueki, K.; Kikuchi, K.; Takehara, K.; Kadowaki, T.; Yazaki, Y.; Nojima, Y. Matrix/Integrin Interaction Activates the Mitogen-Activated Protein Kinase, P44 and P42. *J. Biol. Chem.* **1995**, *270*, 269–273.

(**6**) Xiong, J.-P.; Stehle, T.; Diefenbach, B.; Zhang, R.; Dunker, R.; Scott, D. L.; Joachimiak, A.; Goodman,S. L.; Arnaout, M. A. Crystal Structure of the Extracellular Segment of Integrin $\alpha_v\beta_3$. *Science* **2001**, *294*, 339–345.

(**7**) Xiong, J.-P. Crystal Structure of the Extracellular Segment of Integrin $\alpha_v\beta_3$ in Complex with an Arg-Gly-Asp Ligand. *Science* **2002**, *296*, 151–155.

(**8**) Kreuger, J.; Phillipson, M. Targeting Vascular and Leukocyte Communication in Angiogenesis, Inflammation and Fibrosis. *Nat. Rev. Drug Discov.* **2016**, *15*, 125–142.

(**9**) Gottschalk, K.; Kessler, H. The Structures of Integrins and Integrin-Ligand Complexes : Implications for Drug Design and Signal Transduction. *Angew. Chem. Int. Ed.* **2002**, *41*, 3767–3774.

(**10**) Lepzelter, D.; Bates, O.; Zaman, M. Integrin Clustering in Two and Three Dimensions. *Langmuir* **2012**, *28*, 5379–5386.

(**11**) Pierschbacher, M. D.; Ruoslahti, E. Cell Attachment Activity of Fibronectin Can Be Duplicated by Small Synthetic Fragments of the Molecule. *Nature* **1984**, *309*, 30–33.

(**12**) Niu, J.; Li, Z. The Roles of Integrin $\alpha_v\beta_6$ in Cancer. *Cancer Lett.* **2017**, *403*, 128–137.

(**13**) Ruoslahti, E.; Pierschbacher, M. New Perspectives in Cell Adhesion: RGD and Integrins. *Science* **1987**, *238*, 491–497.

(**14**) Kapp, T. G.; Rechenmacher, F.; Neubauer, S.; Maltsev, O. V.; Cavalcanti-Adam, E. A.; Zarka, R.; Reuning, U.; Notni, J.; Wester, H. J.; Mas-Moruno, C.; Spatz, J.; Geiger, B.; Kessler, H. A Comprehensive Evaluation of the Activity and Selectivity Profile of Ligands for RGD-Binding Integrins. *Sci. Rep.* **2017**, *7*, 1–13.

(**15**) Margadant, C.; Sonnenberg, A. Integrin-TGFβ Crosstalk in Fibrosis, Cancer and Wound Healing. *EMBO Rep.* **2010**, *11*, 97–105.

(**16**) Huang, J.; Li, X.; Shi, X.; Zhu, M.; Wang, J.; Huang, S.; Huang, X.; Wang, H.; Li, L.; Deng, H.; Zhou, Y.; Mao, J.; Long, Z.; Ma, Z.; Ye, W.; Pan, J.; Xi, X.; Jin, J. Platelet Integrin αIIbβ3: Signal Transduction, Regulation, and Its Therapeutic Targeting. *J. Hematol. Oncol.* **2019**, *12*, 26.

(**17**) Henninot, A.; Collins, J. C.; Nuss, J. M. The Current State of Peptide Drug Discovery: Back to the Future? *J. Med. Chem.* **2018**, *61*, 1382–1414.

(**18**) Isidro-Llobet, A.; Kenworthy, M. N.; Mukherjee, S.; Kopach, M. E.; Wegner, K.; Gallou, F.; Smith, A. G.; Roschangar, F. Sustainability Challenges in Peptide Synthesis and Purification: From R&D to Production. *J. Org. Chem.* **2019**, *84*, 4615–4628

(**19**) Seguin, L.; Desgrosellier, J. S.; Weis, S. M.; Cheresh, D. A. Integrins and Cancer: Regulators of Cancer Stemness, Metastasis, and Drug Resistance. *Trends Cell Biol.* **2015**, *25*, 234–240.

(**20**) Vagner, J.; Qu, H.; Hruby, V. J. Peptidomimetics, a Synthetic Tool of Drug Discovery. *Curr. Opin. Chem. Biol.* **2008**, *12*, 292–296.

(**21**) Lenci, E.; Trabocchi, A. Peptidomimetic Toolbox for Drug Discovery. *Chem. Soc. Rev.* **2020**, *49*,

3262–3277.
(**22**) Pelay-Gimeno, M.; Glas, A.; Koch, O.; Grossmann, T. N. Structure-Based Design of Inhibitors of Protein-Protein Interactions: Mimicking Peptide Binding Epitopes. *Angew. Chem. Int. Ed.* **2015**, *54*, 8896–8927.
(**23**) Cox, D. How Not to Discover a Drug - Integrins. *Expert Opin. Drug Discov.* **2020**, *00*, 1–15.
(**24**) Mas-Moruno, C.; Rechenmacher, F.; Kessler, H. Cilengitide: The First Anti-Angiogenic Small Molecule Drug Candidate. Design, Synthesis and Clinical Evaluation. *Anti-Cancer Agents Med. Chem.* **2011**, *10*, 753–768.
(**25**) John, A. E.; Graves, R. H.; Pun, K. T.; Vitulli, G.; Forty, E. J.; Mercer, P. F.; Morrell, J. L.; Barrett, J. W.; Rogers, R. F.; Hafeji, M.; Bibby, L. I.; Gower, E.; Morrison, V. S.; Man, Y.; Roper, J. A.; Luckett, J. C.; Borthwick, L. A.; Barksby, B. S.; Burgoyne, R. A.; Barnes, R.; Le, J.; Flint, D. J.; Pyne, S.; Habgood, A.; Organ, L. A.; Joseph, C.; Edwards-Pritchard, R. C.; Maher, T. M.; Fisher, A. J.; Gudmann, N. S.; Leeming, D. J.; Chambers, R. C.; Lukey, P. T.; Marshall, R. P.; Macdonald, S. J. F.; Jenkins, R. G.; Slack, R. J. Translational Pharmacology of An Inhaled Small Molecule $\alpha_v\beta_6$ Integrin Inhibitor for Idiopathic Pulmonary Fibrosis. *Nat. Commun.* **2020**, *11* (1), 1–14.
(**26**) Hatley, R. J. D.; Macdonald, S. J. F.; Slack, R. J.; Le, J.; Ludbrook, S. B.; Lukey, P. T. An Av-RGD Integrin Inhibitor Toolbox: Drug Discovery Insight, Challenges and Opportunities. *Angew. Chem. Int. Ed.* **2018**, *57*, 3298–3321.
(**27**) Alipour, M.; Baneshi, M.; Hosseinkhani, S.; Mahmoudi, R.; Jabari Arabzadeh, A.; Akrami, M.; Mehrzad, J.; Bardania, H. Recent Progress in Biomedical Applications of RGD-Based Ligand: From Precise Cancer Theranostics to Biomaterial Engineering: A Systematic Review. *J. Biomed. Mater. Res. - Part A* **2020**, *108*, 839–850.
(**28**) Srinivasarao, M.; Low, P. S. Ligand-Targeted Drug Delivery. *Chem. Rev.* **2017**, *117*, 12133–12164.
(**29**) Srinivasarao, M.; Galliford, C. V.; Low, P. S. Principles in the Design of Ligand-Targeted Cancer Therapeutics and Imaging Agents. *Nat. Rev. Drug Discovery* **2015**, *14*, 203–219.
(**30**) Chari, R. V. J.; Miller, M. L.; Widdison, W. C. Antibody-Drug Conjugates: An Emerging Concept in Cancer Therapy. *Angew. Chem. Int. Ed.* **2014**, *53*, 3796–3827.
(**31**) Zhuang, C.; Guan, X.; Ma, H.; Cong, H.; Zhang, W.; Miao, Z. Small Molecule-Drug Conjugates: A Novel Strategy for Cancer-Targeted Treatment. *Eur. J. Med. Chem.* **2019**, *163*, 883–895.
(**32**) Dal Corso, A. Targeted Small-Molecule Conjugates: The Future Is Now. *ChemBioChem* **2020**, 1–3.
(**33**) Chittasupho, C. Multivalent Ligand: Design Principle for Targeted Therapeutic Delivery Approach. *Therapeutic Delivery* **2012**, *3*, 1171–1187.
(**34**) Dal Corso, A.; Pignataro, L.; Belvisi, L.; Gennari, C. Innovative Linker Strategies for Tumor-Targeted Drug Conjugates. *Chem. Eur. J.* **2019**, *25*, 14740–14757.
(**35**) Arosio, D.; Casagrande, C. Advancement in Integrin Facilitated Drug Delivery. *Adv. Drug Deliv. Rev.* **2016**, *97*, 111–143.
(**36**) Moreno-Layseca, P.; Icha, J.; Hamidi, H.; Ivaska, J. Integrin Trafficking in Cells and Tissues. *Nat. Cell Biol.* **2019**, *21*, 122–132.
(**37**) He, R.; Finan, B.; Mayer, J. P.; DiMarchi, R. D. Peptide Conjugates with Small Molecules Designed to Enhance Efficacy and Safety. *Molecules* **2019**, *24*, 1855.
(**38**) Gottschalk, K.-E.; Kessler, H. The Structures of Integrins and Integrin–Ligand Complexes: Implications for Drug Design and Signal Transduction. *Angew. Chemie Int. Ed.* **2002**, *41*, 3767–3774.
(**39**) Hein, C. D.; Liu, X.-M.; Wang, D. Click Chemistry, A Powerful Tool for Pharmaceutical Sciences. *Pharm. Res.* **2008**, *25*, 2216–2230.
(**40**) Massaguer, A.; González-Cantó, A.; Escribano, E.; Barrabés, S.; Artigas, G.; Moreno, V.; Marchán, V. Integrin-Targeted Delivery into Cancer Cells of a Pt(IV) pro-Drug Through Conjugation to RGD-Containing Peptides. *Dalton Trans.* **2015**, *44*, 202–212.
(**41**) Pilkington-Miksa, M.; Arosio, D.; Battistini, L.; Belvisi, L.; De Matteo, M.; Vasile, F.; Burreddu, P.; Carta, P.; Rassu, G.; Perego, P.; Carenini, N.; Zunino, F.; De Cesare, M.; Castiglioni, V.; Scanziani, E.; Scolastico, C.; Casiraghi, G.; Zanardi, F.; Manzoni, L. Design, Synthesis, and Biological Evaluation

of Novel cRGD–Paclitaxel Conjugates for Integrin-Assisted Drug Delivery. *Bioconjug. Chem.* **2012**, *23*, 1610–1622.
(**42**) Bianchi, A.; Arosio, D.; Perego, P.; De Cesare, M.; Carenini, N.; Zaffaroni, N.; De Matteo, M.; Manzoni, L. Design, Synthesis and Biological Evaluation of Novel Dimeric and Tetrameric CRGD-Paclitaxel Conjugates for Integrin-Assisted Drug Delivery. *Org. Biomol. Chem.* **2015**, *13*, 7530–7541.
(**43**) Piras, M.; Andriu, A.; Testa, A.; Wienecke, P.; Fleming, I. N.; Zanda, M. Design and Synthesis of an RGD Peptidomimetic-Paclitaxel Conjugate Targeting $\alpha_V\beta_3$ Integrin for Tumour-Directed Drug Delivery. *Synlett* **2017**, *28*, 2769–2776.
(**44**) Bianchini, F.; Portioli, E.; Ferlenghi, F.; Vacondio, F.; Andreucci, E.; Biagioni, A.; Ruzzolini, J.; Peppicelli, S.; Lulli, M.; Calorini, L.; Battistini, L.; Zanardi, F.; Sartori, A. Cell-Targeted c(AmpRGD)-Sunitinib Molecular Conjugates Impair Tumor Growth of Melanoma. *Cancer Lett.* **2019**, *446*, 25–37.
(**45**) Sartori, A.; Corno, C.; De Cesare, M.; Scanziani, E.; Minoli, L.; Battistini, L.; Zanardi, F.; Perego, P. Efficacy of a Selective Binder of $\alpha_V\beta_3$ Integrin Linked to the Tyrosine Kinase Inhibitor Sunitinib in Ovarian Carcinoma Preclinical Models. *Cancers* **2019**, *11*, 531.
(**46**) Sartori, A.; Portioli, E.; Battistini, L.; Calorini, L.; Pupi, A.; Vacondio, F.; Arosio, D.; Bianchini, F.; Zanardi, F. Synthesis of Novel c(AmpRGD)–Sunitinib Dual Conjugates as Molecular Tools Targeting the $\alpha_V\beta_3$ Integrin/VEGFR2 Couple and Impairing Tumor-Associated Angiogenesis. *J. Med. Chem.* **2017**, *60*, 248–262.
(**47**) Gilad, Y.; Noy, E.; Senderowitz, H.; Albeck, A.; Firer, M. A.; Gellerman, G. Synthesis, Biological Studies and Molecular Dynamics of New Anticancer RGD-Based Peptide Conjugates for Targeted Drug Delivery. *Bioorg. Med. Chem.* **2016**, *24*, 294–303.
(**48**) Gilad, Y.; Waintraub, S.; Albeck, A.; Gellerman, G. Synthesis of Novel Protected Nα(ω-Drug) Amino Acid Building Units for Facile Preparation of Anticancer Drug-Conjugates. *Int. J. Pept. Res. Ther.* **2016**, *22*, 301–316.
(**49**) Gilad, Y.; Noy, E.; Senderowitz, H.; Albeck, A.; Firer, M. A.; Gellerman, G. Dual-Drug RGD Conjugates Provide Enhanced Cytotoxicity to Melanoma and Non-Small Lung Cancer Cells. *Biopolymers* **2016**, *106*, 160–171.
(**50**) Yu, H.; Mei, S.; Zhao, L.; Zhao, M.; Wang, Y.; Zhu, H.; Wang, Y.; Wu, J.; Cui, C.; Xu, W.; Peng, S. RGD-Peptides Modifying Dexamethasone: To Enhance the Anti-Inflammatory Efficacy and Limit the Risk of Osteoporosis. *MedChemComm* **2015**, *6*, 1345–1351.
(**51**) López Rivas, P.; Müller, C.; Breunig, C.; Hechler, T.; Pahl, A.; Arosio, D.; Belvisi, L.; Pignataro, L.; Dal Corso, A.; Gennari, C. β-Glucuronidase Triggers Extracellular MMAE Release from An Integrin-Targeted Conjugate. *Org. Biomol. Chem.* **2019**, *17*, 4705–4710.
(**52**) Borbély, A.; Thoreau, F.; Figueras, E.; Kadri, M.; Coll, J. L.; Boturyn, D.; Sewald, N. Synthesis and Biological Characterization of Monomeric and Tetrameric RGD-Cryptophycin Conjugates. *Chem. Eur. J.* **2020**, *26*, 2602–2605.

Chapter 2. Targeting $\alpha_V\beta_6$ integrin

The work described in this Chapter was published in the following article:
Bugatti, K.; Bruno, A.; Arosio, D.; Sartori, A.; Curti, C.; Augustijn, L.; Zanardi, F.; Battistini, L. Shifting Towards $\alpha_V\beta_6$ Integrin Ligands Using Novel Aminoproline-Based Cyclic Peptidomimetics. *Chem. Eur. J.* **2020**, *26*, 13468–13475.

2.1. Introduction

2.1.1. $\alpha_V\beta_6$ integrin

Among the RGD-recognizing integrins, involved in the onset and progression of several pathologies, $\alpha_V\beta_6$ has emerged as an ideal pharmacological target in recent past years.[1] This receptor is exclusively expressed in epithelial cells; indeed, it is not expressed (or it is poorly expressed) in healthy adult epithelia, while it is overexpressed during embryogenesis and wound healing. The $\alpha_V\beta_6$ integrin recognizes all its endogenous ligands in the ECM (i.e. fibronectin, osteopontin, tenascin-C, and vitronectin) by the RGD-sequence. In addition, this integrin binds the Latency Associated Peptide (LAP) of the cytokine TGFβ (Transforming Growth Factor β) leading to cytokine activation.

The research of novel integrin ligands with high binding affinity and selectivity toward a unique integrin subtype are the key pharmacological tools for an unambiguous understanding of the precise biological role and cross-talk among different integrins. In particular, finding novel compounds which can efficiently distinguish between $\alpha_V\beta_6$ and $\alpha_V\beta_3$ is an ambitious goal, since these receptors possess the same α_V domain and are expressed on different tissues.

In recent years, many disease states have been associated with $\alpha_V\beta_6$ overexpression, such as different epithelial tumors, metastasis and fibrotic pathologies.[2,3] Moreover, this receptor plays an essential role in mediating cell entry of the Food-and-Mouth Disease Virus (FMDV);[2] thanks to the interaction between $\alpha_V\beta_6$ and the capsid proteins of this virus, the first $\alpha_V\beta_6$ ligand was indeed identified and characterized.[4]

The most important biological role attributed to $\alpha_V\beta_6$ integrin is the activation of the cytokine TGFβ, and this process has implications in both physiological and pathological contexts. In fact, TGFβ mediates the Epithelial-to-Mesenchymal Transition (EMT) of type I and II, which are important for embryogenesis and wound healing in physiological conditions; on the other hand, TGFβ mediates EMT of type III, crucial for tumor progression and metastasization.[5,6]

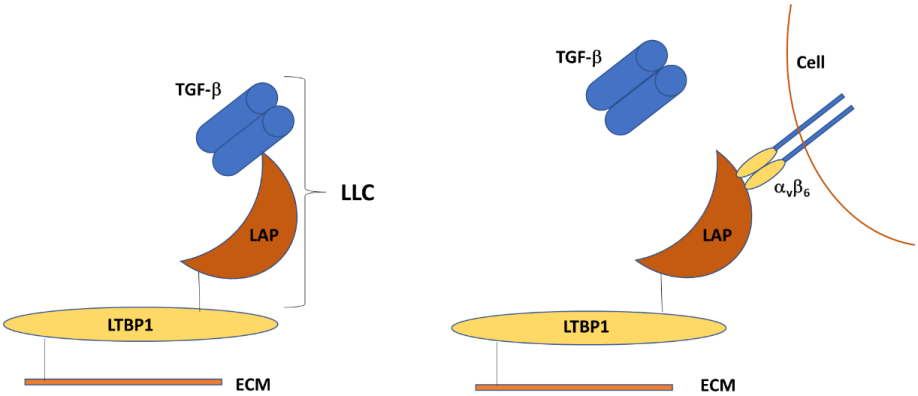

Figure 1. *Structure of the pro-TGFβ complex and role of $\alpha_V\beta_6$ integrin in its activation. Adapted from Ref. 2.*

TGFβ is a potent inhibitor of the proliferation of epithelial, endothelial and hematopoietic cells; it has been described in three different isoforms, TGFβ1, TGFβ2 and TGFβ3. These isoforms are synthesized starting from pro-TGFβ, a complex constituted by the TGFβ covalently bound to a protein, called Latency Associated Peptide (LAP).[2] Pro-TGFβ is partially activated by proteases in the intracellular microenvironment, but it still binds LAP in a non-covalent manner, creating a new complex called Small Latency Complex (SLC). In addition, the SLC forms a disulphide bond with the

Latency TGFβ Binding Proteins (LTBPs), creating the Large Latency Complex (LLC). The LLC anchors the ECM through the LTBPs, and this guarantees the presence of a reservoir of TGFβ in the ECM, which can be activated when it is necessary (Figure 1).

The $\alpha_V\beta_6$ integrin has a crucial role in the TGFβ activation by two alternative yet complementary mechanisms, based on the different "rigidity" of the ECM. On one hand, $\alpha_V\beta_6$ binds the RGD-sequence of LAP in the ECM and the actin filaments in the intracellular environment, exerting a large mechanical force; this causes different conformational changes in LLC, ultimately leading to the release of the TGFβ. On the other hand, if the ECM is not enough rigid, metalloproteases (such as MMP-9 and MMP-2) can assist $\alpha_V\beta_6$ during the proteolytic cleavage.

The free TGFβ binds the receptor TGFβRIII, which subsequently recruits TGFβRII, creating an active receptor complex. This novel unit starts the phosphorylation cascade involving SMAD2 and SMAD3, which ends up with SMAD4 nucleus translocation and activation of genes promoting cell differentiation, Epithelial-to-Mesenchymal Transition (EMT), migration, and apoptosis. This signalling mechanism is involved in many physiological and pathological processes (such as tumor progression and fibrosis), rendering $\alpha_V\beta_6$ a useful biomarker of such diseased states, as well as an interesting target for the development of new pharmacological agents.

2.1.2. Epithelial-To-Mesenchymal Transition (EMT)

The Epithelial-to-Mesenchymal Transition (EMT) is a physiological process acting during embryogenesis, gastrulation and wound healing, but it can also be a pathological phenomenon which leads to tumor progression, metastasis spread and fibrotic states.[7] The physiological EMT is defined as the loss of the epithelial characteristic by cells (polarity, adhesion, basal protein synthesis, …) followed by the acquisition of mesenchymal properties (migration, ECM proteins and integrin interactions, …). Three different types of EMTs have been described (EMT-I, EMT-II, EMT-III), the first two being associated with physiological processes, and the latter being related to pathological conditions.[8] As mentioned before, TGFβ plays an important role for the promotion of EMT. When this cytokine binds its receptor, the phosphorylation of SMAD2/3 is triggered and, once activated, they bind SMAD4. This new complex goes in the nucleus and promotes the activation of mesenchymal genes and the suppression of the epithelial ones. In addition, TGFβ can activate other factors, such as Ras, MAPK, PI3, AKT and Rho, stimulating cell proliferation by a non-canonical SMAD-independent signalling pathway (Figure 2).

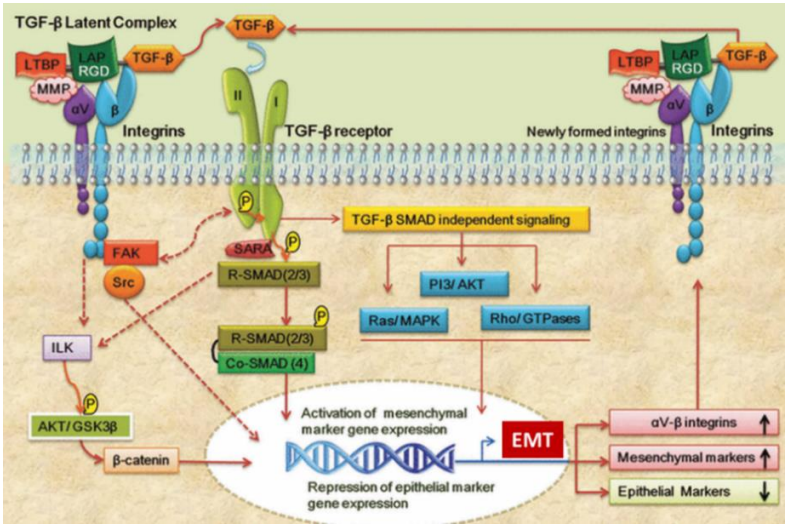

Figure 2. *Role of TGFβ and $\alpha_V\beta_6$ integrin in EMT. Adapted from Ref. 8.*

As TGFβ has a crucial role in EMT, also $\alpha_V\beta_6$ integrin is a key factor during this transition, since it is overexpressed in EMT of type II and III. In particular, both the integrin and the cytokine sustain EMT with a self-amplification process: $\alpha_V\beta_6$ integrin activates TGFβ, which starts an intracellular pathway, whose ending is the promotion of EMT-sustaining gene activation, including the $\alpha_V\beta_6$ expression. This fact causes a vicious circle which sustains and aggravates the Epithelial-to-Mesenchymal Transition (Figure 2).

In addition, all integrins of the α_V family can activate certain types of metalloproteases (MMPs), a group of Zinc-dependent endopeptidases which contribute to ECM degradation and, consequently, to cell proliferation and migration. For instance, MMP2 and MMP9 cleave fibronectin, producing a 120kDa fragment; it has been demonstrated that $\alpha_V\beta_6$ overexpressing cells show high level of these fibronectin fragments.[2] In fact, high level of both MMP2/9 and $\alpha_V\beta_6$ create a positive feedback which promotes cancer progression and metastasization. Moreover, MMPs can participate in the TGFβ activation, as described in the previous paragraph.

To conclude, EMT is a complicated and delicate process in which many factors are involved, and TFG-β plays a central role. However, its pleiotropic distribution and the associated multiple functions make its direct inhibition very challenging; on the contrary, its activator, the $\alpha_V\beta_6$ integrin, has good chances to be targeted by a pharmaceutical agent. For this reason, research toward the synthesis of new ligands targeting $\alpha_V\beta_6$ is highly pursued, in order to find new drugs for the treatment of different pathologies, including aggressive epithelial tumors and pulmonary or liver fibrosis.

2.1.3. $\alpha_V\beta_6$ integrin ligands: state of the art

The search for exogenous $\alpha_V\beta_6$ integrin ligands started with the study on the FMDV, a very contagious infectious virus of the *Picornaviridae* family, particularly dangerous for cloven-hoofed animals; it is not lethal for adults, but it induces extremely high mortality in young exemplars. Integrin $\alpha_V\beta_6$ has a crucial role in mediating the virus entry into cells and consequently the progression of the infection. For instance, it has been shown[9] that $\alpha_V\beta_6$ is constitutively expressed on the surface of cells at sites where infectious lesions occur during natural infection (such as on tracheal sheep and tonsillar cattle epithelia), but not at sites where lesions are not normally formed.

The interactions between $\alpha_V\beta_6$ and the FMDV capsid proteins were used as the starting point for the development of exogenous $\alpha_V\beta_6$ ligands. In fact, Hausner et al. synthesized in 2007[10] the first $\alpha_V\beta_6$ peptide ligand A20FMDV2 (NAVPNLRGDLQVLAQKVART) and they demonstrated its antagonist activity. This was a pioneering work of utmost relevance not only due to the high receptor affinity of this peptide (IC_{50} 3.0 nM, calculated by competitive binding ELISA assay),[10] but also because this compound binds selectively $\alpha_V\beta_6$ and not the other RGD-recognizing integrins. Kraft et al.[11] had already demonstrated via high-throughput screening studies that sequences like RGDLQVL were extremely important for the affinity toward $\alpha_V\beta_6$. In this study, all peptides showing high $\alpha_V\beta_6$ selectivity possess the amino acid sequence DLXXL (where X are variable amino acids); thus, this domain was already identified, but its role in the receptor recognition was initially unknown. It was the research group of Springer et al.[8] in 2014 that clarified via X-ray crystallography and affinity studies how the RGDLXXL sequence of pro-TGFβ3 interacts with $\alpha_V\beta_6$. They showed that the sequence GRGDLGRL of the cytokine is the one with the best affinity toward the receptor (K_d 8.5 nM) and they demonstrated that the aspartic residue of this peptide (Asp243) interacts with the MIDAS-Mg^{2+} of the integrin, while establishing hydrogen bonds with Asn218 and Ala126 (Figure 3). Moreover, they showed that the guanidine residue of arginine (Arg241) makes hydrogen bonds

with Asp218 in the β-propeller region of α subunit, and the remaining arginine residue interacts with Thr221 in the β_6 subunit; this is a crucial element for the selectivity toward $\alpha_V\beta_6$, because other integrins (such as β_5 and β_3) cannot establish this interaction, as they have an Ala residue at position 221.

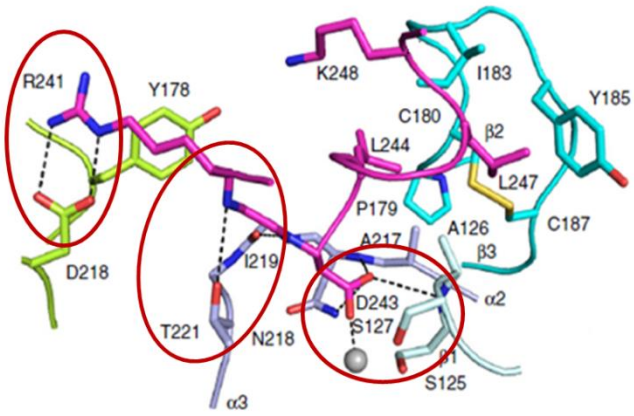

Figure 3. *Interactions between pro-TGFβ3 (depicted in purple) and $\alpha_V\beta_6$. Adapted from Ref. 12.*

Given the potential of $\alpha_V\beta_6$ integrin as an interesting pharmacological target, different research groups started to synthesize different peptide, peptidomimetic and non-peptide molecules, and some of them have reached the step of clinical studies. For instance, the longstanding experience of Kessler's group in the field of integrin ligands drove them in developing two novel cyclic peptidomimetic compounds, the antagonist nonapeptide c[FRGDLAFp(NMe)K] (**I**, Figure 4, IC_{50} $\alpha_V\beta_6$ 0.26 nM, solid phase binding assay)[13] and the more recent c(RGD-Chg-E)-$CONH_2$ (**II**, Figure 4, IC_{50} $\alpha_V\beta_6$ 1.6 nM, competitive ELISA assay).[14] Both these compounds have the RGD sequence in their pharmacophore portion; in particular, this three-amino acid sequence is flanked by apolar and/or hydrophobic residues. The importance of this domain is underlined by the high potency and selectivity of these two molecules. Moreover, Kessler's group also developed a [^{68}Ga]-radiolabelled version of the nonapeptide c[FRGDLAFp(NMe)K] called *Avebehexin,* that was tested as PET imaging agent in models of severe combined immunodeficiency mice bearing human lung adenocarcinoma xenografts.[15]

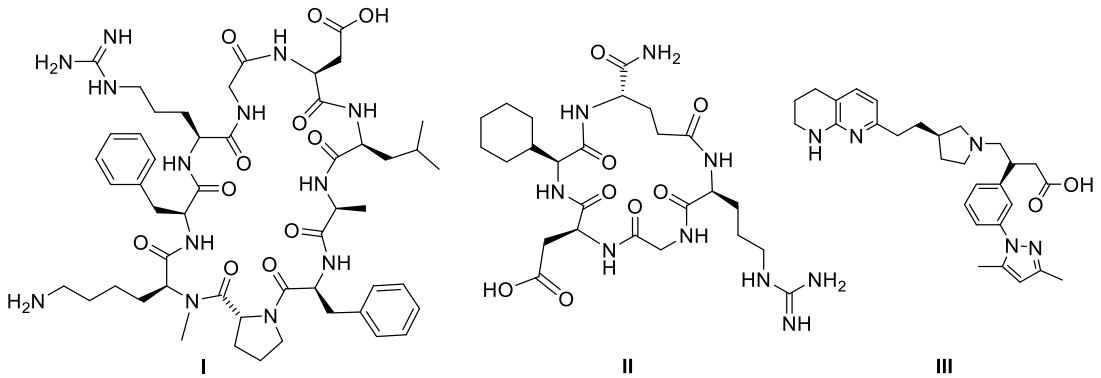

Figure 4. *Structures of the $\alpha_V\beta_6$ integrin ligands c[FRGDLAFp(NMe)K] (**I**), c(RGD-Chg-E)-$CONH_2$ (**II**) and GSK compound (**III**).*

In recent years, a non-peptide small-molecule compound developed by GSK (**III**, Figure 4) has successfully reached the phase II clinical trial for the treatment of Idiopathic Pulmonary Fibrosis.[16,17] This compound has a different structure in comparison to the ones shown before, but it still possesses important pharmacophore elements, such as a carboxylic acid residue (mimicking the Aspartic acid) and a guanidine-mimetic portion, represented by a tetrahydro-naphthyridine group.

Despite other $\alpha_V\beta_6$ integrin ligands have been described so far,[18] research efforts in this field are still required, as wider structural diversification among ligands may lead to renewed and improved physico-chemical properties playing crucial roles toward truly druggable active substances.

2.2. Aim of the project

Based on this background, the synthesis of novel $\alpha_V\beta_6$ integrin ligands represents an ambitious goal in the field of bio-medical research, as this receptor is implicated in several complex pathologies with still unmet solutions. For this reason, the aim of the following project is the design and synthesis of new potent and selective aminoproline-based small molecule peptidomimetics targeting $\alpha_V\beta_6$ integrin.

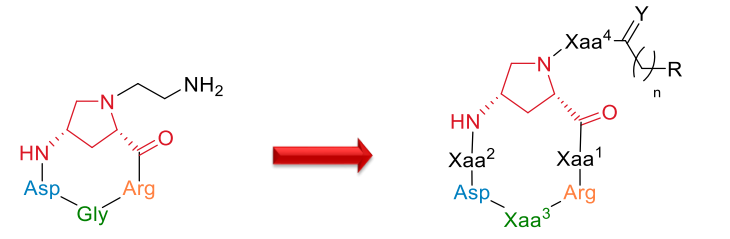

c[Amp($C_2H_4NH_2$)RGD]

IC_{50} ($\alpha_V\beta_3$): 6.1 nM[a]
IC_{50} ($\alpha_V\beta_5$): 315 nM[a]
IC_{50} ($\alpha_5\beta_1$): 151.6 nM[b]
IC_{50} ($\alpha_V\beta_6$): 146.1 nM[c]

IV

Xaa^1 = none, Phe, DiPhe, Leu
Xaa^2 = none, Phe, Leu
Xaa^3 = Gly, Leu
Xaa^4 = none, Phe
Y = O; H,H; R = N_3, NH_2; n = 3,5

Figure 5. *Structure and affinity of known cyclopentapeptide c[Amp($C_2H_4NH_2$)RGD] and general structure of the designed compounds of type* ***IV*** *in this study. [a]Solid phase binding assay, ligand displacement.*[19] *[b]Solid phase binding assay, ligand displacement.*[20] *[c]As determined during the present work.*

In particular, starting from the known c[Amp($C_2H_4NH_2$)RGD, whose ligand properties have been widely investigated,[19,20] the newly designed molecules have been planned to possess three different points of variability concerning the *size of the peptide ring* (cyclotetra-, cyclopenta-, and cyclohexapeptides), the *nature of the amino acid sequence* within the cycle (by introducing phenylalanine, leucine and β,β-diphenylalanine units flanking the RGD sequence), and the *nature of the N^{α}-side chain* (by modifying the length and nature of the amine/amide linkage and evaluating the influence of an additional bulky amino acid) (Figure 5).

The synthesis plan entails the use of Solid Phase Peptide Synthesis and in-solution cyclization procedures, while purification and characterization steps are ensured by HPLC analysis and NMR/HRMS studies.

All the final compounds are intended to be tested by the solid-phase receptor binding assay on isolated, human $\alpha_V\beta_6$ integrins, and the most potent representative compounds are planned to be assayed also toward $\alpha_V\beta_3$ integrin for evaluating the $\alpha_V\beta_6$ *vs* $\alpha_V\beta_3$ selectivity. In addition, for the most promising candidates, rationalization of in vitro activities is proposed, via docking simulation experiments. The results taken together will drive us to the development of new candidates potentially useful for the treatment and/or diagnosis of diverse $\alpha_V\beta_6$ integrin-related diseases.

2.3. Results and discussion

2.3.1. Design of novel $\alpha_V\beta_6$ integrin ligands

The rational design of new Amp-based (Aminoproline-based) $\alpha_V\beta_6$ integrin ligands was performed based on information available in the literature: first, the X-ray structure (PDB: 4UM9) of $\alpha_V\beta_6$ integrin headpiece in complex with the pro-TGFβ3 undecapeptide[1212] and, second, the X-ray crystal structure (PDB: 4MMY) of $\alpha_V\beta_3$ integrin co-crystallized with the high-affinity form of fibronectin (wtFN10).[21] As shown in Figure 6a, pro-TGFβ3 establishes key interactions with $\alpha_V\beta_6$ manly through the RGD domain; in particular, the aspartic residue (D243) within the RGD motif chelates the Mg^{2+} ion in the MIDAS region (subβ_6) and the arginine residue (R241) binds to α_V-Asp218 through a bidentate H-bonding interaction.

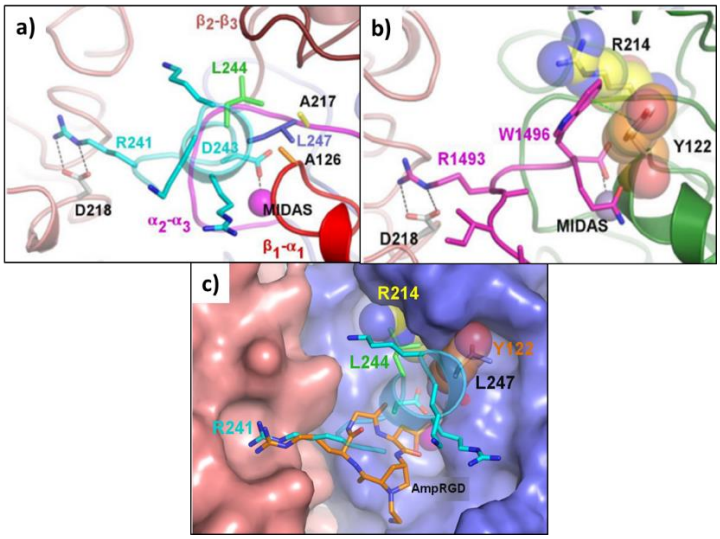

***Figure 6. a**) Binding mode of pro-TGFβ3(cyan sticks and cartoon) into the α_V (pink cartoon)-β_6 (blue cartoon, unless otherwise specified) receptor. The Leu244 and Leu247 residues of pro-TGFβ3 (green and blue sticks) interact with Ala217 (yellow sticks) and Ala126 (orange sticks) within β_6, respectively. The β_6 loops, β_1-α_1, β_2-β_3 and α_2-α_3, accounting for pro-TGFβ3 selectivity, are depicted in red, brown, and purple cartoons, respectively. **b**) Binding mode of wtFN10 (purple sticks and cartoon) into the $\alpha_V\beta_3$ (pink and green cartoons, unless otherwise specified) receptor. The Arg214 and Tyr122 residues within β_3 are highlighted with yellow and orange sticks and spheres, respectively. **c**) The $\alpha_V\beta_6$ receptor is depicted as pink (subα_V) and blue (subβ_6) surfaces, while the pro-TGFβ3 is depicted as reported in **a**. The Arg214 and Tyr122 residues, hampering the accommodation of the pro-TGFβ3 LXXL/X motif into the $\alpha_V\beta_3$ receptor, are highlighted with yellow and orange sticks and spheres. c[Amp($C_2H_4NH_2$)RGD] is depicted as orange sticks. Adapted from Ref. 22.*

In addition, the key tetrapeptide LXXL/X motif of TGFβ assumes amphipathic α-helix characteristics and protrudes Leu244 into a hydrophobic pocket of subβ_6 delimited by Ala217, while Leu247 of the cytokine interacts with Ala126 further burying the Leu244 residue. Particularly, in this kind of conformation, the LXXL/X motif interacts with specific loops of subβ_6 (β_1- α_1, β_2-β_3 and α_2- α_3 loops): this could explain why the pro-TGFβ3 achieves high specificity toward $\alpha_V\beta_6$ integrin.

Concerning this high specificity, other considerations can be done moving to the $\alpha_V\beta_3$ integrin receptor, since relevant amino acidic differences emerge when comparing the corresponding α_2-α_3 loops (Figure 6a,b). In fact, the Ala126 of the β_1-α_1 loop and the Ala217 of α_2-α_3 loop (subβ_6) are mutated into bulkier Tyr122 and Arg214 residues (subβ_3), rendering the LXXL/X interaction of the ligand with β_3 not as favourite as for β_6.

Based on this background and the previous experience of our research group on Amp-RGD compounds, docking studies starting from the hit compound *c*[Amp($C_2H_4NH_2$)RGD] were performed, in order to switch potency and selectivity from $\alpha_v\beta_3$ to $\alpha_v\beta_6$ integrin. Figure 6c shows the binding mode of *c*[Amp($C_2H_4NH_2$)RGD] into the $\alpha_v\beta_6$ binding site, revealing that the peptide RGD motif establishes the same previously described key interactions observed for pro-TGFβ3. However, due to its shorter sequence and the absence of the LXXL/X motif, *c*[Amp($C_2H_4NH_2$)RGD] is not able to adequately fill the hydrophobic pockets within the β_1-α_1 and α_2-α_3 loops, thus explaining the low selectivity index toward the two receptors (SI = $IC_{50(\alpha V\beta 3)}/IC_{50(\alpha V\beta 6)}$ = 0.04).

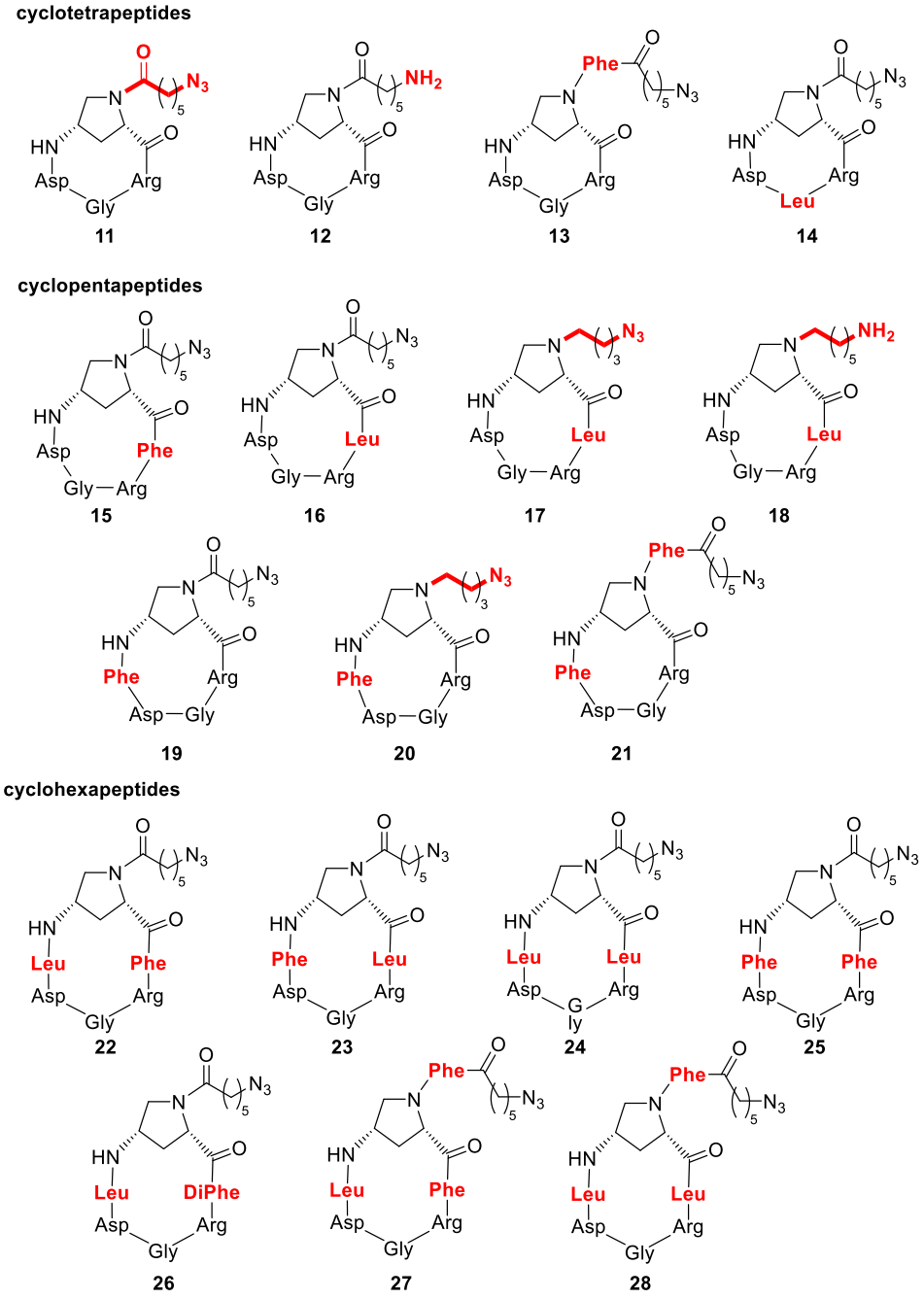

Figure 7. *Molecular structure of the eighteen newly designed and synthesized cyclopeptidomimetics* ***11-28*** *(DiPhe = β-phenyl-Phe; the main structural differences from the starting reference compound c[Amp($C_2H_4NH_2$)RGD] are highlighted in red).*

These observations were used to rationally modify the structure of the cyclic peptide *c*[Amp($C_2H_4NH_2$)RGD] and, as suggested by the proposed binding mode, the following strategy was advanced. First, the exploration of the cyclopeptide size was considered, moving from RGD-containing Amp-based tetrapeptides to more expanded penta- and hexa-cyclic rings, to evaluate whether the overall constrained conformation of the cyclopeptides, which is suitable for the interaction within the integrin binding site, is preserved upon ring enlargement. As a second intervention, the introduction of apolar/bulky side-chain amino acids flanking the RGD sequence was evaluated, to mimic the favorable interaction between the LXXL/X motif and subβ_6. As a third point of intervention, the side chain at the N$^{\alpha}$-aminoproline was modified, to investigate the influence of this region in reaching high $\alpha_V\beta_6$ affinity and selectivity, while concomitantly preserving useful anchoring points in this handle for possible further covalent conjugation.

With these aims in mind, a library of eighteen cyclopeptidomimetics (**11-28**, Figure 7) was designed, whose synthesis is described in the following paragraph.

2.3.2. Synthesis of the $\alpha_V\beta_6$ ligands

The synthesis of the library of new cyclic peptidomimetic compounds started with the in-solution preparation of the different aminoproline (Amp) building blocks (**4**, **6**, **8**, **10**), as shown in Scheme 1.

Scheme 1. *Synthesis of decorated 4-aminoproline (Amp) scaffolds **2**, **4**, **6**, **8** and **10**.*[a]

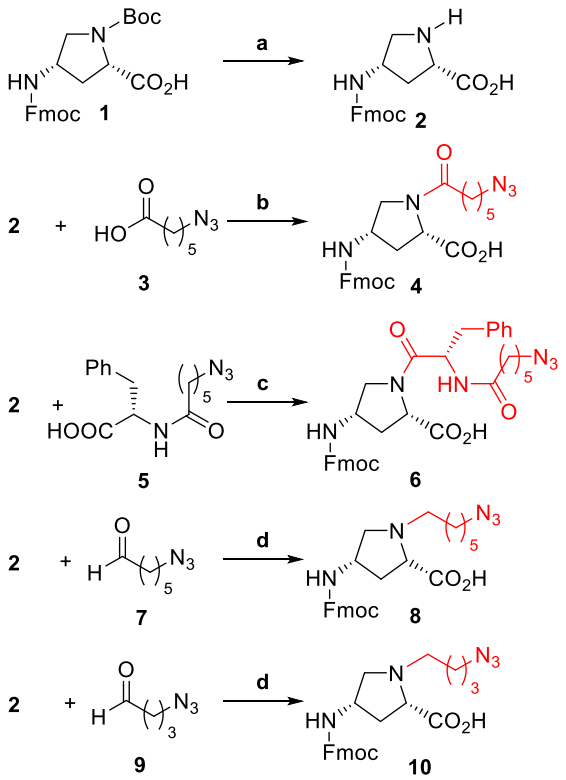

[a]Reagents and conditions: **a**) TFA: DCM, 0-25 °C, 1h, quant yield; **b**) HATU, DIPEA, DMF, rt, 6h, 76% yield; **c**) HATU, HOAt, DIPEA, DMF, rt, 6h, 66% yield; **d**) $NaBH(OAc)_3$, DCE, rt, 63-95% yield.

The commercially available N^{α},N^{γ}-bis-protected *cis*-4-amino-L-proline **1** was chemoselectively deprotected at the N^{α} position under acidic conditions, yielding the Fmoc-Amp nucleus **2**, which was differently functionalized using either acylation or alkylation reaction steps. For the synthesis of the acylated Amp nucleus **4**, compound **2** was treated with HATU, 6-azidohexanoic acid, and

DIPEA, while the use of HOAt was avoided, as this reagent renders the following purification step very challenging. The formation of the undesired dimeric-aminoproline byproduct was successfully avoided by separately activating the 6-azidohexanoic acid **3** with HATU and DIPEA, and the activated acid was following added to the solution of Fmoc-Amp nucleus **2**. To access scaffold **6**, the synthesis of compound **5** was first necessary; thus, 6-azidohexanoic acid was treated with HATU/HOAt/DIPEA and *O*-*t*Bu-Phenylalanine (not shown) and the resulting product was then deprotected on the acid residue to obtain carboxylic acid **5**. This compound was reacted with Amp nucleus **2** using almost the same conditions described for compound **4**, giving the building block **6** in 66% yield over 2 steps. The alkyl-substituted aminoprolines **8** and **10** were both synthesized via reductive amination starting from the common precursor **2** and using 6-azidohexanal (**7**) and 4-azidobutanal (**9**), respectively.

All the synthesized Amp scaffolds were used in the following Fmoc-based Solid Phase Peptide Synthesis (SPPS), the very useful technique often used for the synthesis of peptide/peptidomimetic compounds.

Scheme 2. *General procedure for the synthesis of the cyclic peptidomimetics in this work.*[a]

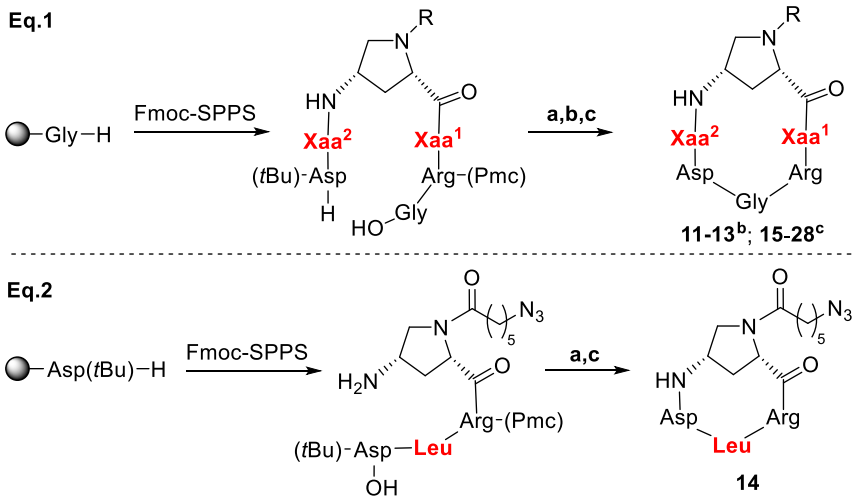

[a]Reagents and conditions: Fmoc-SPPS: (i) Fmoc-Arg(Pmc)-OH, Fmoc-Xaa1-OH (**Xaa^1** = none, Phe, DiPhe, Leu), Fmoc-Amp(R)-OH **4**, **6**, **8**, or **10**, Fmoc-**Xaa^2**-OH (Xaa^2 = none, Phe, Leu), Fmoc-Asp(*t*Bu)-OH; HATU, HOAt, collidine, DMF, rt, (ii) piperidine, DMF, rt, (iii) AcOH, TFE, DCM, rt, 40-97% yield ; **a**) HATU, HOAt, collidine, DCM:DMF (15:1), 1-3 mM, rt, 5-7h, 31-85% yield; **b**) for target compounds **12** and **18**: H_2, Pd/C, HCO_2H, EtOH, rt, 4-5h, 75% yield; **c**) TFA:TIS:H_2O (95:2.5:2.5), rt, 1h, 72-98% yield.
[b]**11**, c[Amp(HexN_3)Arg-Gly-Asp]; **12**, c[Amp(HexNH_2)Arg-Gly-Asp]; **13**, c[Amp(Phe-HexN_3) Arg-Gly-Asp];
[c]**15**, c[Amp(HexN_3)Phe-Arg-Gly-Asp]; 16, c[Amp(HexN_3)Leu-Arg-Gly-Asp]; **17**, c[Amp($C_4H_8N_3$) Leu-Arg-Gly-Asp]; **18**, c[Amp($C_6H_{12}NH_2$)Leu-Arg-Gly-Asp]; **19**, c[Amp(HexN_3)Arg-Gly-Asp-Phe]; **20**, c[Amp($C_4H_8N_3$)Arg-Gly-Asp-Phe]; **21**, c[Amp(Phe-HexN_3)Arg-Gly-Asp-Phe]; **22**, c[Amp(HexN_3)Phe-Arg-Gly-Asp-Leu]; **23**, c[Amp (HexN_3)Leu-Arg-Gly-Asp-Phe]; **24**, c[Amp(HexN_3)Leu-Arg-Gly-Asp-Leu]; **25**, c[Amp(HexN_3)Phe-Arg-Gly-Asp-Phe]; **26**, c[Amp(HexN_3)DiPhe-Arg-Gly-Asp-Leu]; **27**, c[Amp(Phe-HexN_3)Phe-Arg-Gly-Asp-Leu]; **28**, c[Amp (Phe-HexN_3)Leu-Arg-Gly-Asp-Leu].

According to a general procedure, the peptide molecules are synthesized "step-by-step" on a solid and insoluble resin as a support, and the amino acids are added (as Fmoc-protected at the amine group, in order to avoid side reactions) using suitable coupling reagents. Once the desired sequence is completed, the resin-attached molecules are cleaved using different conditions depending on the resin type. The advantages of this technique are *(i)* skipping the purification step after each coupling/deprotection step, and *(ii)* consequently getting faster reaction-rates and higher overall yields, also due to the excess of the used reagents. Completion of each deprotection/coupling reaction is usually checked by Kaiser Test,[23] which allows the qualitative and quantitative detection

of free amine residues by making the resin beads developing a blue colour (for details, see the experimental section).

All the linear peptides were synthesized using the Fmoc-based SPPS protocol starting from the preloaded H-Gly-2-ClTrt resin (Scheme 2, Eq.1), with the exception of the precursor of cyclopeptide **14** for which the H-Asp(*t*Bu)-2-ClTrt resin was used (Scheme 2, Eq.2). The chose of the resin and of the coupling reagents was made based on the matured experience of our research group in this peptide synthesis; in particular, using a H-Gly-2-ClTrt resin allows to perform the following cyclization step by activating a non-steric hindrance carboxylic acid, and, in turn, to improve the reaction yield. Each amino acid was sequentially added to the growing sequence, alternating coupling steps (HATU, HOAt and collidine) and Fmoc cleavage procedures (piperidine/DMF). In some cases, especially for compounds **19** and **20**, the yield of SPPS was unexpectedly low, probably due to the side-chain steric hindrance of the flanking amino acids, as in the case of phenylalanine flanking Pmc-protected arginine. For this reason, in these circumstances, double coupling and double deprotection procedures were performed in the SPPS sequence. At the end of each desired SPPS sequence, cleavage from the resin was performed using acidic conditions (AcOH:TFE:DCM), to obtain the respective linear peptides. Overall, yields for SPPS were variable, ranging from a rather poor 40% yield to excellent 97% yield.

The subsequent quite delicate in-solution cyclization reactions were carried out for all the synthesized peptides using diluted conditions (15:1 DCM/DMF solvent mixture, 1-3 mM) and HATU/HAOt as coupling reagents; the high dilution conditions were required to avoid competitive intermolecular side reactions. With this protocol, most of the cyclic peptidomimetics were obtained in discrete to high yields (45-88%), apart few exceptions (31-32%).

In two cases (compounds **12** and **18**), a N^{α} side chain modification was required after the in-solution cyclization; in particular, a catalytic hydrogenation reduction of the terminal azido groups was performed for both peptides in the same conditions (EtOH, H_2, Pd/C, catalytic formic acid). This step required careful selection of solvent (EtOH instead of MeOH) to avoid the methylation of the newly formed terminal amino group; moreover, catalytic amounts of formic acid were required to get complete conversion of the starting azido precursors.

Lastly, a deprotection step was performed under acidic conditions (TFA:TIS:H_2O) and each final compound was purified by semi-preparative HPLC, providing the library of eighteen cyclopeptides **11**-**28** as TFA salts in 72-98% yields.

2.3.3. Solid phase receptor binding assay

All the final cyclopeptidomimetics **11-28** were evaluated in vitro for their affinity toward $\alpha_V\beta_6$ integrin and, for the most promising candidates of the library, the affinity toward $\alpha_V\beta_3$ integrin was also assayed, to check their $\alpha_V\beta_6$ *vs* $\alpha_V\beta_3$ selectivity. Integrin affinity was estimated as the ability to compete with either biotinylated fibronectin (FN) for binding to isolated human $\alpha_V\beta_6$ receptors, or biotinylated vitronectin (VN) for $\alpha_V\beta_3$, according to previously reported procedures.[24] The binding affinity for each compound was compared to those observed for the reference compounds *c*[Amp($C_2H_4NH_2$)RGD] and the commercially available *c*(RGDfV).[25] The collected IC_{50} values toward $\alpha_V\beta_6$ integrin of all eighteen compounds **11**-**28** are comprised in the 4.6 nM-15.3 μM range and are shown in Table 1.

Based on this biological evaluation, a preliminary SAR study could be carried out. As expected, the substitution of Gly residue in the RGD sequence for Leu is extremely detrimental to the $\alpha_V\beta_6$ affinity (see **14** vs **11** and *c*[Amp($C_2H_4NH_2$)RGD]), underlying the important and "untouchable" role of this

pharmacophore residue. The introduction of an additional RGD-flanking amino acid in the sequence, such as Phe or Leu, has beneficial effects (**15-20** vs **11-13**), leading to middle-low nanomolar $IC_{50(\alpha V\beta 6)}$ values (**15-20**). This improvement maybe be associated to an increased backbone flexibility, which allows the cyclopentapeptides to reach a better accommodation into the $\alpha_V\beta_6$ binding site as compared to the cyclotetrapeptides, and to better fit the ancillary pockets of this integrin. Interestingly, the introduction of Phe or Leu residues has generally beneficial effects on the $\alpha_V\beta_6$ affinity, while it does not alter the selectivity (*c*[Amp($C_2H_4NH_2$)RGD] *vs* **15** and **16**).

When passing to further ring enlargement from cyclopentapeptides to cyclohexapeptides, improvement of the $\alpha_V\beta_6$ affinity was witnessed (**15-21** *vs* **22-28**), leading to compounds **22**, **24**, **26** and **28** with one-digit nanomolar IC_{50} values and appealing reversed selectivity profile ($\alpha_V\beta_6$ over $\alpha_V\beta_3$). In addition, concerning the hexapeptide series, other interesting considerations could be done: *(i)* compounds having Leu residue following the aspartic acid of RGD motif show the best affinity and selectivity profiles (**22**, **24**, **26**, **27** and **28**), while the introduction of bulkier and rigid residues at the same position is detrimental to the selectivity (**23**, **25**); *(ii)* new amino acid residues flanking the Arg unit (Phe, DiPhe and Leu) are tolerated with satisfying selectivity profile (**22**, **25**, **26** and **27**); *(ii)* the presence of a Phe residue in the side chain of Amp nucleus interestingly leads to a further improvement of selectivity (**28** *vs* **24**).

Table 1. Inhibition of Biotinylated FN and VN Binding to $\alpha_V\beta_6$ and $\alpha_V\beta_3$ receptors, respectively.

	Compound[a]	IC_{50} (nM) ± SD for $\alpha_V\beta_6$[b]	IC_{50} (nM) ± SD for $\alpha_V\beta_3$[c]	SI[d]
11	c[Amp($HexN_3$)Arg-Gly-Asp]	1156±442		
12	c[Amp($HexNH_2$)Arg-Gly-Asp]	929±81		
13	c[Amp(Phe-$HexN_3$)Arg-Gly-Asp]	940±137		
14	c[Amp($HexN_3$)Arg-Leu-Asp]	15300±6900		
15	c[Amp($HexN_3$)Phe-Arg-Gly-Asp]	83.5±10.4	1.8±0.1	0.02
16	c[Amp($HexN_3$)Leu-Arg-Gly-Asp]	84.0±1.2	1.9±0.6	0.02
17	c[Amp($C_4H_8N_3$)Leu-Arg-Gly-Asp]	85.7±0.6		
18	c[Amp($C_6H_{12}NH_2$)Leu-Arg-Gly-Asp]	45.7±8.9		
19	c[Amp($HexN_3$)Arg-Gly-Asp-Phe]	90.0±7.1	131.6±18.4	1.46
20	c[Amp($C_4H_8N_3$)Arg-Gly-Asp-Phe]	108.0±9.4		
21	c[Amp(Phe-$HexN_3$)Arg-Gly-Asp-Phe]	89.8±15.4		
22	c[Amp($HexN_3$)Phe-Arg-Gly-Asp-Leu]	4.6±2.7	2887±1135	628
23	c[Amp($HexN_3$)Leu-Arg-Gly-Asp-Phe]	90.6±5.6	29.8±20.5	0.33
24	c[Amp($HexN_3$)Leu-Arg-Gly-Asp-Leu]	8.3±0.4	2122±266	255
25	c[Amp($HexN_3$)Phe-Arg-Gly-Asp-Phe]	73.3±2.0	39.0±9.6	0.53
26	c[Amp($HexN_3$)DiPhe-Arg-Gly-Asp-Leu]	58.5±1.8	14230±5614	243
27	c[Amp(Phe-$HexN_3$)Phe-Arg-Gly-Asp-Leu]	14.4±3.3	1217±37	84.5
28	c[Amp(Phe-$HexN_3$)Leu-Arg-Gly-Asp-Leu]	8.5±0.6	4432±4738	521
	c[Amp($C_2H_4NH_2$)Arg-Gly-Asp]	146±40	6.1±1.6[c]	0.04
	c[Arg-Gly-Asp-phe-Val]	104.7±18.9[e]	3.2±1.3[c]	0.03

[a]Hex = hexanoyl, DiPhe = β-phenyl-Phe. [b]IC_{50} values were calculated as the concentration of compound required for 50% inhibition of biotinylated FN binding to human, isolated receptors. Each data point represents the average of triplicate wells; data analysis was carried out by nonlinear regression analysis using GraphPad Prism software. Each experiment was repeated in duplicate. [c]IC_{50} values were calculated as the concentration of compound required for 50% inhibition of biotinylated VN binding to human, isolated receptors according to a reported procedure.[19] [d]Selectivity Index: ratio between $IC_{50(\alpha V\beta 3)}$ and $IC_{50(\alpha V\beta 6)}$ (the higher the number, the higher the selectivity toward $\alpha_V\beta_6$). [e]*Ref.* 24.

Concerning this last point, modifications at the N^{α}-site (amide *vs* amine linkage, side chain length) caused a drop of $\alpha_V\beta_6$ affinity in the tetrapeptide series (*c*[Amp($C_2H_4NH_2$)RGD] *vs* **11**-**13**), but it seems to be tolerated in the enlarged cycles (e.g. **17**, **18**, **20**, **21**, **27** and **28**), without conditioning both affinity and selectivity. On these evidences, the N^{α}-side chain could be further exploited for future structural functionalization of these ligands.

In conclusion, the analysis of the biological data reveals important structural features instrumental to the design of effective and selective $\alpha_V\beta_6$ integrin ligands; for better understanding the binding pose of these ligands and their selectivity profiles, a docking study on hit compounds was performed, which will be described in the following paragraph.

2.3.4. Docking studies of hit compounds

Among the library of the eighteen synthesized compounds, the most promising representatives namely, compounds **22**, **24**, **26** and **28**, were selected for docking studies (in collaboration with Dr. Agostino Bruno, University of Parma) using the same protocol described for the reference peptide *c*[Amp($C_2H_4NH_2$)RGD], with the aim to rationalize the selectivity profile of such cyclopeptidomimetics.

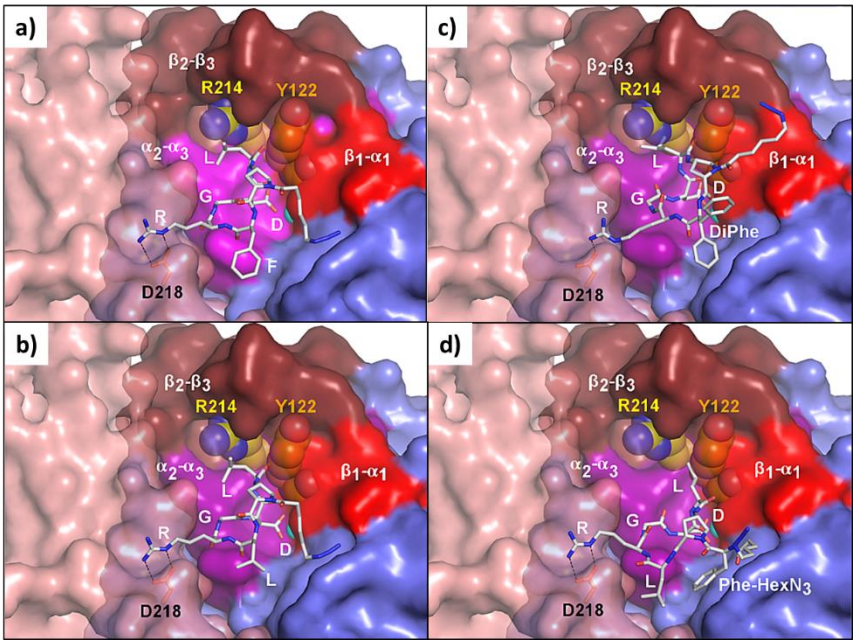

Figure 8. *Proposed binding modes for* ***22*** *(a),* ***24*** *(b),* ***26*** *(c) and* ***28*** *(d). Compounds are reported as white sticks and single-letter code, while the $\alpha_V\beta_6$ receptor is depicted as pink (sub α_V) and blue (sub β_6) surfaces (unless otherwise specified) and receptor residues are labelled using single-letter code. Arg214 and Tyr122 residues of $\alpha_V\beta_3$ are depicted as yellow and orange spheres. The dashed-black lines depict the interaction between the ligand Arg (R) guanidine group and Asp218. The β_6 loops, β_1-α_1, β_2-β_3 and α_2-α_3, accounting for $\alpha_V\beta_6$ receptor selectivity, are depicted in red, brown, and purple surfaces, respectively. Adapted from Ref. 22.*

Accordingly, Figure 8a shows compound **22** which well-accommodates into the $\alpha_V\beta_6$ binding site, exhibiting a binding pose which agrees with the selectivity profile shown in the *in vitro* assay. Similarly, to what observed for reference compound *c*[Amp($C_2H_4NH_2$)RGD], the guanidine group of Arg forms a bidentate H-bond interaction with Asp218 and the carboxylate of Asp coordinates Mg^{2+} ion in the MIDAS domain. In addition, the Phe residue fills a hydrophobic pocket at the α_V and β_6 interface and the Leu residue points to the accessible $\alpha_V\beta_6$ sub-pocket by the β_1-α_1, β_2-β_3 and α_2-α_3 loops, as observed for the natural ligand pro-TGFβ3 (Figure 6). On the other hand, this Leu residue

is not able to fix the same region in the $\alpha_V\beta_3$ receptor, since in this region $\alpha_V\beta_3$ has two bulkier residues (Arg214, yellow sphere and Tyr122, orange sphere, Figure 8a) replacing Ala217 and Ala126 within $\alpha_V\beta_6$; these observations can explain the high $\alpha_V\beta_6$ selectivity profile observed for compound **22** (SI = 628).

Continuing the docking studies, the cyclopeptide **24** (Figure 8b) adopts a conformation very similar to that assumed by compound **22**, with the exception of the Asp-flanking Leu residue which does not completely fill the hydrophobic pocket at the α_V and β_6 interface; this can explain the decrease in the $\alpha_V\beta_6$ affinity in comparison to **22**.

The replacement of the Phe residue of compound **22** with the non-natural DiPhe (β–phenyl-Phe) within cyclopeptide **26** induces a modest, yet interesting modification of the binding conformation (Figure 8a,c), explaining the affinity drop toward both $\alpha_V\beta_3$ and $\alpha_V\beta_6$. In fact, the Arg interaction with Asp218 and accommodation of diphenyl groups at the α_V and β_6 are not optimal as for **22**; indeed, the DiPhe residue within **26** results more solvent-exposed than the Phe of peptide **22**. Nevertheless, compound **26** still shows a good selectivity (SI = 243), probably due to the beneficial interaction between the Leu portion and β_1-α_1, β_2- β_3 and α_2- α_3 loops.

Supporting these observations, when Phe residue is incorporated into the N^{α}-side chain as in compound **28** (Figure 8d), the peptide well accommodates into the $\alpha_V\beta_6$ binding site and the Phe residue deeply fills the pocket at the interface between α_V and β_6. These features could explain not only the improved $\alpha_V\beta_6$ affinity of **26** and **28**, but also the selectivity profile of compound **28** (SI = 521).

All the binding poses proposed in Figure 8 agree with the *in vitro* assay results, confirming that a fine selection of amino acids flanking the RGD motif and a suitable N^{α} side chain functionalization could open the way to the synthesis of novel potent and selective $\alpha_V\beta_6$ integrin ligands.

2.4. Conclusions and perspectives

In the previous pharagraphs, the design and synthesis of a library of eighteen Amp-based cyclopeptidomimetic ligands of integrin $\alpha_V\beta_6$ have been reported, and a preliminary SAR study has been suggested. Starting from the lead compound *c*[Amp($C_2H_4NH_2$)RGD], novel peptidomimetics have been initially designed, supported by docking studies. Then, all the compounds have been synthesized and characterized to investigate the impact of different structural modifications on the affinity and selectivity profiles. In particular, the role of the cyclopeptide size, the nature of amino acids flanking the RGD moiety, and the functionalization of aminoproline N^{α} side chain have been investigated. All the final compounds, synthesized through Solid Phase Peptide Synthesis followed by in-solution cyclization and deprotection, have been evaluated by Solid Phase Receptor Binding Assays toward $\alpha_V\beta_6$ integrin and, for the most promising molecules, also affinity toward $\alpha_V\beta_3$ was tested. Four out of the eighteen synthesized cyclopeptidomimetics namely compounds **22**, **24**, **26** and **28** (Figure 9), have shown very promising results in terms of both affinity and selectivity, exhibiting low nanomolar IC_{50} values (IC_{50} from 4.6 to 58.5 nM) and high selectivity indexes (SI from 243 to 628). With these promising results, further steps in the research will include the evaluation of agonist/antagonist activity of the best candidates by cellular assays and preclinical models of $\alpha_V\beta_6$-related diseases possibly paving the way to optimized ligands to be used in biomedical applications as novel diagnostic and/or therapeutic tools, either *per se*, or as $\alpha_V\beta_6$-targeting component within novel covalent conjugates.

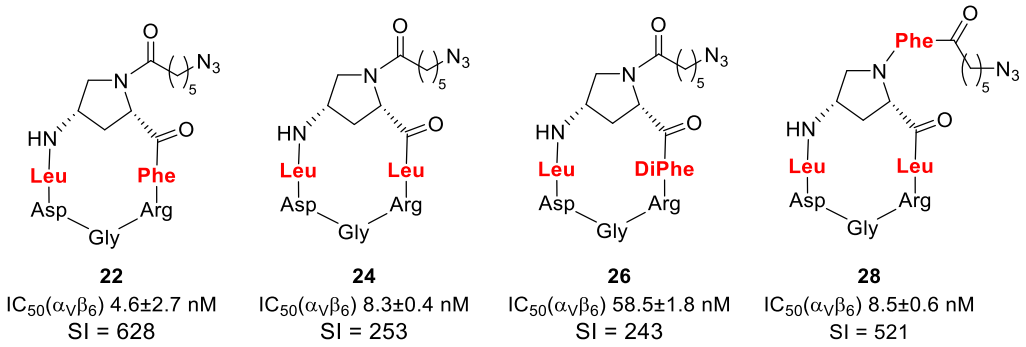

***Figure 9**. Structure, $\alpha_V\beta_6$ binding affinity and Selectivity Indexes of the most promising cyclopeptides accessed in this work (SI= $IC_{50(\alpha V\beta 3)}/IC_{50(\alpha V\beta 6)}$).*

2.5. Experimental Section

2.5.1. Docking Studies

Protein setup: 4UM9[12] crystal structure was used for docking studies: the complex was prepared by using the Protein Preparation Wizard tool of Maestro 9.1 (https://www.schrodinger.com) minimized by a multi-step protocol in which the harmonic restraints were gradually scaled. The complex obtained was used for the following docking studies.

Ligand docking calculations. All docking studies were carried out using the same experimental protocol. In particular, the structures of the different antagonists were prepared from the fragment-building tool available in Maestro 9.1 and the geometries were optimized using the force field OPLS-20054. The docking grid was centred on the Mg^{2+} atom and a grid size of 12×12×12 Å was used. Docking studies were performed using Glide as software, the SP method and the enhanced sampling method for conformational exploration of different ligands. The remaining docking parameters were used as default.

2.5.2. Chemistry

2.5.2.1. General methods and materials

General. All chemicals were of the highest commercially available quality and were used without further purification. Solvents were dried by standard procedures and reactions requiring anhydrous conditions were performed under nitrogen or argon atmosphere. H-Gly-2-ClTrt resin (loading 0.58 mmol/g) and H-Asp(*t*Bu)-2-ClTrt resin (loading 0.74 mmol/g) were purchased from Novabiochem, (2*S*,4*S*)-Fmoc-4-amino-1-Boc-pyrrolidine-2-carboxylic acid (**1**) from PolyPeptide and all other reagents from Alfa Aesar, TCI, or Merck-Sigma-Aldrich. The automated flash chromatography and HPLC solvents respond to ACS standard and they were used without further purification. Analytical thin layer chromatography (TLC) was performed on silica gel 60 F_{254} pre-coated plates with visualization under short-wavelength UV light and by dipping the plates with molybdate reagent (aqueous H_2SO_4 solution of ceric sulphate/ammonium molybdate) followed by heating. Flash column chromatography was performed using 40-63 µm silica gel and the indicated solvent mixtures. Automated flash column chromatography was carried out with the Biotage Isolera One system using Biotage KP-Sil cartridges (direct phase) and KP-C18-HS cartridges (reverse phase). ESI-mass spectra were recorded on UHPLC/ESI-MS system (ACQUITY Ultra Performance LC; ESI, positive ions, Single Quadrupole analyzer) and are reported in the form of (*m/z*). HPLC purifications were performed on a Prostar 210 apparatus (Varian, UV detection) equipped with C18-10 µm columns (Discovery BIO Wide Pore 10 × 250 mm or 21.2 × 250 mm). Routine NMR spectra were recorded on Avance 300 or 400 (Bruker) NMR spectrometers. Chemical shifts (δ) are reported in parts per million (ppm) with TMS ($CDCl_3$), CD_2HOD, and HOD resonance peaks set at 0, 3.31, and 4.80 ppm, respectively. Multiplicities are indicated as s (singlet), d (doublet), t (triplet), q (quartet), m (multiplet), and b (broad). Coupling constants, *J*, are reported in Hertz. ^1H and ^{13}C NMR assignments are corroborated by 1D and 2D experiments (^1H-^1H COSY, ^1H-^1H TOCSY, ^1H-^{13}C DEPT experiments). High resolution mass analysis (ESI) was performed on LTQ ORBITRAP XL Thermo apparatus. Purity of the final compounds was checked by HPLC on a Prostar 210 apparatus (Varian, UV detection) equipped with a semipreparative column (C18-10 µm column Discovery BIO Wide Pore 10 × 250

mm, column A) or a preparative column (C_{18}-10 μm column Discovery BIO Wide Pore 21.2 × 250 mm, column B). The solvent system were H_2O+0.1% TFA (Solvent A) and ACN (solvent B).

Materials. H-Gly-2-ClTrt resin, H-Asp(*t*Bu)-2-ClTrt resin, (2*S*,4*S*)-Fmoc-4-amino-1-Boc-pyrrolidine-2-carboxylic acid, Fmoc-Asp(*t*Bu)-OH; Fmoc-Arg(Pmc)-OH, Fmoc-Phe-OH, H-Phe-O*t*Bu·HCl, Fmoc-Leu-OH, Fmoc–β-Phenyl-Phe-OH, 6-azidohexanoic acid, 2,4,6-collidine, glacial acetic acid, DIPEA, HATU, HOAt, DMP were commercially available and were used as such without further purification. 4-azidobutanal (**9**) and N^{α}-(4-azidobutyl)-4-*N*-(Fmoc)aminoproline (**10**) were prepared according to a reported procedure.[26]

General procedure for final peptide purification: All the final peptides were purified by HPLC equipped with a preparative column (C_{18}-10 μm, 21.2 × 250 mm column) and the following solvent system: H_2O+0.1%TFA (solvent A) and ACN (solvent B). Flow rate 8.0 mL/min; detection at 220 nm.

General procedure for Kaiser test. A few drops of *solution A* (80% phenol solution in ethanol), *solution B* (6% ninhydrin solution in ethanol) and *solution C* (98:2 – pyridine/KCN aq. 0.1 mM) were added to a small sample of the resin [pre-washed with MeOH (2x)], and then heated to 100 °C for 2 min. If resin beads maintained their yellow colour, quantitative coupling was achieved. In case of blue resin beads, the coupling step was not fully completed, and it was then repeated.

Experimental synthetic procedures and characterization data

(2*S*,4*S*)-4-*N*-(9-Fluorenylmethoxycarbonyl)aminoproline 2

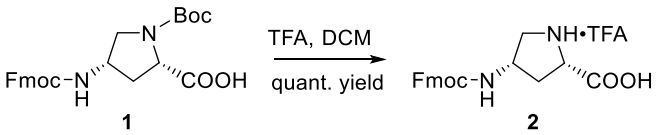

To a solution of commercial aminoproline **1** (1.0 g, 2.2 mmol, 1 eq) in dry DCM (24 mL) at 0 °C, TFA (3 mL) was added dropwise. The ice bath was removed, and the reaction was kept under stirring at room temperature for 1 h. The solvent was evaporated under reduced pressure and Et_2O (4×) was used to favour the complete removal of TFA. The N^{α}-deprotected aminoproline **2** was obtained as a white solid (1.03 g, TFA salt, quantitative yield). ^{1}H NMR (400 MHz, DMSO-d_6) δ 7.89 (d, *J* = 7.4 Hz, 2H, ArH), 7.67 (d, *J* = 7.4 Hz, 2H, ArH), 7.43 (dd, *J* = 7.4, 7.4 Hz, 2H, ArH), 7.33 (dd, *J* = 7.4, 7.4 Hz, 2H, ArH), 4.35 (m, 2H, CH_2 Fmoc), 4.23 (dd, *J* = 6.6, 6.6 Hz, 1H, CH Fmoc), 4.08 (m, 1H, H4), 3.85 (dd, *J* = 8.1, 8.1 Hz, 1H, H2), 3.28 (m, 1H, H5a), 3.02 (m, 1H, H5b), 2.42 (m, 1H, H3a), 1.86 (m, 1H, H3b). ^{13}C NMR (101 MHz, DMSO-d_6) δ 170.0 (Cq), 156.1 (Cq), 144.3 (2C, Cq), 141.2 (2C, Cq), 128.1 (2C, CH), 127.6 (2C, CH), 125.5 (2C, CH), 120.6 (2C, CH), 65.9 (CH_2), 59.4 (CH), 50.3 (CH), 49.4 (CH), 47.1 (CH_2), 34.5 (CH_2). MS (ES^+) *m/z* 353.2 $[M+H]^+$.

(2*S*,4*S*)-1-(6-Azidohexanoyl)-4-*N*-(9-fluorenylmethoxycarbonyl)aminoproline 4

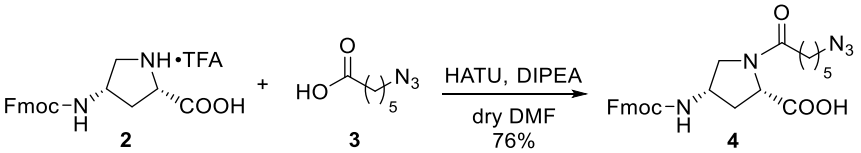

A solution of 6-azidohexanoic acid **3** (158.4 mg, 1.0 mmol, 1.1 eq), HATU (383.3 mg, 1.0 mmol, 1.1 eq), and DIPEA (96.7 μL, 1.0 mmol, 1.1 eq) in dry DMF (4.5 mL) was added dropwise to a solution of aminoproline **2** (426.8 mg, 0.9 mmol, 1 eq) and DIPEA (175.5 μL, 1.8 mmol, 2 eq) in dry DMF (7.5 mL). The reaction was stirred under nitrogen at room temperature for 6 h, then was quenched by

adding HCl 0.1 N until pH=3 and extracted with EtOAc (3×). The combined organic layers were dried with $MgSO_4$, filtered, and evaporated under reduced pressure. The crude residue was purified by reverse phase flash chromatography (eluent: from 80:20 H_2O+0.1%TFA:ACN to 20:80) affording the aminoproline **4** as a colourless glassy solid (342.0 mg, 76% yield). TLC: EtOAc/MeOH/AcOH 94.95:4.95:0.1, R*f*: 0.4. ^{1}H NMR (400 MHz, MeOD) δ 7.80 (bd, *J* = 8.0 Hz, 2H, ArH), 7.64 (bd, *J* = 8.0 Hz, 2H, ArH), 7.40 (dd, *J* = 7.5, 7.5 Hz, 2H, ArH), 7.31 (dd, *J* = 7.5, 7.5 Hz, 2H, ArH), 4.38 (d, *J* = 6.8 Hz, 2H, CH_2 Fmoc), 4.32 (d, *J* = 6.2 Hz, 1H, H2), 4.25-4.17 (m, 2H, H4, CH Fmoc), 3.92 (m, 1H, H5a), 3.39 (m, 1H, H5b), 3.28 (t, *J* = 6.8 Hz, 2H, H6'), 2.54 (m, 1H, H3a), 2.35 (bt, *J* = 7.0 Hz, 2H, H2'), 1.93 (m, 1H, H3b), 1.66-1.56 (m, 4H, H3', H5'), 1.43 (m, 2H, H4'). ^{13}C NMR (101 MHz, MeOD) δ 174.2 (Cq), 172.9 (Cq), 156.7 (Cq), 143.8 (2C, Cq), 141.2 (2C, Cq), 127.4 (2C, CH), 126.8 (2C, CH), 124.8 (2C, CH), 119.6 (2C, CH), 66.4 (CH_2), 57.5 (CH), 51.7 (CH_2), 50.9 (CH_2), 50.1 (CH), 48.6 (CH), 34.2 (CH_2), 33.6 (CH_2), 28.3 (CH_2), 25.9 (CH_2), 23.8 (CH_2). MS (ES$^+$) *m/z* 492.2 $[M+H]^+$.

(*S*)-*N*-(6-Azidohexanoyl)phenylalanine *tert*-butyl ester 5a

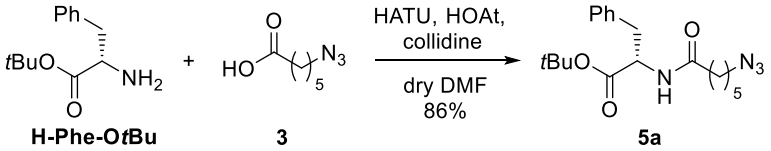

A solution of L-Phe *tert*-butyl ester (160.0 mg, 0.62 mmol, 1.1 eq) and 2,4,6-collidine (68.3 μL, 0.62 mmol, 1.1 eq) in dry DMF (3 mL) was added dropwise to a solution of 6-azidohexanoic acid (**3**) (89.1 mg, 0.57 mmol, 1 eq), HATU (237.3 mg, 0.62 mmol, 1.1 eq), HOAt (114.3 mg, 0.62 mmol, 1.1 eq) and 2,4,6-collidine (126 μL, 1.13 mmol, 2 eq) in dry DMF (4.5 mL). The reaction was stirred under nitrogen at room temperature for 5 h and quenched by adding aq NH_4Cl saturated solution until pH=7. The mixture was extracted with EtOAc (3×) and the combined organic layers were dried with $MgSO_4$, filtered, and evaporated under reduced pressure. The crude residue was purified by flash chromatography (eluent: from 80:20 petroleum ether:EtOAc to 20:80) to afford compound **5a** as a colourless glassy solid (185.4 mg, 86% yield). TLC: petroleum ether/EtOAc 50:50, R*f*: 0.8. ^{1}H NMR (400 MHz, $CDCl_3$) δ 7.32-7.23 (m, 3H, ArH), 7.16 (m, 2H, ArH), 5.94 (bd, *J* = 7.5 Hz, 1H, NH), 4.78 (dt, *J* = 7.8, 6.0 Hz, 1H, Hα Phe), 3.26 (t, *J* = 7.5 Hz, 2H, H6'), 3.13 (dd, *J* = 13.9, 6.3 Hz, 1H, Hβ Phe), 3.08 (dd, *J* = 13.9, 6.3 Hz, 1H, Hβ Phe), 2.20 (m, 2H, H2'), 1.70-1.56 (m, 4H, H3', H5'), 1.43 (s, 9H, *t*Bu), 1.42-1.33 (m, 2H, H4'). ^{13}C NMR (101 MHz, $CDCl_3$) δ 172.0 (Cq), 170.9 (Cq), 136.2 (Cq), 129.5 (2C, CH), 128.4 (2C, CH), 126.9 (CH), 82.4 (Cq), 53.3 (CH_2), 51.2 (CH), 38.1 (CH_2), 36.3 (CH_2), 33.6 (CH_2), 28.6 (CH_2), 28.0 (CH_2), 26.3 (3C, CH_3). MS (ES$^+$) *m/z* 361.1 $[M+H]^+$.

(*S*)-*N*-(6-Azidohexanoyl)phenylalanine 5

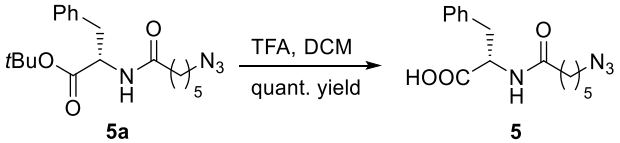

Protected phenylalanine **5a** (185.4 mg, 0.49 mmol, 1 eq) was treated with a solution of TFA:DCM 80:20 (25 mL) and the reaction was kept under stirring for 1 h. The mixture was then concentrated under reduced pressure giving compound **5** as a yellowish glassy solid (149.0 mg, quantitative yield), which was used as such in the following step. ^{1}H NMR (400 MHz, $CDCl_3$) δ 8.92 (bs, 1H, OH), 7.33-7.25 (m, 3H, ArH), 7.18 (m, 2H, ArH), 6.22 (bd, *J* = 7.2 Hz, 1H, NH), 4.91 (m, 1H, Hα Phe), 3.26 (dd, *J* = 13.5, 5.6 Hz, 1H, Hβ Phe), 3.24 (m, 2H, H6'), 3.13 (dd, *J* = 13.5, 6.3 Hz, 1H, Hβ Phe), 2.22 (bt, *J* = 6.6

Hz, 2H, H2'), 1.65-1.53 (m, 4H, H3', H5'), 1.40-1.26 (m, 2H, H4'). ^{13}C NMR (101 MHz, $CDCl_3$) δ 173.2 (Cq), 170.9 (Cq), 136.2 (Cq), 129.5 (2C, CH), 128.4 (2C, CH), 126.9 (CH), 53.3 (CH_2), 51.2 (CH), 38.1 (CH_2), 36.3 (CH_2), 33.6 (CH_2), 28.6 (CH_2), 28.0 (CH_2). MS (ES^+) *m/z* 305.2 $[M+H]^+$.

(2*S*,4*S*)-1-[*N*-(6-Azidohexanoyl)phenylalanyl]-4-*N*-(9-fluorenylmethoxycarbonyl) aminoproline 6

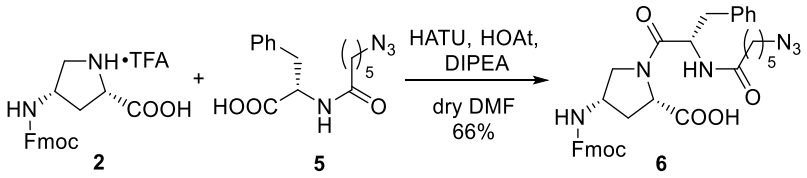

To a solution of compound **5** (149.0 mg, 0.49 mmol, 1.2 eq), HATU (186.3 mg, 0.49 mmol, 1.2 eq), HOAt (66.7 mg, 0.49 mmol, 1.2 eq) and DIPEA (85 μL, 0.49 mmol 1.2 eq) in dry DMF (7.5 mL), a solution of aminoproline **2** (191.2 mg, 0.41 mmol, 1 eq) and DIPEA (143 μL, 0.82 mmol, 2 eq) in dry DMF (9 mL) was added dropwise. The reaction was kept under stirring at room temperature for 6 h. After this time, the reaction was quenched by adding aq NH_4Cl saturated solution until pH=7. The mixture was extracted with EtOAc (3×) and the combined organic layers were dried with $MgSO_4$, filtered and evaporated under reduced pressure. The crude residue was purified by reverse phase flash chromatography (eluent: from 80:20 H_2O+0.1%TFA:ACN to 20:80] affording compound **6** as a colourless glassy solid (172.8 mg, 66% yield). TLC: EtOAc:MeOH:AcOH 94.95:4.95:0.1, R*f*: 0.4. ^{1}H NMR (400 MHz, MeOD) δ 7.80 (bd, *J* = 6.9 Hz, 2H, ArH), 7.63 (dd, *J* = 6.4, 6.4 Hz, 2H, ArH), 7.40 (dd, *J* = 7.2, 7.2 Hz, 2H, ArH), 7.35-7.19 (m, 7H, ArH), 4.94 (dd, *J* = 7.3, 7.3 Hz, 1H, Hα Phe), 4.42-4.30 (m, 3H, H2, CH_2 Fmoc), 4.29-4.15 (m, 2H, H4, CH Fmoc), 3.92 (m, 1H, H5a), 3.49 (m, 1H, H5b), 3.26-3.19 (m, 2H, H6'), 3.22-3.14 (m, 1H, Hβ Phe), 2.96-2.84 (m, 1H, Hβ Phe), 2.57-2.45 (m, 1H, H3a), 2.22-2.14 (m, 2H, H2'), 1.96-1.83 (m, 1H, H3b), 1.57-1.47 (m, 4H, H3', H5'), 1.32-1.24 (m, 2H, H4'). ^{13}C NMR (101 MHz,MeOD) δ 173.9 (Cq), 173.6 (Cq), 170.8 (Cq), 156.6 (Cq), 143.8 (2C, Cq), 141.2 (2C, Cq), 136.5 (Cq), 129.1 (2C, CH), 128.2 (2C, CH), 127.4 (2C, CH), 126.8 (2C, CH), 126.7 (CH), 124.8 (2C, CH), 119.6 (2C, CH), 66.5 (CH_2), 57.9 (CH), 57.7 (CH), 52.5 (CH_2), 52.1 (CH), 50.9 (CH_2), 50.0 (CH), 37.7 (CH_2), 35.0 (CH_2), 34.1 (CH_2), 28.1 (CH_2), 25.8 (CH_2), 24.9 (CH_2). MS (ES^+) *m/z* 639.3 $[M+H]^+$.

6-Azidohexanal 7

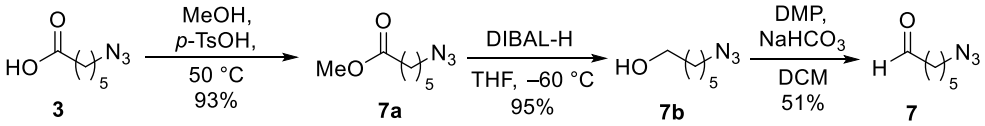

To a stirred solution of 6-azido hexanoic acid (**3**) (200.0 mg, 1.27 mmol, 1 eq) in methanol (10 mL) at 50 °C, *p*-toluene sulfonic acid (24.2 mg, 0.12 mmol, 0.1 eq) was added. The reaction was kept under stirring at 50 °C for 4 h; then, the solvent was removed under reduced pressure. The crude was purified by flash chromatography (eluent: petroleum ether:EtOAc, 70:30) affording ester **7a** as a yellow oil (202 mg, 93% yield). TLC: petroleum ether/EtOAc 70:30, R*f*: 0.8. ^{1}H NMR (400 MHz, $CDCl_3$) δ 3.54 (s, 3H, Me), 3.16 (t, *J* = 6.7 Hz, 2H, H6), 2.21 (t, *J* = 8.0 Hz, 2H, H2), 1.58-1.46 (m, 4H, H3, H5), 1.29 (m, 2H, H4). MS (ES^+) *m/z* 172.3 $[M+H]^+$.

To a stirred solution of ester **7a** (202.0 mg, 1.18 mmol, 1 eq) in THF (12 mL) cooled to –60 °C, a solution of DIBAL-H (1 M in toluene, 3.54 mL, 3.54 mmol, 3 eq) was added dropwise under argon. After 4 h, the reaction was quenched by adding methanol (2 mL) and water (2 mL) and the mixture was allowed to reach room temperature and kept under stirring for 30 min. The mixture was

extracted with EtOAc (3×) and the combined organic layers were dried with $MgSO_4$, filtered and evaporated under reduced pressure. The crude residue was purified by flash chromatography (eluent: petroleum ether:EtOAc, 70:30) affording compound **7b** as a yellow liquid (160.5 mg, 95% yield). TLC: petroleum ether/EtOAc 70:30, R*f*: 0.3. ^{1}H NMR (400 MHz, $CDCl_3$): δ 3.67 (t, *J* = 6.6 Hz, 2H, H1), 3.29 (t, *J* = 7.1 Hz, 2H, H6), 1.72-1.55 (m, 5H, OH, H2, H5), 1.48-1.37 (m, 2H, H4). MS (ES^+) *m/z* 144.3 $[M+H]^+$.

To a stirred solution of **7b** (160.5 mg, 1.12 mmol, 1 eq) in dry DCM (7.5 mL) under nitrogen, $NaHCO_3$ (282 mg, 3.36 mmol, 3 eq) and DMP (712 mg, 1.68 mmol, 1.5 eq) were added. The reaction was kept under stirring for 2 h, and then quenched by adding aq Na_2SO_4 saturated solution (3 mL) and aq $NaHCO_3$ saturated solution (3 mL). The mixture was extracted with EtOAc (3×) and the combined organic layers were dried with $MgSO_4$, filtered and evaporated under reduced pressure. The crude residue was purified by flash chromatography (eluent: petroleum ether:EtOAc, 60:40) affording aldehyde **7** (80.6 mg, 51% yield) as a yellow oil. TLC: DCM/EtOAc 80:20, R*f*= 0.2. ^{1}H NMR (400 MHz, $CDCl_3$): δ 9.75 (bs, 1H, H1), 3.26 (t, *J* = 6.7 Hz, 2H, H6), 2.45 (bt, *J* = 7.2 Hz, 2H, H2), 1.70-1.54 (m, 4H, H3, H5), 1.45-1.34 (m, 2H, H4). MS (ES^+) *m/z* 142.1 $[M+H]^+$.

(2*S*,4*S*)-1-(6-Azidohexyl)-4-*N*-(9-fluorenylmethoxycarbonyl)aminoproline 8

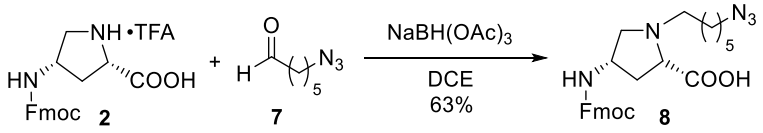

To a solution of N^{α}-deprotected aminoproline **2** (78.8 mg, 0.17 mmol, 1 eq) in dry DCE (10 mL), $NaBH(OAc)_3$ (79.0 mg, 0.37 mmol, 2.2 eq) was added followed by addition of a solution of 4-azidohexanal **7** (30.9 mg, 0.22 mmol, 1.3 eq) in dry DCE (2 mL) was added. The reaction was stirred under argon at room temperature for 5 h, then the mixture was quenched with aq $NaHSO_3$ saturated solution and extracted with DCM (1×) and EtOAc (3×). The combined organic layers were dried with $MgSO_4$, filtered and evaporated under reduced pressure. The crude residue was subjected to reverse phase flash chromatographic purification (eluent: from 80:20 H_2O+0.1%TFA:ACN to 20:80) affording aminoproline **8** as a yellow glassy solid (63.0 mg, 63% yield). TLC: EtOAc/MeOH 60:40, R*f*: 0.2. ^{1}H NMR (400 MHz, MeOD): δ 7.79 (bd, *J* = 7.5 Hz, 2H, ArH), 7.63 (bd, *J* = 7.5 Hz, ArH), 7.40 (dd, *J* = 7.5, 7.5 Hz, 2H, ArH), 7.31 (dd, *J* = 7.5, 7.5 Hz, ArH), 4.43 (m, 2H, CH_2 Fmoc), 4.40-4.28 (m, 2H, H2, CH Fmoc), 4.19 (m, 1H, H4), 3.73 (bd, 1H, *J* = 11.1 Hz, H5a), 3.49 (m, 1H, H5b), 3.42-3.32 (m, 1H, H1'a), 3.29 (t, *J* = 6.7 Hz, 2H, H6'), 3.13 (m, 1H, H1'b), 2.86 (m, 1H, H3a), 2.19 (m, 1H, H3b), 1.71 (m, 2H, H2'), 1.59 (m, 2H, H5'), 1.49-1.34 (m, 4H, H3', H4'). ^{13}C NMR (101 MHz, MeOD): δ 169.1 (Cq), 156.9 (Cq), 143.7 (2C, Cq), 141.3 (2C, Cq), 127.4 (2C, CH), 126.8 (2C, CH), 124.5 (2C, CH), 119.6 (2C, CH), 66.4 (CH_2), 66.2 (CH_2), 58.6 (CH), 55.5 (CH_2), 50.8 (CH_2), 48.7 (CH), 48.1 (CH), 33.9 (CH_2), 28.2 (CH_2), 25.8 (CH_2), 25.5 (CH_2), 25.1 (CH_2). MS (ES^+) *m/z* 478.2 $[M+H]^+$.

***Cyclo*[1-(6-azidohexanoyl)Amp-Arg-Gly-Asp] 11**

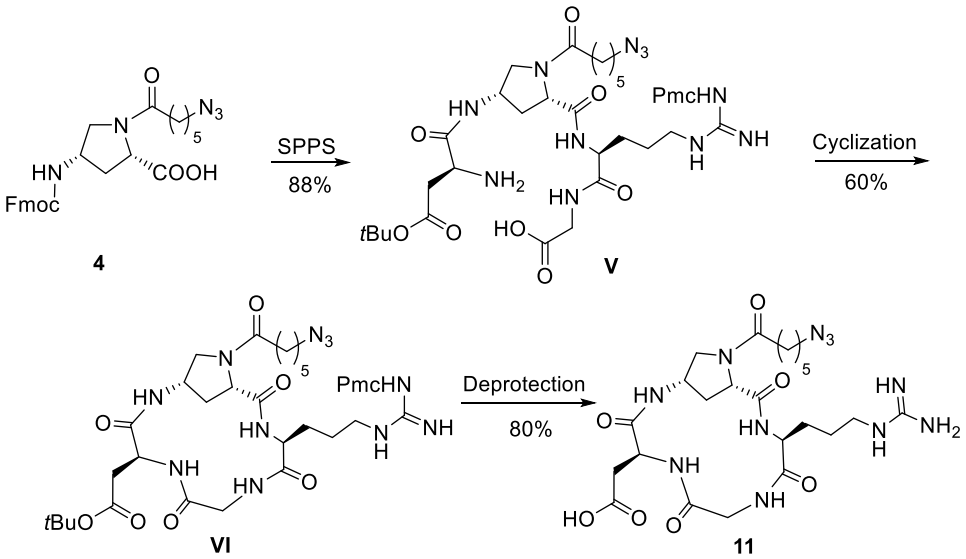

General Procedure for Cyclopeptide Synthesis.

Solid Phase Synthesis. The synthesis of linear tetrapeptide H-Asp(*t*Bu)-1-(6-azidohexanoyl)Amp-Arg(Pmc)-Gly-OH (**V**) was performed using the preloaded 2-chlorotrityl-Gly-H resin (loading 0.58 mmol/g). *Resin swelling*: the resin (265 mg, 0.15 mmol, 1.0 eq) was swollen in a solid phase reaction vessel with dry DMF (5 mL) under mechanical stirring; after 40 min the solvent was drained, and the resin was washed with DMF (3×). *Peptide coupling:* A preformed solution of Fmoc-Arg(Pmc)-OH (143 mg, 0.23 mmol, 1.5 eq) in dry DMF (4 mL) was treated with HATU (117 mg, 0.31 mmol, 2.0 eq), HOAt (42 mg, 0.31 mmol, 2.0 eq) and 2,4,6-collidine (41 µL, 0.308 mmol, 2.0 eq) and stirred for 10 min before adding to the resin. The mixture was shaken at room temperature for 3 h. Completion of the reaction was checked by the Kaiser test. The solution was drained and the resin was washed with DMF (2×), *i*PrOH, (2×), Et_2O (2×), DCM (2×). The resin was washed again with DMF and treated with 20% v/v piperidine in DMF (5 mL) and the mixture was stirred for 40 min. The solution was drained and the resin was washed with DMF (2×), *i*PrOH, (3×), Et_2O (2×), DCM (2×). The couplings of the aminoproline module (**4**) (113 mg, 0.23 mmol, 1.5 eq) and the Fmoc-Asp(*t*Bu)-OH (95 mg, 0.23 mmol, 1.5 eq) were carried out under the same conditions. *Resin cleavage*: the resin was treated with 5 mL of the cleavage mixture DCM:TFE:glacial AcOH (3:1:1) and kept under mechanical stirring for 20 min at room temperature. The solution was recovered and the resin was carefully washed with DCM (2×). This protocol was repeated twice. The combined solution was evaporated under reduced pressure affording the linear tetrapeptide **I** (132 mg, AcOH salt, 88% yield) as a colourless glassy solid, which was used in the following step without further purification. MS (ES^+) *m/z* 920.4 $[M+H]^+$.

In-solution cyclization. To a solution of linear tetrapeptide **V** (132 mg, 0.135 mmol, 1 eq) in dry DCM (40 mL), 2,4,6-collidine (54 µL, 0.40 mmol, 3.0 eq) was added. The mixture was stirred under argon at room temperature for 10 min, then was added dropwise to a solution of HATU (154 mg, 0.40 mmol, 3.0 eq) and HOAt (55 mg, 0.40 mmol, 3.0 eq) in dry DMF (4 mL) and dry DCM (20 mL) to a final peptide concentration of 2.1 mM. The reaction mixture was degassed by argon/vacuum cycles (3×) and left to stir under argon at room temperature for 5 h. After completion, the solution was concentrated under vacuum and extracted with EtOAc (3×). The combined organic layers were dried with $MgSO_4$, filtered, and concentrated under reduced pressure. The crude product was purified by reverse phase chromatography (eluent: from 80:20 H_2O+0.1%TFA:ACN to 20:80) affording the protected cyclopeptide **VI** as a colourless glassy solid (82 mg, TFA salt, 60 % yield).

^{1}H NMR (400 MHz, MeOD): δ 4.69 (dd, *J* = 5.6, 5.6 Hz, 1H, Hα Asp), 4.63 (bd, *J* = 9.2 Hz, 1H, H2), 4.59 (bdd, *J* = 7.3, 6.9 Hz, 1H, H4), 4.16 (d, *J* = 13.7 Hz, 1H, Hα Gly), 4.07 (dd, *J* = 7.3, 7.3 Hz, 1H, Hα Arg), 3.92 (dd, *J* = 11.7, 6.2 Hz, 1H, H5a), 3.64 (bd, *J* = 11.6 Hz, 1H, H5b), 3.34 (m, 1H, Hα Gly), 3.30 (t, *J* = 6.7 Hz, 2H, H6'), 3.28-3.15 (m, 2H, Hδ Arg), 2.73 (dd, *J* = 5.6, 5.6 Hz, 2H, Hβ Asp), 2.68 (t, *J* = 6.9 Hz, 2H, CH_2 Pmc), 2.58 (s, 3H, CH_3 Pmc), 2.57 (s, 3H, CH_3 Pmc), 2.49 (m, 1H, H3a), 2.44-2.31 (m, 2H, H2'), 2.18 (bd, *J* = 13.8 Hz, 1H, H3b), 2.12 (s, 3H, CH_3 Pmc), 1.86 (t, *J* = 6.8 Hz, 2H, CH_2 Pmc), 1.79-1.51 (m, 8H, Hβ Arg, Hγ Arg, H3', H5'), 1.48 (s, 9H, *t*Bu), 1.45 (m, 2H, H4'), 1.33 (s, 6H, CH_3 Pmc). MS (ES$^+$) *m/z* 902.4 $[M+H]^+$.

Side chain deprotection and peptide purification. The protected cyclic tetrapeptide **VI** (82 mg, 0.081 mmol, 1 eq) was treated with 4.1 mL of a TFA:TIS:H_2O (95:2.5:2.5) solution and stirred at room temperature for 1 h. Then, the mixture was evaporated under vacuum and the crude residue was thoroughly washed with Et_2O (4×) and petroleum ether (2×). Preparative RP-HPLC purification was performed as described in the general procedure, using a linear gradient from 95% A to 40% B over 25 min at room temperature; R_t = 22.0 min. The removal of the solvent under vacuum afforded compound **6** as a colorless glassy solid (45 mg, TFA salt, 80% yield). Purity of final cyclopeptide was checked by HPLC and found as 99.7%.

^{1}H NMR (400 MHz, D_2O): δ 4.63 (dd, *J* = 5.7, 5.7 Hz, 1H, Hα Asp), 4.57 (bd, *J* = 9.6 Hz, 1H, H2), 4.48 (bdd, *J* = 6.5, 6.5 Hz, 1H, H4), 4.07 (d, *J* = 14.1 Hz, 1H, Hα Gly), 4.04 (dd, 1H, *J* = 7.4, 7.4 Hz, Hα Arg), 3.88 (dd, *J* = 11.8, 6.0 Hz, 1H, H5a), 3.62 (bd, *J* = 11.8 Hz, 1H, H5b), 3.46 (d, *J* = 14.0 Hz, 1H, Hα Gly), 3.21 (t, *J* = 6.9 Hz, 2H, H6'), 3.12 (t, *J* = 6.9 Hz, 2H, Hδ Arg), 2.81 (m, 2H, Hβ Asp), 2.52 (ddd, *J* = 14.8, 10.2, 6.7 Hz, 1H, H3a), 2.29 (t, *J* = 7.3 Hz, 2H, H2'), 2.02 (d, *J* = 14.1 Hz, 1H, H3b), 1.76-1.62 (m, 4H, Hβ Arg, Hγ Arg), 1.58-1.44 (m, 4H, H3', H5'), 1.38-1.22 (m, 2H, H4'). ^{13}C NMR (101 MHz, D_2O): δ 175.7 (Cq), 175.4 (Cq), 175.2 (Cq), 174.8 (Cq), 170.8 (Cq), 170.7 (Cq), 156.7 (Cq), 58.3 (CH), 55.34 (CH), 54.0 (CH_2), 51.0 (CH_2), 49.6 (CH), 49.5 (CH_2), 44.3 (CH_2), 40.4 (CH_2), 34.8 (CH_2), 33.7 (CH_2), 33.6 (CH_2), 27.7(CH_2), 26.3 (CH_2), 25.5 (CH_2), 24.4 (CH_2), 23.7(CH_2).

HRMS(ES$^+$) $C_{23}H_{38}N_{11}O_7$ calcd for $[M+H]^+$ 580.2956, found 580.2949.

***Cyclo*[1-(6-aminohexanoyl)Amp-Arg-Gly-Asp] 12**

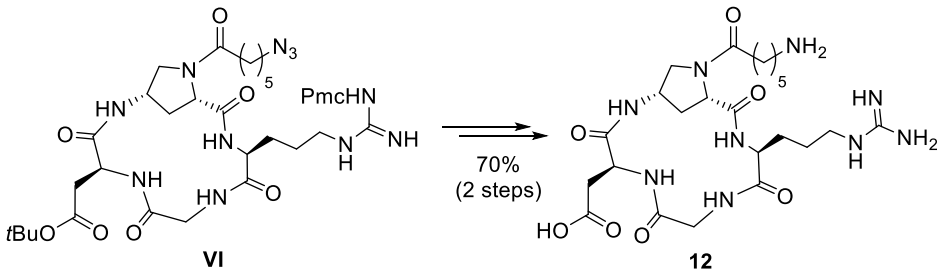

Compound **12** was prepared starting from protected cyclopeptide **VI**, a common intermediate in the preparation of cyclopeptide **11**.

General procedure for side chain reduction. The protected 6-azidohexanoyl cyclopeptide **VI** (20 mg, 0.02 mmol, 1.0 eq) was dissolved in EtOH (2.5 mL), and catalytic amounts of 10% Pd/C and formic acid were added. The reaction vessel was degassed under vacuum, and thoroughly purged with hydrogen (3×). The resulting heterogeneous mixture was stirred at room temperature for 2 h. After completion, the reaction was filtered under suction, and the filtrate was concentrated to afford the amine-terminating protected cyclopeptide (13.4 mg, HCO_2H salt, 74%) as a glassy solid, which was used in the following step without further purification. TLC: EtOAc:MeOH 70:30, R*f*: 0.1.

^{1}H NMR (400 MHz, MeOD) δ 4.72 (dd, *J* = 5.8, 5.8 Hz, 1H, Hα Asp), 4.65 (bd, *J* = 9.8 Hz, 1H, H2), 4.54

(m, 1H, H4), 4.14 (d, *J* = 13.9 Hz, 1H, Hα Gly), 4.10 (m, 1H, Hα Arg), 3.92 (dd, *J* = 11.5, 6.1 Hz, 1H, H5a), 3.67 (d, *J* = 11.7 Hz, 1H, H5b), 3.35 (m, 1H, Hα Gly), 3.29-3.16 (m, 2H, Hδ Arg), 2.95 (t, *J* = 7.9 Hz, 2H, H6'), 2.73 (m, 2H, Hβ Asp), 2.69 (t, *J* = 6.9 Hz, 2H, CH_2 Pmc), 2.59 (s, 3H, CH_3 Pmc), 2.58 (s, 3H, CH_3 Pmc), 2.55-2.40 (m, 3H, H3a, H2'), 2.27 (bd, *J* = 14.4 Hz, 1H, H3b), 2.12 (s, 3H, CH_3 Pmc), 1.86 (t, *J* = 6.8 Hz, CH_2 Pmc), 1.79-1.56 (m, 8H, Hβ Arg, Hγ Arg, H3', H5'), 1.52-1.43 (m, 11H, *t*Bu, H4'), 1.33 (m, 6H, CH_3 Pmc). MS (ES^+) *m/z* 876.5 $[M+H]^+$.

The amine-terminating protected cyclopeptide (13.4 mg, 0.014 mmol, 1 eq) was elaborated according to the above-described deprotection and purification general procedure. Preparative RP-HPLC purification was performed as described in the general procedure, using a linear gradient from 90% A to 40% B over 25 min at room temperature; R_t = 17.1 min. Removal of the solvent afforded cyclopeptide **7** as a colorless glassy solid (10.4 mg, TFA salt, 95% yield). Purity of final cyclopeptide was checked by HPLC and found as 99%. ^{1}H NMR (400 MHz, D_2O): δ 4.67 (dd, *J* = 6.0, 6.0 Hz, 1H, Hα Asp), 4.58 (bd, *J* = 9.9 Hz, 1H, H2), 4.46 (dd, *J* = 6.3, 6.3 Hz, 1H, H4), 4.10-4.01 (m, 2H, Hα Gly, Hα Arg), 3.88 (dd, *J* = 11.9, 5.9 Hz, 1H, H5a), 3.62 (bd, *J* = 11.9 Hz, 1H, H5b), 3.46 (d, *J* = 14.1 Hz, 1H, Hα Gly), 3.15 (t, *J* = 6.7 Hz, 2H, Hδ Arg), 2.91 (t, *J* = 7.2 Hz, 2H, H6'), 2.82 (dd, *J* = 5.4, 5.4 Hz, 1H, Hβ Asp), 2.52 (m, 1H, H3a), 2.33 (m, 2H, H2'), 2.05 (bd, *J* = 13.9 Hz, 1H, H3b), 1.75-1.47 (m, 8H, Hβ Arg, Hγ Arg, H3', H5'), 1.32 (m, 2H, H4'). HRMS(ES^+) $C_{23}H_{39}N_9O_7$ calcd for $[M+H]^+$ 554.2972, found 554.3057.

***Cyclo*{1-[*N*-(6-azidohexanoyl)phenylalanyl]Amp-Arg-Gly-Asp} 13**

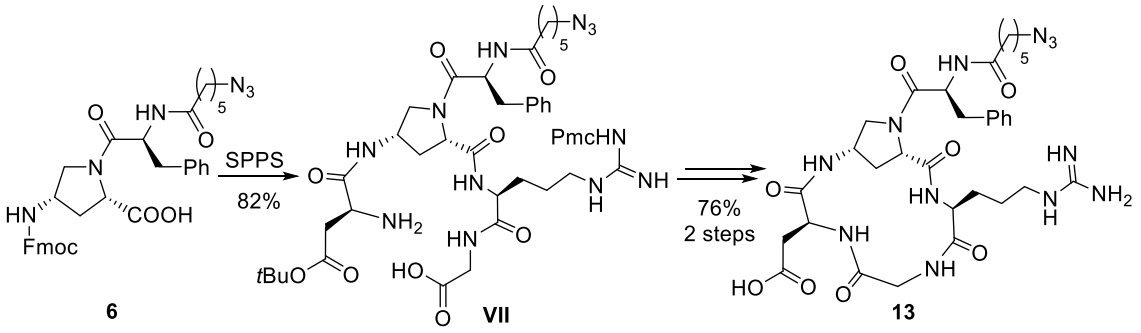

Cyclopeptide **13** was prepared according to the general procedure described for compound **11** by using the module **6** in place of **4**. The linear tetrapeptide **VII**, precursor of compound **13**, was prepared according to the procedure described for linear tetrapeptide **I** by using 2-chlorotrityl-Gly-H resin (26.7 mg, 0.015 mmol, 1.0 eq), Fmoc-Arg(Pmc)-OH (14.4 mg, 0.023 mmol, 1.5 eq), the aminoproline module **6** (14.7 mg, 0.023 mmol, 1.5 eq) and Fmoc-Asp(*t*Bu)-OH (9.5 mg, 0.023 mmol, 1.5 eq). After the resin cleavage, compound **VII** (16.1 mg, AcOH salt, 92% yield) was recovered as a colourless glassy solid and was used in the following step without further purification. MS (ES^+) *m/z* 1067.6 $[M+H]^+$.

The protected cyclopeptide intermediate was prepared starting from V**II** (16.1 mg, 0.014 mmol, 1 eq) according to the cyclization general procedure and was obtained as a glassy solid (14.1 mg, TFA salt 85% yield). TLC: EtOAc:MeOH 70:30, R*f* = 0.7. ^{1}H NMR (400 MHz, MeOD): δ 7.33-7.22 (m, 5H, ArH), 4.81 (dd, *J* = 7.8, 7.8 Hz, 1H, Hα Phe), 4.71-4.67 (m, 1H, Hα Asp), 4.59 (bd, *J* = 9.6 Hz, 1H, H2), 4.55-4.51 (m, 1H, H4), 4.20 (m, 1H, Hα Gly), 4.01 (dd, *J* = 7.8, 7.8 Hz, 1H, Hα Arg), 3.84 (dd, *J* = 13.2, 6.4 Hz, 1H, H5a), 3.66 (bd, *J* = 13.4 Hz, 1H, H5b), 3.29-3.10 (m, 6H, Hα Gly, H6', Hδ Arg, Hβ Asp), 3.04-2.82 (m, 3H, Hβ Phe, HβAsp), 2.76-2.72 (m, 1H, H3a), 2.70 (t, *J* = 5.2 Hz, 2H, CH_2 Pmc), 2.59 (s, 3H, CH_3 Pmc), 2.58 (s, 3H, CH_3 Pmc), 2.38 (bd, *J* = 13.8 Hz, 1H, H3b), 2.24-2.16 (m, 2H, H2'), 2.13 (s,

3H, CH_3 Pmc), 1.86 (t, *J* = 6.4 Hz, 2H, CH_2 Pmc), 1.84-1.63 (m, 4H, Hβ Arg, Hγ Arg), 1.61-1.49 (m, 4H, H3', H5'), 1.47 (s, 9H, *t*Bu), 1.33 (s, 6H, CH_3 Pmc), 1.30 (m, 1H, H4'). MS (ES^+) *m/z* 1071.5 $[M+Na]^+$.

Cyclopeptide **13** was recovered after deprotection and purification by preparative RP-HPLC as described in the general, using linear gradient from 80% A to 40% B over 25 min at room temperature (R_t = 16.0 min) as a colourless glassy solid (9.2 mg, TFA salt, 90% yield). Purity of the final cyclopeptide was checked by HPLC and found as 96.2%. ^{1}H NMR (400 MHz, D_2O): δ 7.41-7.23 (m, 5H, ArH), 4.73-4.63 (m, 2H, Hα Phe, Hα Asp), 4.58-4.47 (m, 1H, H2), 4.46-4.38 (m, 1H, H4), 4.13 (d, *J* = 13.7 Hz, 1H, Hα Gly), 4.10-4.02 (m, 1H, Hα Arg), 3.88 (m, 1H, H5a), 3.64-3.47 (m, 2H, H5b, Hα Gly), 3.29-3.16 (m, 4H, H6', Hδ Arg), 3.03 (m, 1H, Hβ Phe), 2.2.97-2.80 (m, 3H, Hβ Phe, Hβ Asp), 2.32 (m, 1H, H3a), 2.25-2.11 (m, 2H, H2'), 1.98 (bd, *J* = 14.4 Hz, 1H, H3b), 1.83-1.55 (m, 4H, Hβ Arg, Hγ Arg); 1.54-1.36 (m, 4H, H3', H5'), 1.24-1.12 (m, 2H, H4'). HRMS(ES^+) $C_{32}H_{47}N_{12}O_8$ calcd for $[M+H]^+$ 727.3634, found 727.3649.

***Cyclo*[1-(6-azidohexanoyl)Amp-Arg-Leu-Asp] 14**

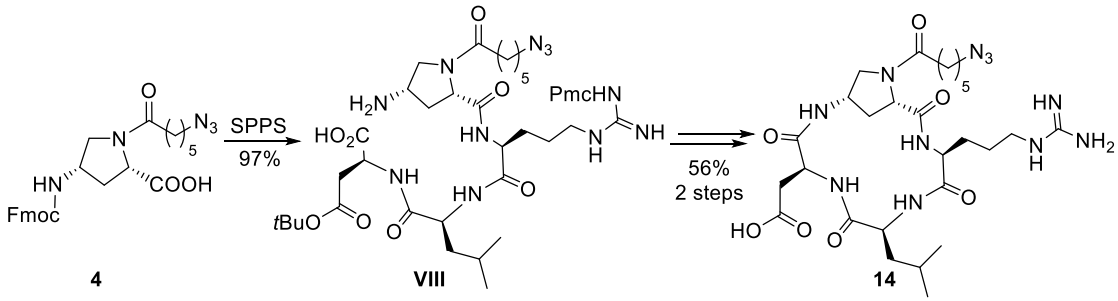

Cyclopeptide **14** was prepared according to the general procedure described for compound **11** by using the preloaded H-Asp(*t*Bu)-2-ClTrt resin (loading 0.74 mmol/g) and the aminoproline module **4**. The linear tetrapeptide **VIII**, precursor of compound **14**, was prepared according to the procedure described for linear tetrapeptide **V** by using the H-Asp(*t*Bu)-2-ClTrt resin (61.8 mg, 0.046 mmol, 1.0 eq), Fmoc-Leu-OH (24.2 mg, 0.069 mmol, 1.5 eq), Fmoc-Arg(Pmc)-OH (42.4 mg, 0.069 mmol, 1.5 eq), the aminoproline module **4** (33.7 mg, 0.069 mmol, 1.5 eq). After the resin cleavage, compound **VIII** (46.0 mg, AcOH salt, 97% yield) was recovered as a colourless glassy solid and was used in the following step without further purification. MS (ES^+) *m/z* 976.5 $[M+H]^+$.

The protected cyclopeptide intermediate was prepared starting from **VIII** (46.0 mg, 0.045 mmol, 1 eq) according to the cyclization general procedure and, after purification by reverse phase chromatography (eluent: from 80:20 H_2O+0.1%TFA:CAN to 10:90), was obtained as a glassy solid (29.0 mg, TFA salt, 61% yield). TLC: EtOAc:MeOH 70:30, R*f* = 0.7. ^{1}H NMR (400 MHz, MeOD): δ 4.82 (m, 1H, H4), 4.60 (d, *J* = 9.6 Hz, 1H, H2), 4.30-4.22 (m, 2H, Hα Asp, Hα Leu), 3.99-3.91 (m, 2H, H5a, Hα Arg), 3.62 (d, *J* = 11.2 Hz, 1H, H5b), 3.31-3.17 (m, 4H, H6', Hδ Arg), 2.90 (dd, *J* = 15.9, 5.7 Hz, 1H, Hβ Asp), 2.73-2.67 (m, 3H, Hβ Asp, CH_2 Pmc), 2.59 (s, 3H, CH_3 Pmc), 2.58 (s, 3H, CH_3 Pmc), 2.52-2.43 (m, 1H, H3a), 2.42-2.32 (m, 2H, H2'), 2.12 (s, 3H, CH_3 Pmc), 2.02 (bd, *J* = 14.0 Hz, 1H, H3b), 1.85 (t, *J* = 6.2 Hz, 2H, CH_2 Pmc), 1.82-1.49 (m, 11H, Hβ Leu, Hγ Leu, H3', H5', Hβ Arg, Hγ Arg), 1.48-1.41 (m, 11H, *t*Bu, H4'), 1.32 (s, 6H, CH_3 Pmc), 0.94 (d, *J* = 6.4 Hz, 3H, Hδ Leu), 0.93 (d, *J* = 6.4 Hz, 3H, Hδ Leu). MS (ES^+) *m/z* 958.5 $[M+H]^+$.

Cyclopeptide **14** was recovered after deprotection and purification by preparative RP-HPLC as described in the general procedure, using a linear gradient from 90% A to 40% B over 20 min, room temperature (R_t = 18.0 min), as a colourless glassy solid (16.3 mg, TFA salt, 92% yield). Purity of final

cyclopeptide was checked by HPLC and found as 95.6%. ^{1}H NMR (400 MHz, D_2O): δ 4.67-4.63 (m, 1H, H4), 4.51 (bd, *J* = 10.8 Hz, 1H, H2), 4.43 (dd, *J* = 8.2, 8.2 Hz, 1H, Hα Leu), 4.21 (dd, *J* = 6.0, 6.0 Hz, 1H, Hα Asp), 3.93-3.87 (m, 2H, H5a, Hα Arg), 3.61 (d, *J* = 12.0 Hz, 1H, H5b), 3.24 (t, *J* = 6.4 Hz, 2H, H6'), 3.20-3.10 (m, 2H, Hδ Arg), 3.01 (dd, *J* = 16.8, 6.8 Hz, 1H, Hβ Asp), 2.67 (dd, *J* = 16.5, 7.2 Hz, 1H, Hβ Asp), 2.50 (m, 1H, H3a), 2.35-2.29 (m, 2H, H2'), 1.82-1.74 (m, 2H, H3b, Hβ Leu), 1.71-1.58 (m, 2H, Hβ Arg), 1.55-1.24 (m, 7H, Hβ Leu, Hγ Arg, H5', H3'), 1.40-1.23 (m, 3H, Hγ Leu, H4'), 0.82 (d, *J* = 6.6 Hz, 3H, Hδ Leu), 0.79 (d, *J* = 6.6 Hz, 3H, Hδ Leu). HRMS(ES$^+$) $C_{27}H_{46}N_{11}O_7$ calcd for $[M+H]^+$ 636.3582, found 636.3591.

***Cyclo*[1-(6-azidohexanoyl)Amp-Phe-Arg-Gly-Asp] 15**

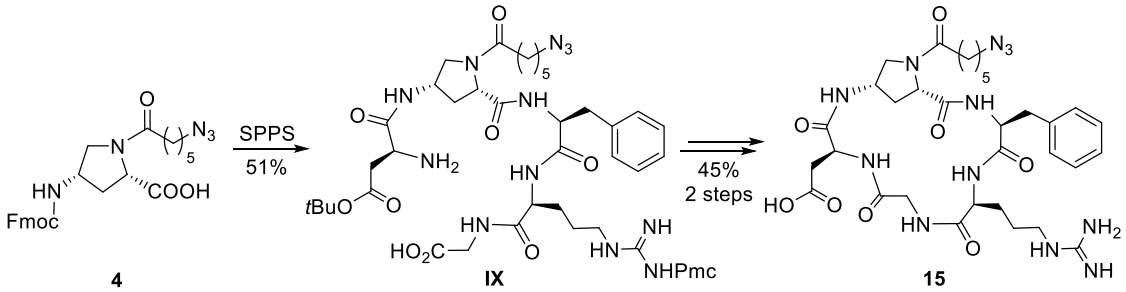

Cyclopeptide **15** was prepared according to the general procedure described for compound **11** by using the aminoproline module **4**. The linear pentapeptide **IX**, precursor of compound **15**, was prepared according to the procedure described for linear tetrapeptide **I** by using 2-chlorotrityl-Gly-H resin (97.2 mg, 0.056 mmol, 1.0 eq), Fmoc-Arg(Pmc)-OH (52.3 mg, 0.084 mmol, 1.5 eq), Fmoc-Phe-OH (32.5 mg, 0.084 mmol, 1.5 eq), the aminoproline module **4** (41.3 mg, 0.084 mmol, 1.5 eq) and Fmoc-Asp(*t*Bu)-OH (34.5 mg, 0.084 mmol, 1.5 eq). After the resin cleavage, compound **V** (32.2 mg, AcOH salt, 51% yield) was recovered as a colourless glassy solid and was used in the following step without further purification. MS (ES$^+$) *m/z* 1067.4 $[M+H]^+$.

The protected cyclopeptide intermediate was prepared starting from **IX** (32.2 mg, 0.028 mmol, 1 eq) according to the cyclization general procedure and, after reverse phase chromatography (eluent: from 80:20 H_2O+0.1%TFA:ACN to 10:90] was obtained as a glassy solid (19.2 mg, TFA salt 58% yield). TLC: EtOAc:MeOH 70:30, R*f* = 0.7. ^{1}H NMR (400 MHz, MeOD): δ 7.31-7.20 (m, 5H, ArH), 4.70 (dd, *J* = 7.8, 4.7 Hz, 1H, Hα Asp), 4.54 (m, 2H, H4, H2), 4.59 (dd, *J* = 8.1, 8.1 Hz, 1H, Hα Phe), 4.01 (d, *J* = 16.5 Hz,1H, Hα Gly), 3.85 (m, 1H, Hα Arg), 3.84 (dd, *J* = 11.3, 5.6 Hz, 1H, H5a), 3.68 (d, *J* = 16.5 Hz, 1H, Hα Gly), 3.59 (bd, *J* = 11.0 Hz, 1H, H5b), 3.29 (t, *J* = 6.0 Hz, 2H, H6'), 3.21-3.04 (m, 4H, Hβ Phe, Hδ Arg), 2.97 (dd, *J* = 16.9, 5.6 Hz, 1H, Hβ Asp), 2.75 (dd, *J* = 16.9, 8.1 Hz, 1H, Hβ Asp), 2.68 (t, *J* = 6.2 Hz, 2H, CH_2 Pmc), 2.58 (s, 3H, CH_3 Pmc), 2.57 (s, 3H, CH_3 Pmc), 2.55 (m, 1H, H3a), 2.46-2.29 (m, 2H, H2'), 2.17 (bd, *J* = 14.4 Hz, 1H, H3b), 2.13 (s, 3H, CH_3 Pmc), 1.86 (t, *J* = 7.6 Hz, 2H, CH_2 Pmc), 1.66-1.57 (m, 4H, H3', H5'), 1.54-1.39 (m, 13H, Hβ Arg, Hγ Arg, *t*Bu), 1.33-1.20 (m, 8H, CH_3 Pmc, H4'). MS (ES$^+$) *m/z* 1049.5 $[M+H]^+$.

Cyclopeptide **15** was recovered after deprotection and purification by preparative RP-HPLC as described in the general procedure, using a linear gradient from 80% A to 40% B over 20 min, room temperature (R_t = 17.2 min), as a colourless glassy solid (10.9 mg, TFA salt, 78% yield). Purity of the final cyclopeptide was checked by HPLC and found as 99%. ^{1}H NMR (400 MHz, D_2O): δ 7.48-7.30 (m, 5H, ArH), 4.74 (dd, *J* = 7.4, 7.4 Hz, 1H, Hα Asp), 4.59 (d, *J* = 10.2 Hz, 1H, H2), 4.53 (m, 1H, H4), 4.44 (dd, *J* = 7.8, 7.8 Hz, 1H, Hα Phe), 4.05 (dd, *J* = 9.4, 4.4 Hz, 1H, Hα Arg), 4.00 (d, *J* = 17.2 Hz, 1H, Hα Gly), 3.90 (dd, *J* = 11.7, 5.5 Hz, 1H, H5a), 3.78 (d, *J* = 16.9 Hz, 1H, Hα Gly), 3.71 (bd, *J* = 11.5 Hz, 1H,

H5b), 3.33 (t, *J* = 6.8 Hz, 2H, H6'), 3.28 (dd, J = 14.2, 7.0 HZ, 1H, Hβ Phe), 3.18-3.00 (m, 4H, Hβ Phe, Hδ Arg, Hβ Asp), 2.77 (dd, *J* = 15.9, 7.1 Hz, 1H, Hβ Asp), 2.66 (m, 1H, H3a), 2.49-2.32 (m, 2H, H2'), 2.16 (bd, *J* = 13.9 Hz, 1H, H3b), 1.95-1.77 (m, 1H, Hβ Arg), 1.70-1.28 (m, 8H, Hβ Arg, H3', H5', H4', Hγ Arg), 1.28-1.12 (m, 1H, Hγ Arg). HRMS(ES$^+$) $C_{32}H_{47}N_{12}O_8$ calcd for $[M+H]^+$ 727.3634, found 727.3628.

***Cyclo*[1-(6-azidohexanoyl)Amp-Leu-Arg-Gly-Asp] 16**

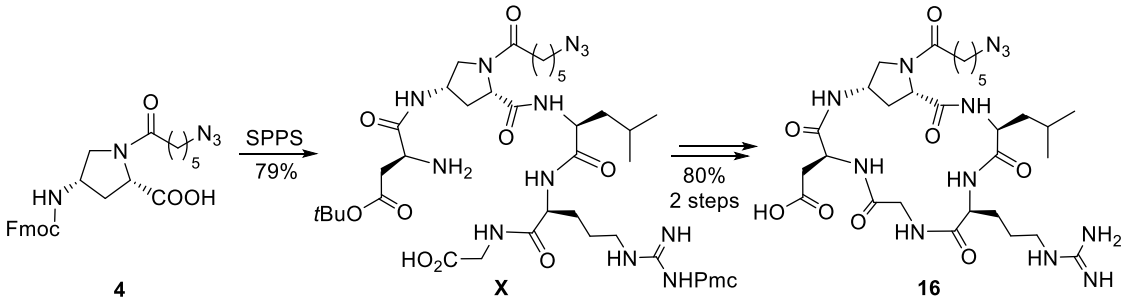

Cyclopeptide **16** was prepared according to the general procedure described for compound **11** by using the aminoproline module **4**. The linear pentapeptide **X**, precursor of compound **11**, was prepared according to the procedure described for linear tetrapeptide **I** by using 2-chlorotrityl-Gly-H resin (103 mg, 0.06 mmol, 1.0 eq), Fmoc-Arg(Pmc)-OH (55.7 mg, 0.09 mmol, 1.5 eq), Fmoc-Leu-OH (31.8 mg, 0.09 mmol, 1.5 eq), the aminoproline module **4** (44.2 mg, 0.09 mmol, 1.5 eq) and Fmoc-Asp(*t*Bu)-OH (37.0 mg, 0.09 mmol, 1.5 eq). After the resin cleavage, compound **X** (51.6 mg, AcOH salt, 79% yield) was recovered as a colourless glassy solid and was used in the following step without further purification. MS (ES$^+$) *m/z* 1033.6 $[M+H]^+$.

The protected cyclopeptide intermediate was prepared starting from **X** (51.6 mg, 0.047 mmol, 1 eq) according to the cyclization general procedure and, after reverse phase chromatography (eluent: from 90:10 H_2O+0.1%TFA:ACN to 10:90] was obtained as a glassy solid (42.5 mg, TFA salt 80% yield). TLC: EtOAc:MeOH 70:30, R*f* = 0.7. ^{1}H NMR (400 MHz, MeOD): δ 4.69 (dd, *J* = 7.6, 6.6 Hz, 1H, Hα Asp), 4.60 (bd, *J* = 9.9 Hz, 1H, H2), 4.51 (m, 1H, H4), 4.13-4.04 (m, 2H, Hα Arg, Hα Leu), 4.00 (d, *J* = 16.4 Hz, 1H, Hα Gly), 3.90 (dd, *J* = 11.2, 5.5 Hz, 1H, H5a), 3.63 (d, *J* = 16.4 Hz, 1H, Hα Gly), 3.59 (d, *J* = 10.8 Hz, 1H, H5b), 3.33-3.27 (m, 4H, H6', Hδ Arg), 2.92 (dd, *J* = 16.9, 5.1 Hz, 1H, Hβ Asp), 2.70 (t, *J* = 6.7 Hz, 2H, CH_2 Pmc), 2.65-2.54 (m, 8H, Hβ Asp, CH_3 Pmc, H3a), 2.43-2.29 (m, 2H, H2'), 2.19 (bd, *J* = 14.7 Hz, 1H, H3b), 2.13 (s, 3H, CH_3 Pmc), 2.06-1.92 (m, 1H, Hβ Leu) 1.89-1.78 (m, 3H, CH_2 Pmc, Hβ Leu), 1.72-1.55 (m, 9H, Hγ Leu, Hβ Arg, Hγ Arg, H5', H3'), 1.48-1.42 (m, 11H, *t*Bu, H4'), 1.34 (s, 6H, CH_3 Pmc), 1.04 (d, *J* = 5.7 Hz, 3H, Hδ Leu), 0.98 (d, *J* = 6.5 Hz, 3H, Hδ Leu). MS (ES$^+$) *m/z* 1015.4 $[M+H]^+$.

Cyclopeptide **16** was recovered after deprotection and purification by preparative RP-HPLC as described in the general procedure, using linear gradient from 90% A to 40% B over 30 min, room temperature (R_t = 15.7 min), as a colourless glassy solid (30.4 mg, TFA salt, quantitative yield). Purity of the final cyclopeptide was checked by HPLC and found as 99%. ^{1}H NMR (400 MHz, D_2O): δ 4.64 (dd, *J* = 7.1, 6.8 Hz, 1H, Hα Asp). 4.50 (d, *J* = 11.2 Hz, 1H, H2), 4.43 (m, 1H, H4), 4.16-4.10 (m, 1H, Hα Arg), 4.03-3.98 (m, 1H, Hα Leu), 3.87-3.80 (m, 2H, Hα Gly, H5a), 3.67 (d, *J* = 17.2 Hz, 1H, Hα Gly), 3.60 (d, *J* = 11.5 Hz, 1H, H5b), 3.21 (t, *J* = 7.1 Hz, 2H, H6'), 3.14-3.06 (m, 2H, Hδ Arg), 2.94 (dd, *J* = 16.9, 6.6 Hz, 1H, Hβ Asp), 2.62 (dd, *J* = 17.1, 7.3 Hz, 1H, Hβ Asp), 2.57 (m, 1H, H3a), 2.37-2.22 (m, 2H, H2'), 2.04 (d, *J* = 15.1 Hz, 1H, H3b), 1.89-1.57 (m, 4H, Hβ Arg, Hβ Leu, Hγ Leu) 1.54-1.42 (m, 7H,

H3', H5', Hγ Arg, Hβ Leu), 1.32-1.23 (m, 2H, H4'), 0.87 (d, *J* = 5.6 Hz, 3H, Hδ Leu), 0.82 (d, *J* = 6.4 Hz, 3H, Hδ Leu). HRMS(ES$^+$) $C_{29}H_{49}N_{12}O_8$ calcd for $[M+H]^+$ 693.3791, found 693.3805.

***Cyclo*[1-(4-azidobutyl)Amp-Leu-Arg-Gly-Asp] 17**

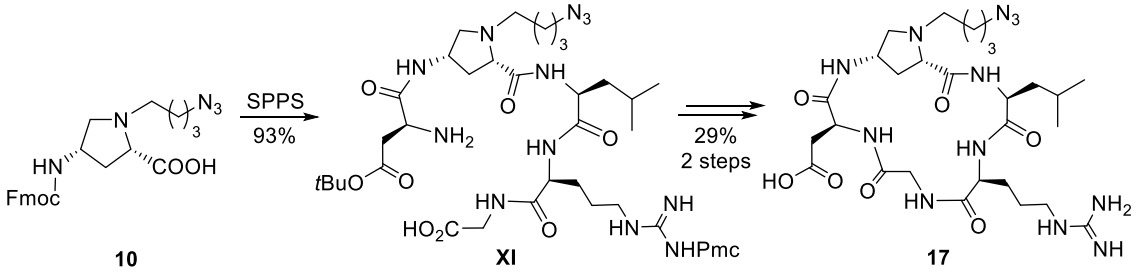

Cyclopeptide **17** was prepared according to the general procedure described for compound **11** by using the aminoproline module **10**. The linear pentapeptide **XI**, precursor of compound **17**, was prepared according to the procedure described for linear tetrapeptide **I** by using 2-chlorotrityl-Gly-H resin (76.7 mg, 0.045 mmol, 1.0 eq), Fmoc-Arg(Pmc)-OH (41.3 mg, 0.067 mmol, 1.5 eq), Fmoc-Leu-OH (23.6 mg, 0.067 mmol, 1.5 eq), the aminoproline module **10** (30 mg, 0.067 mmol, 1.5 eq) and Fmoc-Asp(*t*Bu)-OH (27.4 mg, 0.067 mmol, 1.5 eq). After the resin cleavage, compound **XI** (43.5 mg, AcOH salt, 93% yield) was recovered as a colourless glassy solid and was used in the following step without further purification. MS (ES$^+$) *m/z* 991.6 $[M+H]^+$.

The protected cyclopeptide intermediate was prepared starting from **XI** (43.5 mg, 0.041 mmol, 1 eq) according to the cyclization general procedure and, after reverse phase chromatography (eluent: from 90:10 H_2O+0.1%TFA:ACN to 10:90) was obtained as a glassy solid (15.6 mg, TFA salt, 32% yield). TLC: EtOAc:MeOH 70:30, R*f* = 0.7. ^{1}H NMR (400 MHz, MeOD): δ 4.71 (dd, *J* = 6.8, 6.8 Hz, 1H, Hα Asp), 4.51 (m, 1H, H4), 4.47-4.42 (m, 2H, H2, Hα Leu), 4.20 (m, 1H, Hα Arg), 4.00 (bd, *J* = 12.2 Hz, 1H, H5a), 3.82 (d, *J* = 15.8 Hz, 1H, Hα Gly), 3.64 (d, *J* = 15.8 Hz, 1H, Hα Gly), 3.46 (m, 1H, H5b), 3.38 (t, *J* = 6.7 Hz, 2H, H4'), 3.31-3.24 (m, 2H, Hδ Arg), 3.24-3.14 (m, 2H, H1'), 3.12-3.01 (m, 1H, H3a), 2.95 (dd, *J* = 16.4, 6.2 Hz, 1H, Hβ Asp), 2.69 (m, 3H, H3b, CH_2 Pmc), 2.62 (dd, *J* = 16.6, 7.1 Hz, 1H, Hβ Asp) 2.58 (s, 3H, CH_3 Pmc), 2.57 (s, 3H, CH_3 Pmc), 2.12 (s, 3H, CH_3 Pmc), 1.92-1.83 (m, 3H, Hβ Leu, CH_2 Pmc), 1.80-1.52 (m, 10H, H2', H3', Hβ Leu, Hγ Leu, Hβ Arg, Hγ Arg), 1.46 (s, 9H, *t*Bu), 1.33 (s, 6H, CH_3 Pmc), 1.02 (d, *J* = 6.8 Hz, 3H, Hδ Leu), 0.96 (d, *J* = 6.3 Hz, 3H, Hδ Leu). MS (ES$^+$) *m/z* 973.7 $[M+H]^+$.

Cyclopeptide **17** was recovered after deprotection and purification by preparative RP-HPLC as described in the general procedure, using linear gradient from 90% A to 40% B over 20 min, room temperature (R_t = 12.1 min), as a colourless glassy solid (10.5 mg, TFA salt, 90% yield). Purity of the final cyclopeptide was checked by HPLC and found as 99%. ^{1}H NMR (400 MHz, D_2O): δ 4.69 (m, 1H, Hα Asp), 4.44-4.38 (m, H2, H2, H4), 4.32 (dd, *J* = 9.9, 4.7 Hz, 1H, Hα Leu), 4.08 (m, 1H, Hα Arg), 3.92 (bd, *J* = 12.2 Hz, 1H, H5a), 3.78 (d, *J* = 16.9 Hz, 1H, Hα Gly), 3.68 (d, *J* = 16.4, 1H, Hα Gly), 3.40 (m, 1H, H5a), 3.27 (t, *J* = 6.4, 2H, H4'), 3.24-3.16 (m, 2H, Hδ Arg), 3.16-3.06 (m, 2H, H1'), 2.98 (m, 1H, H3a), 2.93 (dd, *J* = 17.4, 6.9 Hz, 1H, Hβ Asp), 2.68 (dd, *J* = 17.2, 7.0 Hz, 1H, Hβ Asp), 2.37 (dd, *J* = 15.1, 3.9 Hz, 1H, H3b), 1.85-1.74 (m, 1H, Hβ Leu), 1.71-1.44 (m, 10H, H3', H2', Hβ Leu, Hγ Leu, Hβ Arg, Hγ Arg), 0.88 (d, *J* = 6.1 Hz, 3H, Hδ Leu), 0.84 (d, *J* = 6.2 Hz, 3H, Hδ Leu). HRMS(ES$^+$) $C_{27}H_{46}N_{12}O_7$ calcd for $[M+H]^+$ 651.3612, found 651.3684.

***Cyclo*[1-(6-aminohexyl)Amp-Leu-Arg-Gly-Asp] 18**

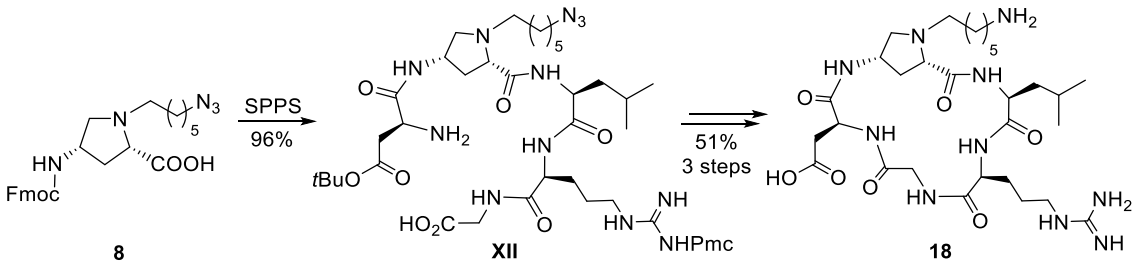

Cyclopeptide **18** was prepared according to the general procedure described for compound **11** by using the aminoproline module **8**. The linear pentapeptide **XII**, precursor of compound **18**, was prepared according to the procedure described for linear tetrapeptide **I** by using 2-chlorotrityl-Gly-H resin (49.5 mg, 0.029 mmol, 1.0 eq), Fmoc-Arg(Pmc)-OH (26.6 mg, 0.043 mmol, 1.5 eq), Fmoc-Leu-OH (15.2 mg, 0.043 mmol, 1.5 eq), the aminoproline module **8** (23 mg, 0.043 mmol, 1.5 eq) and Fmoc-Asp(*t*Bu)-OH (17.7 mg, 0.043 mmol, 1.5 eq). After the resin cleavage, compound **XII** (31.3 mg, AcOH salt, 96% yield) was recovered as a colourless glassy solid and was used in the following step without further purification. MS (ES^+) *m/z* 1019.7 $[M+H]^+$.

The protected cyclopeptide intermediate was prepared starting from **XII** (31.3 mg, 0.027 mmol, 1 eq) according to the cyclization general procedure and, after reverse phase chromatography (eluent: from 90:10 H_2O+0.1%TFA:ACN to 10:90] was obtained as a glassy solid (21.7 mg, TFA salt 71% yield). TLC: EtOAc:MeOH 70:30, R*f* = 0.7. ^{1}H NMR (400 MHz, MeOD): δ 4.72 (dd, *J* = 6.3, 6.3 Hz, 1H, Hα Asp), 4.52 (m, 1H, Hα Leu), 4.72-4.42 (m, 2H, H2, H4), 4.20 (dd, *J* = 9.9, 5.8 Hz, 1H, Hα Arg), 3.99 (d, *J* = 12.2 Hz, 1H, H5a), 3.82 (d, *J* = 15.9 Hz, 1H, Hα Gly), 3.63 (d, *J* = 16.4 Hz, 1H, Hα Gly), 3.46 (m, 1H, H5b), 3.33 (t, *J* = 1.7 Hz, 2H, H6'), 3.30-3.16 (m, 4H, Hδ Arg, H1'), 3.12-3.02 (m, 1H, H3a), 2.94 (dd, *J* = 16.4, 6.2 Hz, 1H, Hβ Asp), 2.69 (t, *J* = 6.9 Hz, 2H, CH_2 Pmc), 2.66-2.61 (m, 2H, H3b, Hβ Asp), 2.59 (s, 3H, CH_3 Pmc), 2.58 (s, 3H, CH_3 Pmc), 2.12 (s, 3H, CH_3 Pmc), 1.92-1.52 (m, 13H, Hβ Arg, Hγ Arg, H5', H3', Hβ Leu, Hγ Leu, CH_2 Pmc), 1.46 (s, 9H, *t*Bu), 1.42 (m, 4H, H2', H4'), 1.33 (s, 6H, CH_3 Pmc), 1.01 (d, *J* = 6.4 Hz, 3H, Hδ Leu), 0.96 (d, *J* = 6.9 Hz, 3H, Hδ Leu). MS (ES^+) *m/z* 1001.4 $[M+H]^+$

The azido-terminating cyclopeptide intermediate (21.7 mg, 0.019 mmol, 1 eq) was subjected to the reduction of the terminal azido group according to the procedure described for compound **12**. The amine-terminating cyclopeptide (15.6 mg, HCO_2H salt, 75%) was recovered as a glassy solid and was used in the following step without further purification. TLC: EtOAc:MeOH 70:30, R*f*: 0.1. ^{1}H NMR (400 MHz, MeOD): δ 4.75 (dd, *J* = 7.1, 7.1 Hz, 1H, Hα Asp), 4.43-4.35 (m, 2H, H2, H4), 4.05 (m, 1H, Hα Arg), 3.94 (d, *J* = 16.1 Hz, 1H, Hα Gly), 3.62 (d, *J* = 16.2 Hz, 1H, Hα Gly), 3.50 (m, 1H, Hα Leu), 3.27-3.12 (m, 3H, Hδ Arg, H5a), 3.03-2.87 (m, 3H, H6', Hβ Asp), 2.82 (dd, *J* = 10.2, 2.1 Hz, 1H, H5b), 2.75-2.65 (m, 4H, H1', CH_2 Pmc), 2.64-2.54 (m, 8H, Hβ Asp, H3a, CH_3 Pmc), 2.14 (m, 1H, H3b), 2.12 (s, 3H, CH_3 Pmc), 1.86 (t, *J* = 7.1 Hz, 2H, CH_2 Pmc), 1.80-1.48 (m, 13H, Hβ Arg, Hγ Arg, Hβ Leu, Hγ Leu, H2', H3', H5'), 1.46 (m, 11H, H4', *t*Bu), 1.43 (m, 6H, CH_3 Pmc), 1.01 (d, *J* = 6.0 Hz, 3H, Hδ Leu), 0.95 (d, *J* = 6.2 Hz, 3H, Hδ Leu). MS (ES^+) *m/z* 975.5 $[M+H]^+$

Cyclopeptide **18** was recovered after deprotection and purification by preparative RP-HPLC as described in the general procedure, using linear gradient from 90% A to 40% B over 30 min, room temperature; R_t = 15.7 min] as a colourless glassy solid (14 mg, TFA salt, 97% yield). The purity of the final peptide was checked by HPLC and found as 99%. ^{1}H NMR (400 MHz, D_2O): δ 4.68 (m, 1H, Hα Asp), 4.45-4.35 (m, 3H, H2, H4, Hα Leu), 4.07 (m, 1H, Hα Arg), 3.93 (bd, *J* = 13.0 Hz, 1H, H5a),

3.77 (d, *J* = 16.7 Hz, 1H, Hα Gly), 3.68 (d, *J* = 16.4 Hz, 1H, Hα Gly), 3.39 (m, 1H, H5b), 3.22-3.05 (m, 4H, H6', Hδ Arg), 3.02-2.84 (m, 4H, H1', Hβ Asp, H3a), 2.71 (dd, *J* = 17.6, 7.2 Hz, 1H, Hβ Asp), 2.37 (dd, *J* = 15.3, 4.3 Hz, 1H, H3b), 1.84-1.44 (m, 12H, Hβ Arg, Hγ Arg, Hβ Leu, Hγ Leu, H2', H3', H5'), 1.34-1.25 (m, 3H, Hβ Leu, H4') 0.88 (d, *J* = 6.2 Hz, 3H, Hδ Leu), 0.84 (d, *J* = 6.1 Hz, 3H, Hδ Leu). HRMS(ES$^+$) $C_{29}H_{52}N_{10}O_7$ calcd for $[M+H]^+$ 653.4020, found 653.4093.

***Cyclo*[1-(6-azidohexanoyl)Amp-Arg-Gly-Asp-Phe] 19**

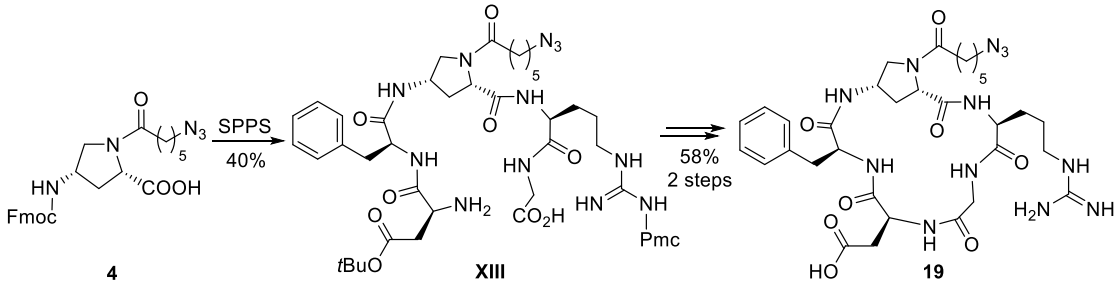

Cyclopeptide **19** was prepared according to the general procedure described for compound **11** by using the aminoproline module **4**. The linear pentapeptide **XIII**, precursor of compound **19**, was prepared according to the procedure described for linear tetrapeptide **I** by using 2-chlorotrityl-Gly-H resin (57 mg, 0.033 mmol, 1.0 eq), Fmoc-Arg(Pmc)-OH (30.9 mg, 0.050 mmol, 1.5 eq), the aminoproline module **4** (24.6 mg, 0.050 mmol, 1.5 eq), Fmoc-Phe-OH (19.4 mg, 0.050 mmol, 1.5 eq), and Fmoc-Asp(*t*Bu)-OH (20.6 mg, 0.050 mmol, 1.5 eq). Coupling with Fmoc-Phe-OH was repeated twice in the same conditions (19.4 mg, 0.050 mmol, 1.5 eq). After the resin cleavage, compound **XIII** (14.6 mg, AcOH salt, 40% yield) was recovered as a colourless glassy solid and was used in the following step without further purification. MS (ES$^+$) *m/z* 1067.5 $[M+H]^+$.

The protected cyclopeptide intermediate was prepared starting from **XIII** (14.6 mg, 0.013 mmol, 1 eq) according to the cyclization general procedure and, after reverse phase chromatography (eluent: from 90:10 to H_2O+0.1%TFA:ACN to 10:90) was obtained as a glassy solid (10.3 mg, TFA salt 67% yield). TLC: EtOAc:MeOH 70:30, R*f* = 0.7. ^{1}H NMR (400 MHz, MeOD): δ7.29 (m, 5H, ArH), 4.59 (m, 2H, H2, H4), 4.40 (m, 1H, Hα Asp), 4.29 (m, 1H, Hα Phe), 4.08 (m, 2H, Hα Arg, Hα Gly), 4.05 (dd, *J* = 11.4, 5.3 Hz, 1H, H5a), 3.64-3.54 (m, 2H, H5b, Hα Gly), 3.28 (m, 3H, H6', Hβ Phe), 3.25-3.15 (m, 2H, Hδ Arg), 3.04 (dd, *J* = 13.9, 10.6 Hz, 1H, Hβ Phe), 2.77 (m, 2H, Hβ Asp), 2.68 (t, *J* = 6.9 Hz, 2H, CH_2 Pmc), 2.58 (s, 3H, CH_3 Pmc), 2.57 (s, 3H, CH_3 Pmc), 2.50 (m, 1H, H3a), 2.44-2.27 (m, 2H, H2'), 2.14-2.12 (m, 4H, CH_3 Pmc, H3b), 1.96-1.81 (m, 4H, CH_2 Pmc, Hβ Arg), 1.68-1.56 (m, 6H, Hγ Arg, H5', H3'), 1.43 (m, 11H, *t*Bu, H4'), 1.32 (s, 6H, CH_3 Pmc). MS (ES$^+$) *m/z* 1049.2 $[M+H]^+$.

Cyclopeptide **19** was recovered after deprotection and purification by preparative RP-HPLC as described in the general procedure, using linear gradient from 80% A to 40% B over 20 min, room temperature (R_t = 16.1 min), as a colourless glassy solid (5.4 mg, TFA salt, 72% yield). Purity of final peptide was checked by HPLC and found as 99%. ^{1}H NMR (400 MHz, D_2O): δ7.30 (m, 2H, ArH), 7.23 (m, 1H, ArH), 7.17 (m, 2H, ArH), 4.53-4.47 (m, 2H, H2, H4), 4.41 (dd, *J* = 10.5, 4.9 Hz, 1H, Hα Phe), 4.33 (t, *J* = 4.3 Hz, 1H, Hα Asp), 4.02 (t, *J* = 7.4 Hz, 1H, Hα Arg), 3.95 (d, *J* = 17.8 Hz, 1H, Hα Gly), 3.79 (dd, *J* = 11.1, 5.5 Hz, 1H, H5a), 3.69 (d, *J* = 17.2 Hz, 1H, Hα Gly), 3.56 (d, *J* = 12.1 Hz, 1H, H5b), 3.27 (d, *J* = 4.2 Hz, 1H, Hβ Phe), 3.22 (t, *J* = 6.9 Hz, 2H, H6'), 3.16 (t, *J* = 6.9 Hz, 2H, Hδ Arg), 2.89 (dd, *J* = 13.9, 10.5 Hz, 1H, Hβ Phe), 2.71 (m, 2H, Hβ Asp), 2.59-2.51 (ddd, *J* = 14.8, 10.6, 6.8 Hz, 1H, H3a), 3.28-2.23 (m, 2H, H2'), 1.98 (bd, *J* = 14.7 Hz, 1H, H3b), 1.82-1.76 (m, 2H, Hβ Arg), 1.69-1.45 (m, 6H,

Hγ Arg, H3', H5'), 1.34-1.28 (m, 2H, H4'). HRMS(ES$^+$) $C_{32}H_{46}N_{12}O_8Na$ calcd for $[M+Na]^+$ 749.3454, found 749.3459.

***Cyclo*[1-(4-azidobutyl)Amp-Arg-Gly-Asp-Phe] 20**

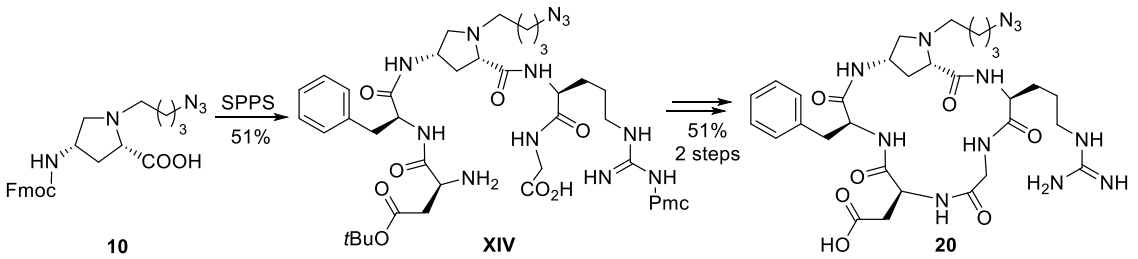

Cyclopeptide **20** was prepared according to the general procedure described for compound **11** by using the aminoproline module **10**. The linear pentapeptide **XIV**, precursor of compound **20**, was prepared according to the procedure described for linear tetrapeptide **I** by using 2-chlorotrityl-Gly-H resin (92 mg, 0.053 mmol, 1.0 eq), Fmoc-Arg(Pmc)-OH (49.5 mg, 0.080 mmol, 1.5 eq), the aminoproline module **10** (45 mg, 0.080 mmol, 1.5 eq), Fmoc-Phe-OH (31 mg, 0.080 mmol, 1.5 eq), and Fmoc-Asp(*t*Bu)-OH (32.9 mg, 0.080 mmol, 1.5 eq). Coupling with Fmoc-Phe-OH was repeated twice in the same conditions (31 mg, 0.080 mmol, 1.5 eq). After the resin cleavage, compound **XIV** (31 mg, AcOH salt, 51% yield) was recovered as a colourless glassy solid and was used in the following step without further purification. MS (ES$^+$) *m/z* 1025.7 $[M+H]^+$.

The protected cyclopeptide intermediate was prepared starting from **XIV** (31 mg, 0.027 mmol, 1 eq) according to the cyclization general procedure and, after reverse phase chromatography (eluent: from 90:10 H_2O+0.1%TFA:ACN to 10:90] was obtained as a glassy solid (18.3 mg, TFA salt 55% yield). TLC: Petroleum Ether:EtOAc 70:30, R*f* = 0.7. ^{1}H NMR (400 MHz, CD_3OD) δ 7.30-7.10 (m, 5H, ArH), 4.58-4.54 (m, 1H, H4), 4.39-4.38 (m, 1H, H2), 4.43-4.35 (m, 2H, Hα Asp, Hα Phe), 4.27 (t, *J* = 6.9 Hz 1H, Hα Arg), 3.97 (d, *J* = 16.7 Hz, 1H, Hα Gly), 3.92 (d, *J* = 11.6 Hz, 1H, H5a), 3.72 (d, *J* = 16.1 Hz, 1H, Hα Gly), 3.52-3.47(m, 1H, H5b), 3.41-3.38 (m, 5H, H4', Hβ Phe, Hδ Arg), 3.23 (t, *J* = 6.6 Hz, 2H, H1'), 3.06-2.87 (m, 3H, Hβ Phe, Hβ Asp, H3a), 2.74-2.64 (m, 3H, Hβ Asp, CH_2 Pmc) 2.58 (s, 3H, CH_3 Pmc), 2.57 (s, 3H, CH_3 Pmc), 2.36 (dd, *J* = 16.7, 9.1 Hz, 1H, H3b), 2.10 (s, 3H, CH_3Pmc), 1.84 (t, *J* = 6.7 Hz, 2H, CH_2 Pmc), 1.82-1.60 (m, 8H, H3', H2', Hβ Arg, Hγ Arg), 1.52 (s, 9H, *t*Bu), 1.31 (s, 6H, CH_3 Pmc). MS (ES$^+$) *m/z* 1006.6 $[M+H]^+$.

Cyclopeptide **20** was recovered after deprotection and purification by preparative RP-HPLC as described in the general procedure, using a linear gradient from 90% A to 40% B over 25 min, room temperature (R_t = 18.6 min), as a colourless glassy solid (12.6 mg, TFA salt, 92% yield). Purity of the final peptide was checked by HPLC and found as 96.8%. ^{1}H NMR (400 MHz, D_2O) δ 7.26 (m, 2H, ArH), 7.19 (m, 1H, ArH), 7.13 (m, 2H, ArH), 4.53-4.47 (m, 2H, H4, Hα Asp), 4.42 (dd, *J* = 8.8, 5.1 Hz, 1H, H2), 4.34 (dd, *J* = 8.4, 5.2 Hz, 1H, Hα Phe), 4.09 (dd, *J* = 7.2, 7.2 Hz, 1H, Hα Arg), 3.83-3.77 (m, 2H, H5a, Hα Gly), 3.74 (d, *J* = 16.4 Hz, 1H, Hα Gly), 3.42 (dd, *J* = 5.8, 6.7 Hz, 1H, H5b), 3.28-3.18 (m, 5H, Hβ Asp, Hδ Arg, H4'), 3.11 (t, *J* = 6.8 2H, H1'), 2.94-2.81 (m, 2H, H3a, Hβ Asp), 2.51 (dd, *J* = 12.3, 4.9 Hz, 1H, Hβ Phe), 2.33 (dd, *J* = 12.0, 8.5 Hz, 1H, Hβ Phe), 2.23 (bd, *J* = 14.7 Hz, 1H, H3b), 1.72-1.48 (m, 8H, H3', H2', Hβ Arg, Hγ Arg). HRMS(ES$^+$) $C_{30}H_{44}N_{12}O_7$ calcd for $[M+H]^+$ 685.3436, found 685.3441.

***Cyclo*{1-[*N*-(6-azidohexanoyl)phenylalanyl]Amp-Arg-Gly-Asp-Phe} 21**

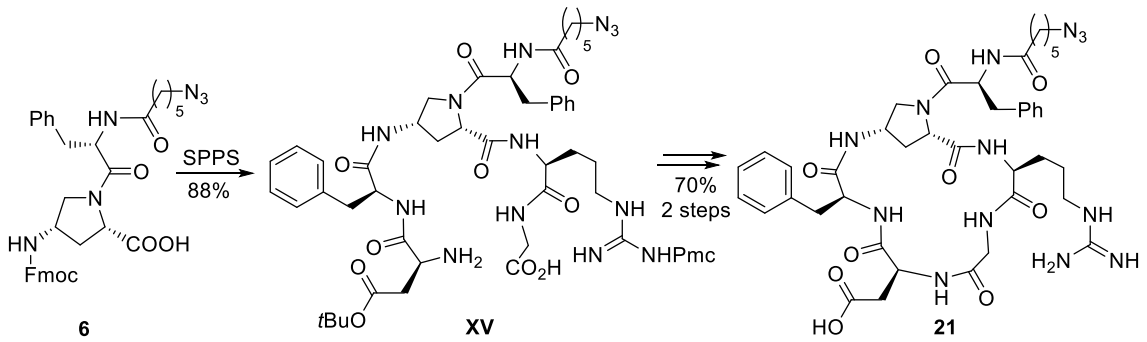

Cyclopeptide **19** was prepared according to the general procedure described for compound **11** by using the aminoproline module **6**. The linear pentapeptide **XV**, precursor of compound **21**, was prepared according to the procedure described for linear tetrapeptide **I** by using 2-chlorotrityl-Gly-H resin (47.7 mg, 0.027 mmol, 1.0 eq), Fmoc-Arg(Pmc)-OH (25.7 mg, 0.041 mmol, 1.5 eq), the aminoproline module **6** (26.5 mg, 0.041 mmol, 1.5 eq), Fmoc-Phe-OH (31.8 mg, 0.082 mmol, 3.0 eq), and Fmoc-Asp(*t*Bu)-OH (17 mg, 0.041 mmol, 1.5 eq). Coupling with Fmoc-Phe-OH was repeated twice in the same conditions (31.8 mg, 0.082 mmol, 3.0 eq). After the resin cleavage, compound **XV** (30.5 mg, AcOH salt, 88% yield) was recovered as a colourless glassy solid and was used in the following step without further purification. MS (ES^+) *m/z* 1215.1 $[M+H]^+$.

The protected cyclopeptide intermediate was prepared starting from **XV** (30.5 mg, 0.024 mmol, 1 eq) according to the cyclization general procedure and, after reverse phase chromatography (eluent: from 80:20 H_2O+0.1%TFA:ACN to 10:90) was obtained as a glassy solid (24.8 mg, TFA salt 80% yield). TLC: EtOAc:MeOH 70:30, R*f* = 0.7. ^{1}H NMR (400 MHz, MeOD) δ7.31-7.12 (m, 10H, ArH), 4.79 (dd, *J* = 7.7, 7.7 Hz, 1H, Hα Phe), 4.65 (d, *J* = 9.9 Hz, 1H, H2) 4.61-4.50 (m, 2H, H4, Hα Asp), 4.30 (m, 1H, Hα Phe), 4.18-4.10 (m, 1H, Hα Arg), 4.09 (d, *J* = 17.7 Hz, 1H, Hα Gly), 3.95 (m, 1H, H5a), 3.69 (m, 1H, H5b), 3.58 (d, *J* = 17.8 Hz, 1H, Hα Gly), 3.24 (t, *J* = 6.7 Hz, 2H, H6'), 3.20-3.14 (m, 4H, Hβ Phe, Hδ Arg), 3.08-2.96 (m, 2H, Hβ Phe), 2.74.2.60 (m, 4H, Hβ Asp, CH_2 Pmc), 2.59 (s, 3H, CH_3 Pmc), 2.58 (s, 3H, CH_3 Pmc), 2.53 (m, 1H, H3a), 2.18-2.13 (m, 3H, H3b, H2'), 2.12 (s, 3H, CH_3 Pmc), 1.89-1.79 (m, 4H, Hβ Arg, CH_2 Pmc), 1.73-1.50 (m, 8H, Hγ Arg, H3', H5', H4'), 1.44 (s, 9H, *t*Bu), 1.32 (s, 6H, CH_3 Pmc). MS (ES^+) *m/z* 1196.7 $[M+H]^+$.

Cyclopeptide **21** was recovered after deprotection and purification by preparative RP-HPLC as described in the general procedure, using a linear gradient from 80% A to 30% B over 25 min, room temperature (R_t = 22.7 min) as a colourless glassy solid (17.2 mg, TFA salt, 92% yield). Purity of final compound was checked by HPLC and found as 99%.^{1}H NMR (400 MHz, MeOD) δ 7.34-7.18 (m, 10H, ArH), 4.78 (t, *J* = 7.7 Hz, 1H, Hα Phe), 4.50 (bd, *J* = 8.2 Hz, 1H, H2), 4.40 (dd, *J* = 13.8, 6.8 Hz, 1H, Hα Phe), 4.35 (m, 1H, Hα Asp), 4.28 (m, 1H, H4), 4.12 (d, *J* = 16.9 Hz, 1H, Hα Gly), 4.01-3.96 (m, 2H, Hα Arg, H5a), 3.70 (d, *J* = 15.7 Hz, 1H, H5b), 3.61 (d, *J* = 17.1 Hz, 1H, Hα Gly), 3.31-3.21 (m, 4H, Hδ Arg, H6'), 3.12-2.95 (m, 3H, Hβ Phe, Hβ Asp), 2.93-2.82 (m, 1H, Hβ Asp), 2.81-2.75 (m, 2H, Hβ Phe), 2.27-2.11 (m, 3H, H2', H3a), 2.03 (bd, *J* = 14.7 Hz, 1H, H3b), 1.98-1.85 (m, 2H, Hβ Arg), 1.84-1.67 (m, 2H, Hγ Arg), 1.63-1.46 (m, 4H, H5', H3'), 1.38-1.29 (m, 2H, H4'). HRMS(ES^+) $C_{41}H_{55}N_{13}O_9$ calcd for $[M+H]^+$ 874.4246, found 874.4250.

***Cyclo*[1-(6-azidohexanoyl)Amp-Phe-Arg-Gly-Asp-Leu] 22**

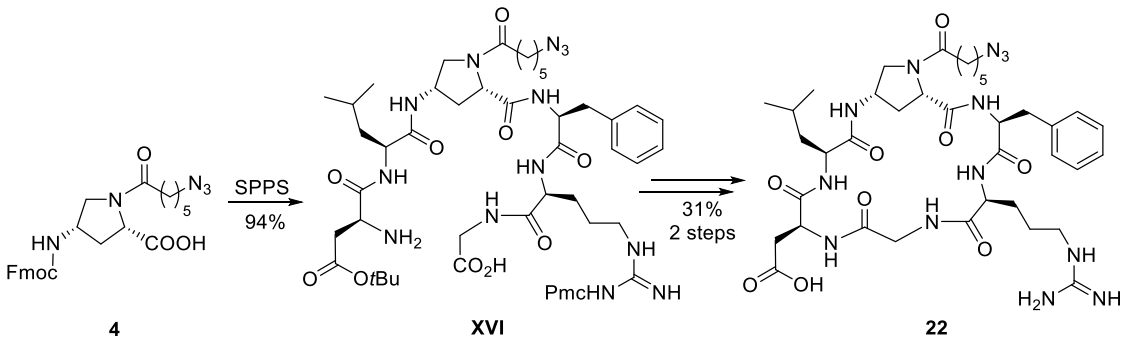

Cyclopeptide **21** was prepared according to the general procedure described for compound **11** by using the aminoproline module **4**. The linear hexapeptide **XVI**, precursor of compound **17**, was prepared according to the procedure described for linear tetrapeptide **I** by using 2-chlorotrityl-Gly-H resin (93.1 mg, 0.054 mmol, 1.0 eq), Fmoc-Arg(Pmc)-OH (50.1 mg, 0.081 mmol, 1.5 eq), Fmoc-Phe-OH (31.4 mg, 0.081 mmol, 1.5 eq), the aminoproline module **4** (40 mg, 0.081 mmol, 1.5 eq), Fmoc-Leu-OH (28.6 mg, 0.081 mmol, 1.5 eq) and Fmoc-Asp(*t*Bu)-OH (33.3 mg, 0.081 mmol, 1.5 eq). Coupling with Fmoc-Phe-OH was repeated twice in the same conditions (31.4 mg, 0.081 mmol, 1.5 eq). After the resin cleavage, compound **XVI** (63.2 mg, AcOH salt, 94% yield) was recovered as a colourless glassy solid and was used in the following step without further purification. MS (ES^+) *m/z* 1180.4 $[M+H]^+$.

The protected cyclopeptide intermediate was prepared starting from **XVI** (63.2 mg, 0.051 mmol, 1 eq) according to the cyclization general procedure and, after reverse phase chromatography (eluent: from 80:20 H_2O+0.1%TFA:ACN to 10:90] was obtained as a glassy solid (20.4 mg, TFA salt 32% yield). TLC: EtOAc:MeOH 70:30, R*f* = 0.7. ^{1}H NMR (400 MHz, MeOD): δ7.33-7.17 (m, 5H, ArH), 4.53 (m, 1H, H2), 4.42 (m, 1H, Hα Asp), 4.39-4.30 (m, 2H, Hα Leu, H4), 4.18 (m, 1H, Hα Phe), 4.01-3.84 (m, 3H, Hα Gly, Hα Arg), 3.81 (dd, *J* = 11.4, 6.4 Hz, 1H, H5a), 3.67 (bd, *J* = 11.9 Hz, 1H, H5b), 3.27 (t, *J* = 7.1 Hz, 2H, H6'), 3.25-3.18 (m, 3H, Hδ Arg, Hβ Phe), 3.14 (dd, *J* = 13.8, 9.6 Hz, 1H, Hβ Phe), 2.90 (m, 1H, Hβ Asp), 2.78 (dd, *J* = 16.9, 9.1 Hz,1H, Hβ Asp), 2.69 (t, *J* = 6.9 Hz, 2H, CH_2 Pmc), 2.58 (s, 3H, CH_3 Pmc), 2.57 (s, 3H, CH_3 Pmc), 2.56-2.43 (m, 2H, H3a, H2'), 2.32 (dt, *J*= 15.5, 7.3 Hz, 1H, H2'), 2.12 (s, 3H, CH_3 Pmc), 1.99-1.82 (m, 5H, H3b, Hβ Leu, CH_2 Pmc), 1.82-1.50 (m, 9H, Hγ Leu, H3', H5', Hβ Arg, Hγ Arg), 1.46 (s, 9H, *t*Bu), 1.44-1.38 (m, 2H, H4'), 1.33 (s, 6H, CH_3 Pmc), 0.93 (d, *J* = 6.9 Hz, 3H, Hδ Leu), 0.89 (d, *J* = 6.4 Hz, 3H, Hδ Leu). MS (ES^+) *m/z* 1162.7 $[M+H]^+$.

Cyclopeptide **22** was recovered after deprotection and purification by preparative RP-HPLC as described in the general procedure, using a linear gradient from 80% A to 40% B over 20 min, room temperature (R_t = 17.8 min), as a colourless glassy solid (15 mg, TFA salt, 97% yield). Purity of final peptide was check by HPLC and found as 96.4%. ^{1}H NMR (400 MHz, D_2O): δ7.34-7.19 (m, 5H, ArH), 4.46-4.39 (m, 2H, Hα Asp, H4), 4.37-4.27 (m, 3H, H2, Hα Leu, Hα Phe), 4.18 (dd, *J* = 7.7, 7.7 Hz, 1H, Hα Arg), 4.08 (d, *J* = 17.5 Hz, 1H, Hα Gly), 3.91 (dd, *J* = 10.6, 7.1 Hz, 1H, H5a), 3.76 (d, *J* = 17.6 Hz, Hα Gly), 3.25 (dd, *J* = 10.6, 7,1 Hz, 1H, H5b), 3.22 (t, *J* = 7.4 Hz, 2H, H6'), 3.18-2.99 (m, 4H, Hδ Arg, Hβ Phe), 2.93 (dd, *J* = 17.0, 5.1 Hz, 1H, Hβ Asp), 2.85 (dd, *J* = 16.7, 7.1 Hz, 1H, Hβ Asp), 2.54-2.47 (m, 1H, H3a), 2.36-2.25 (m, 2H, H2'), 1.73-1.24 (m, 14H, H3b, H3', H4', H5', Hβ Arg, Hγ Arg, Hβ Leu, Hγ Leu), 0.83 (d, *J* = 6.1 Hz, 3H, Hδ Leu), 0.77 (d, *J* = 6.1 Hz, 3H, Hδ Leu). HRMS(ES^+) $C_{37}H_{55}N_{13}O_9$ calcd for $[M+H]^+$ 840.4402, found 840.4404.

***Cyclo*[1-(6-azidohexanoyl)Amp-Leu-Arg-Gly-Asp-Phe] 23**

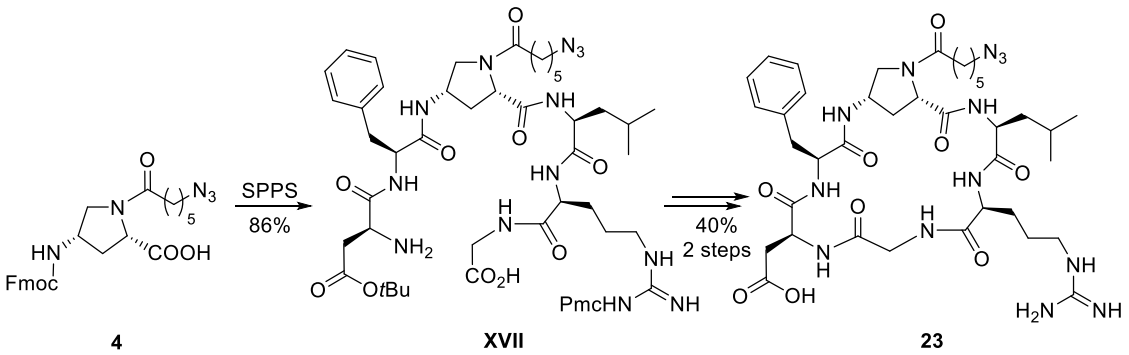

Cyclopeptide **23** was prepared according to the general procedure described for compound **11** by using the aminoproline module **4**. The linear hexapeptide **XVII**, precursor of compound **23**, was prepared according to the procedure described for linear tetrapeptide **I** by using 2-chlorotrityl-Gly-H resin (117 mg, 0.068 mmol, 1.0 eq), Fmoc-Arg(Pmc)-OH (63.1 mg, 0.102 mmol, 1.5 eq), Fmoc-Leu-OH (36 mg, 0.102 mmol, 1.5 eq), the aminoproline module **4** (50 mg, 0.102 mmol, 1.5 eq), Fmoc-Phe-OH (65.8 mg, 0.17 mmol, 2.5 eq) and Fmoc-Asp(*t*Bu)-OH (42 mg, 0.102 mmol, 1.5 eq). Coupling with Fmoc-Phe-OH was repeated twice in the same conditions (65.8 mg, 0.17 mmol, 2.5 eq). After the resin cleavage, compound **XVII** (72 mg, AcOH salt, 86% yield) was recovered as a colourless glassy solid and was used in the following step without further purification. MS (ES^+) *m/z* 1180.9 $[M+H]^+$.

The protected cyclopeptide intermediate was prepared starting from **XVII** (72 mg, 0.058 mmol, 1 eq) according to the cyclization general procedure and, after reverse phase chromatography (eluent: from 80:20 H_2O+0.1%TFA:ACN to 10:90] was obtained as a glassy solid (30.6 mg, TFA salt 42% yield). TLC: EtOAc:MeOH 70:30, R*f* = 0.7. ^{1}H NMR (400 MHz, CD_3OD) δ 7.32-7.19 (m, 5H, ArH), 4.62-4.49 (m, 2H, H4, Hα Asp), 4.48-4.39 (m, 2H, H2, Hα Phe), 4.33-4.28 (m, 1H, Hα Leu), 4.20-4.15 (m, 1H, Hα Arg), 4.10 (dd, *J* = 17.1, 5.8 Hz, 1H, Hα Gly), 3.93 (dd, *J* = 10.4, 7.2 Hz, 1H, H5a), 3.67 (dd, *J* = 17.1, 5.0 Hz, 1H, Hα Gly), 3.42 (dd, *J* = 9.9, 7.0 Hz, 1H, H5b), 3.38 (m, 1H, Hβ Asp), 3.29 (t, *J* = 6.6 Hz, 2H, H6'), 3.21-3.16 (m, 2H, Hδ Arg), 2.93 (m, 1H, Hβ Asp), 2.69 (t, *J* = 6.2 Hz, 2H, CH_2 Pmc), 2.66-2.60 (m, 2H, Hβ Phe, H3a), 2.59 (s, 3H, CH_3 Pmc), 2.58 (s, 3H, CH_3 Pmc), 2.48-2.31 (m, 3H, Hβ Phe, H2'), 2.12 (s, 3H, CH_3 Pmc), 1.95-1.52 (m, 14H, H3b, H3', H5', Hβ Arg, Hγ Arg, Hβ Leu, Hγ Leu, CH_2 Pmc), 1.44 (m, 11H, H4', *t*Bu), 1.33 (s, 6H, CH_3Pmc), 1.00 (d, *J* = 6.9 Hz, 3H, Hδ Leu), 0.96 (d, *J* = 6.2 Hz, 3H, Hδ Leu). MS (ES^+) *m/z* 1162.6 $[M+H]^+$.

Cyclopeptide **23** was recovered after deprotection and purification by preparative RP-HPLC as described in the general procedure, using a linear gradient from 80% A to 40% B over 30 min, room temperature (R_t = 22.6 min), as a colourless glassy solid (21.9 mg, TFA salt, 95% yield). Purity of final peptide was checked by HPLC and found as 95.7%. ^{1}H NMR (400 MHz, MeOD) δ 7.32-7.21 (m, 5H, ArH), 4.58-4.48 (m, 2H, H4, Hα Asp), 4.47-4.37 (m, 2H, H2, Hα Phe), 4.26 (bt, *J* = 6.6 Hz, 1H, Hα Leu), 4.16-4.07 (m, 2H, Hα Gly, Hα Arg), 3.93 (dd, *J* = 10.6, 7.1 Hz, 1H, H5a), 3.70 (d, *J* = 16.7 Hz, 1H, Hα Gly), 3.41 (m, 1H, H5b), 3.27 (t, *J* = 7.0 Hz, 2H, H6'), 3.22-3.11 (m, 3H, Hδ Arg, Hβ Asp), 2.96 (dd, *J* = 14.0, 10.2 Hz, 1H, Hβ Asp), 2.68-2.31 (m, 5H, Hβ Phe, H2', H3a), 2.04-1.55 (m, 12H, H3b, H3', H5', Hβ Arg, Hγ Arg, Hβ Leu, Hγ Leu), 1.47-1.41 (m, 2H, H4'), 0.98 (d, *J* = 6.5 Hz, 3H, Hδ Leu), 0.94 (d, *J* = 6.3 Hz, 3H, Hδ Leu). HRMS(ES^+) $C_{37}H_{55}N_{13}O_9$ calcd for $[M+H]^+$ 840.4402, found 840.4410.

***Cyclo*[1-(6-azidohexanoyl)Amp-Leu-Arg-Gly-Asp-Leu] 24**

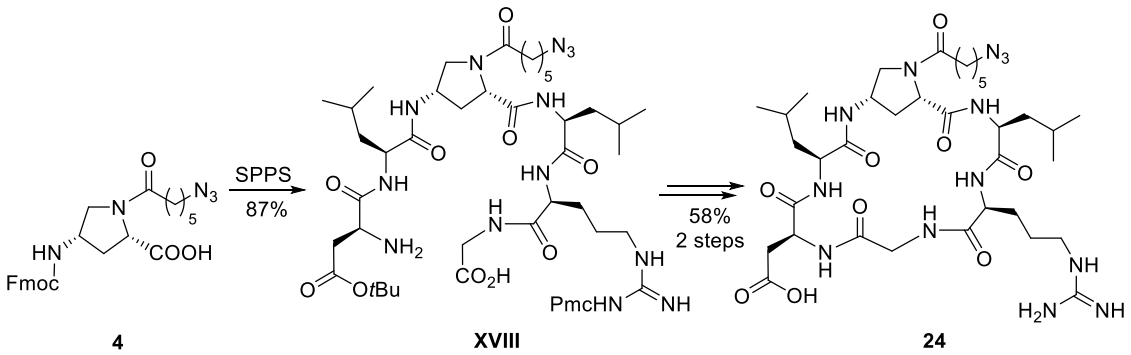

Cyclopeptide **24** was prepared according to the general procedure described for compound **6** by using the aminoproline module **27**. The linear hexapeptide **XVIII**, precursor of compound **24**, was prepared according to the procedure described for linear tetrapeptide **I** by using 2-chlorotrityl-Gly-H resin (66 mg, 0.038 mmol, 1.0 eq), Fmoc-Arg(Pmc)-OH (35.2 mg, 0.057 mmol, 1.5 eq), Fmoc-Leu-OH (20.1 mg, 0.057 mmol, 1.5 eq), the aminoproline module **4** (28.4 mg, 0.057 mmol, 1.5 eq), Fmoc-Leu-OH (20.1 mg, 0.057 mmol, 1.5 eq) and Fmoc-Asp(*t*Bu)-OH (23.4 mg, 0.057 mmol, 1.5 eq). After the resin cleavage, compound **XVIII** (39.8 mg, AcOH salt, 87% yield) was recovered as a colourless glassy solid and was used in the following step without further purification. MS (ES^+) *m/z* 1146.8 $[M+H]^+$.

The protected cyclopeptide intermediate was prepared starting from **XVIII** (39.8 mg, 0.033 mmol, 1 eq) according to the cyclization general procedure and, after reverse phase chromatography (eluent: from 90:10 H_2O+0.1%TFA:ACN to 10:90] was obtained as a glassy solid (29.8 mg, TFA salt 74% yield). TLC: EtOAc:MeOH 70:30, R*f* = 0.7. ^{1}H NMR (400 MHz, MeOD): δ 4.53 (m, 1H, Hα Asp), 4.46 (m, 2H, H4, Hα Leu), 4. 39 (m, 1H, Hα Leu), 4.15 (m, 1H, H2), 4.09 (dd, *J* = 8.7, 5.3 Hz, 1H, Hα Arg), 4.01 (d, *J* = 17.1 Hz, 1H, Hα Gly), 3.87 (dd, *J* = 10.6, 6.9 Hz, 1H, H5a) 3.75 (d, *J* = 17.1 Hz, 1H, Hα Gly), 3.49 (dd, *J* = 10.6, 3.9 Hz, 1H, H5b), 3.28 (t, *J* = 6.9 Hz, 2H, H6'), 3.25-3.18 (m, 2H, Hδ Arg), 2.94 (dd, *J* = 16.5 Hz, 4.4 Hz, 1H, Hβ Asp), 2.80 (dd, *J* = 16.0 Hz, 8.9 Hz, 1H, Hβ Asp), 2.70 (t, *J* = 6.6 Hz, 2H, CH_2 Pmc), 2.58 (s, 3H, CH_3 Pmc), 2.57 (s, 3H, CH_3 Pmc), 2.54 (m, 1H, H3a), 2.47-2.28 (m, 2H, H2'), 2.12 (s, 3H, CH_3 Pmc), 1.97-1.89 (m, 1H, H3b), 1.82-1.55 (m, 16H, H3', H5', Hβ Leu, Hγ Leu, Hβ Arg, Hγ Arg, CH_2 Pmc), 1.48 (s, 9H, *t*Bu), 1.45-1.37 (m, 2H, H4'), 1.33 (s, 6H, CH_3 Pmc), 1.00 (d, *J* = 6.5 Hz, 3H, Hδ Leu), 0.96 (d, *J* = 6.5 Hz, 3H, Hδ Leu), 0.94 (d, *J* = 6.6 Hz, 3H, Hδ Leu), 0.90 (d, *J* = 6.4 Hz, 3H, Hδ Leu). MS (ES^+) *m/z* 1128.5 $[M+H]^+$.

Cyclopeptide **24** was recovered after deprotection and purification by preparative RP-HPLC as described in the general procedure, using a linear gradient from 80% A to 40% B over 20 min, room temperature (R_t = 12.3 min) as a colourless glassy solid (17.4 mg, TFA salt, 79% yield). Purity of final peptide was checked by HPLC and found as 99%. ^{1}H NMR (400 MHz, D_2O): δ 4.45 (dd, *J* = 7.4, 4.9 Hz, 1H, Hα Asp), 4.39 (dd, *J* = 6.9, 6.9 Hz, 1H, H4), 4.35-4.27 (m, 3H, Hα Leu, H2), 4.07 (d, *J* = 17.4 Hz, 1H, Hα Gly), 4.02 (dd, *J* = 8.9, 6.2 Hz, 1H, Hα Arg), 3.91 (dd, *J* = 9.9, 7.2 Hz, 1H, H5a), 3.73, (d, *J* = 17.7 Hz, 1H, Hα Gly), 3.18 (m, 3H, H5b, H6'), 3.08 (m, 2H, Hδ Arg), 2.89 (dd, *J* = 16.9, 5.1 Hz, 1H, Hβ Asp), 2.82 (dd, *J* = 17.1, 7.6 Hz, 1H, Hβ Asp), 2.54-2.45 (m, 1H, H3a), 2.32-2.19 (m, 2H, H2'), 1.74-1.40 (m, 15H, H3b, H3', H4', H5', Hβ Arg, Hβ Leu, Hγ Arg), 1.29-1.20 (m, 2H, Hγ Leu), 0.85 (d, *J* = 6.1 Hz, 3H, Hδ Leu), 0.80 (m, 6H, Hδ Leu), 0.73 (d, *J* = 6.3 Hz, 3H, Hδ Leu). HRMS(ES^+) $C_{35}H_{59}N_{13}O_9$ calcd for $[M+H]^+$ 806.4559, found 806.4565.

***Cyclo*[1-(6-azidohexanoyl)Amp-Phe-Arg-Gly-Asp-Phe] 25**

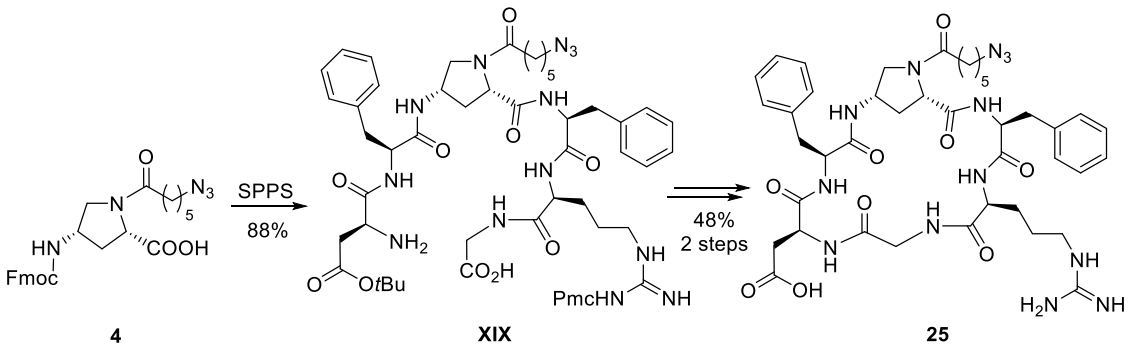

Cyclopeptide **25** was prepared according to the general procedure described for compound **11** by using the aminoproline module **4**. The linear hexapeptide **XIX**, precursor of compound **25**, was prepared according to the procedure described for linear tetrapeptide **I** by using 2-chlorotrityl-Gly-H resin (172 mg, 0.1 mmol, 1.0 eq), Fmoc-Arg(Pmc)-OH (92.8 mg, 0.15 mmol, 1.5 eq), Fmoc-Phe-OH (116.2 mg, 0.30 mmol, 3.0 eq), the aminoproline module **4** (73.7 mg, 0.15 mmol, 1.5 eq), Fmoc-Phe-OH (116.2 mg, 0.30 mmol, 3.0 eq) and Fmoc-Asp(*t*Bu)-OH (61.7 mg, 0.15 mmol, 1.5 eq). The couplings involving Fmoc-Phe-OH and the following Fmoc-removal step were repeated twice in the same conditions (Fmoc-Phe-OH, 116.2 mg, 0.30 mmol, 3.0 eq). After the resin cleavage, compound **XIX** (112 mg, AcOH salt, 88% yield) was recovered as a colourless glassy solid and was used in the following step without further purification. MS (ES^+) *m/z* 1214.1 $[M+H]^+$.

The protected cyclopeptide intermediate was prepared starting from **XIX** (112 mg, 0.088 mmol, 1 eq) according to the cyclization general procedure and, after reverse phase chromatography (eluent: from 80:20 H_2O+0.1%TFA:ACN to 90:10] was obtained as a glassy solid (64.2 mg, TFA salt 56% yield). TLC: EtOAc:MeOH 70:30, R*f* = 0.7. ^{1}H NMR (400 MHz, MeOD): δ 7.34-7.18 (m, 10H, ArH), 4.64-4.36 (m, 5H, Hα Asp, H2, H4, Hα Phe), 4.26 (m, 1H, Hα Arg), 4.15-3.96 (m, 2H, Hα Gly, H5a), 3.87 (d, *J* = 17.0 Hz, 1H, Hα Gly), 3.60 (m, 1H, H5b), 3.27 (t, *J* = 7.1 Hz, 2H, H6'), 3.25-2.99 (m, 6H, Hβ Phe, Hδ Arg), 2.74-2.61 (m, 3H, Hβ Asp, CH_2 Pmc), 2.59 (s, 3H, CH_3 Pmc), 2.58 (s, 3H, CH_3 Pmc), 2.54-2.41 (m, 2H, Hβ Asp, H3a), 2.39-2.25 (m, 2H, H2'), 2.12 (s, 3H, CH_3 Pmc), 1.99-1.50 (m, 13H, H3b, Hβ Arg, Hγ Arg, H3', H5', H4', CH_2 Pmc,), 1.44 (s, 9H, *t*Bu), 1.33 (s, 6H, CH_3 Pmc). MS (ES^+) *m/z* 1196.9 $[M+H]^+$.

Cyclopeptide **25** was recovered after deprotection and purification by preparative RP-HPLC as described in the general procedure, using a linear gradient from 80% A to 40% B over 30 min, room temperature (R_t = 25.2 min), as a colourless glassy solid (41.5 mg, TFA salt, 85% yield). Purity of the final peptide was checked by HPLC and found as 99.5%. ^{1}H NMR (400 MHz, MeOD): δ 7.26-7.13 (m, 10H, ArH), 4.47-4.41 (m, 2H, Hα Phe, H4), 4.33-4.27 (m, 2H, Hα Asp, H2), 4.14 (dd, *J* = 9.6, 5.6 Hz, 1H, Hα Phe), 3.94 (d, *J* = 17.1 Hz, 1H, Hα Gly), 3.90 (m, 1H, Hα Arg), 3.81 (d, *J* = 17.5 Hz, 1H, Hα Gly), 3.78 (m, 1H, H5a), 3.56 (m, 1H, H5b), 3.19 (t, *J* = 6.9 Hz, 2H, H6'), 3.17-3.05 (m, 4H, Hδ Arg, Hβ Phe), 3.05-2.94 (m, 2H, Hβ Phe), 2.61 (dd, *J* = 17.6, 4.1 Hz, 1H, Hβ Asp), 2.49-2.37 (m, 2H, H3a, Hβ Asp), 2.31-2.20 (m, 1H, H3b), 2.01-1.81 (m, 2H, H2'), 1.57-1.46 (m, 4H, H5', H3'), 1.36-1.23 (m, 6H, H4', Hβ Arg, Hγ Arg). HRMS(ES^+) $C_{41}H_{55}N_{13}O_9$ calcd for $[M+H]^+$ 874.4246, found 874.4257.

***Cyclo*[1-(6-azidohexanoyl)Amp-DiPhe-Arg-Gly-Asp-Leu] 26**

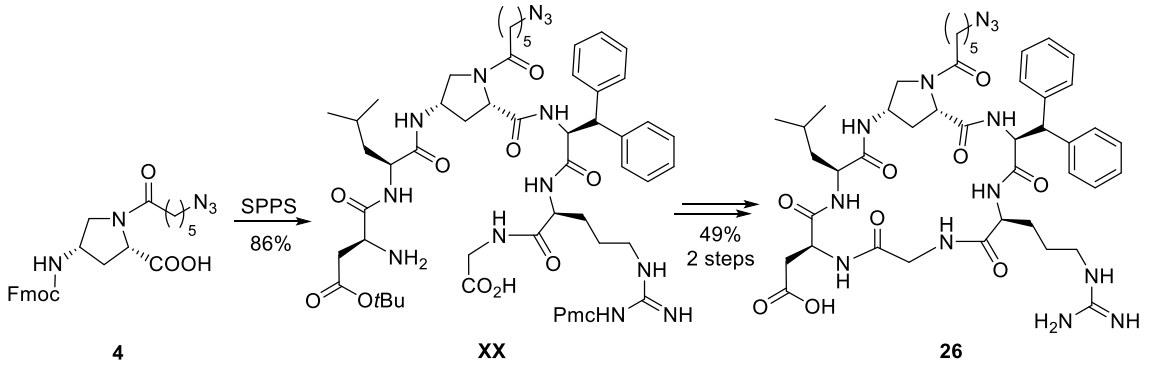

Cyclopeptide **26** was prepared according to the general procedure described for compound **11** by using the aminoproline module **4**. The linear hexapeptide **XX**, precursor of compound **26**, was prepared according to the procedure described for linear tetrapeptide **I** by using 2-chlorotrityl-Gly-H resin (138 mg, 0.08 mmol, 1.0 eq), Fmoc-Arg(Pmc)-OH (74.2 mg, 0.12 mmol, 1.5 eq), Fmoc-β-Phenyl-Phe-OH (74.2 mg, 0.16 mmol, 2.0 eq), the aminoproline module **4** (58.2 mg, 0.12 mmol, 1.5 eq), Fmoc-Leu-OH (42.4 mg, 0.12 mmol, 1.5 eq) and Fmoc-Asp(*t*Bu)-OH (49.4 mg, 0.12 mmol, 1.5 eq). Coupling involving Fmoc-β–Phenyl-Phe-OH and the following Fmoc-removal step were repeated twice in the same conditions (Fmoc-β-Phenyl-Phe-OH, 74.2 mg, 0.16 mmol, 2.0 eq). After the resin cleavage, compound **XX** (95 mg, AcOH salt, 86% yield) was recovered as a colourless glassy solid and was used in the following step without further purification. MS (ES$^+$) *m/z* 1257.0 $[M+H]^+$.

The protected cyclopeptide intermediate was prepared starting from **XX** (95 mg, 0.069 mmol, 1 e) according to the cyclization general procedure and, after reverse phase chromatography (eluent: from 80:20 H_2O+0.1%TFA:ACN 90:10] was obtained as a glassy solid (49.2 mg, TFA salt 53% yield). TLC: EtOAc:MeOH 70:30, R*f* = 0.7. ^{1}H NMR (400 MHz, MeOD): δ 7.38-7.08 (m, 10H, ArH), 4.57-4.29 (m, 5H, Hα Asp, H4, Hα DiPhe, H2, Hα Leu), 3.91 (bd, *J* = 17.0 Hz, 1H, Hα Gly), 3.86-3.76 (m, 2H, Hα Arg, H5a), 3.69 (bd, *J* = 17.2 Hz, 1H, Hα Gly), 3.50 (m, 1H, H5b), 3.30 (t, *J* = 6.7 Hz, 2H, H6'), 3.22-3-10 (m, 2H, Hδ Arg), 3.04-2.94 (m, 1H, Hβ Asp) 2.80 (dd, *J* = 16.3, 8.9 Hz, 1H, Hβ Asp) 2.69 (t, J = 6.4 Hz, 2H, CH_2 Pmc), 2.64-2.54 (m, 7H, Hβ DiPhe, CH_3 Pmc), 2.47-2.24 (m, 3H, H3a, H2'), 2.12 (s, 3H, CH_3 Pmc), 1.87-1.53 (m, 14H, H3b, Hβ Arg, Hγ Arg, Hβ Leu, Hγ Leu, H3', H5', CH_2 Pmc), 1.48 (s, 9H, *t*Bu), 1.43 (m, 2H, H4'), 1.33 (s, 6H, CH_3 Pmc), 0.96 (d, *J* = 5.9 Hz, 3H, Hδ Leu), 0.91 (d, *J* = 6.1 Hz, 3H, Hδ Leu). MS (ES$^+$) *m/z* 1260.7 $[M+Na]^+$.

Cyclopeptide **26** was recovered after deprotection and purification by preparative RP-HPLC as described in the general procedure, using a linear gradient from 80% A to 50% B over 25 min, room temperature (R_t = 25.0 min), as a colourless glassy solid (35 mg, TFA salt, 93% yield). Purity of the final compound was checked by HPLC and found as 99%. ^{1}H NMR (400 MHz, MeOD): δ 7.46-7.16 (m, 10H, ArH), 4.60 (d, *J* = 10.7 Hz, 1H, Hα DiPhe), 4.50-4.40 (m, 2H, H2, Hα Asp), 4.36 (m, 1H, Hα Leu), 4.28 (dd, *J* = 9.9, 5.3 Hz, 1H, H4), 4.03 (d, *J* = 17.0 Hz, 1H, Hα Gly), 3.89 (m, 1H, Hα Arg), 3.84-3.76 (m, 2H, Hα Gly, H5a), 3.50 (m, 1H, H5b), 3.29 (t, *J* = 6.8 Hz, 2H, H6'), 3.18-3.04 (m, 2H, Hδ Arg), 2.98 (dd, *J* = 17.1, 4.4 Hz,1H, Hβ Asp) 2.88-2.79 (m, 2H, Hβ Asp, Hβ DiPhe) 2.44 (m, 1H, H2'), 2.33 (m, 2H, H3a, H2'), 1.92-1.35 (m, 12H, H3b, Hβ Arg, Hγ Arg, Hβ Leu, Hγ Leu, H3', H5'), 1.28 (m, 2H, H4'), 1.01 (d, *J* = 6.0 Hz, 3H, Hδ Leu), 0.96 (d, *J* = 6.0 Hz, 3H, Hδ Leu). HRMS(ES$^+$) $C_{44}H_{61}N_{13}O_9$ calcd for $[M+H]^+$ 916.4715, found 916.4724.

***Cyclo*{1-[*N*-(6-azidohexanoyl)phenylalanyl]Amp-Phe-Arg-Gly-Asp-Leu} 27**

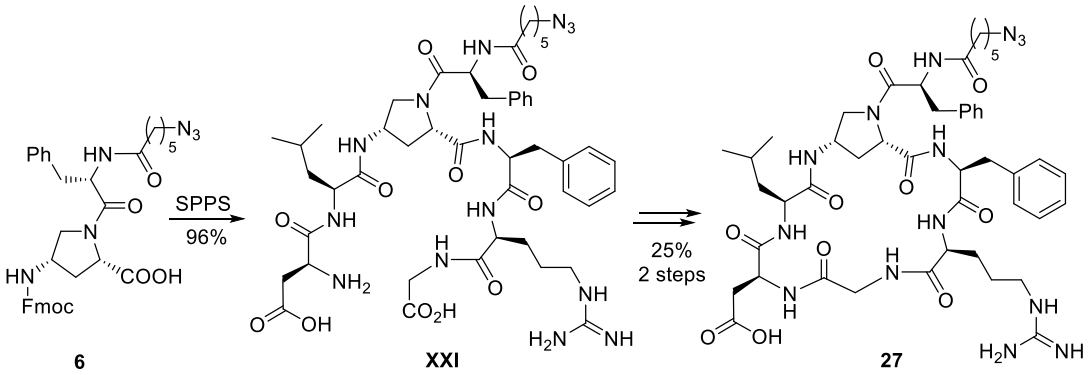

Cyclopeptide **27** was prepared according to the general procedure described for compound **11** by using the aminoproline module **6**. The linear hexapeptide **XXI**, precursor of compound **26**, was prepared according to the procedure described for linear tetrapeptide **I** by using 2-chlorotrityl-Gly-H resin (80.5 mg, 0.046 mmol, 1.0 eq), Fmoc-Arg(Pmc)-OH (43.3 mg, 0.07 mmol, 1.5 e), Fmoc-Phe-OH (35.6 mg, 0.092 mmol, 2.0 eq), the aminoproline module **6** (44.7 mg, 0.07 mmol, 1.5 eq), Fmoc-Leu-OH (24.7 mg, 0.07 mmol, 1.5 eq) and Fmoc-Asp(*t*Bu)-OH (28.8 mg, 0.07 mmol, 1.5 eq). Coupling involving Fmoc-Phe-OH and the following Fmoc-removal step were repeated twice in the same conditions (Fmoc-Phe-OH, 35.6 mg, 0.92 mmol, 2.0 eq). After the resin cleavage, compound **XXI** (62 mg, AcOH salt, 96% yield) was recovered as a colourless glassy solid and was used in the following step without further purification. MS (ES^+) *m/z* 1328.1 $[M+H]^+$.

The protected cyclopeptide intermediate was prepared starting from **XXI** (62 mg, 0.045 mmol, 1 eq) according to the cyclization general procedure and, after reverse phase chromatography (eluent: from 80:20 H_2O+0.1%TFA:ACN to 90:10] was obtained as a glassy solid (19.8 mg, TFA salt 31% yield). TLC: EtOAc:MeOH 70:30, R*f* = 0.7. ^{1}H NMR (400 MHz, MeOD): δ7.36-7.05 (m, 10H, ArH), 4.99 (dd, *J* = 6.6, 6.6Hz, 1H, Hα Phe), 4.80 (dd, *J* = 9.6, 4.8 Hz, 1H, Hα Asp), 4.57-4.38 (m, 2H, H2, Hα Phe), 4.37-4.14 (m, 2H, H4, Hα Leu), 4.03 (m, 1H, Hα Arg), 3.96 (d, *J* = 17.5 Hz, 1H, Hα Gly), 3.77 (d, *J* = 17.6 Hz, 1H, Hα Gly), 3.68 (bd, *J* = 11.1 Hz, 1H, H5a), 3.49 (dd, *J* = 11.1, 5.7 Hz, 1H, H5b), 3.29-3.14 (m, 4H, H6', Hδ Arg), 3.15-2.73 (m, 6H, Hβ Asp, Hβ Phe), 2.68 (t, *J* = 6.5 Hz, 2H, CH_2 Pmc), 2.59 (s, 3H, CH_3 Pmc), 2.58 (m, 3H, CH_3 Pmc), 2.49-2.27 (m, 1H, H3a), 2.16 (m, 2H, H2'), 2.12 (s, 3H, CH_3 Pmc), 2.00-1.46 (m, 14H, H3b, Hβ Arg, Hγ Arg, CH_2 Pmc, Hβ Leu, Hγ Leu, H3', H5'), 1.44 (s, 9H, *t*Bu), 1.32 (s, 6H, CH_3Pmc), 1.30 (m, 2H, H4'), 0.93-0.87 (m, 6H, Hδ Leu). MS (ES^+) *m/z* 1309.1 $[M+H]^+$.

Cyclopeptide **27** was recovered after deprotection and purification by preparative RP-HPLC as described in the general procedure, using a linear gradient from 80% A to 35% B over 22 min, room temperature (R_t = 24.4 min), as a colourless glassy solid (12.4 mg, TFA salt, 80% yield). Purity of the final peptide was checked by HPLC and found as 98.9%. ^{1}H NMR (400 MHz, MeOD): δ7.35-7.11 (m, 10H, ArH), 5.03 (d, *J* = 7.3, 7.3 Hz, 1H, Hα Phe), 4.53 (dd, *J* = 8.1. 4.0 Hz, 1H, Hα Asp), 4.39 (m, 1H, H2), 4.30 (m, 2H, Hα Leu, H4), 4.20-4.10 (m, 1H, Hα Phe), 4.03 (m, 1H, Hα Arg), 3.98 (d, *J* = 17.3 Hz, 1H, Hα Gly), 3.83 (d, *J* = 17.3 Hz, 1H, Hα Gly), 3.76 (bd, *J* = 11.4 Hz, 1H, H5a), 3.48 (dd, *J* = 11.4, 6.2 Hz, 1H, H5b), 3.31-3.22 (m, 4H, Hδ Arg, H6'), 3.18-2.98 (m, 4H, Hβ Phe), 2.96-2.83 (m, 2H, Hβ Asp), 2.40-2.28 (m, 1H, H3a), 2.21-1.44 (m, 12H, H3b, H2', Hβ Leu, Hγ Leu, Hβ Arg, H3', H5'), 1.36-1.21 (m, 4H, H4', Hγ Arg), 0.95-0.88 (m, 6H, Hδ Leu). HRMS(ES^+) $C_{47}H_{66}N_{14}O_{10}$ calcd for $[M+H]^+$ 987.5086, found 987.5097.

***Cyclo*{1-[*N*-(6-azidohexanoyl)phenylalanyl]Amp-Leu-Arg-Gly-Asp-Leu} 28**

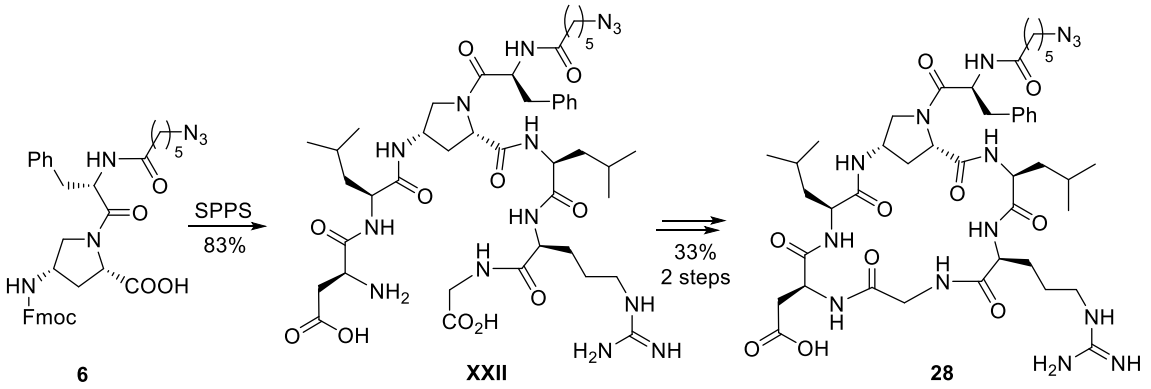

Cyclopeptide **28** was prepared according to the general procedure described for compound **11** by using the aminoproline module **6**. The linear hexapeptide **XXII**, precursor of compound **28**, was prepared according to the procedure described for linear tetrapeptide **I** by using 2-chlorotrityl-Gly-H resin (80.5 mg, 0.047 mmol, 1.0 eq), Fmoc-Arg(Pmc)-OH (43.3 mg, 0.07 mmol, 1.5 eq), Fmoc-Leu-OH (24.7 mg, 0.07 mmol, 1.5 eq), the aminoproline module **6** (44.7 mg, 0.07 mmol, 1.5 eq), Fmoc-Leu-OH (24.7 mg, 0.07 mmol, 1.5 eq) and Fmoc-Asp(*t*Bu)-OH (28.8 mg, 0.07 mmol, 1.5 eq). After the resin cleavage, compound **XXII** (52.7 mg, AcOH salt, 83% yield) was recovered as a colourless glassy solid and was used in the following step without further purification. MS (ES^+) *m/z* 1293.9 $[M+H]^+$.

The protected cyclopeptide intermediate was prepared starting from **XXII** (52.7 mg, 0.039 mmol, 1 eq) according to the cyclization general procedure and, after reverse phase chromatography (eluent: from 80:20 H_2O+0.1%TFA:ACN to 90:10] was obtained as a glassy solid (21.6 mg, TFA salt 40% yield). TLC: EtOAc:MeOH 70:30, R*f* = 0.7. ^{1}H NMR (400 MHz, MeOD): δ 7.30-7.16 (m, 5H, ArH), 4.94 (dd, *J* = 7.4, 7.4 Hz, 1H, Hα Asp), 4.43 (m, 1H, Hα Phe), 4.39-4.24 (m, 2H, H2, Hα Leu), 4.23-3.98 (m, 3H, H4, Hα Leu, Hα Arg), 3.96-3.86 (m, 2H, H5a, Hα Gly), 3.60 (d, *J* = 17.0 Hz, 1H, Hα Gly), 3.48 (m, 1H, H5b), 3.20-3.07 (m, 4H, H6', Hδ Arg), 3.03-2.78 (m, 3H, Hβ Phe, Hβ Asp), 2.70 (dd, *J* = 16.5. 8.5 Hz, 1H, Hβ Asp), 2.60 (t, *J* = 6.3 Hz, 2H, CH_2 Pmc), 2.59 (s, 3H, CH_3 Pmc), 2.58 (s, 3H, CH_3 Pmc), 2.46-2.37 (m, 1H, H3a), 2.08 (t, *J* = 6.9 Hz, 2H H2'), 2.03 (s, 3H, CH_3 Pmc), 1.87 (m, 1H, H3b), 1.77 (t, *J* = 6.3 Hz, 2H, CH_2 Pmc), 1.74-1.40 (m, 14H, Hβ Arg, HγArg, Hγ Leu, Hβ Leu, H3', H5'), 1.39 (s, 9H, *t*Bu), 1.24 (s, 6H, CH_3 Pmc), 1.21 (m, 2H, H4'), 1.04-0.88 (m, 12H, Hδ Leu). MS (ES^+) *m/z* 1297.9 $[M+Na]^+$.

Cyclopeptide **28** was recovered after deprotection and purification by preparative RP-HPLC as described in the general procedure, using a linear gradient from 90% A to 35% B over 21 min, room temperature (R_t = 21.6 min), as a colourless glassy solid (12.8 mg, TFA salt, 77% yield). Purity of the final compound was checked by HPLC and found as 99%. ^{1}H NMR (400 MHz, MeOD): δ 7.26-7.06 (m, 5H, ArH), 4.88 (m, 1H, Hα Asp), 4.50-4.35 (m, 2H, H2, Hα Phe), 4.34-4.24 (m, 2H, H4, Hα Leu), 4.20-3.92 (m, 4H, Hα Arg, Hα Leu, Hα Gly, H5a), 3.64 (d, *J* = 17.1 Hz, 1H, Hα Gly), 3.45 (dd, *J* = 10.6, 6.8 Hz, 1H, H5b), 3.22-3.09 (m, 4H, Hδ Arg, H6'), 3.05-2.69 (m, 4H, Hβ Phe, Hβ Asp), 2.40 (m, 1H, H3a), 2.16 (m, 2H, H2'), 1.85 (m, 1H, H3b), 1.81-1.37 (m, 14H, Hβ Arg, Hγ Arg, Hβ Leu, Hγ Leu, H3', H5'), 1.28-1.07 (m, 2H, H4'), 1.00-0.73 (m, 12H, Hδ Leu). HRMS(ES^+) $C_{44}H_{68}N_{14}O_{10}$ calcd for $[M+H]^+$ 953.5243, found 953.5252.

2.5.2.2. HPLC chromatograms

Purity determination of final compounds. Purity of the final compounds was checked by HPLC on a Prostar 210 apparatus (Varian, UV detection) equipped with a semipreparative column (C18-10 µm Discovery BIO Wide Pore 10 × 250 mm, column A) or a preparative column (C_{18}-10 µm Discovery BIO Wide Pore 21.2 × 250 mm, column B). The solvent system was H_2O+0.1% TFA (Solvent A) and ACN (solvent B).

Data for compound 6. Column A (from 80% to 60% of Solvent A over 14 min, then 40% of Solvent A for 6 min), 220 nm, 3.0 mL min^{-1}, R_t = 11.1 min, 99.7% purity.

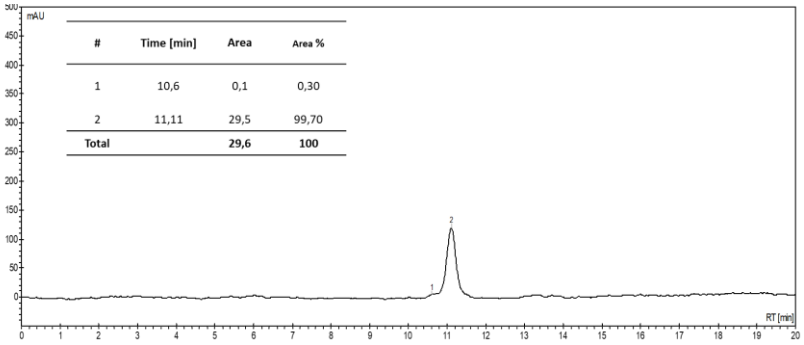

#	Time [min]	Area	Area %
1	10,6	0,1	0,30
2	11,11	29,5	99,70
Total		**29,6**	**100**

Data for compound 7. Column B (from 80% to 40% of Solvent A over 25 min, then 40% of Solvent A for 2 min, then from 40% to 80% of Solvent A over 3 min), 220 nm, 8.0 mL min^{-1}, R_t = 17.1 min, >99.5% purity.

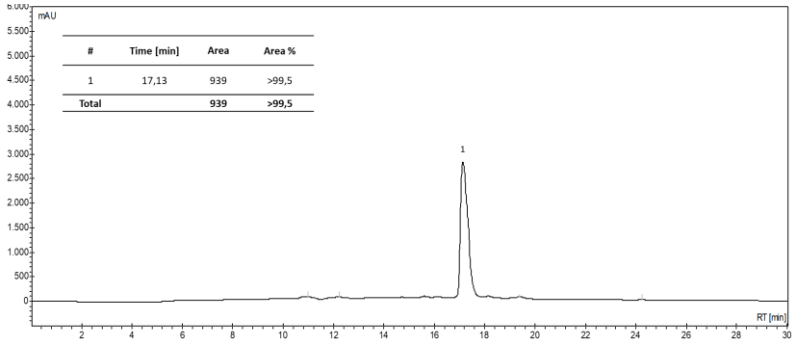

#	Time [min]	Area	Area %
1	17,13	939	>99,5
Total		**939**	**>99,5**

Data for compound 8. Column A (from 80% to 50% of Solvent A over 14 min, then 50% of Solvent A for 6 min), 220 nm, 3.0 mL min^{-1}, R_t = 11.6 min, 96.2% purity.

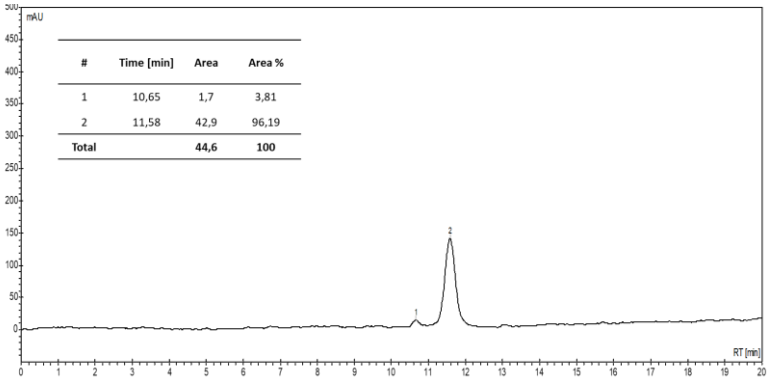

#	Time [min]	Area	Area %
1	10,65	1,7	3,81
2	11,58	42,9	96,19
Total		**44,6**	**100**

Data for compound 9. Column A (from 80% to 50% of Solvent A over 14 min, then 50% of Solvent A for 6 min), 220 nm, 3.0 mL min^{-1}, R_t = 11.4 min, 95.6% purity**.**

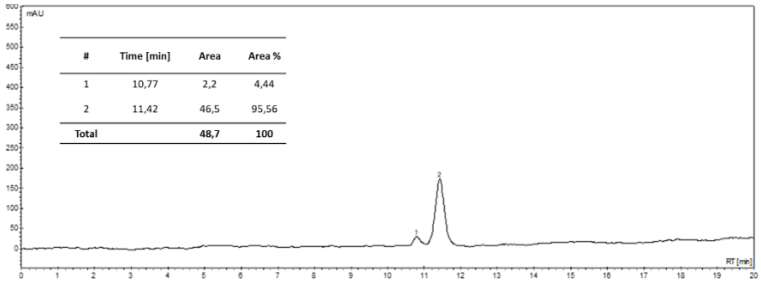

#	Time [min]	Area	Area %
1	10,77	2,2	4,44
2	11,42	46,5	95,56
Total		**48,7**	**100**

Data for compound 10. Column A (from 80% to 50% of Solvent A over 14 min, then 50% of Solvent A for 6 min), 220 nm, 3.0 mL min^{-1}, R_t = 11.4 min, >99.5% purity**.**

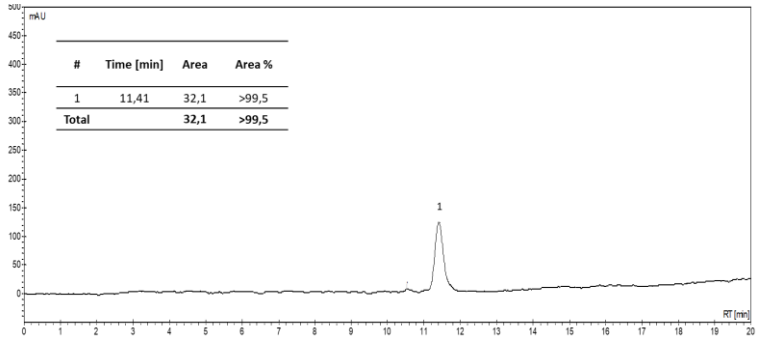

#	Time [min]	Area	Area %
1	11,41	32,1	>99,5
Total		**32,1**	**>99,5**

Data for compound 11. Column B (from 80% to 40% of Solvent A over 25 min, then 40% of Solvent A for 2 min, then from 40% to 80% of Solvent A over 3 min), 220 nm, 8.0 mL min^{-1}, R_t = 15.7 min, >99.5% purity**.**

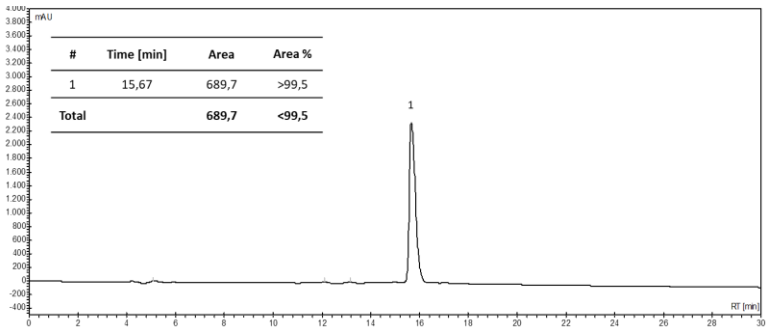

#	Time [min]	Area	Area %
1	15,67	689,7	>99,5
Total		**689,7**	**<99,5**

Data for compound 12. Column A (from 80% to 50% of Solvent A over 14 min, then 50% of Solvent A for 6 min), 220 nm, 3.0 mL min^{-1}, R_t = 11.2 min, >99.5% purity**.**

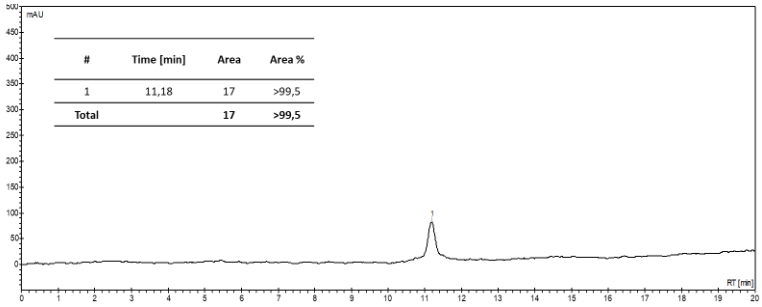

#	Time [min]	Area	Area %
1	11,18	17	>99,5
Total		**17**	**>99,5**

Data for compound 13. Column B (from 80% to 40% of Solvent A over 25 min, then 40% of Solvent A for 2 min, then from 40% to 80% of Solvent A over 3 min), 220 nm, 8.0 mL min^{-1}, R_t = 15.7 min, >99.5% purity.

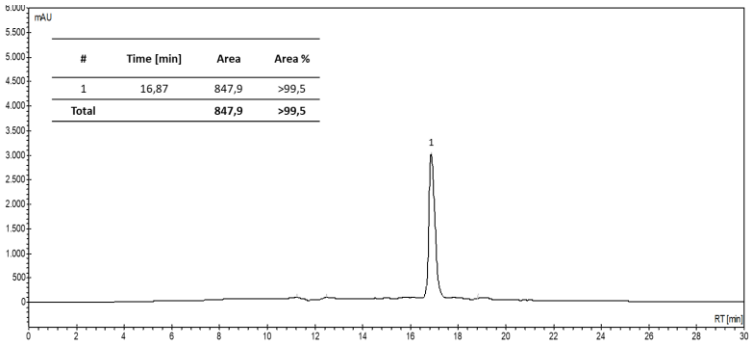

Data for compound 14. Column A (from 80% to 50% of Solvent A over 14 min, then 50% of Solvent A for 6 min), 220 nm, 3.0 mL min^{-1}, R_t = 11.4 min, >99.5% purity.

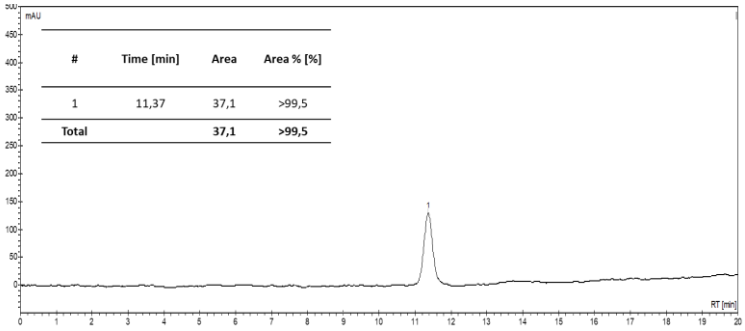

Data for compound 15. Column B (from 90% to 40% of Solvent A over 25 min), 220 nm, 8.0 mL min^{-1}, R_t = 18.6 min, 96.8% purity.

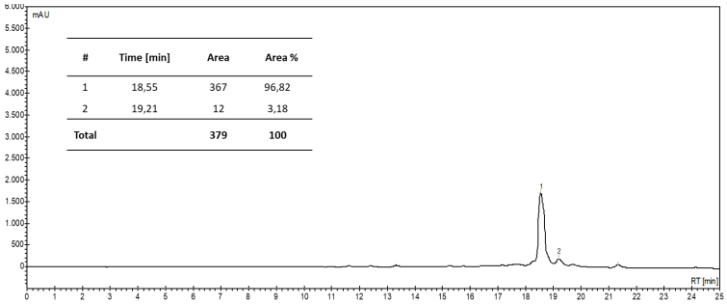

Data for compound 16. Column B (from 80% to 30% of Solvent A over 25 min, then 30% of Solvent A for 2 min, then from 30% to 80% over 3 min), 220 nm, 8.0 mL min^{-1}, R_t = 22.7 min, >99.5% purity.

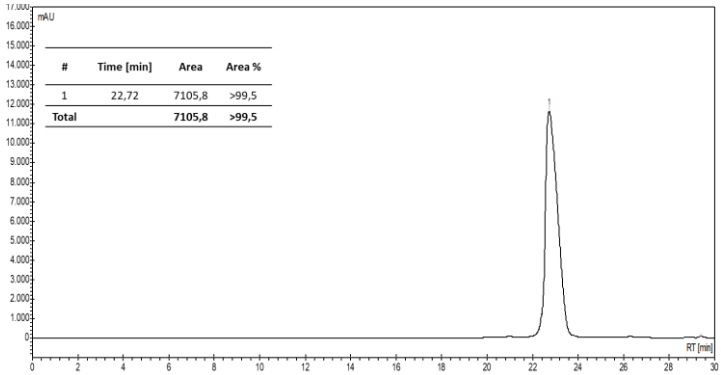

Data for compound 17. Column A (from 80% to 50% of Solvent A over 14 min, then 50% of Solvent A for 5 min), 220 nm, 3.0 mL min^{-1}, R_t = 11.8 min, 96.4% purity**.**

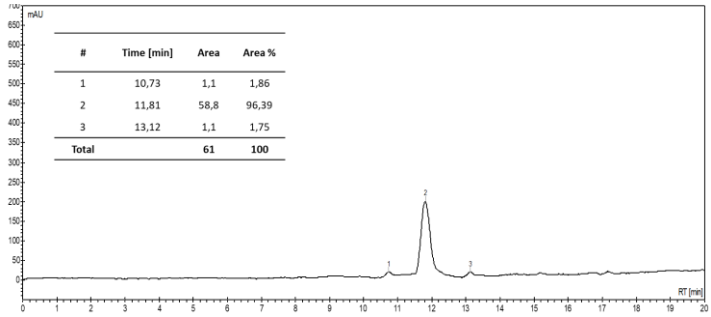

#	Time [min]	Area	Area %
1	10,73	1,1	1,86
2	11,81	58,8	96,39
3	13,12	1,1	1,75
Total		**61**	**100**

Data for compound 18. Column B (from 80% to 40% of Solvent A over 25 min, then 40% of Solvent A for 2 min, then from 40% to 80% over 3 min), 220 nm, 8.0 mL min^{-1}, R_t = 22.6 min, 95.7% purity**.**

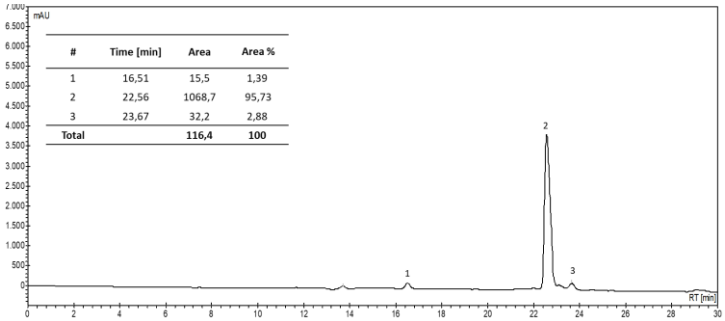

#	Time [min]	Area	Area %
1	16,51	15,5	1,39
2	22,56	1068,7	95,73
3	23,67	32,2	2,88
Total		**116,4**	**100**

Data for compound 19. Column A (from 80% to 50% of Solvent A over 14 min, then 50% of Solvent A for 5 min), 220 nm, 3.0 mL min^{-1}, R_t = 11.7 min, >99.5% purity**.**

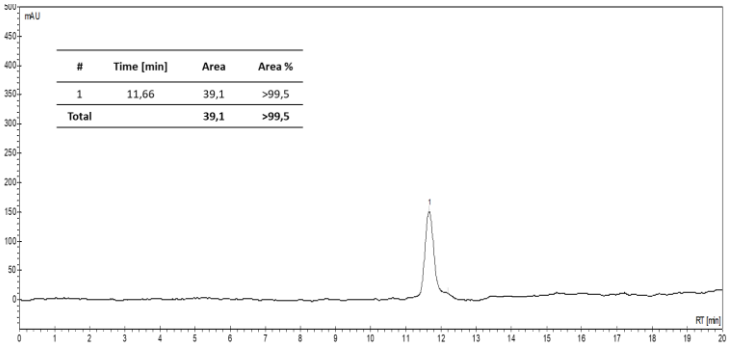

#	Time [min]	Area	Area %
1	11,66	39,1	>99,5
Total		**39,1**	**>99,5**

Data for compound 20. Column B (from 80% to 50% of Solvent A over 25 min, then 50% of Solvent A for 2 min, then from 50% to 80% over 3 min), 220 nm, 8.0 mL min^{-1}, R_t = 25.2 min, 99.5% purity**.**

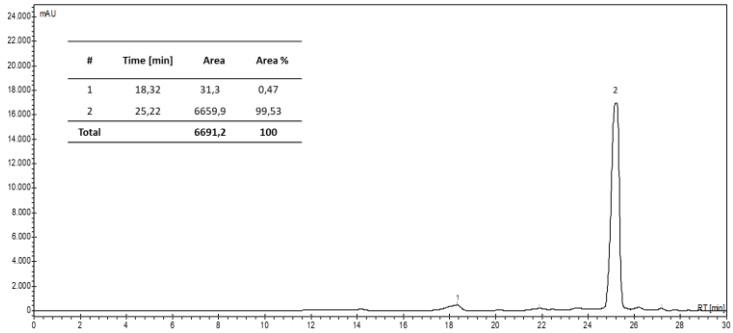

#	Time [min]	Area	Area %
1	18,32	31,3	0,47
2	25,22	6659,9	99,53
Total		**6691,2**	**100**

Data for compound 21. Column B (from 80% to 50% of Solvent A over 25 min, then 50% of Solvent A for 2 min, then from 50% to 80% over 3 min), 220 nm, 8.0 mL min^{-1}, R_t = 25.0 min, >99.5% purity**.**

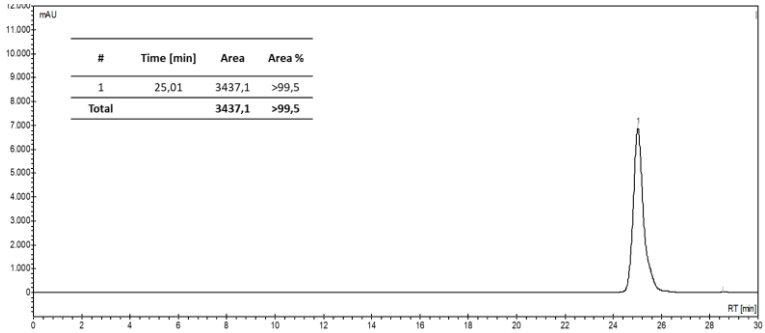

#	Time [min]	Area	Area %
1	25,01	3437,1	>99,5
Total		**3437,1**	**>99,5**

Data for compound 22. Column B (from 90% to 35% of Solvent A over 22 min, then 35% of Solvent A for 3 min, then from 35% to 90% over 3 min), 220 nm, 8.0 mL min^{-1}, R_t = 24.4 min, 98.9% purity**.**

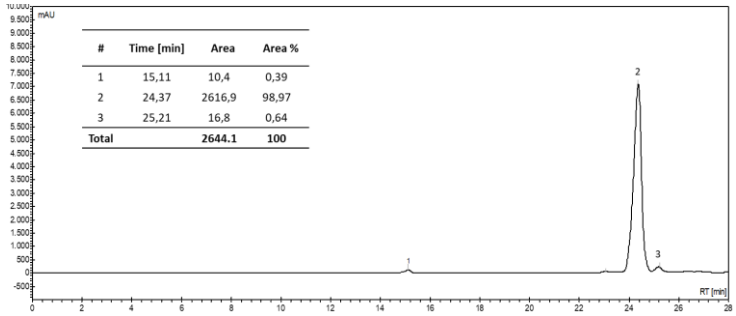

#	Time [min]	Area	Area %
1	15,11	10,4	0,39
2	24,37	2616,9	98,97
3	25,21	16,8	0,64
Total		**2644.1**	**100**

Data for compound 23. Column B (from 90% to 35% of Solvent A over 21 min, then 35% of Solvent A for 4 min), 220 nm, 8.0 mL min^{-1}, R_t = 21.6 min, >99.5% purity**.**

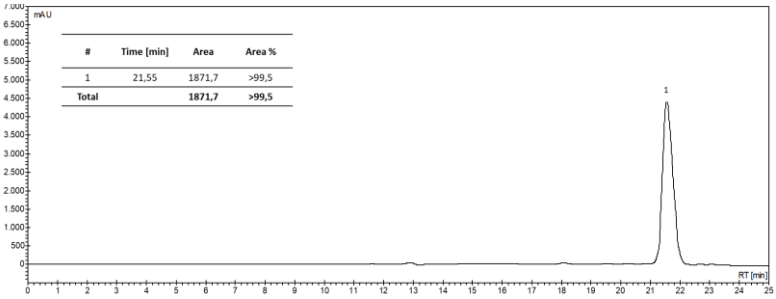

#	Time [min]	Area	Area %
1	21,55	1871,7	>99,5
Total		**1871,7**	**>99,5**

2.5.3. Biology

Solid-phase $\alpha_v\beta_6$ receptor binding assay. Recombinant human integrin $\alpha_v\beta_6$ receptor (R&D Systems, Minneapolis, MN, USA) was diluted to 1.0 μg/mL in coating buffer containing 20 mM Tris-HCl (pH 7.4), 150 mM NaCl, 1 mM $MnCl_2$, 2 mM $CaCl_2$, and 1 mM $MgCl_2$. An aliquot of diluted receptor (100 μL/well) was added to 96-well microtiter plates (Nunc MaxiSorp, Thermo Fisher Scientific, Roskilde, Denmark) and incubated overnight at 4 °C. The plates were incubated with blocking solution (coating buffer plus 1% bovine serum albumin) for additional 2 h at room temperature to block nonspecific binding. After washing twice with blocking solution, plates were incubated 3 h at room temperature, in the dark, with various concentrations (10^{-4}–10^{-11} M) of test compounds in the presence of 1 μg/mL biotinylated fibronectin (Molecular Innovations, Novi, MI, USA). Biotinylation was performed using an EZ-Link Sulfo-NHS-Biotinylation kit (Pierce, Rockford, IL, USA). After thorough washing (3 times), the plates were incubated for 1 h, at room temperature, with streptavidin-biotinylated peroxidase complex (Amersham Biosciences, Uppsala, Sweden). Plates were washed 3 times with blocking solution, followed by 30 min incubation in the dark with 100 μL/well Substrate Reagent Solution (R&D Systems, Minneapolis, MN, USA) before stopping the reaction with the addition of 50 μL/well 2N H_2SO_4. Absorbance at 415 nm was read in a SynergyTM HT Multi-Detection Microplate Reader (BioTek Instruments, Inc.). Each data point represents the average of triplicate wells; data analysis was carried out by nonlinear regression analysis with GraphPad Prism software. Each experiment was repeated in duplicate.

Solid-phase $\alpha_v\beta_3$ receptor binding assay. The assay was performed according to a reported procedure.[19]

2.6. References

(**1**) Koivisto, L.; Bi, J.; Häkkinen, L.; Larjava, H. Integrin $\alpha_V\beta_6$: Structure , Function and Role in Health and Disease. *Int. J. Biochem. Cell Biol.* **2018**, *99*, 186–196.
(**2**) Bandyopadhyay, A.; Raghavan, S. Defining the Role of Integrin $\alpha_V\beta_6$ in Cancer. *Curr. Drug Targets* **2009**, *10*, 645–652.
(**3**) Goodwin, A.; Jenkins, G. Role of Integrin-Mediated TGFβ Activation in the Pathogenesis of Pulmonary Fibrosis. *Biochem. Soc. Trans.* **2009**, *37*, 849–854.
(**4**) Wang, G.; Wang, Y.; Shang, Y.; Zhang, Z.; Liu, X. How Foot-and-Mouth Disease Virus Receptor Mediates Foot-and-Mouth Disease Virus Infection. *Virol. J.* **2015**, *12*, 1–7.
(**5**) Lamouille, S.; Xu, J.; Derynck, R. Molecular Mechanisms of Epithelial–Mesenchymal Transition. *Nat. Rev. Mol. Cell Biol.* **2014**, *15*, 178–196.
(**6**) Ramos, D. M.; Dang, D.; Sadler, S. The Role of the Integrin $\alpha_V\beta_6$ in Regulating the Epithelial to Mesenchymal Transition in Oral Cancer. *Anticancer Res.* **2009**, *29*, 125–130.
(**7**) Nieto, M. A.; Cano, A. The Epithelial-Mesenchymal Transition under Control: Global Programs to Regulate Epithelial Plasticity. *Semin. Cancer Biol.* **2012**, *22*, 361–368.
(**8**) Mamuya, F. A.; Duncan, M. K. α_V Integrins and TGFβ-Induced EMT: A Circle of Regulation. *J. Cell. Mol. Med.* **2012**, *16*, 445–455.
(**9**) Monaghan, P.; Gold, S.; Simpson, J.; Zhang, Z.; Weinreb, P. H.; Violette, S. M.; Alexandersen, S.; Jackson, T. The $\alpha_V\beta_6$ Integrin Receptor for Foot-and-Mouth Disease Virus Is Expressed Constitutively on the Epithelial Cells Targeted in Cattle. *J. Gen. Virol.* **2005**, *86*, 2769–2780.
(**10**) Hausner, S. H.; DiCara, D.; Marik, J.; Marshall, J. F.; Sutcliffe, J. L. Use of a Peptide Derived from Foot-and-Mouth Disease Virus for the Noninvasive Imaging of Human Cancer: Generation and Evaluation of 4-[18 F]Fluorobenzoyl A20FMDV2 for In Vivo Imaging of Integrin $\alpha_V\beta_6$ Expression with Positron Emission Tomography. *Cancer Res.* **2007**, *67*, 7833–7840.
(**11**) Kraft, S.; Diefenbach, B.; Mehta, R.; Jonczyk, a.; Luckenbach, G. a.; Goodman, S. L. Definition of an Unexpected Ligand Recognition Motif for $\alpha_V\beta_6$ Integrin. *J. Biol. Chem.* **1999**, *274*, 1979–1985.
(**12**) Dong, X.; Hudson, N. E.; Lu, C.; Springer, T. A. Structural Determinants of Integrin β-Subunit Specificity for Latent TGFβ. *Nat. Struct. Mol. Biol.* **2014**, *21*, 1091–1096.
(**13**) Maltsev, O. V.; Marelli, U. K.; Kapp, T. G.; Di Leva, F. S.; Di Maro, S.; Nieberler, M.; Reuning, U.; Schwaiger, M.; Novellino, E.; Marinelli, L.; Kessler, H. Stable Peptides Instead of Stapled Peptides: Highly Potent $\alpha_V\beta_6$-Selective Integrin Ligands. *Angew. Chem. Int. Ed.* **2016**, *55*, 1535–1539.
(**14**) Di Leva, F. S.; Tomassi, S.; Di Maro, S.; Reichart, F.; Notni, J.; Dangi, A.; Marelli, U. K.; Brancaccio, D.; Merlino, F.; Wester, H.; Novellino, E.; Kessler, H.; Marinelli, L. From a Helix to a Small Cycle: Metadynamics-Inspired $\alpha_V\beta_6$ Integrin Selective Ligands. *Angew. Chem. Int. Ed.* **2018**, *57*, 14645–14649.
(**15**) Notni, J.; Reich, D.; Maltsev, O. V.; Kapp, T. G.; Steiger, K.; Hoffmann, F.; Esposito, I.; Weichert, W.; Kessler, H.; Wester, H.-J. In Vivo PET Imaging of the Cancer Integrin $\alpha_V\beta_6$ Using ^{68}Ga-Labeled Cyclic RGD Nonapeptides. *J. Nucl. Med.* **2017***, 58, 671– 677.*
(**16**) Anderson, N. A.; Campbell, I. B.; Fallon, B. J.; Lynn, S. M.; Macdonald, S. J. F.; Pritchard, J. M.; Procopiou, P. A.; Sollis, S. L.; Thorp, L. R. Synthesis and Determination of Absolute Configuration of a Non-Peptidic $\alpha_v\beta_6$ Integrin Antagonist for the Treatment of Idiopathic Pulmonary Fibrosis. *Org. Biomol. Chem.* **2016**, *14*, 5992–6009.
(**17**) Maden, C. H.; Fairman, D.; Chalker, M.; Costa, M. J.; Fahy, W. A.; Garman, N.; Lukey, P. T.; Mant, T.; Parry, S.; Simpson, J. K.; Slack, R. J.; Kendrick, S.; Marshall, R. P. Safety, Tolerability and Pharmacokinetics of GSK3008348, a Novel Integrin $\alpha_V\beta_6$ Inhibitor, in Healthy Participants. *Eur. J. Clin. Pharmacol.* **2018**, *74*, 701–709.
(**18**) Hatley, R. J. D.; Macdonald, S. J. F.; Slack, R. J.; Le, J.; Ludbrook, S. B.; Lukey, P. T. An α_V-RGD Integrin Inhibitor Toolbox: Drug Discovery Insight, Challenges and Opportunities. *Angew. Chem. Int. Ed.* **2018**, *57*, 3298–3321.
(**19**) Battistini, L.; Burreddu, P.; Carta, P.; Rassu, G.; Auzzas, L.; Curti, C.; Zanardi, F.; Manzoni, L.;

Araldi, E. M. V; Scolastico, C.; Casiraghi, G. 4-Aminoproline-Based Arginine-Glycine-Aspartate Integrin Binders with Exposed Ligation Points: Practical in-Solution Synthesis, Conjugation and Binding Affinity Evaluation. *Org. Biomol. Chem.* **2009**, *7*, 4924–4935.
(**20**) Sartori, A.; Bianchini, F.; Migliari, S.; Burreddu, P.; Curti, C.; Vacondio, F.; Arosio, D.; Ruffini, L.; Rassu, G.; Calorini, L.; Pupi, A.; Battistini, L. Synthesis and preclinical evaluation of a novel, selective ^{111}In-labelled aminoproline-RGD-peptide for non-invasive melanoma tumor imaging *MedChemComm* **2015**, *6*, 2175–2183.
(**21**) Van Agthoven, J. F.; Xiong, J.-P.; Alonso, J. L.; Rui, X.; Adair, B. D.; Goodman, S. L.; Arnaout, M. A. Structural Basis for Pure Antagonism of Integrin $\alpha_V\beta_3$ by a High-Affinity Form of Fibronectin. *Nat. Struct. Mol. Biol.* **2014**, *21*, 383–388.
(**22**) Bugatti, K.; Bruno, A.; Arosio, D.; Sartori, A.; Curti, C.; Augustijn, L.; Zanardi, F.; Battistini, L. Shifting Towards $\alpha_V\beta_6$ Integrin Ligands Using Novel Aminoproline-Based Cyclic Peptidomimetics. *Chem. Eur. J.* **2020**, *26*, 13468–13475.
(**23**) Kaiser, E.; Colescott, R. L.; Bossinger, C. D.; Cook, P. I. Color Test for Detection of Free Terminal Amino Groups in the Solid-Phase Synthesis of Peptides. *Anal. Biochem.* **1970**, *34*, 595–598.
(**24**) Civera, M.; Arosio, D.; Bonato, F.; Manzoni, L.; Pignataro, L.; Zanella, S.; Gennari, C.; Piarulli, U.; Belvisi, L. Investigating the Interaction of Cyclic RGD Peptidomimetics with $\alpha_V\beta_6$ Integrin by Biochemical and Molecular Docking Studies. *Cancers* **2017**, *9*, 128.
(**25**) Kapp, T. G.; Rechenmacher, F.; Neubauer, S.; Maltsev, O. V.; Cavalcanti-Adam, E. A.; Zarka, R.; Reuning, U.; Notni, J.; Wester, H. J.; Mas-Moruno, C.; Spatz, J.; Geiger, B.; Kessler, H. A Comprehensive Evaluation of the Activity and Selectivity Profile of Ligands for RGD-Binding Integrins. *Sci. Rep.* **2017**, *7*, 1–13.
(**26**) Sartori, A.; Portioli, E.; Battistini, L.; Calorini, L.; Pupi, A.; Vacondio, F.; Arosio, D.; Bianchini, F.; Zanardi, F. Synthesis of Novel c(AmpRGD)–Sunitinib Dual Conjugates as Molecular Tools Targeting the $\alpha_V\beta_3$ Integrin/VEGFR2 Couple and Impairing Tumor-Associated Angiogenesis. *J. Med. Chem.* **2017**, *60*, 248–262.

Chapter 3. Targeting PAR2

The work described in this chapter is confidential.

3.1. Introduction

3.1.1. PAR2: structure and generalities

Proteinase-activated receptors (PAR) are a family of seven-transmembrane-domain receptors, belonging to the G protein-coupled receptors (GPCR). Described for the first time in the early 1990s,[1] these receptors are characterized by a unique activation mechanism involving a protease that cleaves the extracellular pro-domain, thus exposing a new N-terminus which activates the receptor. Nowadays, four different members of the PARs family have been identified (PAR1, PAR2, PAR3 and PAR4), which have different functions and physio-pathological roles, despite their overlapping tissue expression patterns.[2] Typically, PARs consist of seven transmembrane helices (TM1-TM7), an amino-terminal extracellular domain, three intracellular loops (ICL1-ICL3), three extracellular loops (ECL1-ECL3) and a carboxy-terminal intracellular domain (Figure 1). In particular, a disulphide bond between the ECL2 and the TM3 increases the stability and ensures the integrity of the receptor, as for many other GCPRs.

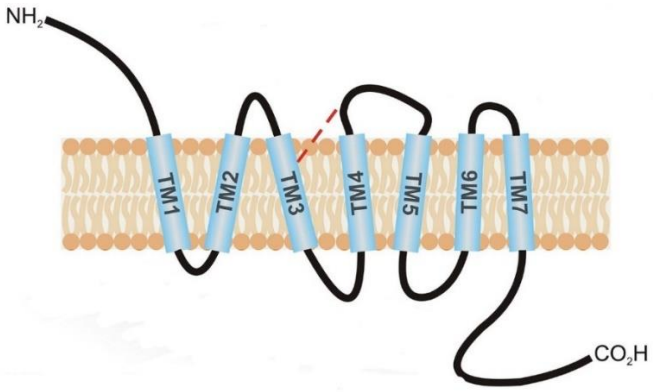

Figure 1. *General structure of PARs. Adapted from Ref. 2.*

In the last decades, different mechanisms of activation have been recognized, showing that the activation processes, which regulate the activity of PARs, are more complex than those initially described for these receptors. Therefore, the different mechanisms can be listed as follows: *(i) Classical activation:* PARs are activated by a specific protease that cleaves the N-terminus on a precise site, unmasking the tethered ligand (TL) which, in turn, binds the ECL2 and activates the receptor. Beside this so-called "canonical activation", a "non-canonical activation" entails other proteases that cleave PARs at different sites[3,4] and cause distinct cell responses; (*ii) Peptide activation*: PARs are activated by exogenous peptide agonists, which bind the ECL2 as for the tethered ligand; (*iii) Biased activation:* PARs are disabled by a disarming proteinase, which can "silence" the response of the receptor to other proteases (Figure 2). However, it has been demonstrated that some proteases (including the elastases) can activate a specific intracellular pathway by means of such disarming process (biased agonism).[1,5]

After receptor activation, ligand interaction leads to PAR desensitization (as for the other GCPR), followed by endocytosis and recycling of the receptor or degradation, depending on the respective receptor system involved. In many cases, after phosphorylation, the receptors recruit β-arrestin and the novel complexes undergo a clathrin-dependent endocytosis in the early endosomes; here, the complexes are dephosphorylated and finally recycled or degraded in the lysosomes.

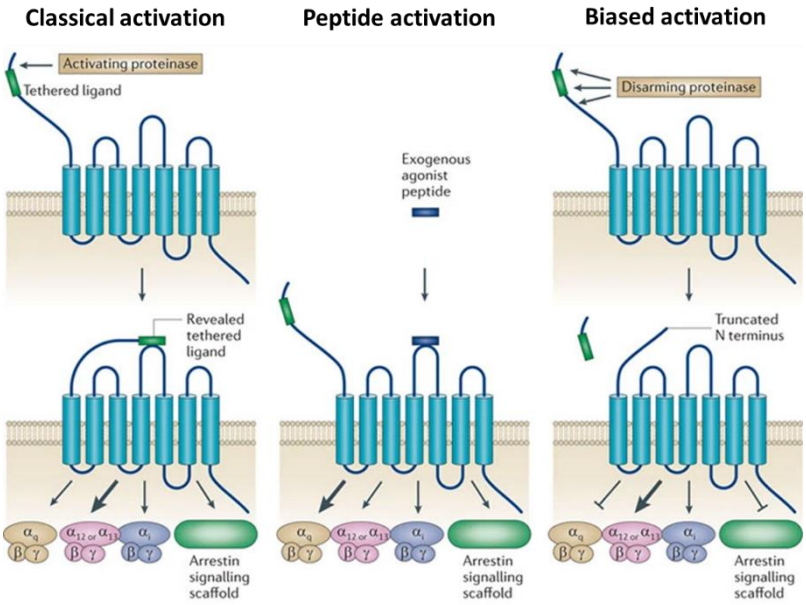

Figure 2. *Scheme of the different mechanisms of PAR activation. Adapted from Ref. 6.*

PARs are involved in many normal and disease states,[2,4] and their diversity as regards the activation mechanisms makes the development of new drugs targeting PARs systems very challenging. Among the proteinase-activated receptors, PAR2 has recently emerged as an attractive therapeutic target being involved in a number of diseases, including cancer.

Initially known as a trypsin-activated receptor, PAR2 was identified and cloned by Sundelin in 1994[7] and it was immediately associated to the PARs family, based on the structure similarity and mechanism of activation of PAR1. The general mechanism of activation is described in the previous section; in particular, according to the canonical activation, the extracellular N-terminus of PAR2 is cleaved mainly by the serine proteinase trypsin, cutting the Arg36-Ser37 linkage and unmasking the canonical tethered Ser-Leu-Ile-Gly-Lys-Val hexapeptide;[6] this, in turn, binds the receptor in a conserved region of the extracellular loop 2 (ECL2) and/or a transmembrane region. Other proteases, such as elastase, proteinase-3 and cathepsin, cleave the N-terminus at distinct sites generating different responses (Figure 3), depending on the coupled G protein:[1,3,8] i) $G\alpha_q$ activates the inositol triphosphate and diacylglycerol pathways, resulting in a downregulation of protein kinase C and mobilization of calcium ions; ii) $G\alpha_s$ activates adenylyl cyclase, which stimulates cAMP production; iii) $G\alpha_i$, on the contrary, inhibits cAMP and activates MAPK pathways, causing cellular proliferation; iv) $G\alpha_{12/13}$ activates JNK (c-Jun N-terminus kinases) and RhoA, promoting migration, differentiation and cell growth.

Concerning expression and localization, PAR2 is expressed in many epithelial and endothelial cells (in lung, skin, kidney, pancreas, liver and other tissues), but also in fibroblasts, nerves and in immune and inflammatory cells.[8] Therefore, it is implicated in different physiological processes and its up-regulation has been associated to different pathological states, such as cancers,[9] arthritis,[10] inflammation,[11] cardiovascular,[12] gastrointestinal,[13] and pulmonary diseases.[14] However, PAR2 activation exerts protective effects in certain pathologies, for instance in ischemia,[15] wound healing[16] and colitis,[13] rendering this receptor an attractive target for the development of both agonist and antagonist ligands.

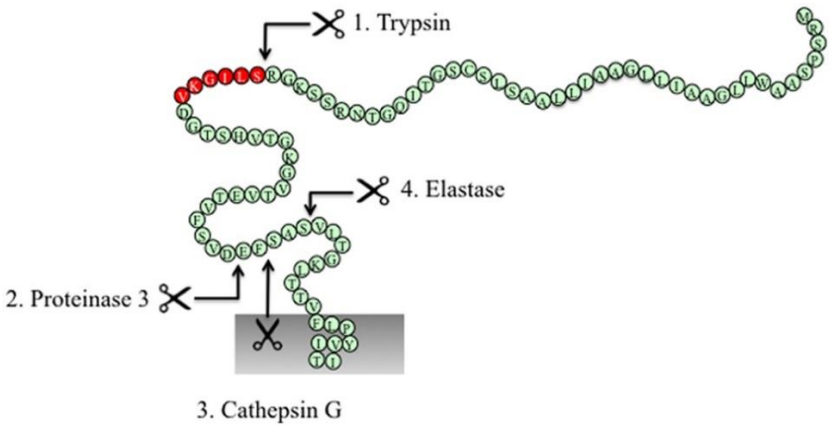

Figure 3. *Cleavage of the N-terminus of PAR2 by different proteases. Adapted from Ref. 1.*

3.1.2. Ligands targeting PAR2 receptors: state of the art

The PAR2 receptor is known to be involved in several physiological and pathological processes and different ligands targeting this receptor have been synthesized and proposed since its discovery and cloning in 1994;[7] however, no PAR2 modulators have yet entered the clinical trials.[1]

The first molecules proposed were based on the structure of the tethered ligand shown in the previous paragraph. Hence, in 1996 different short peptides were synthesized and, among these, only the sequence SLIGRL-NH_2[17] resulted more potent than the native sequence SLIGKV-NH_2.[18] Unfortunately, this peptide could be used only as a tool for biological investigations due to its poor potency (it is active at micromolar concentration). Later, in 2004 Hollenberg and colleagues synthesized a library of more potent and stable peptides modified at the N-terminus,[19] among these the 2-furoyl-LIGRLO-NH_2 ligand **1** (Figure 4), showing the best potency in the series, became a pioneering candidate in the search of PAR2 binders.

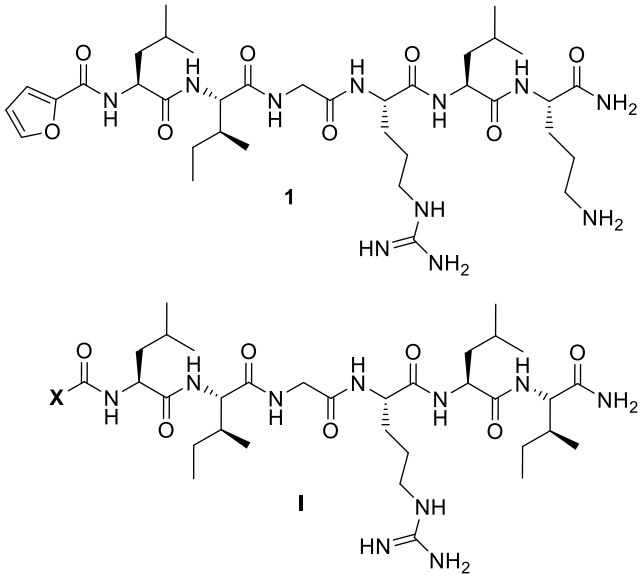

X = 2-furoyl, 4-(2-methyloxazolyl), 5-isoxazolyl, 2 pyrazolyl, 2-pyridoyl, 3-pyridoyl, 2-benzofuranoyl, 2-naphthoyl, 2-benzothienyl

Figure 4. *Structure of the sequence 2-furoyl-LIGRLO-NH_2 (**1**) and other PAR2 agonists (**I**). Adapted from Ref. 20.*

Going further on this direction, other research groups proposed new short peptide sequences of type **I** as PAR2 agonists (Figure 5) with EC_{50} in the 0.1-0.8 mM range (measured by the concentration

of intracellular calcium released in various cell lines), confirming that a terminal heterocyclic ring is beneficial for the agonist activity.[21,20] These results taken together evidenced that agonist activity is positively affected by a C-terminal amide group and a heterocyclic ring linked at the N-terminus, thus opening the way to the development of peptidomimetic PAR2 ligands.

Therefore, the research moved toward the synthesis of small molecules and peptidomimetics having better stability and pharmacokinetic properties. In 2010, Barry et al. described an important SAR study[22] that resulted in the discovery of the novel agonist GB110 (**2**, Figure 5, EC_{50} 0.28 μM, iCa^{2+} release) and the antagonist GB88 (**3**, Figure 5, IC_{50} 2 μM, inhibition of iCa^{2+} release). As for the previously described ligands, GB110 presents an N-terminal heterocycle and two apolar amino acid residues close to this ring, suggesting that these residues are important for the binding to the receptor. On the contrary, GB88 has a bulky residue at the C-terminus, although the rest of the structure is very similar to GB110, once more suggesting that this last portion is crucial for switching agonist/antagonist activity towards PAR2.

Relying on these studies, in 2016 Yau et al.[20] tried to reduce size, polar surface and bond mobility with the aim to synthesize a potent, rule-of-five compliant compound with higher potency and better stability than the previously described ones. During this study, they found the novel potent agonist AY77 (**4**, Figure 5, EC_{50} 33 nM, iCa^{2+} release) and proposed a possible binding mode, where AY77 is supposed to form multiple hydrogen bonds and hydrophobic interactions with PAR2 through its terminal amide group (with Asp228 and Tyr156) and the isoxazole ring (with Tyr82) (Figure 5). The authors hypothesized that isoxazole, cyclohexylalanine and cyclohexylglycine portions should occupy three distinct pockets in the PAR2 binding site; in particular, cyclohexylglycine seems to develop specific hydrophobic interactions with Tyr326 and Leu307.

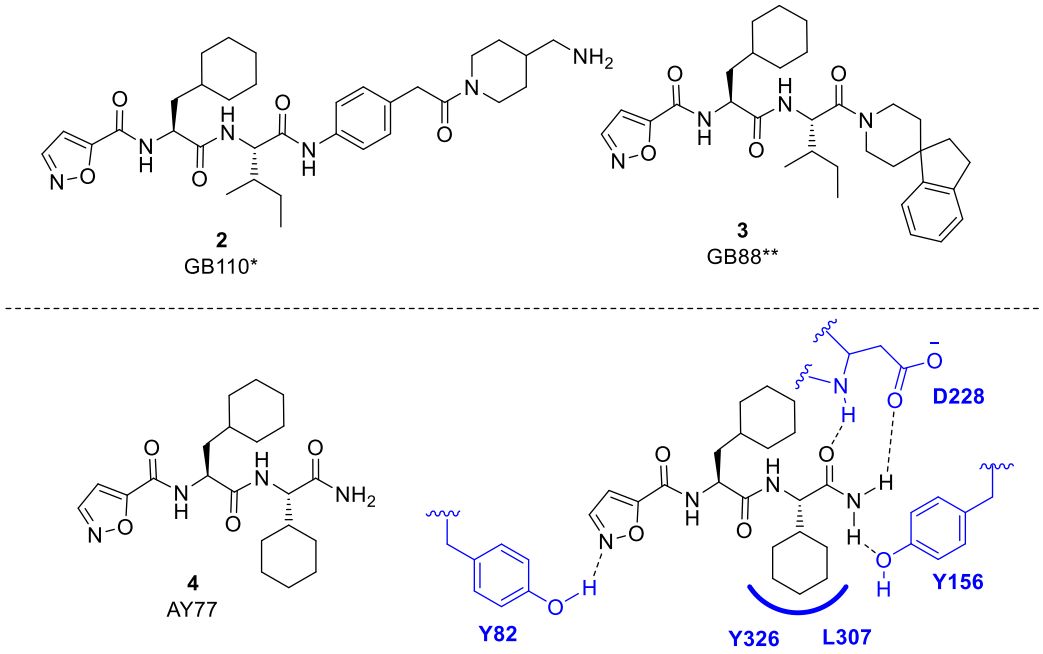

Figure 5. *Structures of the PAR2 agonists **2** and **4**, and the antagonist **3**. The predicted binding mode for **4** in a PAR2 homology model derived from nociceptin/orphanin FQ receptor (PDB code 4EA3)[20] is shown at the bottom right.*

One year later, the same research group synthesized the biased ligand AY117 (**5**, Figure 6),[23] which showed antagonist activity in calcium release induced by trypsin and 2-furoyl-LIGRLO-NH_2 (IC_{50} 2.2 and 0.7 μM), but it also showed selective PAR2 agonist activity in inhibiting cAMP stimulation and in activating ERK1/2 phosphorylation. In fact, in this work the authors described the switching from agonist to antagonist properties for several low micro- to submicromolar PAR2 ligands in the iCa^{2+}

release assays; they demonstrated that the presence of a primary amide or H-bond acceptor at the C-terminus was crucial for the agonist activity and that the switch to antagonist activity depended on the presence of H-bond acceptor units at the N-terminus.

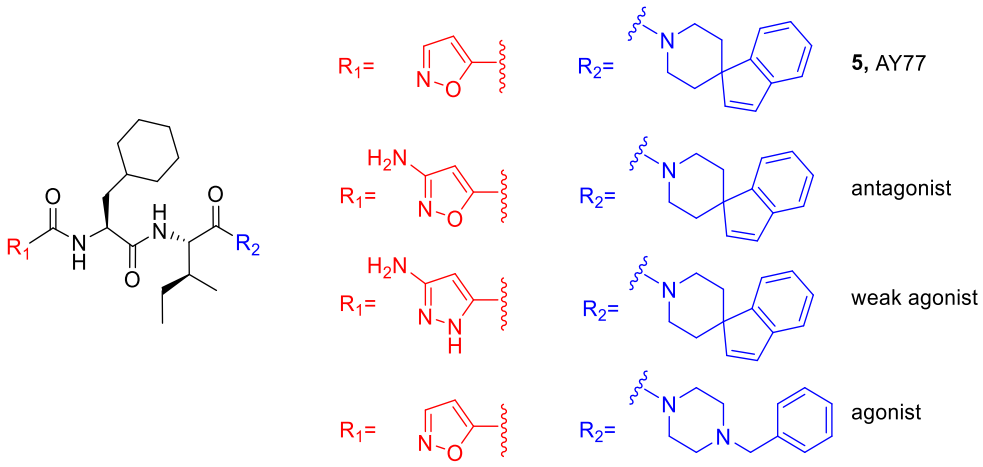

Figure 6. *Structure of the antagonist AY117 (**5**) and examples of compounds with antagonist/agonist activity.*[23]

In the field of non-peptidic small molecular ligands, only a few candidates appeared in the literature up to now. In 2008, Gardell et al. discovered the first non-peptidic small molecular PAR2 agonists AC-55541 and AC-264613 by means of a high-throughput functional screening (**6** and **7**, Figure 7); these compounds were able to activate PAR2 signalling in cellular proliferation, phosphatidylinositol hydrolysis and calcium mobilization assays, with potencies ranging from 200 to 1000 nM for AC-55541 (**6**) and 30 to 100 nM for AC-264613 (**7**).[24] Interestingly, these compounds share a completely non-peptidic scaffold, a *N'-acetyl*-hydrazone central core, on which two hydrophobic portions (the aromatic rings) and the H-bond donor groups (the phthalazin-1(2*H*)-one for AC-55541 and at the γ-lactam for AC-264613) are grafted.

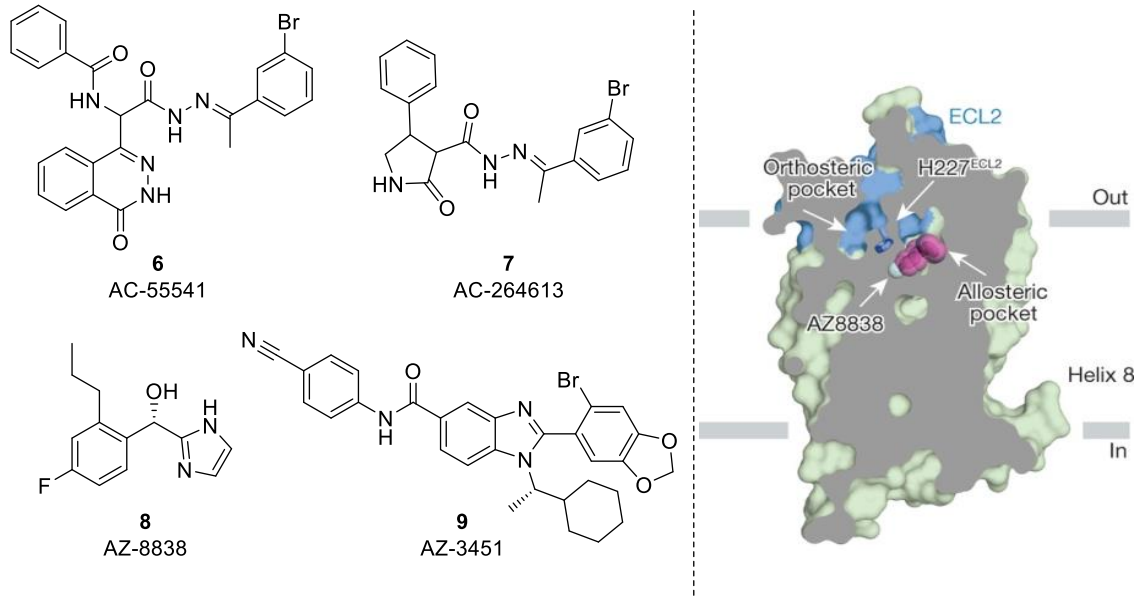

Figure 7. *On the left, structures of the antagonists AC-55541 (**6**), AC-264613 (**7**), AZ8838 (**8**) and AZ3451 (**9**). On the right, the crystal structure (PDB: 5NDD) of PAR2 in complex with AZ8838. Adapted from Ref. 25.*

In 2017, Cheng et al. first reported the crystal structure of PAR2 in complex with two antagonists, AZ8838 and AZ3451 (**8** and **9**, Figure 7).[25] According to these studies, compound AZ8838 (**8**) binds

in a fully occluded pocket near the extracellular surface and exhibits slow binding kinetics, whilst compound AZ3451 (**9**) binds to a remote allosteric site outside the helical bundle; hence, the authors concluded that AZ3451 is not an orthosteric antagonist, as its binding to PAR2 is able to prevent the structural rearrangements required for receptor activation and signalling. This important study allowed to expand considerably the knowledge about PAR2 and prompted the development of new PAR2 ligands.

Along this line, Gmeiner et al. recently published a SAR study concerning a series of peptidomimetic PAR2 agonists.[26] The authors planned to replace the cyclohexylglycine moiety within the previously described ligand **4** AY77 with benzamide-homologues to achieve a better fitting in the lipophilic pocket with respect to compound AY77, synthesizing a panel of compounds of type **II** (Figure 8). However, the three most potent molecules in the Gαq activation (EC_{50} 0.59-0.64 μM) are not enough potent in the β-arrestin recruitment (EC_{50} 6.0-8.9 μM).

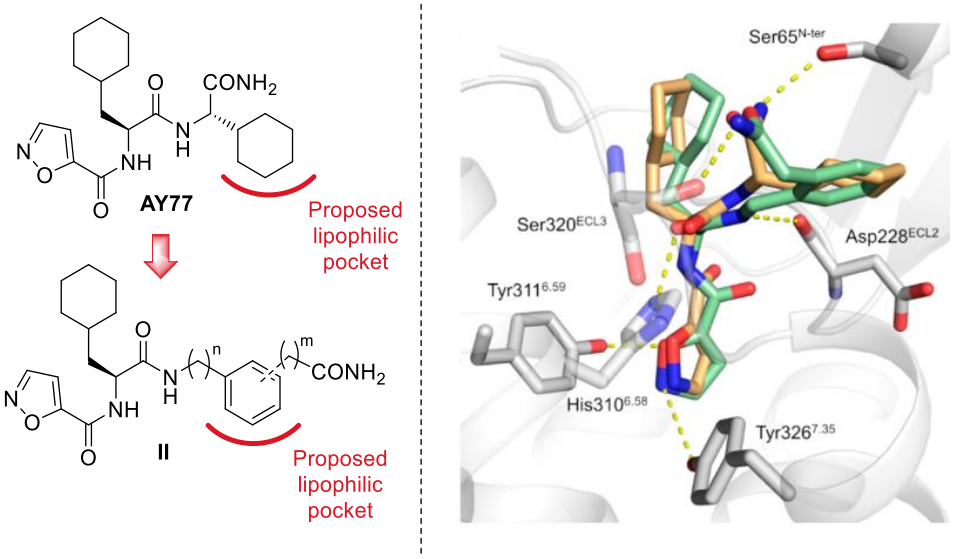

Figure 8. *Left, design of novel nonpeptidic PAR2 agonists. Right, overlay of the best poses for* ***AY77*** *(orange) and type* ***II*** *ligands (green) in the PAR2 model (grey). Adapted from Ref. 26.*

In this research context is inserted the project I carried out during my six-month secondment in the Prof. Dr. Gmeiner group at the University of Erlangen-Nürnberg. Considering the remarkable potential of PAR2 targeting ligands as both therapeutic agents and/or investigating probes, it is not surprising that great efforts are being addressed to the development of new PAR2 modulators; indeed, although several ligands have been reported so far,[27] no drugs addressing PAR2 receptors have been approved yet.

3.2. Aim of the project

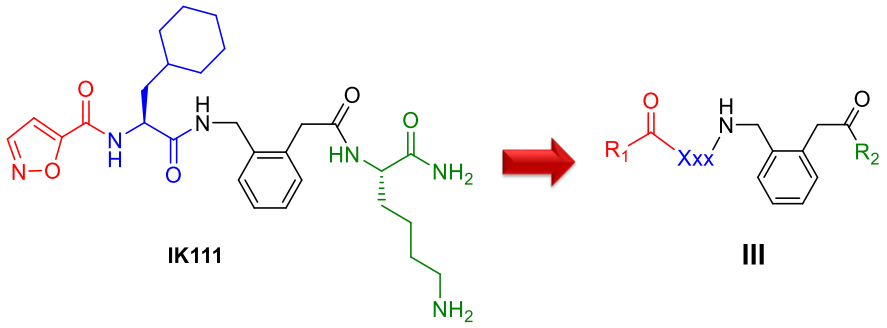

Figure 9. *Structure of compound **IK111** and suggested modification sites in the general formula **III** of this project.*

As described in the previous section, in the last decades remarkable progress was made in profiling the therapeutic potential of PAR2 antagonists, but fewer studies explored the field of PAR2 agonists, which are extremely important tools to investigate the pathophysiological condition related to PAR2. For these reasons, my six-months project at the University of Erlangen-Nürnberg in the Prof. Dr. Gmeiner's research group was focused on the synthesis and characterization of a collection of new small molecule peptidomimetics with PAR2 agonist activity, as a continuation of the PhD project by Dr. Klösel, who described the synthesis and characterization of compound **IK111** (Figure 9); this peptidomimetic ligand was then selected as the starting point to rationally design the new candidates to be synthesized with the aim to obtain functional selectivity by using a basic side chain at the C-terminus.

The following chapters illustrate the design and synthesis of a panel of twenty new small molecules; the microwave-assisted solid phase peptide synthesis was applied to the synthesis of all the peptidomimetic ligands; the final compounds were fully characterized by NMR and HMRS. The compounds are planned to be tested by the IP-One-HEK assay and the arrestin-HEK-PS1K assay to identify the most promising candidates within the library, with the hope to drive the research toward the future development of new potent PAR2 agonists.

3.3. Results and discussion

3.3.1. Design of potential PAR2 agonists

At the beginning of the project, taking inspiration from information found in Dr. Klösel's dissertation and in the literature, we planned to evaluate structural modification of the reference compound **IK111**. To this aim, **IK111** was formally subdivided into four different subunits, marked with different colours in Figure 10. First, modification of the heterocyclic portion (in red) was planned by selecting varied heterocycles (such as pyridine, oxazole, …) or acyclic substituents (oxamic or oxalic acid residues), able to act as H-bond acceptors. Then, the importance of a bulky hydrophobic amino acid side chain (in blue) was explored, by using apolar amino acids (cyclohexylglycine, leucine, isoleucine, …) instead of cyclohexylalanine to maximize interactions in the hydrophobic pocket of the receptor. Finally, various basic residues were selected for the terminal portion (in green) featuring distinct conformational arrangement and/or length and nature of functional group (amine, methyl ester, …).

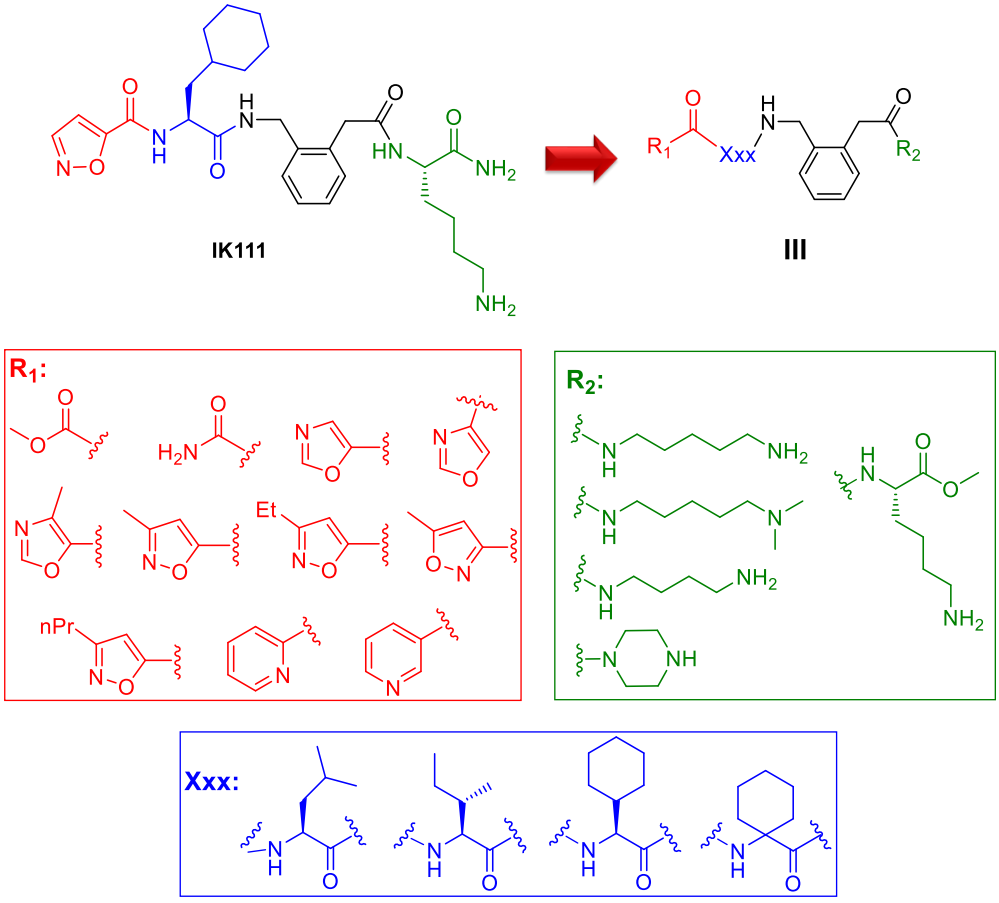

Figure 10. *Planned modifications of compound* ***IK111*** *toward the library of new peptidomimetics* ***III*** *of this work.*

According to this plan, the synthesis of all the peptidomimetics of general formula **III** in Figure 10 was mainly based on the exploitation of the microwave-assisted solid phase synthesis, followed by in-solution modifications for a limited number of molecules, as described in the following chapter.

3.3.2. Synthesis of the designed PAR2 agonists

All the designed peptidomimetics were synthesized by using the microwave-assisted solid phase peptides synthesis (SPPS) according to a Fmoc-based protocol described in the experimental section. The merits of SPPS in the synthesis of peptides and peptidomimetics have been described in Chapter 2 (Paragraph 2.3.2.). The use of microwaves is beneficial for the acceleration of coupling and deprotection steps; indeed, these procedures performed under microwaves take only few minutes to completion making the whole synthetic route rapid and efficient as compared to traditional SPPS. In the implementation of the routine SPPS (resin swelling and loading, alternating deprotection/coupling steps and resin cleavage), two different protocols were adopted to accomplish the synthesis of the designed peptidomimetics, depending on the resin of choice. The type of the resin have been chosen based on the desired final terminal group of the designed peptidomimetic (Rink-Amide resin for terminal amide or 2-Chlorotrityl resin for terminal carboxylic acid, ester or amine).

3.3.2.1. Protocol based on the Rink-Amide resin

The general protocol based on the Rink-Amide resin starts with the resin swelling by DMF and shaking the reaction vessel for 20 minutes. This resin is usually stored as Fmoc-protected, so the first step consists on removal of the protecting group by treatment with a solution of 25% piperidine in DMF (Scheme 1) performing five cycles of irradiation (5 sec, 100 W). Completion of the reaction is usually checked by the Kaiser Test.

Scheme 1. *Microwave-assisted SPPS protocol based on the Rink-Amide resin.*[a]

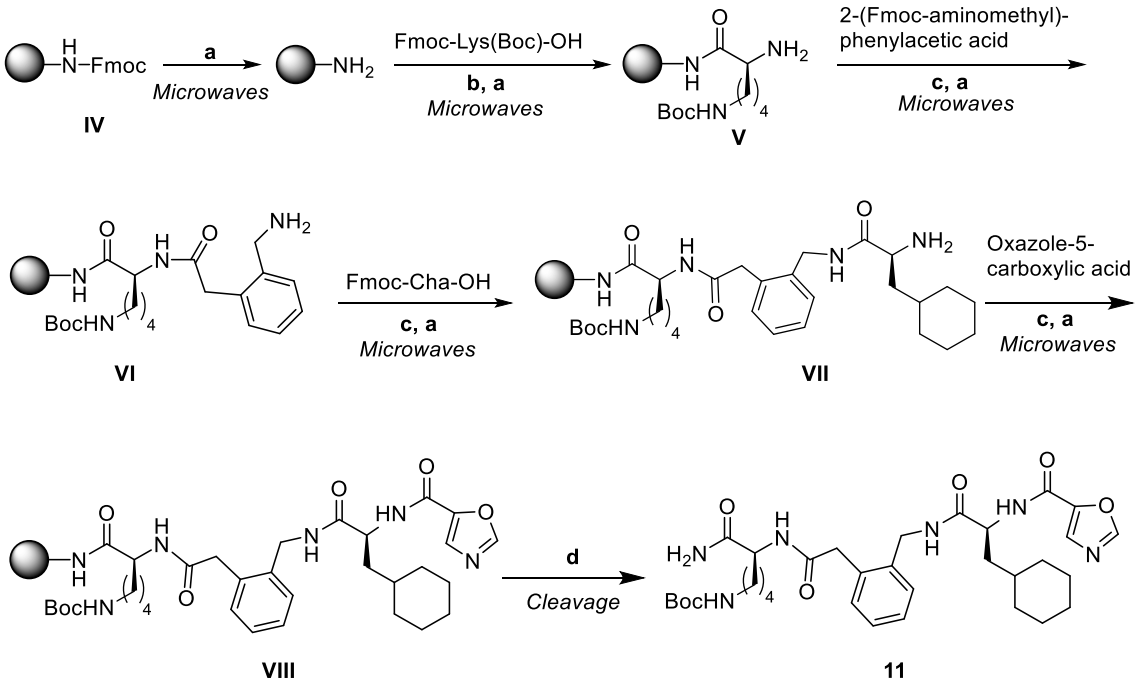

[a]Reagents and conditions: **a**) piperidine 25% in DMF; **b**) HATU, HOBt, DIPEA, DMF; **c**) PyBOP, HOBt, DIPEA, DMF; **d**) TFA:PhOH *liq*:H_2O:TIS 88:6:4:2.

To obtain compound **11**, the loading of the resin required the Fmoc-Lys(Boc)-OH as the first amino acid and HATU; HOBt and DIPEA were used as coupling reagents, 20 cycles of irradiation (10 sec, 50 W) were performed and completion of reaction was checked by Kaiser Test. However, in some cases, the test was positive, and a double coupling procedure was performed by adopting the

conditions described before. After the loading step, the alternating cycles of coupling/deprotection reactions were executed until the planned sequence was accomplished. Coupling reactions required different amino acids or functionalized carboxylic acids and the use of PyBOP instead of HATU as coupling reagent, since the subsequent amine groups are not that sterically hindered as in the case of the benzhydryl amine-based resin. In case of positive Kaiser Test, the double coupling was performed using HATU instead of PyBOP. The final cleavage from the resin was performed using trifluoroacetic acid and the final peptidomimetics were purified by reverse-phase preparative HPLC.

3.3.2.2. Protocol based on the 2-Chlorotrityl resin

For the general protocol employing the 2-Chlorotrityl resin, the swelling was performed by using deacidified dichloromethane and shaking the reactor for 20 minutes. The remarkable acid-sensitivity of 2-Chlorotrityl resin made the use of deacidified solvent necessary, to avoid premature peptide cleavage and decrease of the reaction yield.

Scheme 2. *Eq.1) Loading of the 2-Chlorotrityl resin with 1,4 butanediamine. Eq.2) Loading of the 2-Chlorotrityl resin with a generic amino acid (Fmoc-Aaa-OH).*

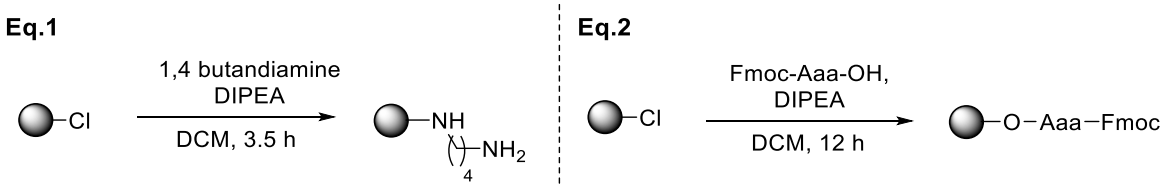

After the swelling step, loading with the amines (Scheme 2, eq. 1) required a solution of DIPEA in a small amount of dichloromethane and shaking for 3.5 hours under nitrogen atmosphere; on the other hand, loading with the amino acidic units required a solution of the Fmoc-protected amino acid and DIPEA in dichloromethane and shaking for 12 hours (Scheme 2, eq. 2). In both cases, the loading step was followed by treatment with a dichloromethane:methanol:DIPEA solution (8.5:1:0.5) as a quenching procedure to avoid the presence of reactive chlorotrityl residues.

Scheme 3. *Microwave-Assisted SPPS protocol based on the 2-Chlorotrityl Resin.*[a]

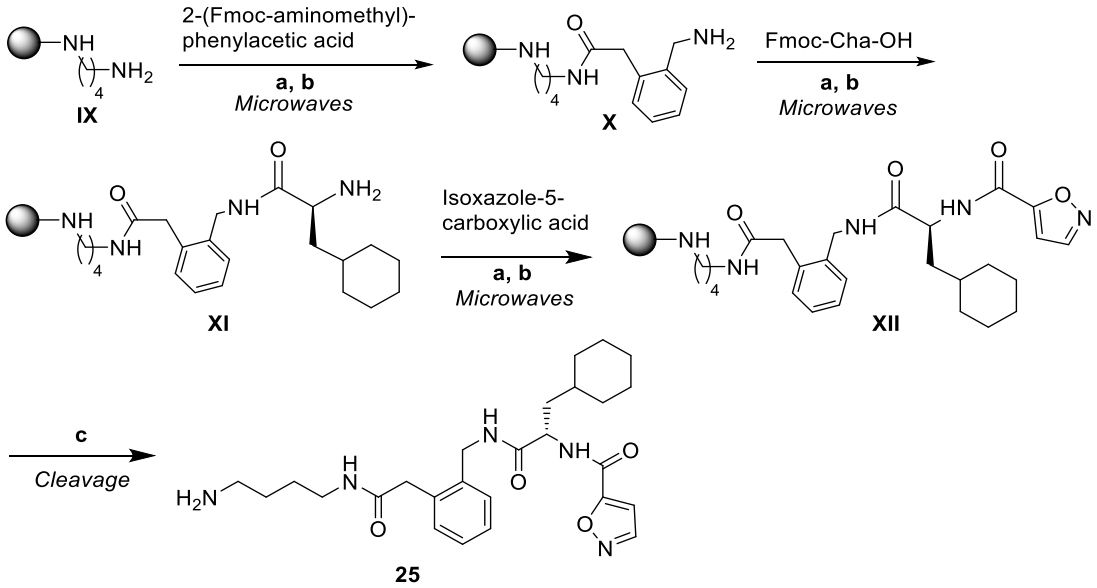

[a]Reagents and conditions: **a**) PyBOP, HOBt, DIPEA, DMF; **b**) piperidine 25% in DMF; **c**) DCM:TFA:TIS (85:10:5).

After the loading step, the alternating cycles of coupling and Fmoc-cleavage were executed as previously described for the Rink-Amide resin, with the only exception of using excess DIPEA, due to the sensitivity of the resin to the acid environment (Scheme 3).

Different conditions were also required for the cleavage procedures, depending on the nature of the first unit loaded and/or the functional groups. In case of sequences terminating with a primary amine, a solution of dichloromethane, trifluoroacetic acid and triisopropylsilane was employed and the reaction was kept under stirring for 2 hours. On the other hand, when the sequence terminated with a carboxylic acid, a solution of hexafluoropropanol and dichloromethane was used, and the reaction vessel was kept under stirring for 18 hours. In all cases, the final peptidomimetics were purified by reverse phase preparative HPLC.

3.3.2.3. Post-SPPS modifications

Two target compounds were obtained by post-SPPS modifications. The preparation of compound **26** required final esterification of precursor **26a**, as shown in Scheme 4 (eq. 1). In this case, a solution of trimethylchlorosilane in methanol was directly added to the crude compound obtained from the resin cleavage and the reaction was stirred at 80 °C for 6 hours. After completion, the reaction was subjected to work up and reverse-phase preparative HPLC purification, giving the final product **26** with an overall yield of 61%.

Scheme 4. *Post-SPPS modifications of compounds **26** and **28**.*[a]

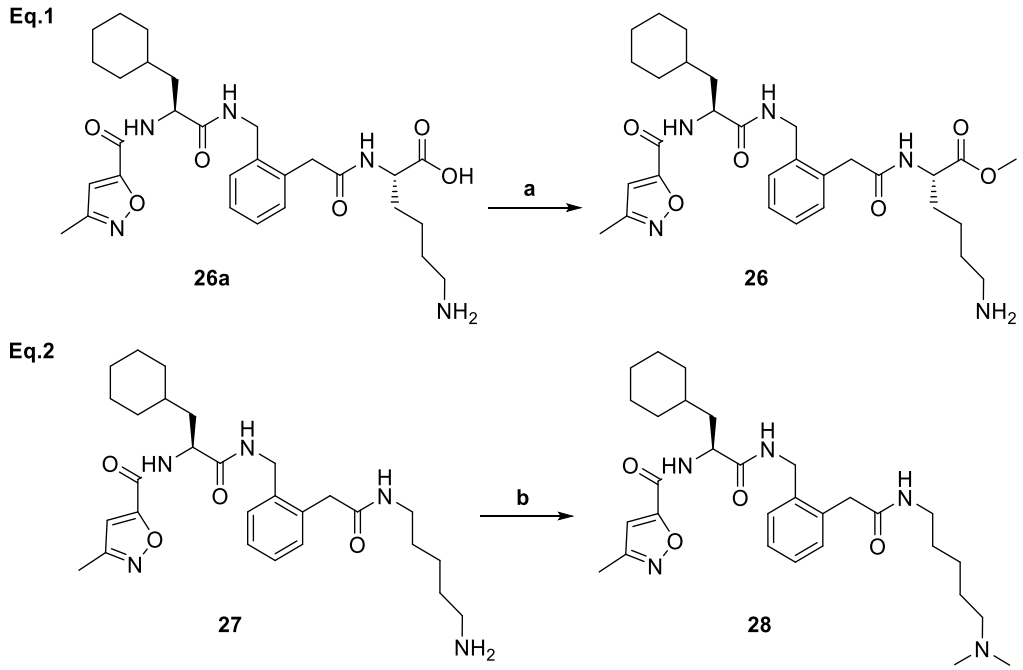

[a]Reagents and conditions: a) TMSCl, MeOH, 80° C, 12 h, 61%; b) HCOH 37%, $NaBH(OAc)_3$, ACN:H_2O 1:1, 12 h, rt, 43%.

In the second instance, precursor **27** was subjected to a reductive amination in the presence of an excess of formaldehyde and $NaBH(OAc)_3$ to afford the dimethylated terminal amine, which was purified by reverse-phase preparative HPLC, giving the final compound **28** in 43% yield.

3.3.3. The library of PAR2-targeting peptidomimetics: a SAR study

The structures of the twenty synthesized compounds are shown in Figure 11, along with the corresponding overall yields (up to 87%). All the final compounds were tested in two PAR2 receptor

systems, namely the IP-One-HEK screening assay and the arrestin-HEK-PK1S assay using **IK111** and 2f-LIGRLO-NH_2 as reference compounds. It is important to state that in the present dissertation the activities of the final peptidomimetics are only qualitatively described and commented. On the basis of the results of IP-One assay, we noticed that any modification at the cyclohexylalanine residue (**21**, **22**, **23**, **24**, Figure 11 middle) was deleterious for the agonist activity, underling the importance of a bulky apolar side-chain to fit the PAR2 hydrophobic pocket. Regarding the substitution of the isoxazole ring with different heteroaromatic moieties (**10**, **11**, **13**, **14**, Figure 11 up) or non-cyclic residues (**15**, **16,** Figure 12 up), we observed a substantial drop of the agonist activity. On the other hand, the introduction of a methyl substituent at C3 within the isoxazole ring (**12**, Figure 11 up) was beneficial, while the positioning of the same group at the C4 was detrimental (**17**, Figure 11 up). These evidences suggested the presence of an additional small hydrophobic pocket close to the isoxazole C3, whose extent was explored by introducing different alkyl chains at this position (**19**, **20**, Figure 11 up). Interestingly, the ethyl- and propyl-substituted compounds were slightly worse agonists when compared to **12**. Finally, the relative position of oxygen and nitrogen within the isoxazole was explored by switching the two heteroatoms (**18**, Figure 11 up) with disappointingly lower activity.

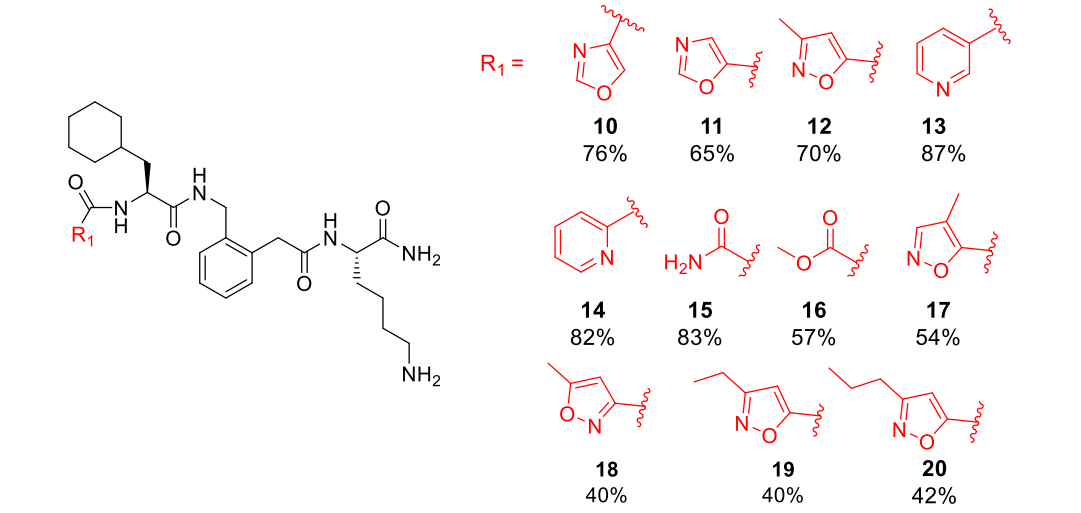

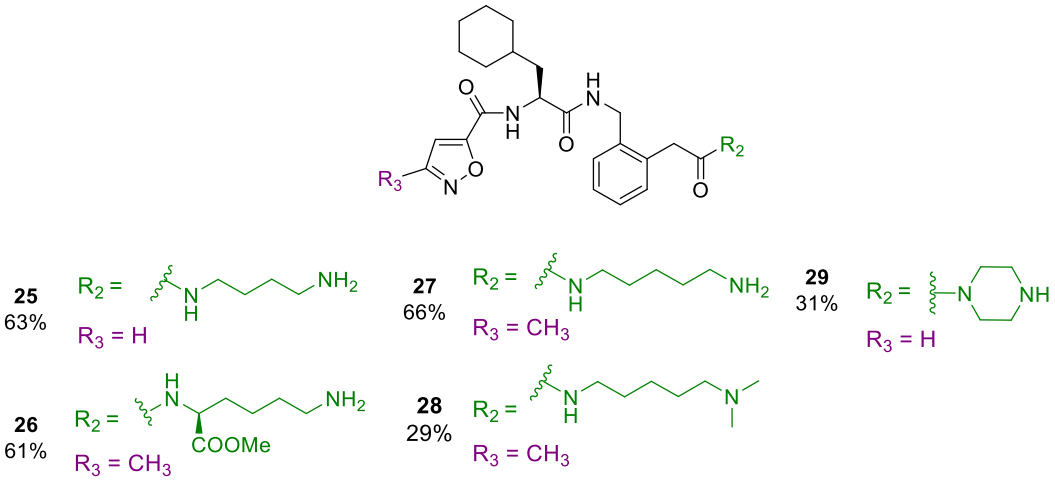

Figure 11. *Structures of the peptidomimetics synthesized in this work with overall yields.*

To complete the qualitative SAR study, the influence of the terminal primary amide was investigated. First, removal of the amide residue by introducing free terminal amines (**25**, **27**, **28**, **29**, Figure 11 bottom) caused a loss in potency with respect to compound **12**, in particular when terminal amino acid was changed by a piperazine nucleus (**29**, Figure 11 bottom). However, compound **27** and its dimethyl derivative **28** showed activities similar to **12**, suggesting that the terminal primary amine could be functionalized without decreasing the activity. Lastly, the substitution of the terminal amide with a methyl ester was beneficial (**26**), supporting the hypothesis that the presence of H-bond acceptor groups is crucial for the agonist activity of this kind of ligands.

The most promising compounds were evaluated in the arrestin-HEK-PK1S assay: the results obtained for compounds **25**, **26**, **28** and **29** (Figure 11, bottom) showed that any modification at the lysine group was detrimental for the arrestin recruitment, in particular, the methylation of the terminal amine (**28** versus **27**, Figure 11 up). In addition, the introduction of a methyl group at the oxazole C3 (**12**, Figure 11 up) showed a positive impact on the arrestin recruitment, meanwhile larger alkyl groups (ethyl, propyl) located at the same position were detrimental to the activity (**19**, **20**, Figure 11 up). Moreover, the substitution of the terminal amide with a methyl ester (**26**, Figure 11 up), which was tolerated in the IP-One assay, was deleterious for the arrestin recruitment.

3.4. Conclusions and perspectives

The present project, carried out in the laboratory of Prof. Dr. Peter Gmeiner at the University of Erlangen-Nürnberg, was focused on the synthesis and the Structure-Activity-Relationship studies of a library of new small-molecular peptidomimetics with potential PAR2 agonist activities.

Starting from the work done by Dr. Klösel, twenty different PAR2 ligands were designed and synthesized, characterized and tested in IP-One screening and arrestin-HEK-PK1S assays. Among these, the most interesting compound was **12** (Figure 12), featuring a methyl group located at the isoxazole C3, which displays an IC_{50} reduced by approximately one third as compared to **IK111**. Compound **26**, differing from **12** by exchanging the primary amide function by a methyl ester, showed a positive iCa^{2+} agonist activity, but failed in the arrestin recruitment assay, proving once more the dichotomy in the role played by the terminal functional group in activating the PAR2.

Further investigations will be necessary to shed light on this controversial behaviour in the search of novel potent PAR2 agonists. As shown in Figure 13, the role of the C3 substituent must be further evaluated with regard to the polarity/apolarity of the residue (i.e., trifluoromethyl, cyclopropyl and hydroxymethyl groups). In addition, the role of the amine appendage in the lysine portion should be explored by varying the amine functionalities. Finally, modifications at the terminal amide should be investigated as well (i.e., secondary/tertiary amides or homologous alkyl esters).

All these structural modifications could drive the research in finding potent peptidomimetic PAR2 agonists, as useful tools to understand the receptor binding/activation properties of new therapeutic agents targeting PAR2.

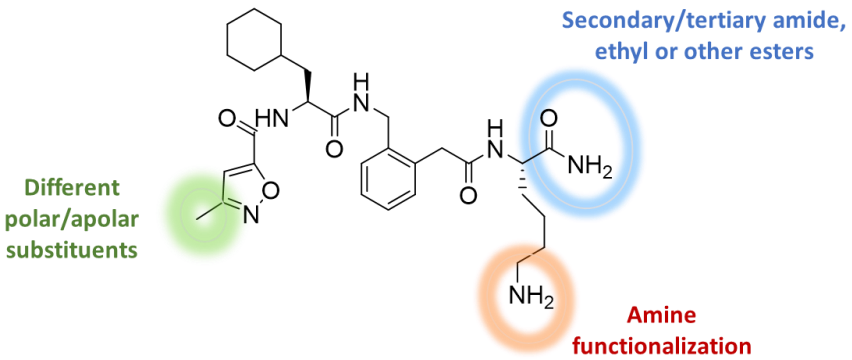

***Figure 12**. Structure of the best synthesized ligand **12** and possible suggestions for further modifications.*

3.5. Experimental section

3.5.1. General methods and materials

Starting Materials. Rink-Amide resin, 2-Cholorotrityl resin, Fmoc-Lys(O*t*Bu)-OH; Fmoc-Cha-OH, Fmoc-Chg-OH, Fmoc-Leu-OH, Fmoc-Ile-OH, 1-*N*-Fmoc-aminocyclohexylcarboxylic acid, Phenol *liquefactum* (86.4% absolute phenol, 13.6% water), DIPEA, HATU, HOAt, PyBoP, oxazole-5-carboxylic acid, oxazole-4-carboxylic acid, isoxazole-3-methyl-5-carboxylic acid, isoxazole-3-ethyl-5-carboxylic acid, isoxazole-3-propyl-5-carboxylic acid, isoxazole-5-methyl-3-carboxylic acid, isoxazole-4-methyl-5-carboxylic acid, nicotinic acid, picolinic acid, oxamic acid, methyl-chlorooxoacetate, 1,4-butandiamine, 1,5-pentandiamine, piperazine, phenol were commercially available and were used as such without further purification.

***General*.** All chemicals were of the highest commercially available quality and were used without further purification. Solvents were dried by standard procedures and reactions requiring anhydrous conditions were performed under nitrogen or argon atmosphere. Flash chromatography was performed using 40-63 μm silica gel using the indicated solvent mixtures. The HPLC solvents respond to HPLC grade for preparative HPLC and gradient grade for analytical HPLC and they were used without other purification. Preparative HPLC was performed on an Agilent 1200 preparative series HPLC system or on an Agilent HPLC 1260 Infinity system combined with an MWD detector and fraction collector, applying a linear gradient and a flow rate of 12 ml/min. As HPLC column, a Zorbax-Eclipse XDB-C8 PrepHT (21.2 mm × 150 mm, 5 μm) was used. α measurement was performed using a JASCO P-2000 apparatus at the temperature and concentration conditions reported for each compound. Routine NMR spectra were recorded on a Bruker Avance III 400 or 600 NMR spectrometers. Chemical shifts (δ) are reported in parts per million (ppm) with TMS ($CDCl_3$) resonance peaks set at 0. Multiplicities are indicated as s (singlet), d (doublet), t (triplet), q (quartet), m (multiplet), and b (broad). Coupling constants *J*, are reported in Hertz. ^{1}H and ^{13}C NMR assignments were corroborated by ^{1}H-^{1}H COSY, ^{1}H-^{13}C DEPTQ experiments. ESI-mass spectra were recorded using LC-MS: Thermo Scientific Dionex Ultimate 3000 UHPLC quaternary pump, autosampler and RS-diode array detector, column: Zorbax-Eclipse XDB-C8 analytical column, 3.0 mm × 100 mm, 3.5 μm, flow rate 0.4 mL/min, detection wavelength: 220 nm, coupled to a Bruker Daltonics Amazon mass spectrometer using ESI as ionization source. High resolution mass analysis (ESI) was performed on on a Bruker Daltonics timsTOF Pro spectrometer using electrospray ionization (ESI) as ionization source.

Final peptides purification: purification of the final peptides was performed by preparative HPLC (Agilent Zorbax XBD-C8, 21.2x150 mm, 5 μm) using H_2O+0.1% TFA (solvent A) and acetonitrile (solvent B) according to the following gradients

- *Gradient A:* 65% solvent A for 2 min, from 65% to 5% solvent A over 10 min, 5% solvent A for 1 min, from 5% to 65% of solvent A over 1 min.
- *Gradient B:* 75% solvent A for 2 min, from 75% to 5% solvent A over 14 min, 5% solvent A for 1 min, from 5% to 75% of solvent A over 1 min.
- *Gradient C:* 75% solvent A for 2 min, from 75% to 5% solvent A over 16 min, 5% solvent A for 2 min, from 5% to 75% of solvent A over 2 min.

General procedure for Microwave-assisted Solid Phase Peptide Synthesis. All the solid phase peptide syntheses (SPPSs) were performed using a CEM Focused Microwave Synthesis System (Model Discover), operating at ambient temperature and with constant power. Every reaction was carried out using silanized glassware.

Silanization: the glassware was soaked in hydrochloric acid (1 M) for 12 hours. Afterwards, it was washed with water (2x) and acetone (2x), and the surface was treated two times with a 5% solution of dimethyldichlorosilane in heptane (Sigma-Aldrich) for 30 seconds; then, the glassware was washed three times with methanol (1x) and DCM (2x) and dried at 60 °C.

Kaiser test: to determinate the completion of either Fmoc-deprotection or coupling steps, the Kaiser test was performed. After the last washing of the corresponding reaction step, a few resin beads were transferred to a small test tube and 2 drops of each of the following solutions were added in sequence: *Kaiser-solution A (*36.6 g phenol dissolved in 40 mL aqua dest. and 10 mL ethanol), *Kaiser-solution B* (2.5 g ninhydrin dissolved in 50 mL ethanol), *Kaiser-solution C* (1.0 mL 0.001 M KCN-solution and 49 mL pyridine). The mixture was heated on a heating plate at 100 °C for 3 minutes. A positive result, indicating free primary amines, is shown by the resin beads developing a blue color.

Loading of the resin: the resin was swollen in the indicated solvent for 20 min before the first reaction step. After that, the solvent was removed, and the resin loading was performed as follows:

▪ *Loading of 2-chlorotrityl resin:*

- *Method A:* 1 eq of the dry 2-chlorotrityl resin was swollen in DCM; then, 0.25 eq of the amino acid was dissolved in a small amount of DCM, 1 eq of DIPEA was added and the resulting mixture was pipetted on the resin. The mixture was shaken or stirred for 12 h, after which time, the reaction mixture was drained. The resin was washed with a mixture of DCM:MeOH:DIPEA (17:2:1) for 5 min (3x), with DCM (2x) and DMF (2x).
- *Method B:* 1 eq of the dry 2-chlorotrityl resin was swollen in DCM; then, 0.5 eq of the amine and 2 eq of DIPEA were dissolved in DCM, and then the mixture was added to the resin. The mixture was shaken or stirred for 3.5 h, after which time the reaction mixture was drained. The resin was washed for 5 min with a mixture of DCM:MeOH:DIPEA (17:2:1) (3x), with DCM (2x) and DMF (2x).

▪ *Loading of Rink-Amide resin:* the dry Rink-Amide resin was swollen using DMF for peptide synthesis. The Fmoc-protecting group was removed using the general method for Fmoc-removal described below. Then, 5 eq of the amino acid, 5 eq of HATU and 7.5 eq of HOBt were dissolved in a small amount of DMF. After addition of 5 eq of DIPEA, the resulting mixture was pipetted on the resin. The resin was loaded using the standard microwave assisted coupling method A (see below), performing 20 cycles of irradiation. After that, the reaction mixture was drained, and the resin was washed with DMF for peptide synthesis (3x). This procedure was repeated twice in the same conditions.

Cleavage of Fmoc-protective group: a 25% (v/v) solution of piperidine in DMF was added to the resin, so that the resin is completely immersed. Deprotection was achieved by irradiating the resin in the microwave reactor (100 W; 5 s) for five times. Between each irradiation step, the reaction tube was cooled in an ethanol/ice bath. After removal of the solvent the resin was washed with DMF (3x).

Coupling reaction: Coupling of the amino acids was performed using the different methods described below. After each coupling, completion of coupling was monitored by Kaiser test. In case of positive Kaiser Test, a double coupling was performed, using 5 eq of HATU instead of PyBOP.

▪ *Method A:* 5 eq of the *N*-Fmoc-protected amino acid, 5 eq of PyBOP and 7.5 eq of HOBt were dissolved in a small amount of DMF. After addition of 5 eq of DIPEA, the resulting mixture was pipetted on the resin. The mixture was irradiated in the microwave reactor (50 W, 10 s) for 20 times. Between each irradiation step, the reaction tube was cooled in an ethanol/ice bath. The reaction mixture was drained, and the resin was washed with DMF (3x).

▪ *Method B:* 2.5 eq of the *N*-Fmoc-protected amino acid, 2.5 eq of HATU and 3.75 eq of HOBt were dissolved in a small amount of DMF. After addition of 5 eq of DIPEA, the resulting solution was pipetted on the resin. The mixture was irradiated in the microwave reactor (50 W, 10 s) for 15 times. Between each irradiation step, the reaction tube was cooled in an ethanol/ice bath. The reaction mixture was withdrawn by suction and the loaded resin was washed with DMF (3x).
▪ *Method C*: 5 eq of the *N*-Fmoc-protected amino acid, 5 eq of HATU and 7.5 eq of HOBt were dissolved in a small amount of DMF. After addition of 10 eq of DIPEA, the resulting mixture was pipetted on the resin. The mixture was irradiated in the microwave reactor (50 W, 10 s) for 20 times. Between each irradiation step, the reaction tube was cooled in an ethanol/ice bath. The reaction mixture was removed, and the resin was washed with DMF (3x).
Peptide cleavage from resin and deprotection: After the last reaction step, the resin was washed with DCM (3x) and dried. Depending on the resin used, the indicated method was used:
▪ *Cleavage from 2-chlorotrityl resin:*
- *Method A*: a solution of DCM:TFA:TIS (8.5:1:0.5) was added to the resin, so that the resin beads were completely immersed. The mixture was stirred or shaken for 2 hours at room temperature and then drained. The residue was washed with a small amount of DCM (2x) and the filtrate was concentrated, to obtain the crude peptide, which was purified by preparative HPLC.
- *Method B:* a solution of HFIP:DCM (1:4) was pipetted on the resin and the reaction was kept under stirring for 18 hours at room temperature, then the solvent was drained. The residue was washed with DCM (2x) and the filtrate was concentrated to obtain the crude peptide, which was purified by preparative HPLC.
▪ *Cleavage from Rink-Amide resin:* a solution of TFA:TIS:phenol *liquefactum:*water (8.8:0.2:0.6:0.4) was pipetted on the resin and the mixture was stirred for 2 h at ambient temperature and then the solvent was drained. The residue was washed with a small amount of TFA (2x). TFA was removed in vacuum using a rotary vane pump equipped with a cooling trap. Then, ice-cooled MTBE was added to the crude product and the resulting white precipitate was separated by centrifugation and washed with ice-cooled MTBE (2x). The solid residue was then purified by preparative HPLC.

Experimental synthetic procedures and characterization data

Synthesis of N-Fmoc-2-aminomethylphenyl acetic acid 31[26]

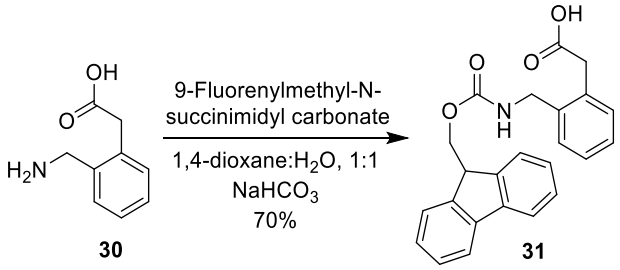

30 **31**

To a solution of 2-aminomethylphenyl acetic acid **30** (1.2 g, 7.26 mmol) in 1,4-dioxane (33 mL), a solution of 9-fluorenylmethyl-*N*-succinimidyl carbonate in aq $NaHCO_3$ (pH = 9, 33 mL) was added. The reaction was left under stirring overnight. After completion of reaction, the mixture was extracted with DCM (2x), then the aqueous phase was acidified with citric acid (pH = 3) and extracted with ethyl acetate (2x). The combined organic layers were dried over Na_2SO_4 and evaporated. The crude product was purified by flash column chromatography (eluent: from hexane:EtOAc 10:1.7+0.1% glacial acetic acid to 100% ethyl acetate + 0.1% glacial acetic acid) to yield **30** as brownish solid (1.9 g, 70%). TLC: ethyl acetate:hexane 6:4+0.1% glacial acetic acid, R*f* = 0.3. ^{1}H-NMR (DMSO-d_6, 400 MHz) δ 12.44 (bs, 1H, COOH), 7.90 (d, *J* = 7.7 Hz, 2H, ArH Fmoc), 7.80

(t, *J* = 6.5, 1H, NH), 7.71 (d, *J* = 7.7 Hz, 2H, ArH Fmoc), 7.43 (t, *J* = 7.4 Hz, 2H, ArH Fmoc), 7.33 (t, *J* = 7.4 Hz, 2H, ArH Fmoc), 7.21 (m, 4H, ArH), 4.34 (d, *J* = 7.0 Hz, 2H, CH_2 Fmoc), 4.22 (m, 3H, CH Fmoc+CH_2CONH), 3.66 (s, 2H, CH_2COOH). MS (ES^+) *m/z* 388.2 $[M+H]^+$.

Synthesis of compound 10

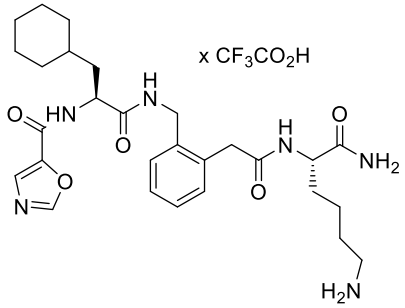

Compound **10** was synthesized according to the SPPS general procedure, using 100.0 mg of Rink-Amide resin (loading: 0.71 mmol/g, 200-400 mesh). The loading was performed following the general procedure, using 166.3 mg of Fmoc-Lys(O*t*Bu)-OH (0.36 mmol, 5 eq). Coupling reactions were performed according to the general procedure (method A), using 137.5 mg of **31** (0.36 mmol, 5 eq), 139.7 mg of Fmoc-Cha-OH (0.36 mmol, 5 eq) and 40.4 mg of oxazole-5-carboxylic acid (0.36 mmol, 5 eq). After the cleavage from the resin, the crude was purified by preparative HPLC (gradient A, t_R= 4.34 min), yielding compound **10** as a TFA salt (white solid, 35.2 mg, 76% yield). Purity determination: system A; t_R= 16.11 min, >98% (254 nm), >99% (220 nm); system B; t_R= 14.05 min, >99% (254 nm), >98% (220 nm). ^{1}H-NMR (DMSO-d_6, 400 MHz) δ 8.68 (d, *J* = 8.1 Hz, 1H, NH Cha), 8.57 (s, 1H, CH 2-oxazole), 8.55 (dd, *J* = 5.8, 5.8 Hz, 1H, N$\underline{H}CH_2$Ar), 8.19 (d, *J* = 8.2 Hz, 1H, NH Lys), 7.89 (s, 1H, CH 4-oxazole), 7.72 (bs, 3H, NH_3^+ Lys), 8.06 (d, *J* = 8.7 Hz, 1H, NH Cha), 7.39 (bs, 1H, NH_2), 7.24-7.17 (m, 4H, ArH), 7.04 (bs, 1H, NH_2), 4.52 (m, 1H, αCha), 4.35 (dd, *J* = 15.4, 5.8 Hz, 1H, CH_2Ar), 4.30 (dd, *J* = 15.4, 5.8 Hz, 1H, CH_2Ar), 4.15 (m, 1H, αLys), 3.58 (s, 2H, ArCH_2), 2.77-2.68 (m, 2H, εLys), 1.74-1.55 (m, 9H, βCha+γLys+δLys+3H cyclohexyl), 1.54-1.44 (m, 2H, βLys), 1.34-1.20 (m, 3H, cyclohexyl), 1.17-1.03 (m, 3H, cyclohexyl), 0.96-0.79 (m, 2H, cyclohexyl). ^{13}C-NMR (DMSO-d_6, 150 MHz) δ 173.7, 171.7, 170.1, 156.6, 153.5, 145.3, 137.7, 134.5, 130.2, 129.5, 127.7, 126.9, 126.7, 50.2, 50.8, 40.2, 39.2, 30.0, 38.8, 33.8, 33.3, 31.9, 31.7, 26.8, 26.2, 25.9, 25.7, 22.4. HRMS(ES^+) $C_{28}H_{41}N_6O_5^+$ calcd for $[M+H]^+$ 541.3132, found 541.3135. $[\alpha]^{22.8}_D$ = -3.5 (*c* 1.0, MeOH).

Synthesis of compound 11

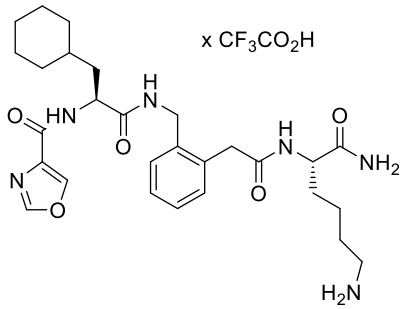

Compound **11** was synthesized according to the SPPS general procedure, using 100.0 mg of Rink-Amide resin (loading: 0.71 mmol/g, 200-400 mesh). Loading was performed according to the general procedure, using 166.3 mg of Fmoc-Lys(O*t*Bu)-OH (0.36 mmol, 5 eq). Coupling reactions were performed by employing the general procedure (method A), using 137.5 mg of **31** (0.36 mmol, 5 eq), 139.7 mg of Fmoc-Cha-OH (0.36 mmol, 5 eq) and 40.4 mg of oxazole-4-carboxylic acid (0.36 mmol, 5 eq). After the cleavage from the resin, the crude was purified by preparative HPLC (gradient A, R_t = 4.31 min), yielding compound **11** as a TFA salt (white solid, 30.1 mg, 65% yield). Purity determination: system A; R_t = 16.58 min, >96% (254 nm), >97% (220 nm); system B; R_t = 14.76 min, >97% (254 nm), >97% (220 nm). ^{1}H-NMR (DMSO-d6, 400 MHz) δ 8.69 (d, *J* = 1.0 Hz, 1H, CH 2-oxazole), 8.56 (dd, *J* = 5.7, 5.7 Hz, 1H, NHCH$_2$Ar), 8.54 (d, *J* = 1.0 Hz, 1H, CH 5-oxazole), 8.19 (d, *J* = 8.2 Hz, 1H, NH Lys), 8.06 (d, *J* = 8.7 Hz, 1H, NH Cha), 7.71 (bs, 3H, NH_3^+ Lys), 7.40 (bs, 1H, NH_2), 7.24-7.17 (m, 4H, ArH), 7.04 (bs, 1H, NH_2), 4.56 (m, 1H, αCha), 4.37 (dd, *J* = 15.5, 5.7 Hz, 1H, CH_2Ar), 4.31 (dd, *J* = 15.5, 5.7 Hz, 1H, CH_2Ar), 4.16 (m, 1H, αLys), 3.58 (s, 2H, ArCH_2), 2.73 (m, 2H, εLys), 1.75-1.69 (m, 2H, βCha), 1.67-1.55 (m, 7H, γLys+δLys+3H cyclohexyl), 1.52-1.45 (m, 2H, βLys), 1.31-1.22 (m, 3H, cyclohexyl), 1.15-1.05 (m, 3H, cyclohexyl), 0.94-0.71 (m, 2H, cyclohexyl). ^{13}C-NMR (DMSO-d6, 150 MHz) δ 173.5, 171.6, 170.0, 159.5, 142.5, 137.4, 135.1, 134.4, 130.1, 127.7, 126.7, 126.5, 52.1, 50.4, 39.7, 38.7, 38.7, 33.7, 33.1, 31.9, 32.5, 26.6, 26.0, 25.7, 25.6, 22.7. HRMS(ES$^+$) $C_{28}H_{41}N_6O_5^+$ calcd for $[M+H]^+$ 541.3133, found 541.3128. $[\alpha]^{23.1}_D$ = +23.3 (c 1.0, MeOH).

Synthesis of compound 12

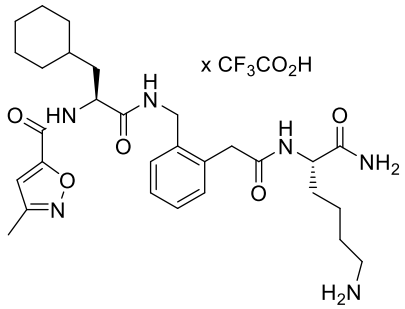

Compound **12** was synthesized according to the SPPS general procedure, using 100.0 mg of Rink Amide resin (loading: 0.71 mmol/g, 200-400 mesh). Loading was performed following the general procedure, using 166.3 mg of Fmoc-Lys(O*t*Bu)-OH (0.36 mmol, 5 eq). Coupling reactions were performed according to the general procedure (method A), using 137.5 mg of **31** (0.36 mmol, 5 eq), 139.7 mg of Fmoc-Cha-OH (0.36 mmol, 5 eq) and 45.1 mg of 3-methyl-isoxazole-5-carboxylic acid (0.36 mmol, 5 eq). After the cleavage from the resin, the crude was purified by preparative HPLC (gradient A, R_t = 4.11 min), yielding compound **12** as a TFA salt. (white solid, 32.4 mg, 70% yield). Purity determination: system A: R_t = 16.89 min, >97% (254 nm), >97% (220 nm); system B: R_t = 16.46

min, >98% (254 nm), >99% (220 nm). ^{1}H-NMR (DMSO-d_6, 400 MHz) δ 8.90 (d, *J* = 8.6 Hz, 1H, NH Cha), 8.53 (dd, *J* = 5.9, 5.9 Hz, 1H, N<u>H</u>CH_2Ar), 8.16 (d, *J* = 8.6 Hz, 1H, NH Lys), 7.71 (bs, 3H, NH_3^+ Lys), 7.36 (s, 1H, NH_2), 7.24-7.18 (m, 4H, ArH), 7.02 (s, 1H, NH_2), 7.01 (s, 1H, CH isoxazole), 4-53-4.49 (m, 1H, αCha), 4.35 (dd, *J* = 15.4, 5.9 Hz, 1H, CH_2Ar), 4.32 (dd, *J* = 15.4, 5.9 Hz, 1H, CH_2Ar), 4.15 (ddd, *J* = 8.6, 8.4, 5.3 Hz, 1H, αLys), 3.59 (s, 2H, ArCH_2), 2.73 (m, 2H, εLys), 2.31 (s, 3H, CH_3), 1.72-1.55 (m, 9H, βCha+γLys+cyclohexyl), 1.54-1.47 (m, 4H, βLys+δLys), 1.32-1.22 (m, 3H, cyclohexyl), 1.16-1.07 (m, 3H, cyclohexyl), 0.95-0.83 (m, 2H, cyclohexyl). ^{13}C-NMR (DMSO-d_6, 150 MHz) δ 173.5, 171.3, 170.0, 162.8, 160.4, 155.8, 137.8, 134.4, 130.0, 127.6, 126.7, 126.5, 107.3, 52.1, 50.9, 40.0, 39.1, 38.7, 38.7, 33.7, 33.3, 31.6, 31.5, 26.7, 26.0, 25.7, 25.6, 22.3, 11.0. HRMS(ES$^+$) $C_{29}H_{43}N_6O_5^+$ calcd for $[M+H]^+$ 555.3289, found 555.3292. $[\alpha]^{23.8}_D$ = +3.3 (c 0.62, MeOH).

Synthesis of compound 13

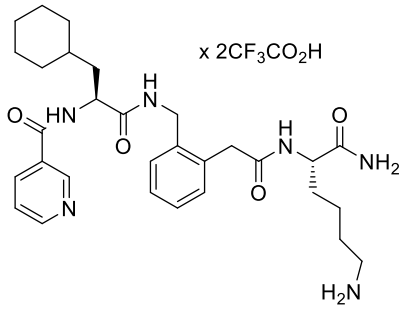

Compound **13** was synthesized according to the SPPS general procedure, using 100.0 mg of Rink Amide resin (loading: 0.71 mmol/g, 200-400 mesh). Loading was performed following the general procedure, using 166.3 mg of Fmoc-Lys(O*t*Bu)-OH (0.36 mmol, 5 eq). Coupling reactions were performed according to the general procedure (method A), using 137.5 mg of **31** (0.36 mmol, 5 eq), 139.7 mg of Fmoc-Cha-OH (0.36 mmol, 5 eq) and 43.7 mg of nicotinic acid (0.36 mmol, 5 eq). After the cleavage from the resin, the crude was purified by preparative HPLC (gradient A, R_t = 2.60 min), yielding compound **13** as a TFA salt. (white solid, 40.2 mg, 87% yield). Purity determination: system A: R_t = 16.49 min, >96% (254 nm), >96% (220 nm); system B: R_t = 13.53 min, >97% (254 nm), >97% (220 nm). ^{1}H NMR (DMSO-d6, 600 MHz) δ 9.10 (bd, *J* = 1.2 Hz, 1H, CH 2-pyridine), 8.77 (d, *J* = 8.1 Hz, 1H, NHCha), 8.75 (bdd, *J* = 4.9, 1.2 Hz, 1H, CH 4-pyridine), 8.50 (dd, *J* = 5.9 Hz, 1H, N<u>H</u>CH_2Ar), 8.32 (ddd, *J* = 7.9, 1.2, 1.2 Hz, CH 6-pyridine), 8.17 (d, *J* = 8.9 Hz, 1H, NH Lys), 7.68 (bs, 3H, NH_3^+ Lys), 7.59 (dd, *J* = 7.9, 4.9 Hz, 1H CH 5-pyridine), 7.38 (s, 1H, NH_2), 7.23 (m, 2H, ArH), 7.19 (m, 2H, ArH), 7.03 (s, 1H, NH_2), 4.59-4.55 (m, 1H, αCha), 4.37 (dd, *J*= 15.5, 5.9 Hz, 1H, CH_2Ar), 4.33 (dd, *J* = 15.5, 5.9 Hz, 1H, CH_2Ar), 4.15 (ddd, *J* = 8.9, 8.5, 5.4 Hz, 1H, αLys), 3.59 (s, 2H, CH_2), 2.73 (m, 2H, εLys), 1.74-1.62 (m, 7H, βCha+γLys+cyclohexyl), 1.58 (m, 1H, cyclohexyl), 1.53-1.46 (m, 3H, βLys+δLys), 1.39-1.21 (m, 3H, cyclohexyl), 1.20-1.06 (m, 3H, cyclohexyl), 0.97-0.83 (m, 2H, cyclohexyl). ^{13}C NMR (DMSO-d6, 150 MHz) δ 173.5, 171.9, 170.0, 164.9, 151.1, 148.1, 137.7, 136.2, 134.4, 130.0, 130.0, 127.6, 126.7, 126.5, 123.7, 52.1, 51.4, 40.0, 39.1, 38.9, 38.7, 33.8, 33.2, 31.7, 31.5, 26.7, 26.1, 25.8, 25.6, 22.3. HRMS(ES$^+$) $C_{43}H_{43}N_6O_4^+$ calcd for $[M+H]^+$ 551.3340, found: 551.332. $[\alpha]^{23.8}_D$ = -1.6 (c 1.0, MeOH).

Synthesis of compound 14

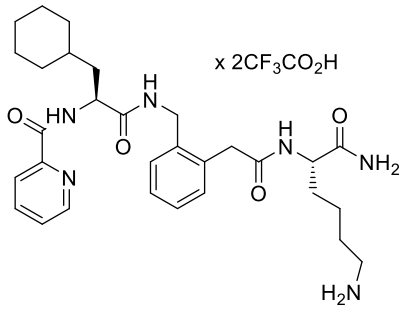

Compound **14** was synthesized according to the SPPS general procedure, using 70.0 mg of Rink Amide resin (loading: 0.71 mmol/g, 200-400 mesh). Loading was performed following the general procedure, using 166.3 mg of Fmoc-Lys(O*t*Bu)-OH (0.25 mmol, 5 eq). Coupling reactions were performed according to the general procedure (method A), using 137.5 mg of **31** (0.25 mmol, 5 eq), 139.7 mg of Fmoc-Cha-OH (0.25 mmol, 5 eq) and 43.7 mg of pipecolic acid (0.25 mmol, 5eq). After the cleavage from the resin, the crude was purified by preparative HPLC (gradient A, R_t = 4.31 min), yielding compound **14** as a TFA salt. (white solid, 27.2 mg, 82% yield). Purity determination: system A: R_t = 17.41 min, >98% (254 nm), >98% (220 nm); system B: R_t = 15.01 min, >99% (254 nm), >98% (220 nm). ^{1}H-NMR (DMSO-d_6, 400 MHz) δ (ppm): 8.68 (bd, *J* = 4.3 Hz, 1H, CH 6-pyridine), 8.64 (dd, *J* = 6.0, 6.0 Hz, 1H, NHCH$_2$Ar), 8.62 (m, 1H, NH Cha), 8.15 (d, *J* = 8.1 Hz, 1H, NH Lys), 8.06 (bd, *J* = 7.5 Hz, 1H, CH 3-pyridine), 8.02 (ddd, *J* = 7.5, 7.5, 1.3 Hz, 1H, CH 4-pyridine), 7.67 (bs, 3H, NH_3^+ Lys), 7.63 (ddd, *J* = 7.5, 4.3, 1.3 Hz, CH 5-pyridine), 7.38 (s, 1H, NH$_2$), 7.24-7.21 (m, 2H, ArH), 7.20-7.17 (m, 2H, ArH), 7.02 (s, 1H, NH$_2$), 4.63 (ddd, *J* = 8.9, 8.9, 5.6 Hz, 1H, αCha), 4.39 (dd, *J* = 15.4, 6.0 Hz, 1H, CH$_2$Ar), 4.31 (dd, *J* = 15.4, 6.0 Hz, 1H, CH$_2$Ar), 4.17 (ddd, *J* = 8.1, 8.1, 5.2 Hz, 1H, αLys), 3.59 (s, 2H, ArCH$_2$), 2.74 (m, 2H, εLys), 1.77 (bd, *J* = 12.3 Hz, 1H, cyclohexyl), 1.72-1.55 (m, 7H, βCha+βLys+γLys+cyclohexyl), 1.54-1.47 (m, 3H, δLys+cyclohexyl), 1.32-1.23 (m, 3H, cyclohexyl), 1.13-1.06 (m, 3H, cyclohexyl), 0.93-0.84 (m, 2H, cyclohexyl). ^{13}C-NMR (DMSO-d_6, 150 MHz) δ 173.4, 171.9, 170.0, 164.8, 151.1, 148.1, 137.7, 136.2, 134.4, 130.0, 129.9, 127.6, 126.7, 126.5, 123.7, 52.1, 51.4, 40.0, 30.1, 38.9, 38.7, 33.8, 33.2, 31.7, 31.5, 26.7, 26.1, 25.8, 25.6, 22.3. HRMS(ES$^+$) $C_{30}H_{43}N_6O_4^+$ calcd for $[M+H]^+$ 551.3340, found: 551.3328. $[\alpha]^{24.2}_D$ = +53.3 (c 1.0, MeOH).

Synthesis of compound 15

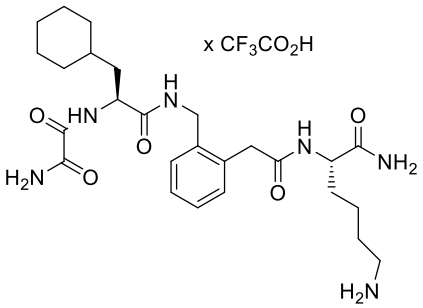

Compound **15** was synthesized according to the SPPS general procedure, using 100.0 mg of Rink Amide resin (loading: 0.72 mmol/g, 200-400 mesh). Loading was performed following the general procedure, using 309.2 mg of Fmoc-Lys(O*t*Bu)-OH (0.36 mmol, 5 eq). Coupling reactions were performed according to the general procedure (method A), using 139.5 mg of **31** (0.36 mmol, 5 eq), 141.7 mg of Fmoc-Cha-OH (0.36 mmol, 5 eq) and 32.1 mg of oxamic acid (0.36 mmol, 5eq). After the cleavage from the resin, the crude was purified by preparative HPLC (gradient A, R_t = 3.67 min),

yielding compound **15** as a TFA salt. (white solid, 37.6 mg, 83% yield). Purity determination: system A: R_t = 16.04 min, >97% (220 nm), >98% (254 nm), system B: R_t = 13.92 min, >99% (220 nm), >99% (254 nm). ^{1}H-NMR (DMSO-d$_6$, 600 MHz) δ 8.50 (dd, *J* = 5.6, 5.6 Hz, 1H, NHCH$_2$Ar), 8.43 (d, *J* = 8.9 Hz, 1H, NH Cha), 8.15 (d, *J* = 8.4 Hz, 1H, NH Lys), 8.13 (bs, 1H, NH$_2$ oxamic acid), 7.86 (bs, 1H, NH$_2$ oxamic acid), 7.66 (bs, 3H, NH$_3^+$ Lys), 7.38 (s, 1H, NH$_2$), 7.23 (m, 1H, ArH), 7.21-7.17 (m, 3H, ArH), 7.02 (s, 1H, NH$_2$), 4.37 (dd, J= 8.9, 8.9, 5.1 Hz, 1H, αCha), 4.34 (dd, *J* = 15.5, 5.6 Hz, 1H, CH$_2$Ar), 4.31 (dd, *J* = 15.5, 5.6 Hz, 1H, CH$_2$Ar) 4.18 (bddd, *J* = 8.4, 8.4, 5.3 Hz, 1H, αLys), 3.58 (m, 2H, ArCH$_2$), 2.74 (m, 2H, εLys), 1.71 (m, 1H, cyclohexyl), 1.67-1.60 (m, 6H, βCha+βLys+γLys), 1.58-1.47 (m, 5H, δLys+cyclohexyl), 1.32-1.07 (m, 6H, cyclohexyl), 0.92-0-81 (m, 2H, cyclohexyl). ^{13}C NMR (DMSO-d$_6$, 150 MHz) δ 173.4, 170.9, 169.9, 161.7, 159.8, 137.2, 134.4, 130.0, 127.6, 126.7, 126.4, 51.9, 50.9, 40.0, 39.2, 38.9, 38.6, 33.5, 33.0, 31.7, 31.4, 26.6, 25.9, 25.6, 25.5, 22.2. HRMS(ES$^+$) $C_{26}H_{41}N_6O_5^+$ calcd for $[M+H]^+$ 517.3133, found: 517.3137. $[\alpha]^{23.9}_D$ = +13.9 (c 1.0, MeOH).

Synthesis of compound 16

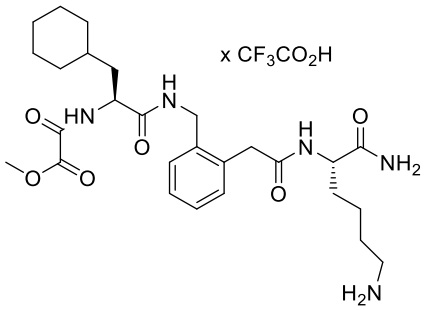

Compound **16** was synthesized according to the SPPS general procedure, using 50.0 mg of Rink Amide resin (loading: 0.72 mmol/g, 200-400 mesh). Loading was performed following the general procedure, using 154.6 mg of Fmoc-Lys(O*t*Bu)-OH (0.18 mmol, 5 eq). Coupling reactions were performed according to the general procedure (method A), using 69.7 mg of **31** (0.18 mmol, 5 eq), 70.9 mg of Fmoc-Cha-OH (0.18 mmol, 5 eq) and, for the final step, 16.1 μl of methylchlorooxoacetate (0.18 mmol, 5 eq) and 62.8 μl of DIPEA (0.36, 10 eq). After the cleavage from the resin, the crude was purified by preparative HPLC (gradient A, R_t = 3.08 min), yielding compound **16** as a TFA salt. (white solid, 13.2 mg, 57% yield). Purity determination: system A: R_t = 16.40 min, >96% (220 nm), >96% (254 nm); system B: R_t = 14.63 min, >96% (220 nm), >96% (254 nm). ^{1}H-NMR (DMSO-d$_6$, 400 MHz) δ 8.91 (d, J = 8.3 Hz, 1H, NH Cha), 8.50 (dd, J = 8.3, 8.3 Hz, 1H, NHCH2Ar), 8.19 (d, J = 8.0 Hz, 1H, NH Lys), 7.66 (bs, 3H, NH$_3$+ Lys), 7.40 (s, 1H, NH2), 7.24-7.21 (m, 1H, ArH), 7.21-7.14 (m, 3H, ArH), 7.05 (s, 1H, NH2), 4.40-4.35 (m, 1H, αCha), 4.33 (m, 1H, CH2Ar), 4.29 (dd, J = 15.4, 8.3 Hz, 1H, CH2Ar), 4.17 (ddd, J = 9.0, 9.0, 5.2 Hz, 1H, αLys), 3.79 (s, 3H, CH$_3$), 3.58 (s, 2H, ArCH2), 2.73 (m, 2H, εLys), 1.71-1-57 (m, 9H, cyclohexyl+βCha+βLys+γLys+δLys), 1.56-1.45 (m, 4H, cyclohexyl), 1.33-1.19 (m, 4H, cyclohexyl), 1.16-1.06 (m, 3H, cyclohexyl), 0.91-0.79 (m, 2H, cyclohexyl). ^{13}C NMR (DMSO-d$_6$, 150 MHz) δ 173.3, 170.7, 169.8, 160.7, 156.9, 137.2, 134.2, 129.9, 127.4, 126.6, 126.4, 52.7, 51.9, 50.9, 39.9, 38.9, 38.6, 38.5, 33.4, 32.9, 31.5, 31.3, 26.5, 25.9, 25.6, 25.4, 22.1. HRMS(ES$^+$) $C_{27}H_{42}N_5O_6^+$ calcd for $[M+H]^+$ 532.3140, found: 532.3139. $[\alpha]^{23.9}_D$ = +6.7 (c 0.74, MeOH).

Synthesis of compound 17

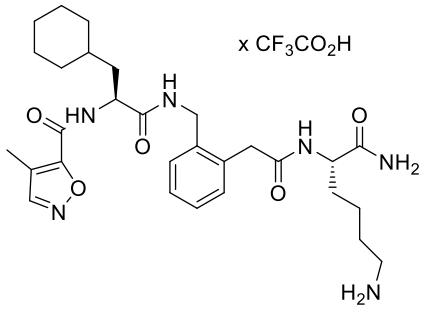

Compound **17** was synthesized according to the SPPS general procedure, using 100.0 mg of Rink Amide resin (loading: 0.72 mmol/g, 200-400 mesh). Loading was performed following the general procedure, using 309.2 mg of Fmoc-Lys(Boc)-OH (0.36 mmol, 5 eq). Coupling reactions were performed according to the general procedure (method A), using 139.5 mg of **31** (0.36 mmol, 5 eq), 141.7 mg of Fmoc-Cha-OH (0.36 mmol, 5 eq) and 45.1 mg of 4-methyl-isoxazole-3-carboxylic acid (0.36 mmol, 5 eq). After the cleavage from the resin, the crude was purified by preparative HPLC (gradient C, R_t = 9.00 min), yielding compound **17** as a TFA salt. (white solid, 23.5 mg, 54% yield). Purity determination: system A: R_t = 17.04 min, >95% (220 nm), >99% (254 nm); system B: R_t = 15.03 min, >97% (220 nm), >99% (254 nm). ^{1}H NMR (DMSO-d_6, 600 MHz) δ 8.74 (d, *J* = 8.0 Hz, 1H, NH Cha), 8.63 (s, 1H, CH isoxazole), 8.49 (dd, *J* = 6.1, 6.1 Hz, 1H, N<u>H</u>CH_2Ar), 8.16 (d, *J* = 8.4 Hz, 1H, NH Lys), 7.70 (bs, 3H, NH_3^+ Lys), 7.37 (s, 1H, NH_2), 7.23 (m, 2H, ArH), 7.19 (m, 2H, ArH), 7.02 (s, 1H, NH_2), 4.51 (m, 1H, αCha), 4.36 (dd, *J* = 15.5, 6.1 Hz, 1H, CH_2Ar), 4.32 (dd, *J* = 15.5, 6.1 Hz, 1H, CH_2Ar), 4.15 (ddd, *J* = 8.4, 8.4, 5.2 Hz, 1H, αLys), 3.60 (d, *J* = 15.0 Hz, 1H, ArCH2), 3.57 (d, *J* = 15.0 Hz, 1H, ArCH_2), 2.74 (m, 2H, εLys), 2.23 (s, 3H, CH_3), 1.72-1.55 (m, 9H, βCha+γLys+cyclohexyl), 1.54-1.47 (m, 4H, βLys+δLys), 1.32-1.22 (m, 3H, cyclohexyl), 1.16-1.07 (m, 3H, cyclohexyl), 0.95-0.83 (m, 2H, cyclohexyl). ^{13}C NMR (DMSO-d_6, 150 MHz) δ 173.5, 171.4, 169.9, 156.8, 156.7, 153.8, 137.5, 134.4, 130.0, 127.6, 126.7, 126.8, 117.8, 52.1, 50.8, 40.0, 39.0, 38.7, 38.6, 33.7, 33.1, 31.7, 31.5, 26.7, 26.0, 25.8, 25.6, 22.3, 7.8. HRMS(ES$^+$) $C_{29}H_{42}N_6O_5^+$ calcd for $[M+H]^+$ 555.3289, found: 555.3290. $[\alpha]^{22.6}_D$ = -11.0 (c 1.0, MeOH).

Synthesis of compound 18

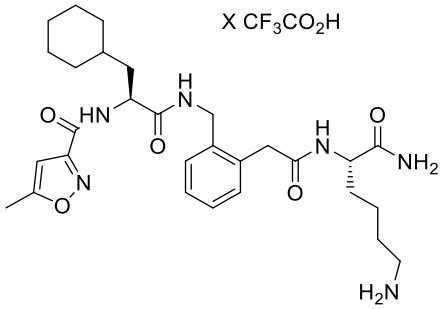

Compound **18** was synthesized according to the SPPS general procedure, using 112.0 mg of Rink Amide resin (loading: 0.72 mmol/g, 200-400 mesh). Loading was performed following the general procedure, using 189.8 mg of Fmoc-Lys(Boc)-OH (0.41 mmol, 5 eq). Coupling reactions were performed according to the general procedure (method A), using 156.9 mg of **31** (0.41 mmol, 5 eq), 159.4 mg of Fmoc-Cha-OH (0.41 mmol, 5 eq) and 51.5 mg of 5-methyl-isoxazole-3-carboxylic acid (0.41 mmol, 5eq). After the cleavage from the resin, the crude was purified by preparative HPLC (gradient B, R_t = 7.16 min), yielding compound **18** as a TFA salt. (white solid, 28.5 mg, 40% yield). Purity determination: system A: t_R= 17.21 min, >96% (220 nm), >96% (254 nm); system B: R_t = 14.93

min, >99% (220 nm), >99% (254 nm). ^{1}H NMR (DMSO-d_6, 600 MHz) δ 8.55 (d, *J* = 8.3 Hz, 1H, NH Cha), 8.49 (dd, *J* = 5.9, 5.9 Hz, 1H, NHCH$_2$Ar), 8.16 (d, *J* = 8.5 Hz, 1H, NH Lys), 7.70 (bs, 3H, NH_3^+), 7.64 (bs, 1H, NH_2), 7.24-7.17 (m, 4H, ArH), 7.02 (bs, 1H, NH_2), 6.59 (d, *J* = 0.8 Hz, 1H, CH isoxazole), 4.54 (m, 1H, αCha), 4.36 (dd, J = 15.5, 5.9 Hz, 1H, NHCH$_2$Ar), 4.32 (dd, *J* = 15.5, 5.9 Hz, 1H, NHCH$_2$Ar), 4.16 (td, *J* = 8.5, 5.3 Hz, 1H, αLys), 3.58 (s, 2H, ArCH$_2$), 2.73 (m, 2H, εLys), 2.47 (d, *J* = 0.8, 3H, CH_3), 1.73-1.56 (m, 8H, βCha+1βLys+cyclohexyl), 1.53-1.48 (m, 3H, δLys+1βLys), 1.28 (m, 3H, γLys+cyclohexyl), 1.12 (m, 3H, cyclohexyl), 0.89 (m, 2H, cyclohexyl). ^{13}C NMR (DMSO-d_6, 150 MHz) δ 173.5, 171.4, 171.1, 170.0, 158.7, 137.5, 134.4, 130.1, 127.6, 126.8, 126.5, 101.4, 52.1, 50.9, 40.1, 39.1, 38.9, 38.7, 33.7, 33.1, 31.8, 31.5, 26.7, 26.0, 25.8, 25.6, 22.3, 11.8. HRMS(ES$^+$) $C_{29}H_{42}N_6O_5^+$ calcd for $[M+H]^+$ 555.3289, found: 555.3289. $[\alpha]^{23.0}_D$ = -10.7 (c 1.0 MeOH).

Synthesis of compound 19

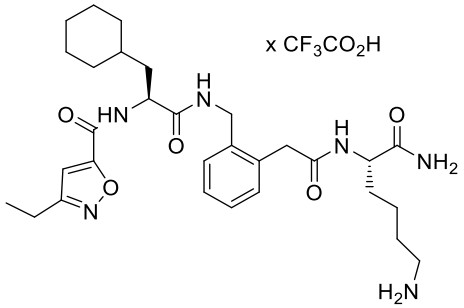

Compound **19** was synthesized according to the SPPS general procedure, using 112.0 mg of Rink Amide resin (loading: 0.72 mmol/g, 200-400 mesh). Loading was performed following the general procedure, using 189.8 mg of Fmoc-Lys(Boc)-OH (0.41 mmol, 5 eq). Coupling reactions were performed according to the general procedure (method A), using 156.9 mg of **31** (0.41 mmol, 5 eq), 159.4 mg of Fmoc-Cha-OH (0.41 mmol, 5 eq) and 57.2 mg of 3-ethyl-isoxazole-5-carboxylic acid (0.41 mmol, 5eq). After the cleavage from the resin, the crude was purified by preparative HPLC (gradient B, R_t = 8.12 min), yielding compound **19** as a TFA salt. (white solid, 29.6 mg, 40% yield). Purity determination: system A: R_t = 17.49 min, >96% (220 nm), >96% (254 nm); system B: R_t = 15.02 min, >99% (220 nm), >99% (254 nm). ^{1}H NMR (DMSO-d_6, 600 MHz) δ 8.89 (d, *J* = 8.0 Hz, 1H, NH Cha), 8.53 (dd, *J* = 5.7, 5.7 Hz, 1H, NHCH$_2$Ar), 8.16 (d, *J* = 8.4 Hz, 1H, NH Lys), 7.71 (bs, 3H, NH_3^+ Lys), 7.36 (bs, 1H, NH_2), 7.24-7.17 (m, 4H, ArH), 7.09 (s, 1H, CH isoxazole), 7.02 (bs, 1H, NH_2), 4.51 (m, 1H, αCha), 4.35 (dd, *J* = 15.5, 5.7, 1H, NHCH$_2$Ar), 4.32 (dd, *J* = 15.5, 5.7, 1H, NHCH$_2$Ar), 4.16 (td, *J* = 8.4, 5.3 Hz, 1H, αLys), 3.59 (s, 2H, ArCH$_2$), 2.74 (m, 2H, εLys), 2.70 (q, *J* = 7.7 Hz, 2H, CH_2 isoxazole), 1.71-1.57 (m, 8H, βCha+1βLys+cyclohexyl), 1.54-1.47 (m, 3H, δLys+1βLys), 1.29 (m, 3H, γLys+cyclohexyl), 1.22 (t, *J* = 7.7 Hz, 3H, CH3 isoxazole), 1.12 (m, 3H, cyclohexyl), 0.89 (m, 2H, cyclohexyl). ^{13}C NMR (DMSO-d_6, 150 MHz) δ 173.5, 171.3, 170.0, 165.6, 162.8, 155.9, 137.5, 134.4, 130.0, 127.5, 126.7, 126.5, 106.1, 52.1, 50.9, 40.0, 39.0, 38.7, 38.7, 33.7, 33.1, 31.6, 31.5, 26.7, 26.0, 25.7, 25.6, 22.3, 18.9, 12.4. HRMS(ES$^+$) $C_{30}H_{45}N_6O_5^+$ calcd for $[M+H]^+$ 569.3446, found: 569.3447. $[\alpha]^{23.4}_D$ = -8.2 (c 1.0, MeOH).

Synthesis of compound 20

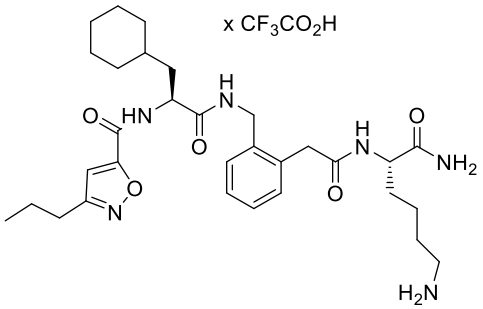

Compound **20** was synthesized according to the SPPS general procedure, using 112.0 mg of Rink Amide resin (loading: 0.72 mmol/g, 200-400 mesh). Loading was performed following the general procedure, using 189.8 mg of Fmoc-Lys(Boc)-OH (0.41 mmol, 5 eq). Coupling reactions were performed according to the general procedure (method A), using 156.9 mg of **31** (0.41 mmol, 5 eq), 159.4 mg of Fmoc-Cha -OH (0.41 mmol, 5 eq) and 62.3 mg of 3-propyl-isoxazole-5-carboxylic acid (0.41 mmol, 5 eq). After the cleavage from the resin, the crude was purified by preparative HPLC (gradient B, R_t = 8.56 min), yielding compound **20** as a TFA salt. (white solid, 31.4 mg, 42% yield). Purity determination: system A: R_t = 17.85 min, >98% (220 nm), >98% (254 nm); system B: R_t = 14.96 min, >99% (220 nm), >98% (254 nm). ^{1}H NMR (DMSO-d$_6$, 600 MHz) δ 8.90 (d, *J* = 8.2 Hz, 1H, NH Cha), 8.53 (dd, *J* = 5.7, 5.7 Hz, 1H, NHCH$_2$Ar), 8.16 (d, *J* = 8.2 Hz, 1H, NH Lys), 7.71 (bs, 3H, NH_3^+ Lys), 7.36 (bs, 1H, NH_2), 7.24-7.17 (m, 4H, ArH), 7.07 (s, 1H, CH isoxazole), 7.02 (bs, 1H, NH_2), 4.51 (m, 1H, αCha), 4.35 (dd, *J* = 15.5, 5.7, 1H, NHCH$_2$Ar), 4.32 (dd, *J* = 15.5, 5.7, 1H, NHCH$_2$Ar), 4.16 (td, *J* = 8.2, 5.2 Hz, 1H, αLys), 3.59 (s, 2H, ArCH$_2$), 2.74 (m, 2H, εLys), 2.65 (q, *J* = 7.5 Hz, 2H, CH$_3$CH$_2$CH$_2$ isoxazole), 1.71-1.56 (m, 10H, βCha+1βLys+cyclohexyl+CH$_3$CH$_2$CH$_2$ isoxazole), 1.54-1.47 (m, 3H, δLys+1βLys), 1.29 (m, 3H, γLys+cyclohexyl), 1.12 (m, 3H, cyclohexyl), 0.93 (t, *J* = 7.3 Hz, 3H, CH$_3$ isoxazole), 0.88 (m, 2H, cyclohexyl). ^{13}C NMR (DMSO-d$_6$, 150 MHz) δ 173.5, 171.1, 170.0, 164.3, 162.8, 155.9, 137.5, 134.4, 130.0, 127.5, 126.7, 126.5, 106.3, 52.1, 50.9, 40.0, 39.1, 38.69, 38.68, 33.6, 33.1, 31.6, 31.5, 27.1, 26.7, 26.0, 25.7, 25.6, 22.3, 20.9, 13.5. HRMS(ES$^+$) $C_{31}H_{47}N_6O_5^+$ calcd for $[M+H]^+$ 583.3602, found: 583.3605. $[\alpha]^{23.7}_D$ = +2.8 (c 0.47, MeOH).

Synthesis of compound 21

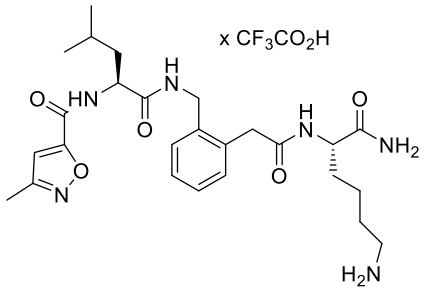

Compound **21** was synthesized according to the SPPS general procedure, using 100.0 mg of Rink Amide resin (loading: 0.72 mmol/g, 200-400 mesh). Loading was performed following the general procedure, using 168.7 mg of Fmoc-Lys(O*t*Bu)-OH (0.36 mmol, 5 eq). Coupling reactions were performed according to the general procedure (method A), using 139.5 mg of **31** (0.36 mmol, 5 eq), 127.2 mg of Fmoc-Leu-OH (0.36 mmol, 5 eq) and 45.8 mg of 3-methylisoxazole-5-carboxylic acid (0.36 mmol, 5eq). After the cleavage from the resin, the crude was purified by preparative HPLC (gradient B, R_t = 6.15 min), yielding compound **21** as a TFA salt. (white solid, 30.7 mg, 68% yield). Purity determination: system A: R_t = 15.06 min, 98% (220 nm), >99% (254); system B: R_t = 13.67

min, >99% (220 nm), >99% (254 nm). ^{1}H NMR (DMSO-d_6, 600 MHz) δ 8.92 (d, *J* = 8.4 Hz, 1H, NH Leu), 8.53 (dd, *J* = 6.0, 6.0 Hz, 1H, N<u>H</u>CH_2Ar), 8.16 (d, *J* = 8.4 Hz, 1H, NH Lys), 7.70 (bs, 3H, NH_3^+ Lys), 7.36 (s, 1H, NH), 7.24-7.17 (m, 4H, ArH), 7.02 (s, 1H, NH), 7.01 (s, 1H, CH isoxazole), 4.51-4.47 (m, 1H, αLeu), 4.35 (dd, *J* = 15.5, 6.0 Hz, CH2Ar), 4.32 (dd, *J* = 15.5, 6.0 Hz, CH_2Ar), 4.15 (ddd, *J* = 8.4, 8.4, 5.2 HZ, 1H, αLys), 3.58 (s, 1H, ArCH_2), 2.74 (m, 2H, εLys), 2.30 (s, 3H, CH3), 1.76-1.48 (m, 7H, βLeu+γLeu+βLys+γLys), 1.34-1.22 (m, 2H, δLys), 0.91 (d, J = 6.4 Hz, 3H, δLeu), 0.86 (d, *J* = 6.4 Hz, 3H, δLeu). ^{13}C NMR (DMSO-d_6, 150 MHz) δ 173.5, 171.3, 170.0, 162.8, 160.4, 155.9, 137.5, 134.4, 130.0, 127.6, 126.7, 126.5, 107.2, 52.1, 51.3, 48.6, 40.1, 39.1, 38.7, 31.5, 26.7, 24.4, 23.0, 22.3, 21.2, 11.0. HRMS(ES$^+$) $C_{26}H_{39}N_6O_5^+$ calcd for $[M+H]^+$ 515.2976, found: 515.2977. $[\alpha]^{22.5}_D$ = +6.5 (c 1.0, MeOH).

Synthesis of compound 22

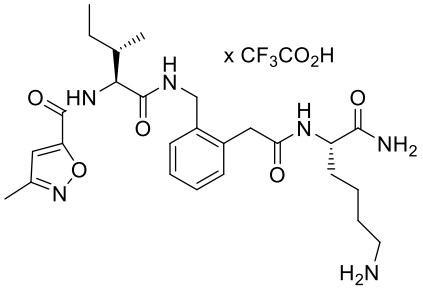

Compound **22** was synthesized according to the SPPS general procedure, using 50.0 mg of Rink Amide resin (loading: 0.72 mmol/g, 200-400 mesh). Loading was performed following the general procedure, using 84.3 mg of Fmoc-Lys(O*t*Bu)-OH (0.18 mmol, 5 eq). Coupling reactions were performed according to the general procedure (method A), using 69.8 mg of **31** (0.18 mmol, 5 eq), 63.6 mg of Fmoc-Ile-OH (0.18 mmol, 5 eq) and 22.9 mg of 3-methylisoxazole-5-carboxylic acid (0.18 mmol, 5eq). After the cleavage from the resin, the crude was purified by preparative HPLC (gradient B, R_t = 6.13 min), yielding compound **22** as a TFA salt. (white solid, 17.6 mg, 78% yield). Purity determination: system A: R_t = 14.96 min, >98% (220 nm), >97% (254 nm); system B: R_t = 13.54 min, >98% (220 nm), >97% (254 nm). ^{1}H NMR (DMSO-d~~6~~, 600 MHz) δ 8.68 (d, *J* = 8.7 Hz, 1H, NH Ile), 8.56 (dd, J = 5.6, 5.6 Hz, 1H, N<u>H</u>CH_2Ar), 8.12 (d, J = 8.4 Hz, 1H, NH Lys), 7.66 (bs, 3H, NH_3^+ Lys), 7.35 (s, 1H, NH), 7.22-7.19 (m, 2H, ArH), 7.16-7.13 (m, 2H, ArH), 7.03 (s, 1H, CH isoxazole), 6.99 (bs, 1H, NH), 4.34 (dd, *J* = 15.9, 5.6 Hz, 1H, CH_2Ar), 4.31 (m, 1H, CH_2Ar), 4.28 (dd, *J* = 8.7, 8.7 Hz, 1H, αIle), 4.15 (m, 1H, αLys), 3.56 (s, 2H, ArCH_2), 2.70 (m, 2H, εLys), 2.27 (s, 3H, CH_3), 1.89 (m, 1H, 1HβIle) 1.64 (m, 1H, 1HβLys), 1.52-1.40 (m, 4H, 1HβLys+δLys+1HγIle), 1.28-1.20 (m, 2H, γLys), 1.12 (m, 1HγIle), 0.81 (d, J = 6.9 Hz, δIle), 0.79 (d, J = 7.5 Hz, δIle). ^{13}C-NMR (DMSO-d_6, 150 MHz) δ 173.5, 170.3, 169.9, 162.6, 160.4, 155.7, 137.4, 134.4, 130.1, 127.8, 126.8, 126.5, 107.3, 57.7, 52.1, 40.1, 39.1, 38.7, 35.7, 31.5, 26.7, 23.7, 22.3, 15.3, 11.0, 10.6. HRMS(ES$^+$) $C_{26}H_{39}N_6O_5^+$ calcd for $[M+H]^+$ 515.2976, found: 515.2974. $[\alpha]^{22.9}_D$ = +4.6 (c 1, MeOH).

Synthesis of compound 23

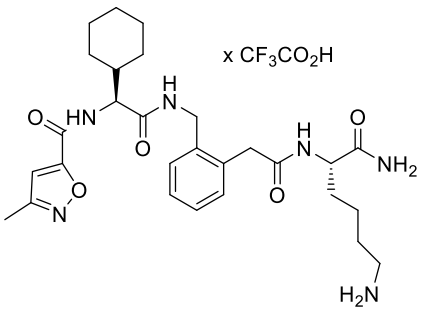

Compound **23** was synthesized according to the SPPS general procedure, using 50.0 mg of Rink Amide resin (loading: 0.72 mmol/g, 200-400 mesh). Loading was performed following the general procedure, using 84.4 mg of Fmoc-Lys(O*t*Bu)-OH (0.18 mmol, 5 eq). Coupling reactions were performed according to the general procedure (method A), using 69.8 mg of **31** (0.18 mmol, 5 eq), 68.3 mg of Fmoc-Chg-OH (0.18 mmol, 5 eq) and 22.9 mg of 3-methylisoxazole-5-carboxylic acid (0.18 mmol, 5eq). After the cleavage from the resin, the crude was purified by preparative HPLC (gradient B, R_t = 7.16 min), yielding compound **23** as a TFA salt. (white solid, 13.7 mg, 61% yield). Purity determination: system A: R_t = 16.08 min, 97% (220 nm), >99% (254 nm); system B: R_t = 14.15 min, >99% (220 nm), >99% (254 nm). ^{1}H NMR (DMSO-d_6, 600 MHz) δ 8.65 (d, J = 8.8 Hz, 1H, NH Chg), 8.57 (t, J = 6.1 Hz, 1H, NHCH2Ar), 8.14 (d, J = 8.4 Hz, 1H, NH Lys), 7.65 (s, 3H, NH3+ Lys), 7.37 (bs, 1H, NH), 7.23 (m, 2H, ArH), 7.18 (m, 2H, ArH), 7.05 (s, 1H, CH isoxazole), 7.02 (bs, 1H, NH), 4.34 (d, J = 6.1 Hz, 2H, NHCH2Ar), 4.29 (dd, J = 8.8 Hz, 1H, αChg), 4.17 (m, 1H, αLys), 3.58 (s, 2H, ArCH2), 2.72 (m, 2H, εLys), 2.29 (s, 3H, CH3), 1.81 (m, 1H, βChg), 1.73-1.62 (m, 4H, cyclohexyl), 1.61-1.45 (m, 5H, βLys+δLys+cyclohexyl), 1.27 (m, 2H, cyclohexyl), 1.20-0.93 (m, 5H, γLys+cyclohexyl). ^{13}C-NMR (DMSO-d_6, 150 MHz) δ 173.4, 170.1, 169.9, 162.6, 160.4, 155.8, 137.4, 134.4, 130.0, 127.8, 126.8, 126.5, 107.3, 58.0, 52.0, 40.0, 39.9, 39.0, 38.7, 31.5, 29.1, 28.7, 26.6, 25.7, 25.4, 25.4, 22.3, 11.0. HRMS(ES$^+$) $C_{28}H_{41}N_6O_5^+$ calcd for $[M+H]^+$ 541.3133, found: 541.3131. $[\alpha]^{23.2}_D$ = +10.0 (c 0.73, MeOH).

Synthesis of compound 24

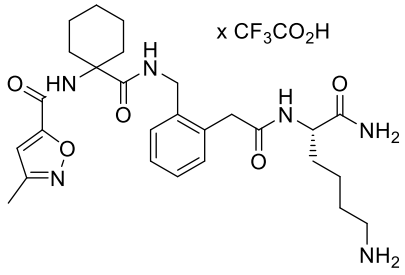

Compound **24** was synthesized according to the SPPS general procedure, using 50.0 mg of Rink Amide resin (loading: 0.72 mmol/g, 200-400 mesh). Loading was performed following the general procedure, using 84.4 mg of Fmoc-Lys(O*t*Bu)-OH (0.18 mmol, 5 eq). Coupling reactions were performed using the general procedure (method A), using 68.3 mg of **31** (0.18 mmol, 5 eq), 68.3 mg of 1-*N*-Fmoc-cyclohexylcarboxylic acid (0.18 mmol, 5 eq) and 22.9 mg of 3-methylisoxazole-5-carboxylic acid (0.18 mmol, 5 eq). After the cleavage from the resin, the crude was purified by preparative HPLC (gradient B, R_t = 6.25 min), yielding compound **24** as a TFA salt. (white solid, 14.2 mg, 61% yield). Purity determination: system A: R_t = 13.73 min, >98% (220 nm), >99% (254 nm); system B: R_t = 13.51 min, >99% (220 nm), >99% (254 nm). ^{1}H-NMR (DMSO-d_6, 600 MHz) δ 8.19 (s, 1H, NH isoxazole), 8.14 (dd, *J* = 5.8, 5.8 Hz, 1H, N<u>H</u>CH$_2$Ar), 8.12 (d, *J* = 8.1 Hz, 1H, NH Lys), 7.67 (bs, 3H, NH_3^+ Lys), 7.35 (bs, 1H, NH_2), 7.22-7.19 (m, 2H, ArH), 7.16-7.14 (m, 2H, ArH), 7.03 (s, 1H, CH isoxazole), 7.02 (bs, 1H, NH_2), 4.32 (dd, J = 15.7, 5.8 Hz, 1H, CH_2Ar), 4.28 (dd, J = 15.7, 5.8 Hz, 1H, CH_2Ar), 4.15 (m, 1H, αLys), 3.56 (s, 2H, ArCH_2), 2.74 (m, 2H, εLys), 2.31 (s, 3H, CH_3), 2.21 (m, 2H, cyclohexyl), 1.77 (m, 2H, cyclohexyl), 1.67 (m, 1H, HβLys), 1.56-1.41 (m, 8H, HβLys+δLys+cyclohexyl), 1.27 (m, 3H, γLys+cyclohexyl). ^{13}C NMR (DMSO-d_6, 150 MHz) δ 173.4, 173.2, 169.8, 163.1, 160.2, 155.7, 137.8, 133.9, 129.9, 126.9, 126.33, 126.29, 107.1, 60.3, 51.5, 40.0, 38.9, 39.86, 39.81, 39.7, 38.6, 31.4, 26.6, 24.8, 22.2, 21.0, 10.9. HRMS(ES$^+$) $C_{27}H_{39}N_6O_5^+$ calcd for $[M+H]^+$ 527.2976, found: 527.2971. $[\alpha]^{23.4}_D$= -4.1(c 0.78, MeOH).

Synthesis of compound 25

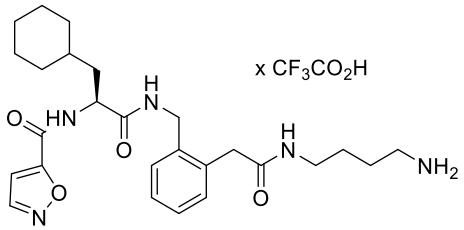

Compound **25** was synthesized according to the SPPS general procedure, using 200.0 mg of 2-chlorotrityl chloride resin (loading: 1.46 mmol/g, 200-400 mesh). The loading was performed according to the general procedure (method B), using 15.8 μl of 1,4-butanediamine (0.16 mmol, 0.5 eq) and 109.4 μl of DIPEA (0.63 mmol, 2 eq). The other couplings were performed according to the general procedure (method B), using 304.1 mg of **31** (0.79 mmol, 2.5 eq), 308.9 mg of Fmoc-Cha-OH (0.79 mmol, 2.5 eq), 88.8 mg of isoxazole 5-carboxylic acid (0.79 mmol, 2.5 eq). After the cleavage from the resin, the crude was purified by preparative HPLC (gradient A, R_t = 3.29 min), yielding compound **25** as a TFA salt. (white solid, 54.4 mg, 63% yield). Purity determination: system A: R_t = 13.73 min, >97% (220 nm), >97% (254 nm); system B: R_t = 16.31 min, >99% (220 nm), >98% (254 nm). ^{1}H NMR (DMSO-d_6, 400 MHz) δ 9.02 (d, *J* = 8.3 Hz, 1H, NH Cha), 8.75 (d, J = 1.9 Hz, 1H, NCH isoxazole), 8.62 (dd, *J* = 5.7, 5.7 Hz, 1H, N<u>H</u>CH$_2$Ar), 8.15 (t, *J* = 5.8 Hz, 1H, ArCH$_2$N<u>H</u>), 7.70 (bs, 3H, NH_3^+), 7.24-7.19 (m, 4H, ArH), 7.17 (d, *J* = 1.9 Hz, 1H, NCHC<u>H</u> isoxazole), 4.15 (m, 1H, αCha), 4.36 (dd, *J* = 15.6, 5.7 Hz, 1H, CH2Ar), 4.15 (dd, *J* = 15.6, 5.7 Hz, 1H, CH$_2$Ar), 3.49 (s, 2H, ArCH$_2$), 3.02 (td, J = 6.8, 6.8 Hz, 2H, NHCH2CH2), 2.78 (m, 2H, C<u>H$_2$</u>NH$_2$), 1.73-1.55 (m, 7H, cyclohexyl), 1.52-1.47 (m, 2H, NHCH$_2$CH$_2$C<u>H$_2$</u>), 1.46-1.38 (m, 2H, NHCH$_2$C<u>H$_2$</u>), 1.33-1.23 (m, 1H, cyclohexyl), 1.19-1.05 (m, 3H, cyclohexyl), 0.96-0.82 (m, 2H, cyclohexyl). ^{13}C NMR (DMSO-d_6, 150 MHz) δ 171.2, 169.9, 162.3, 155.6, 151.5, 137.3, 134.4, 129.9, 127.7, 126.8, 126.5, 105.9, 50.8, 40.1, 39.23, 38.54, 38.48, 37.9, 33.6, 33.0, 31.5, 25.96, 25.94, 25.6, 25.5, 24.4. HRMS(ES$^+$) $C_{26}H_{38}N_5O_4^+$ calcd for $[M+H]^+$ 484.2918, found: 484.2913. $[\alpha]^{23.5}_D$ = +15.3 (c 1.0, MeOH).

Synthesis of compound 29

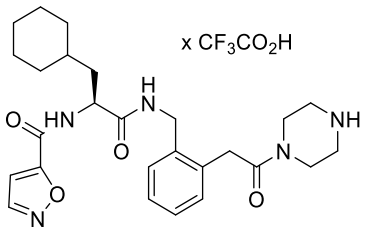

Compound **29** was synthesized according to the SPPS general procedure, using 100.0 mg of 2-chlorotrityl chloride resin (loading: 1.46 mmol/g, 200-400 mesh). The loading was performed according to the general procedure (method B), using 6.9 mg of piperazine (0.073 mmol, 0.5 eq) and 50.9 μl of DIPEA (0.292 mmol, 2 eq). The other couplings were performed according to the general procedure (method B), using 141.4 mg of **31** (0.37 mmol, 2.5eq), 143.6 mg of Fmoc-Cha-OH (0.37 mmol, 2.5 eq), 41.8 mg of isoxazole 5-carboxylic acid (0.37 mmol, 2.5 eq). After the cleavage from the resin, the crude was purified by preparative HPLC (gradient A, R_t = 3.61 min), yielding compound **29** as a TFA salt. (white solid, 13.7mg, 31% yield). Purity determination: system A: R_t = 14.61 min, >98% (254 nm), 99% (220 nm); system B: R_t = 16.44 min, >98% (254 nm), >97% (220 nm). ^{1}H NMR (DMSO-d_6, 600 MHz) δ 8.98 (d, *J* = 8.1 Hz, 1H, NH isoxazole), 8.80 (bs, 2H, NH_2^+ piperazine), 8.75 (d, *J* = 1.9 Hz, 1H, NCH isoxazole), 8.43 (dd, J = 5.7, 5.7 Hz, 1H, N<u>H</u>CH$_2$Ar), 7.26 (dd, *J* = 7.4, 1.9

Hz, 1H, ArH), 7.23 (ddd, *J* = 7.4, 7.4, 1.8 Hz, 1H, ArH), 7.19 (ddd, J = 7.4, 7.4, 1.9 Hz, 1H, ArH), 7.17 (d, *J* = 1.9 Hz, 1H, CHCO isoxazole) 7.10 (dd, *J* = 7.4, 1.9 Hz, 1H, ArH), 4.49 (ddd, J = 8.1, 5.6, 3.1 Hz, 1H, αCha), 4.27 (dd, *J* = 15.2, 6.1 Hz, 1H, NHC$\underline{H_2}$Ar), 4.17 (dd, *J* = 15.2, 6.1 Hz, 1H, NHC$\underline{H_2}$Ar), 3.83 (d, *J* = 16.7 Hz, 1H, ArCH_2N), 3.79 (d, *J* = 16.7 Hz, 1H, ArCH_2N), 3.70-3.62 (m, 4H, CH_2 piperazine, under water signal), 3.10 (bs, 4H, CH_2 piperazine), 1.71-1.57 (m, 7H, cyclohexyl), 1.34-1.28 (m, 1H, cyclohexyl), 1.18-1.07 (m, 3H, cyclohexyl), 0.95-0.83 (m, 2H, cyclohexyl). $\underline{^{13}C\ NMR\ (DMSO\text{-}d_6,\ 150\ MHz)}$ δ 171.2, 168.9, 162.3, 155.6, 151.6, 137.6, 133.8, 129.9, 127.9, 126.8, 126.6, 106.0, 50.9, 42.7, 42.6, 42.1, 39.9, 38.5, 37.9, 36.3, 33.5, 33.0, 31.5, 25.9, 25.6, 25.5. $\underline{HRMS(ES^+)}$ $C_{26}H_{36}N_5O_4^+$ calcd for $[M+H]^+$ 482.2762, found: 482.2751. $[\alpha]^{23.9}_D$ = +7.1 (c 0.47, MeOH).

Synthesis of compound 26

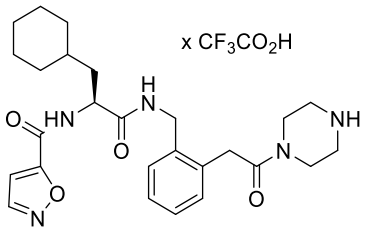

Compound **26** was synthesized according to the SPPS general procedure, using 100.0 mg of 2-chlorotrityl chloride resin (loading: 1.46 mmol/g, 200-400 mesh). The loading was performed according to the general procedure (method A), using 17.3 mg of Fmoc-Lys(Boc)-OH (0.04 mmol, 0.25 eq) and 25.43 μl of DIPEA (0.15 mmol, 1 eq). The other couplings were performed according to the general procedure (method C), using 282.8 mg of **31** (0.73 mmol, 5 eq), 287.2 mg of Fmoc-Cha-OH (0.73 mmol, 5 eq), 92.8 mg of 3-methyl-isoxazole 5-carboxylic acid (0.73 mmol, 5 eq). Cleavage from the resin was performed according to the general procedure (method B). Then, after removing of the cleavage solution, 30.0 mL of MeOH, 150.0 μl of TFA and 17.0 μl of TMSCl (0.29 mmol, 2 eq) were added to the crude, and the reaction was kept under stirring 6 h at 80°C. After competition, the solvent was removed under vacuum and the crude was purified by preparative HPLC (gradient B, R_t = 8.79 min), yielding compound **26** as a TFA salt. (white solid, 15.2 mg, 61% yield). Purity determination: system A: R_t = 17.34 min, >98% (220 nm), >99% (254 nm); system B: R_t = 15.04 min, >97% (220 nm), >97% (254 nm). $\underline{^1H\ NMR\ (DMSO\text{-}d_6,\ 600\ MHz)}$ δ 8.91 (d, *J* = 7.7 Hz, 1H, NH isoxazole), 8.52 (m, 2H, N$\underline{H}$CH_2Ar+NH Lys), 7.71 (bs, 3H, NH_3^+ Lys), 7.23-7.18 (m, 4H, ArH), 7.01 (s, 1H, CH isoxazole), 4.06 (m, 1H, αCha), 4.34 (dd, *J* = 15.5, 5.9 Hz, 1H, NHC$\underline{H_2}$Ar), 4.31 (dd, *J* = 15.5, 5.9 Hz, 1H, NHC$\underline{H_2}$Ar), 4.18 (m, 1H, αLys), 3.62 (s, 3H, OCH_3), 3.59 (d, *J* = 14.8 Hz, 1H, ArCH_2), 3.56 (d, *J* = 14.8 Hz, 1H, ArCH_2), 7.75 (t, *J* = 7.6 Hz, 2H, εLys), 2.31 (s, 3H, CH_3 isoxazole), 1.72-1.55 (m, 9H, βLys+γLys+βCha+cyclohexyl), 1.54-1.48 (m, 2H, δLys), 1.37-1.27 (m, 3H, cyclohexyl), 1.19-1.07 (m, 3H, cyclohexyl), 0.96-0.82 (m, 2H, cyclohexyl). $\underline{^{13}C\ NMR\ (DMSO\text{-}d_6,\ 150\ MHz)}$ δ 172.4, 171.3, 170.4, 162.8, 160.4, 155.9, 137.5, 134.1, 129.9, 127.6, 126.8, 126.6, 107.2, 51.8, 51.7, 50.9, 39.9, 38.8, 38.61, 38.57, 33.7, 32.3, 31.6, 30.3, 26.5, 26.0, 25.7, 25.6, 22.3, 11.0. $\underline{HRMS(ES^+)}$ $C_{30}H_{44}N_5O_6^+$ calcd for $[M+H]^+$ 570.3286, found: 570.3283. $[\alpha]^{23.0}_D$= -11.3 (c 1.0, MeOH).

Synthesis of compound 27

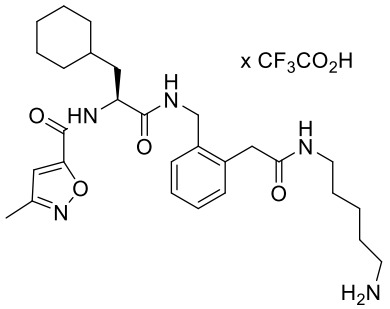

Compound **27** was synthesized according to the SPPS general procedure, using 200.0 mg of 2-chlorotrityl chloride resin (loading: 1.46 mmol/g, 200-400 mesh). The loading was performed according to the general procedure (method B), using 17.1 μl of 1,5-pentadiamine (0.15 mmol, 0.5 eq) and 101.7 μl of DIPEA (0.58 mmol, 2 eq). The other couplings were performed according to the general procedure (method B), using 282.8 mg of **31** (0.73 mmol, 5 eq), 287.2 mg of Fmoc-Cha-OH (0.73 mmol, 5 eq), 92.0 mg of 3-methyl-isoxazole 5-carboxylic acid (0.73 mmol, 5 eq). The cleavage from the resin was performed following the general procedure (method A), and the crude was purified by preparative HPLC (gradient B; R_t = 8.39 min), yielding compound **27** as a TFA salt. (white solid, 59.4 mg, 66% yield). Purity determination: system A: R_t = 17.33 min, >97% (220 nm), >99% (254 nm); system B: R_t = 15.32 min, >99% (220 nm), >99% (254 nm). ^{1}H NMR (DMSO-d_6, 600 MHz) δ 8.90 (d, *J* = 8.1 Hz, 1H, NH Cha), 8.58 (dd, *J* = 5.6 Hz, 1H, N<u>H</u>CH$_2$Ar), 8.09 (t, *J* = 6.4 Hz, 1H, ArCH$_2$N<u>H</u>), 7.74 (bs, 3H, NH_3^+), 7.23-7.18 (m, 4H, ArH), 7.01 (s, 1H, NH isoxazole), 4.49 (ddd, *J* = 8.1, 5.2, 4.9 Hz, 1H, αCha), 4.35 (dd, *J* = 15.2, 5.9 Hz, 1H, NHC<u>H$_2$</u>Ar), 4.32 (dd, *J* = 15.2, 5.9 Hz, 1H, NHC<u>H$_2$</u>Ar), 3.49 (s, 2H, ArC<u>H$_2$</u>NH), 3.01 (td, *J* = 6.4, 6.4 Hz, 2H, NHC<u>H$_2$</u>CH$_2$), 2.76 (m, 2H, C<u>H$_2$</u>NH_3^+), 2.30 (s, 3H, CH_3), 1.72-1.56 (m, 7H, βCha+cyclohexyl), 1.53 (m, 2H, <u>CH_2</u>$CH_2NH_3^+$), 1.40 (m, 2H, NHCH$_2$<u>CH$_2$</u>), 1.28 (m, 3H, NHCH$_2$CH$_2$<u>CH$_2$</u>+cyclohexyl), 1.17-1.05 (m, 3H, cyclohexyl), 0.94-0.88 (m, 2H, cyclohexyl). <u>^{13}C NMR (DMSO-d6, 150 MHz)</u> δ 171.24, 169.99, 162.79, 160.35, 155.84, 137.43, 134.61, 129.96, 127.90, 126.87, 126.58, 107.20, 50.89, 40.18, 39.33, 38.73, 38.63, 38.34, 33.66, 33.14, 31.59, 28.46, 26.64, 26.04, 25.73, 25.57, 23.16, 10.99. <u>HRMS(ES$^+$)</u> $C_{28}H_{42}N_5O_4^+$ calcd for $[M+H]^+$ 512.3231, found: 512.3229. $[\alpha]^{23.4}_D$= -2.0 (c 1.0, MeOH).

Synthesis of compound 28

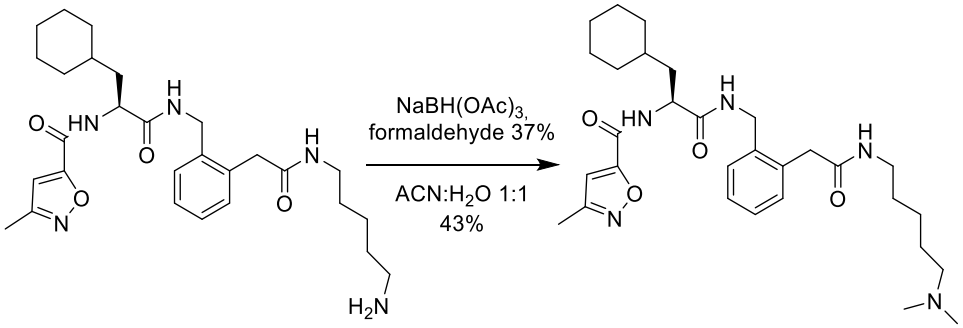

Compound **28** was synthesized through a reductive amination, starting from compound **27** (20.0 mg, 0.04 mmol, 1 eq). **27** was dissolved in 2.5 mL of a solution 1:1 ACN:H_2O, then 15 mg of $NaBH(OAc)_3$ (0.07 mmol, 1.8 eq) and 14.1 μl of formaldehyde 37% v/v in water (0.19 mmol, 5 eq) were added. The reaction was kept under stirring at room temperature overnight. The day after, the reaction was directly purified by preparative HPLC (gradient B, R_t = 8.87), yielding compound **28** as a white solid (10.9 mg, 43%). Purity determination: system A: R_t = 17.29 min, >99% (220 nm),

>99% (254 nm); system B: R_t = 15.67 min, >96% (220 nm), >96% (254 nm). ^{1}H NMR (DMSO-d_6, 600 MHz) δ 9.41 (bs, 1H, N$H^+$$CH_3CH_3$), 8.90 (d, *J* = 8.3 Hz, 1H, NH Cha), 8.57 (dd, *J* = 6.2, 6.2 Hz, 1H, N$H$$CH_2$Ar), 8.16 (d, *J* = 8.2 Hz, 1H, NH Lys), 8.08 (t, *J* = 5.8 Hz, 1H, NHCH_2CH_2), 7.23-7.19 (m, 4H, ArH), 7.01 (s, 1H, CH isoxazole), 4.49 (m, 1H, αCha), 4.35 (dd, *J* = 15.5, 5.8, 1H, NHCH_2Ar), 4.32 (dd, *J* = 15.5, 5.8, 1H, NHCH_2Ar), 3.49 (s, 2H, ArCH_2), 3.03-2.97 (m, 4H, NHCH_2CH_2+CH_2CH_2N$(CH_3)_2$, 2.75 (d, *J* = 4.4 Hz, 6H, N$(CH_3)_2$), 2.31 (s, 3H, CH_3), 1.71-1.55 (m, 9H, βCha+cyclohexyl+CH_2CH_2N$(CH_3)_2$ +$CH_2CH_2CH_2$N$(CH_3)_2$), 1.41 (m, 2H, OCNHCH_2CH_2), 1.31-1.22 (m, 3H, cyclohexyl), 1.18-1.07 (m, 3H, cyclohexyl), 0.95-0.82 (m, 2H, cyclohexyl).^{13}C NMR (DMSO-d_6, 150 MHz) δ 171.3, 170.0, 162.8, 160.4, 155.8, 137.4, 134.6, 130.0, 127.8, 126.9, 126.6, 107.2, 56.6, 50.9, 42.1, 40.1, 40.1, 38.6, 30.2, 33.7, 33.1, 31.6, 28.5, 26.0, 25.7, 25.6, 23.3, 23.2, 11.00. HRMS(ES$^+$) $C_{30}H_{46}N_5O_4^+$ calcd for $[M+H]^+$ 540.3544, found: 540.3544. $[\alpha]^{23.8}_D$ = +4.9 (c 1.0, MeOH).

3.5.2. HPLC chromatograms

Purity determination. Substance purities were assessed by analytical HPLC (Agilent 1200 analytical series, equipped with a quaternary pump and variable wavelength detector; column Zorbax Eclipse XDB-C8 analytical column, 4.6 mm × 150 mm, 5 µm, flow rate 0.5 mL/min, detection wavelengths: 254 nm. Linear gradient solvent systems were used as specified below.

- *System A*: water+0.1% HCOOH (solvent A), methanol (Solvent B), with the following gradient: 90% solvent A for 3 min, from 90% to 10% of solvent A over 15 min, 10% of solvent A for 6 min, from 10% to 90% of solvent A over 3 min, 90% of solvent A for 3 min.
- *System B*: water+0.1% TFA (solvent A), acetonitrile (Solvent B), with the following gradient: 95% solvent A for 3 min, from 95% to 5% of solvent A over 15 min, 5% of solvent A for 6 min, from 5% to 95% of solvent A over 3 min, 90% of solvent A for 3 min.

Compound 10, system A, 254 nm

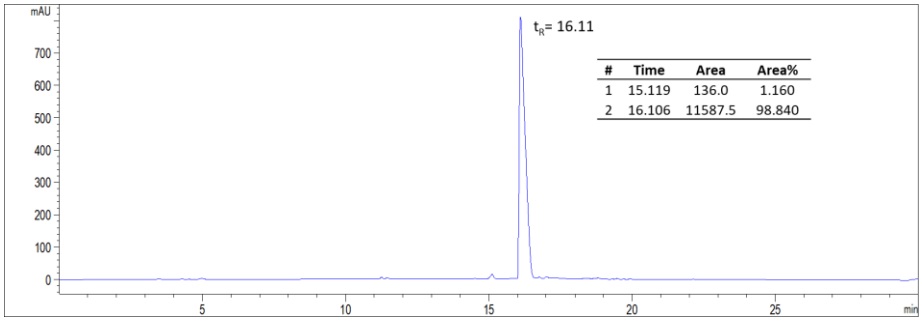

#	Time	Area	Area%
1	15.119	136.0	1.160
2	16.106	11587.5	98.840

Compound 10, system B, 254 nm

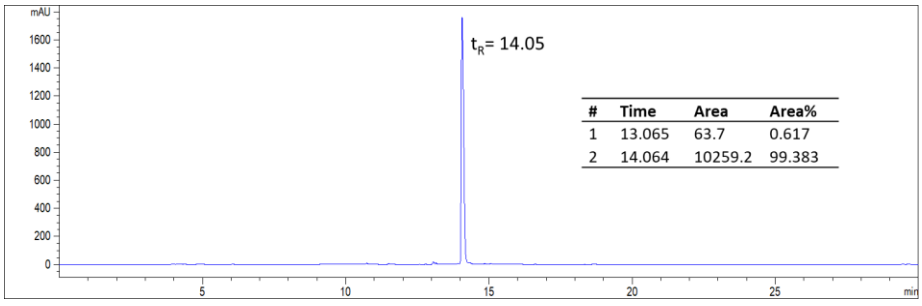

#	Time	Area	Area%
1	13.065	63.7	0.617
2	14.064	10259.2	99.383

Compound 11, system A, 254 nm

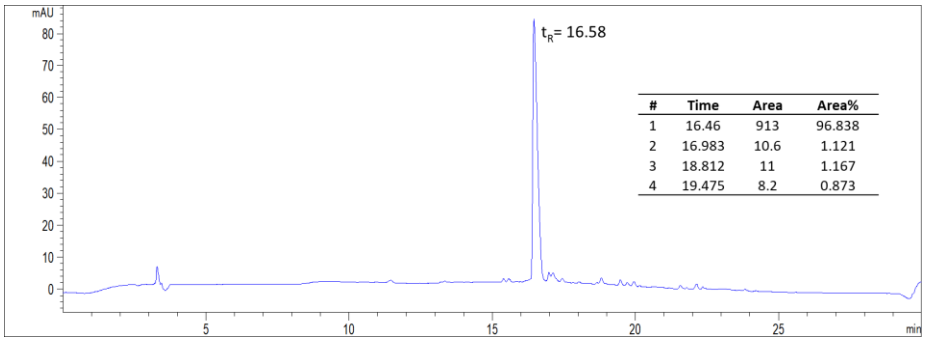

Compound 11, system B, 254 nm

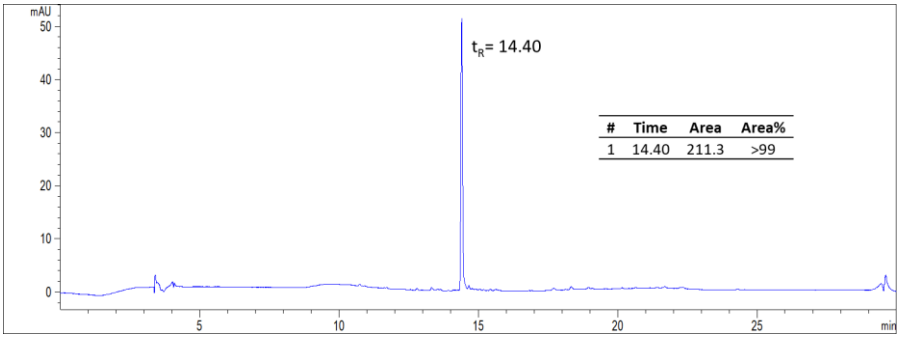

Compound 12, system A, 254 nm

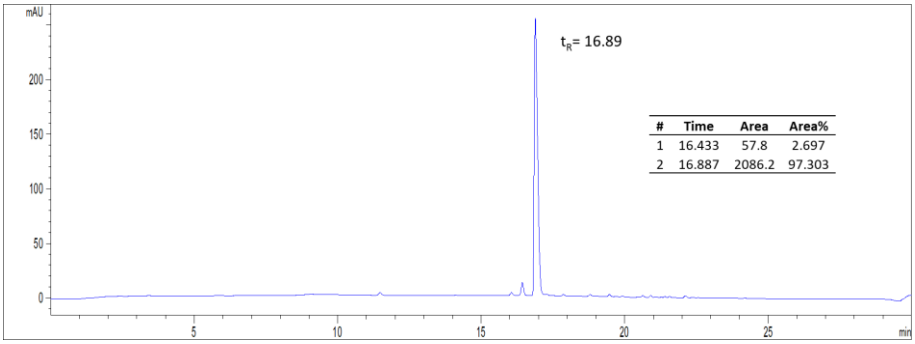

Compound 12, system B, 254 nm

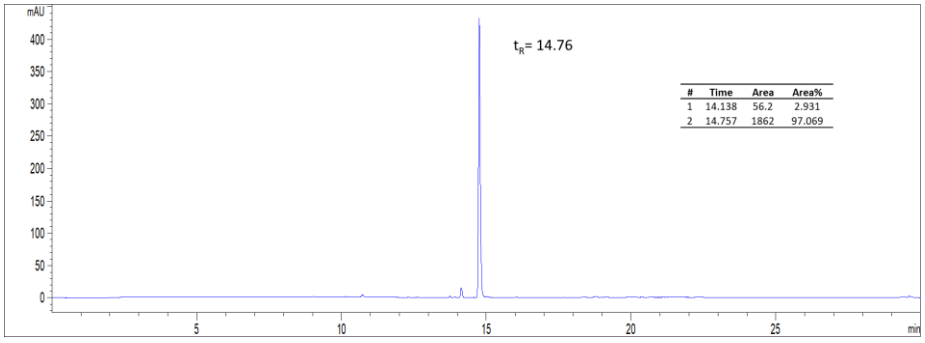

Compound 13, system A, 254 nm

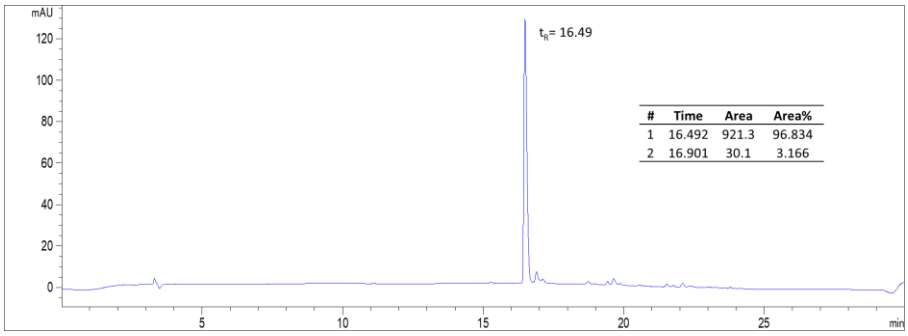

#	Time	Area	Area%
1	16.492	921.3	96.834
2	16.901	30.1	3.166

Compound 13, system B, 254 nm

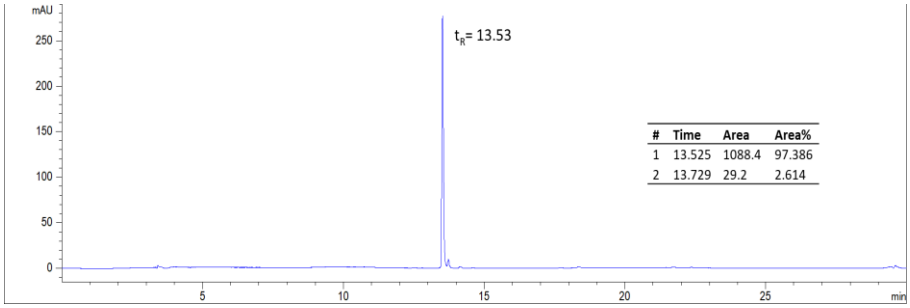

#	Time	Area	Area%
1	13.525	1088.4	97.386
2	13.729	29.2	2.614

Compound 14, system A, 254 nm

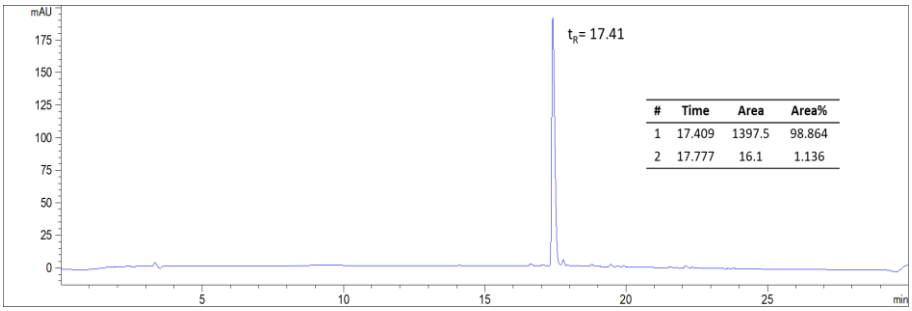

#	Time	Area	Area%
1	17.409	1397.5	98.864
2	17.777	16.1	1.136

Compound 14, system B, 254 nm

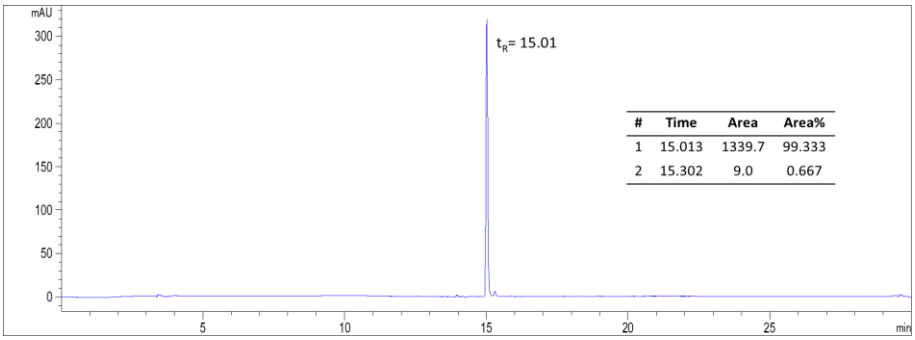

#	Time	Area	Area%
1	15.013	1339.7	99.333
2	15.302	9.0	0.667

Compound 15, system A, 254 nm

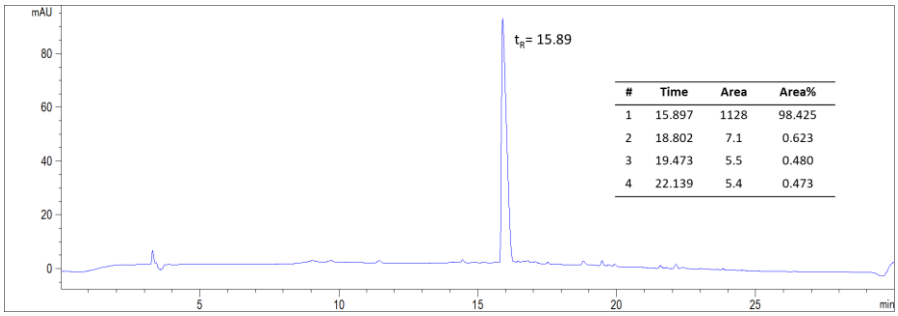

#	Time	Area	Area%
1	15.897	1128	98.425
2	18.802	7.1	0.623
3	19.473	5.5	0.480
4	22.139	5.4	0.473

Compound 15, system B, 254 nm

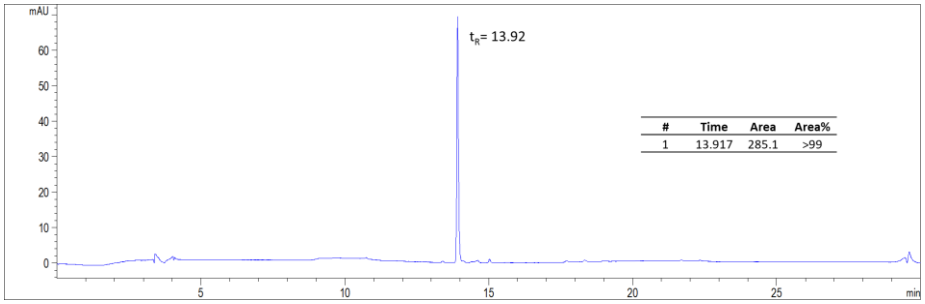

#	Time	Area	Area%
1	13.917	285.1	>99

Compound 16, system B, 254 nm

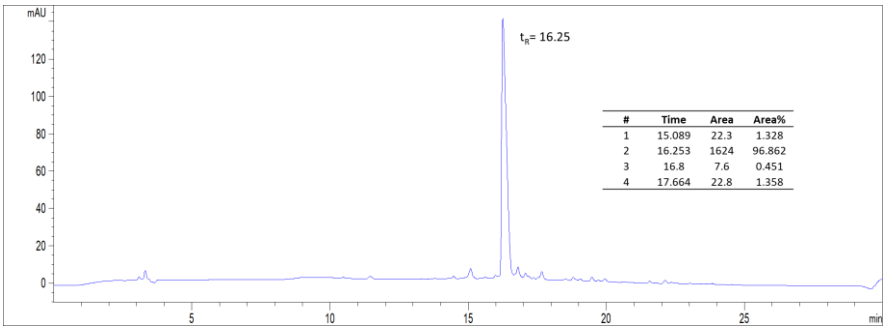

#	Time	Area	Area%
1	15.089	22.3	1.328
2	16.253	1624	96.862
3	16.8	7.6	0.451
4	17.664	22.8	1.358

Compound 16, system B, 254 nm

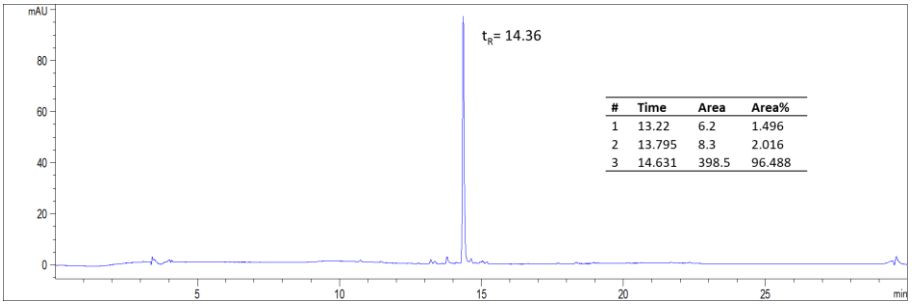

#	Time	Area	Area%
1	13.22	6.2	1.496
2	13.795	8.3	2.016
3	14.631	398.5	96.488

Compound 17, system A, 254 nm

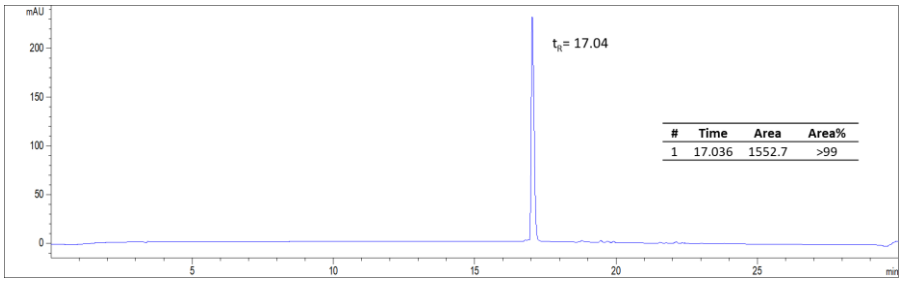

Compound 17, system B, 254 nm

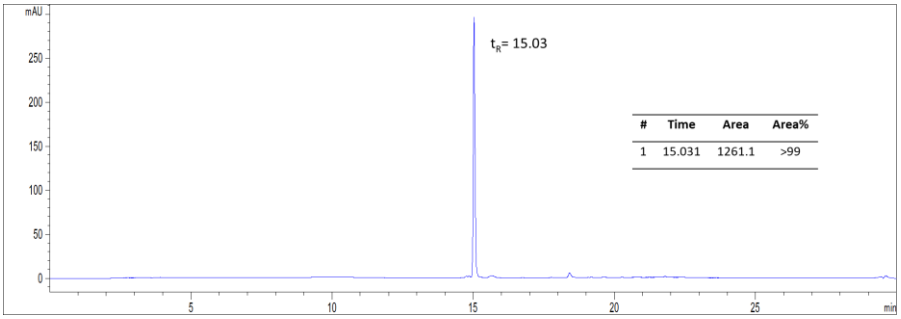

Compound 18, system A, 254 nm

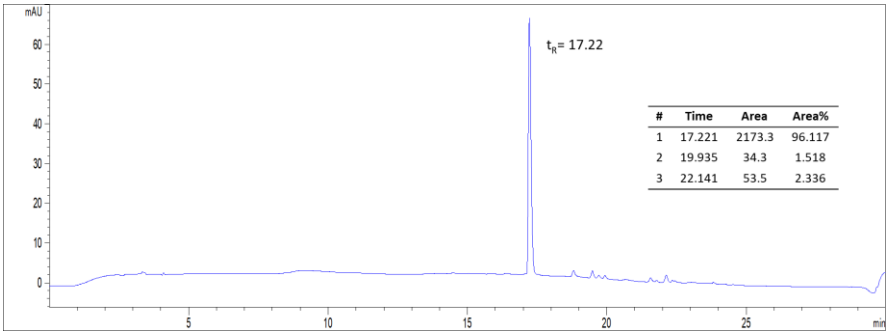

Compound 18, system B, 254 nm

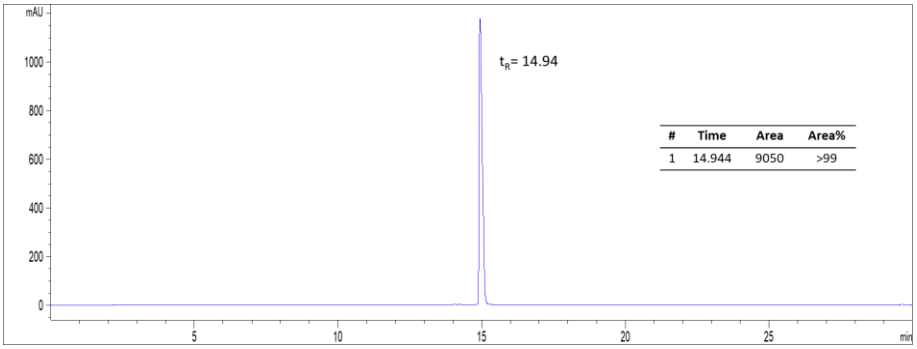

Compound 19, system A, 254 nm

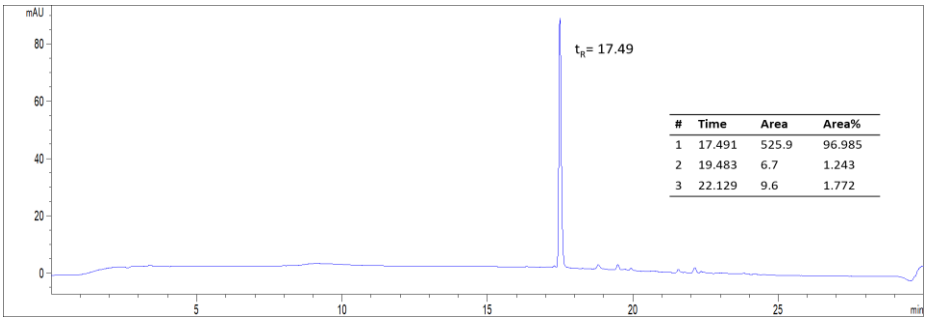

#	Time	Area	Area%
1	17.491	525.9	96.985
2	19.483	6.7	1.243
3	22.129	9.6	1.772

Compound 19, system B, 254 nm

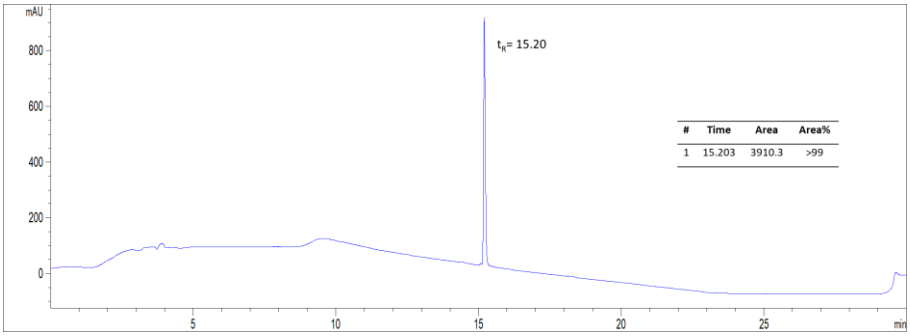

#	Time	Area	Area%
1	15.203	3910.3	>99

Compound 20, system A, 254

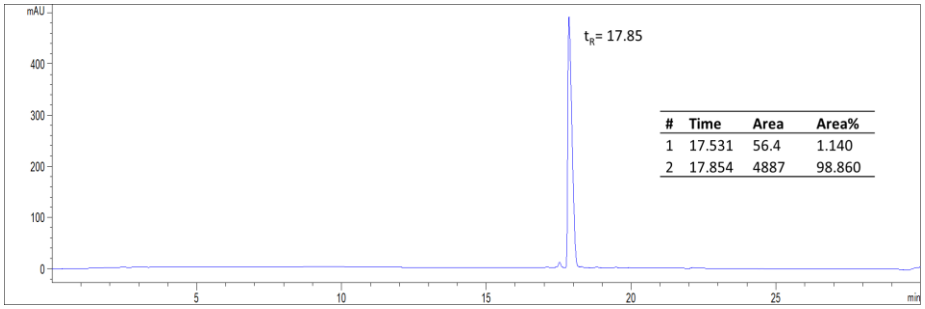

#	Time	Area	Area%
1	17.531	56.4	1.140
2	17.854	4887	98.860

Compound 20, system B, 254 nm

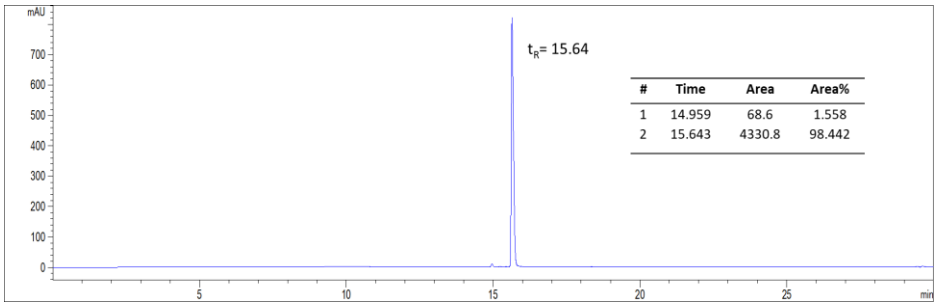

#	Time	Area	Area%
1	14.959	68.6	1.558
2	15.643	4330.8	98.442

Compound 21, System A, 254 nm

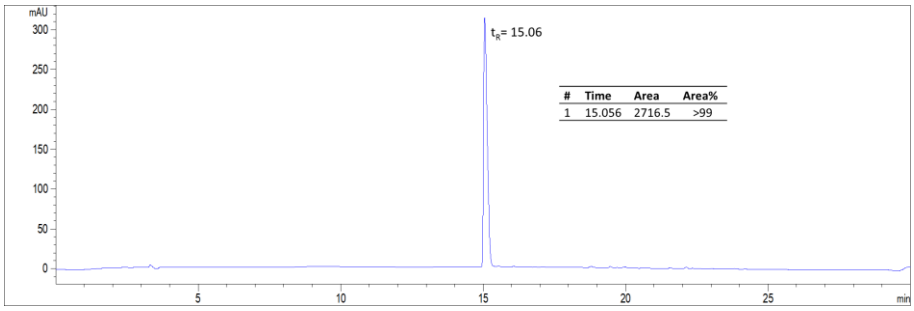

#	Time	Area	Area%
1	15.056	2716.5	>99

Compound 21, system B, 254 nm

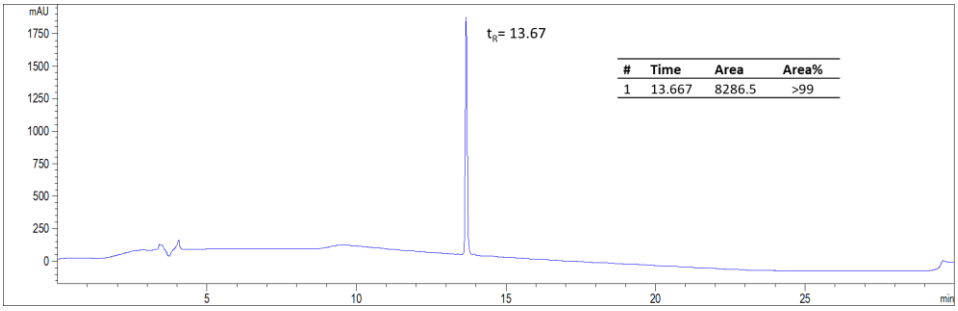

#	Time	Area	Area%
1	13.667	8286.5	>99

Compound 22, system A, 254 nm

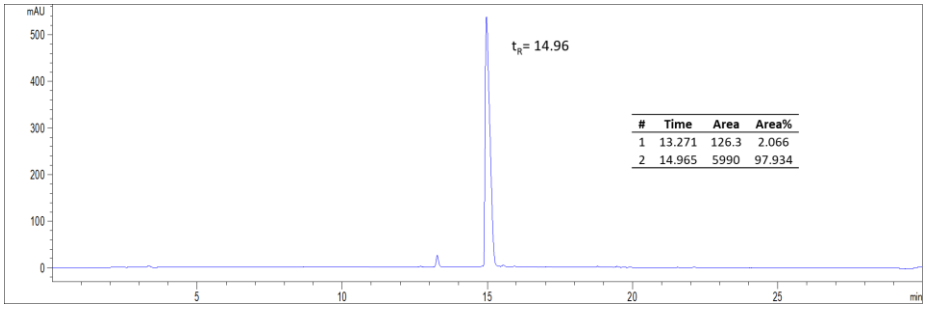

#	Time	Area	Area%
1	13.271	126.3	2.066
2	14.965	5990	97.934

Compound 22, system B, 254 nm

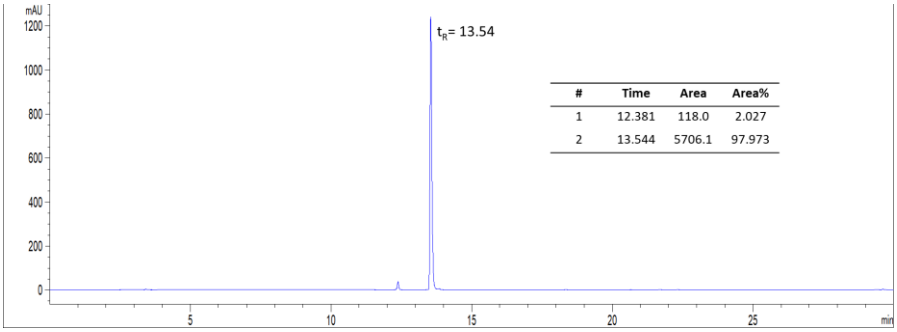

#	Time	Area	Area%
1	12.381	118.0	2.027
2	13.544	5706.1	97.973

Compound 23, system A, 254 nm

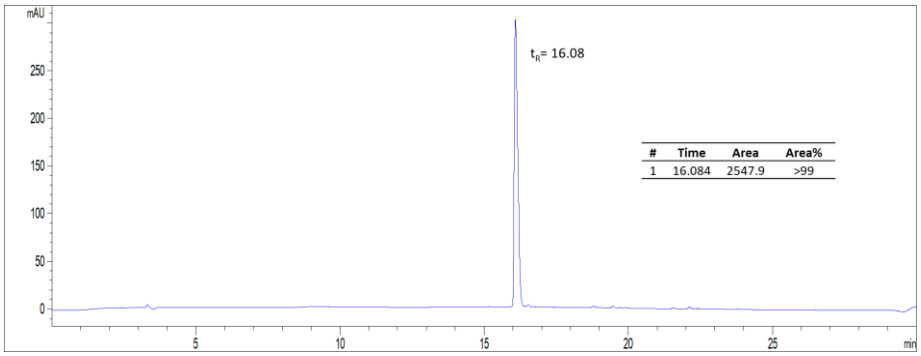

Compound 23, system B, 254 nm

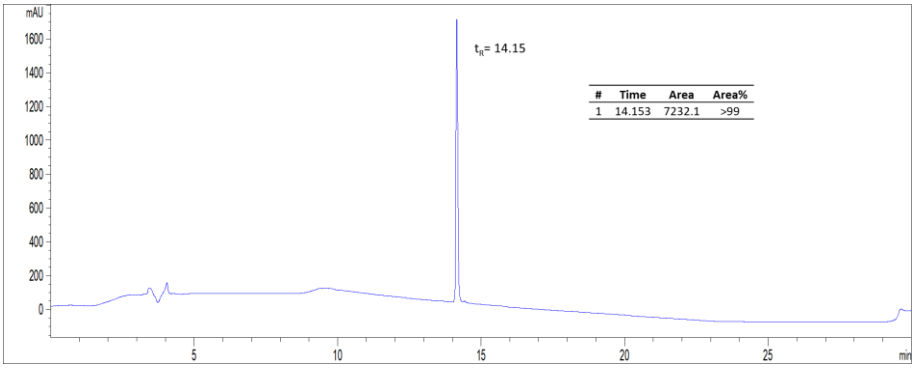

Compound 24, system A, 254 nm

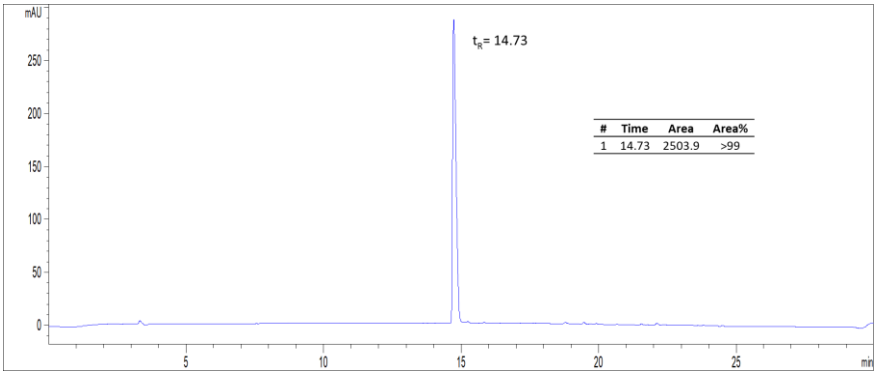

Compound 24, system B, 254 nm

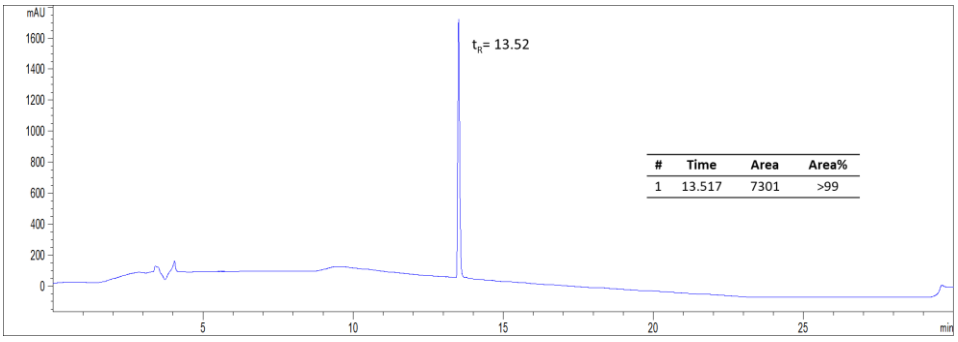

Compound 26, System A, 254 nm

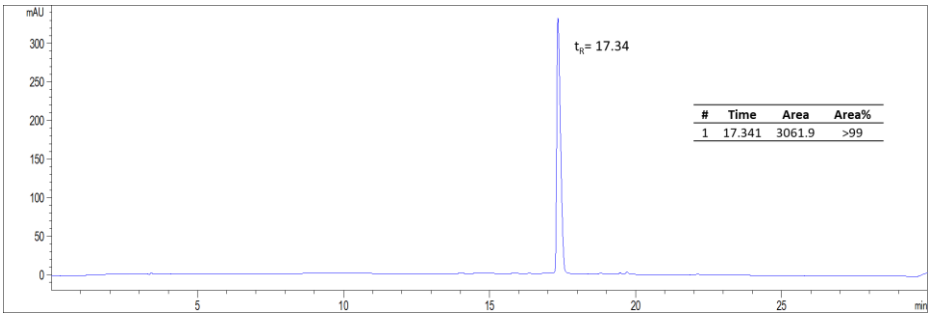

Compound 26, System B, 254 nm

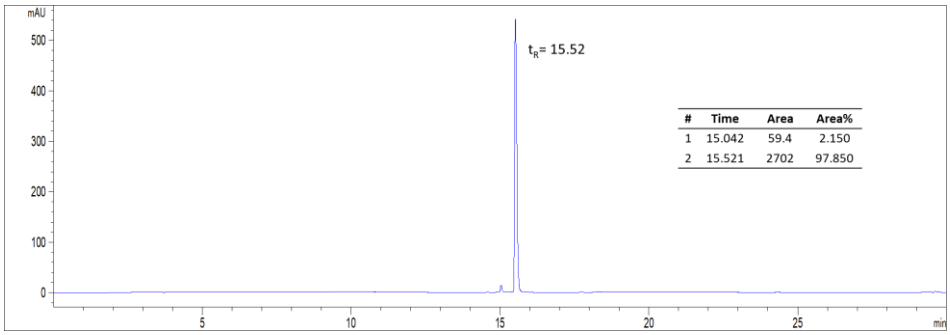

Compound 27, System A, 254 nm

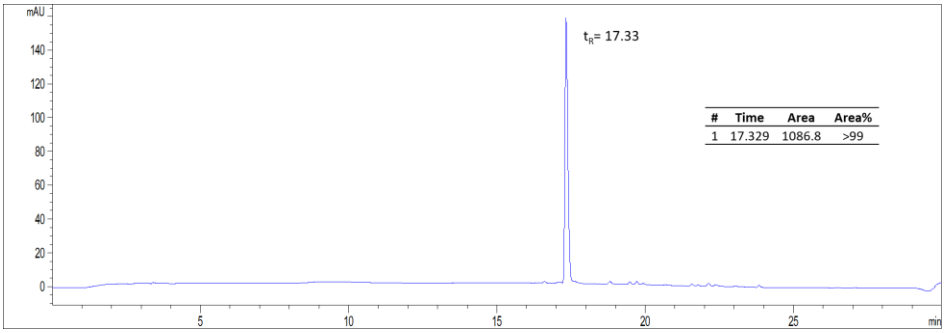

Compound 27, System A, 254 nm

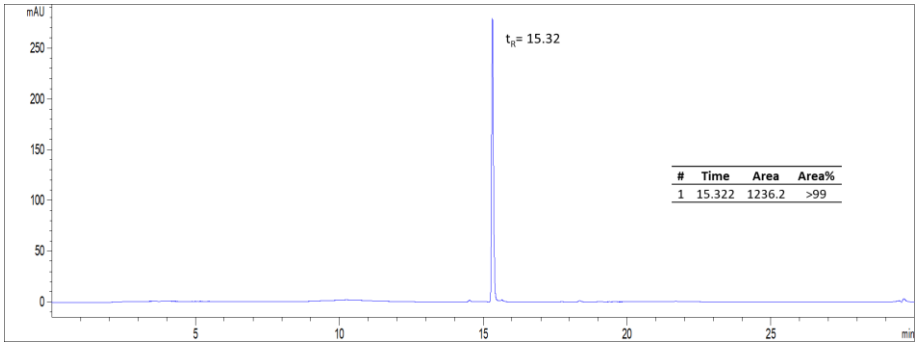

Compound 28, system A, 254 nm

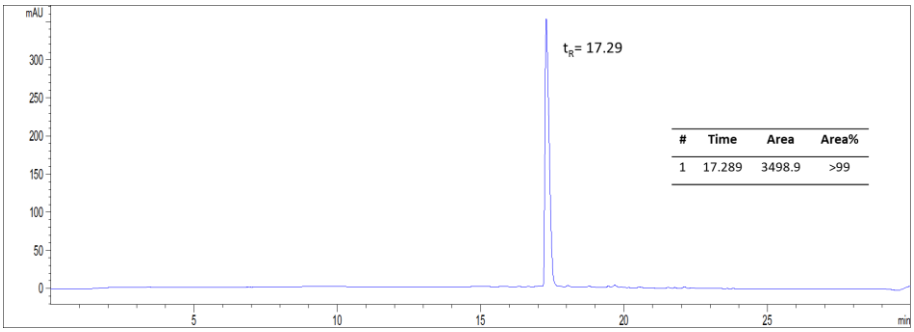

#	Time	Area	Area%
1	17.289	3498.9	>99

Compound 28, system B, 254 nm

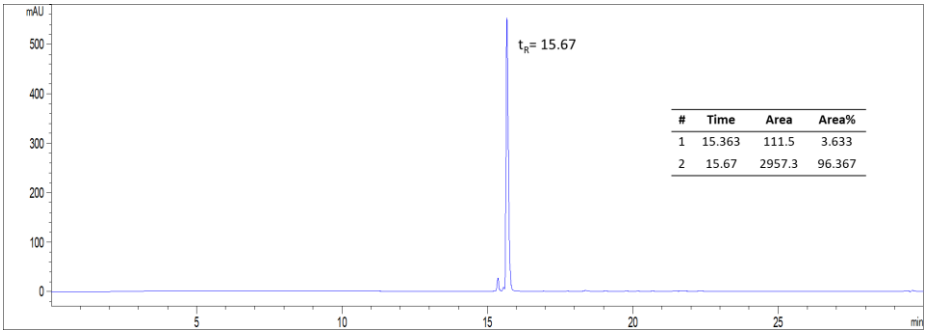

#	Time	Area	Area%
1	15.363	111.5	3.633
2	15.67	2957.3	96.367

3.6. References

(**1**) Zhao, P.; Metcalf, M.; Bunnett, N. W. Biased Signaling of Protease-Activated Receptors. *Front. Endocrinol. (Lausanne).* **2014**, *5*, 1–16.

(**2**) Adams, M. N.; Ramachandran, R.; Yau, M.; Suen, J. Y.; Fairlie, D. P.; Hollenberg, M. D.; Hooper, J. D. Pharmacology & Therapeutics Structure , Function and Pathophysiology of Protease Activated Receptors. *Pharmacol. Ther.* **2011**, *130*, 248–282.

(**3**) Zhao, P.; Lieu, T.; Barlow, N.; Sostegni, S.; Haerteis, S.; Korbmacher, C.; Liedtke, W.; Jimenez-Vargas, N. N.; Vanner, S. J.; Bunnett, N. W. Neutrophil Elastase Activates Protease-Activated Receptor-2 (PAR2) and Transient Receptor Potential Vanilloid 4 (TRPV4) to Cause Inflammation and Pain. *J. Biol. Chem.* **2015**, *290*, 13875–13887.

(**4**) Hollenberg, M. D.; Mihara, K.; Polley, D.; Suen, J. Y.; Han, A.; Fairlie, D. P.; Ramachandran, R. Biased Signalling and Proteinase-Activated Receptors (PARs): Targeting Inflammatory Disease. *Br. J. Pharmacol.* **2014**, *171*, 1180–1194.

(**5**) Ramachandran, R.; Mihara, K.; Chung, H.; Renaux, B.; Lau, C. S.; Muruve, D. A.; DeFea, K. A.; Bouvier, M.; Hollenberg, M. D. Neutrophil Elastase Acts as a Biased Agonist for Proteinase-Activated Receptor-2 (PAR2). *J. Biol. Chem.* **2011**, *286*, 24638–24648.

(**6**) Ramachandran, R.; Noorbakhsh, F.; DeFea, K.; Hollenberg, M. D. Targeting Proteinase-Activated Receptors: Therapeutic Potential and Challenges. *Nat. Rev. Drug Discov.* **2012**, *11*, 69–86.

(**7**) Nystedt, S.; Emilsson, K.; Wahlestedt, C.; Sundelin, J. Molecular Cloning of a Potential Proteinase Activated Receptor. *Proc. Natl. Acad. Sci.* **1994**, *91*, 9208–9212.

(**8**) Yau, M.; Lim, J.; Liu, L.; Fairlie, D. P. Protease Activated Receptor 2 (PAR2) Modulators: A Patent Review (2010–2015). *Expert Opin. Ther. Pat.* **2016**, *26*, 471–483.

(**9**) Kakarala, K. K.; Jamil, K.; Devaraji, V. Structure and Putative Signaling Mechanism of Protease Activated Receptor 2 (PAR2) – A Promising Target for Breast Cancer. *J. Mol. Graph. Model.* **2014**, *53*, 179–199.

(**10**) Crilly, A.; Burns, E.; Nickdel, M. B.; Lockhart, J. C.; Perry, M. E.; Ferrell, P. W.; Baxter, D.; Dale, J.; Dunning, L.; Wilson, H.; Nijjar, J. S.; Gracie, J. A.; Ferrell, W. R.; McInnes, I. B. PAR2 Expression in Peripheral Blood Monocytes of Patients with Rheumatoid Arthritis. *Ann. Rheum. Dis.* **2012**, *71*, 1049–1054.

(**11**) Heuberger, D. M.; Schuepbach, R. A. Protease-Activated Receptors (PARs): Mechanisms of Action and Potential Therapeutic Modulators in PAR-Driven Inflammatory Diseases. *Thromb. J.* **2019**, *17*, 4.

(**12**) Friebel, J.; Weithauser, A.; Witkowski, M.; Rauch, B. H.; Savvatis, K.; Dörner, A.; Tabaraie, T.; Kasner, M.; Moos, V.; Bösel, D.; Gotthardt, M.; Radke, M. H.; Wegner, M.; Bobbert, P.; Lassner, D.; Tschöpe, C.; Schutheiss, H. P.; Felix, S. B.; Landmesser, U.; Rauch, U. Protease-Activated Receptor 2 Deficiency Mediates Cardiac Fibrosis and Diastolic Dysfunction. *Eur. Heart J.* **2019**, *40*, 3318–3332.

(**13**) Kawabata, A.; Matsunami, M.; Sekiguchi, F. Gastrointestinal Roles for Proteinase-Activated Receptors in Health and Disease. *Br. J. Pharmacol.* **2009**, *153*, S230–S240.

(**14**) Lin, C.; von der Thüsen, J.; Daalhuisen, J.; ten Brink, M.; Crestani, B.; van der Poll, T.; Borensztajn, K.; Spek, C. A. Protease-Activated Receptor PAR2 Is Required for PAR1 Signalling in Pulmonary Fibrosis. *J. Cell. Mol. Med.* **2015**, *19*, 1346–1356.

(**15**) Zhong, B.; Ma, S.; Wang, D. Protease-activated Receptor 2 Protects against Myocardial Ischemia-reperfusion Injury through the Lipoxygenase Pathway and TRPV1 Channels. *Exp. Ther. Med.* **2019**, 3636–3642.

(**16**) Fernando, E. H.; Gordon, M. H.; Beck, P. L.; MacNaughton, W. K. Inhibition of Intestinal Epithelial Wound Healing through Protease-Activated Receptor-2 Activation in Caco2 Cells. *J. Pharmacol. Exp. Ther.* **2018**, *367*, 382–392.

(**17**) Hollenberg, M. D.; Saifeddine, M.; Al-Ani, B. Proteinase-Activated Receptor-2 in Rat Aorta: Structural Requirements for Agonist Activity of Receptor-Activating Peptides. *Mol. Pharmacol.* **1996**, *49*, 229–233.

(**18**) Böhm, S. K.; Khitin, L. M.; Grady, E. F.; Aponte, G.; Payan, D. G.; Bunnett, N. W. Mechanisms of Desensitization and Resensitization of Proteinase-Activated Receptor-2. *J. Biol. Chem.* **1996**, *271*, 22003–22016.
(**19**) McGuire, J. J.; Saifeddine, M.; Triggle, C. R.; Sun, K.; Hollenberg, M. D. 2-Furoyl-LIGRLO-Amide: A Potent and Selective Proteinase-Activated Receptor 2 Agonist. *J. Pharmacol. Exp. Ther.* **2004**, *309*, 1124–1131.
(**20**) Yau, M.; Suen, J. Y.; Xu, W.; Lim, J.; Liu, L.; Adams, M. N.; He, Y.; Hooper, J. D.; Reid, R. C.; Fairlie, D. P. Potent Small Agonists of Protease Activated Receptor 2. *ACS Med. Chem. Lett.* **2016**, *7*, 105–110.
(**21**) Barry, G. D.; Suen, J. Y.; Low, H. B.; Pfeiffer, B.; Flanagan, B.; Halili, M.; Le, G. T.; Fairlie, D. P. A Refined Agonist Pharmacophore for Protease Activated Receptor 2. *Bioorg. Med. Chem. Lett.* **2007**, *17*, 5552–5557.
(**22**) Barry, G. D.; Suen, J. Y.; Le, G. T.; Cotterell, A.; Reid, R. C.; Fairlie, D. P. Novel Agonists and Antagonists for Human Protease Activated Receptor 2. *J. Med. Chem.* **2010**, *53* (20), 7428–7440.
(**23**) Yau, M.; Liu, L.; Suen, J. Y.; Lim, J.; Lohman, R.; Jiang, Y.; Cotterell, A. J.; Barry, G. D.; Mak, J. Y. W.; Vesey, D. A.; Reid, R. C.; Fairlie, D. P. PAR2 Modulators Derived from GB88. *ACS Med. Chem. Lett.* **2016**, *7*, 1179–1184.
(**24**) Gardell, L. R.; Ma, J.; Seitzberg, J. G.; Knapp, A. E.; Schiffer, H. H.; Tabatabaei, A.; Davis, C. N.; Owens, M.; Clemons, B.; Wong, K. K.; Lund, B.; Nash, N. R.; Gao, Y.; Lameh, J.; Schmelzer, K.; Olsson, R.; Burstein, E. S. Identification and Characterization of Novel Small-Molecule Protease-Activated Receptor 2 Agonists. *J. Pharmacol. Exp. Ther.* **2008**, *327*, 799–808.
(**25**) Cheng, R. K. Y.; Fiez-Vandal, C.; Schlenker, O.; Edman, K.; Aggeler, B.; Brown, D. G.; Brown, G. A.; Cooke, R. M.; Dumelin, C. E.; Doré, A. S.; Geschwindner, S.; Grebner, C.; Hermansson, N.; Jazayeri, A.; Johansson, P.; Leong, L.; Prihandoko, R.; Rappas, M.; Soutter, H.; Snijder, A.; Sundström, L.; Tehan, B.; Thornton, P.; Troast, D.; Wiggin, G.; Zhukov, A.; Marshall, F. H.; Dekker, N. Structural Insight into Allosteric Modulation of Protease-Activated Receptor 2. *Nature* **2017**, *545*, 112–115.
(**26**) Klösel, I.; Schmidt, M. F.; Kaindl, J.; Hübner, H.; Weikert, D.; Gmeiner, P. Discovery of Novel Nonpeptidic PAR2 Ligands. *ACS Med. Chem. Lett.* **2020**, *11*, 1316–1323.
(**27**) Kennedy, A. J.; Ballante, F.; Johansson, J. R.; Milligan, G.; Sundström, L.; Nordqvist, A.; Carlsson, J. Structural Characterization of Agonist Binding to Protease-Activated Receptor 2 through Mutagenesis and Computational Modeling. *ACS Pharmacol. Transl. Sci.* **2018**, *1*, 119–133.

Chapter 4. Dual conjugates targeting $\alpha_v\beta_6/\alpha_v\beta_3$ and TK

4.1. Introduction

In the last decades, drug resistance to several tumor targeted therapies has been largely demonstrated, despite the subtle mechanisms that sustain tumor cells between initial response and disease progression are not completely understood.[1] An interesting strategy to overcome drug resistance relies on the development of multi-target therapy with the aim to inhibit different targets involved in the tumor genesis and development and, most importantly, to address their intertwined crosstalk.[2]

The crosstalk between certain integrin receptors and Growth Factor Receptors (GFRs) plays a pivotal role in the development of drug resistance in solid tumors.[3] GFRs are membrane-bound glycoproteins and belong to the large family of receptors that have tyrosine kinases activity (RTK). The binding of their natural ligands triggers multiple intracellular cascades (e.g. PI3K, MAPKs, ERK, …), making them key regulators of cell proliferation, survival and growth. These receptors are frequently overexpressed or amplified in a wide variety of solid tumors, and mutations affecting their expression or activity confer a growth advantage to the cells and predispose them to malignant transformations.[3]

Hence, tyrosine kinase inhibitors (TKIs), either monoclonal antibodies or small molecules, have been developed to interrupt several GFR-related pathways. For instance, sunitinib (**1**, Figure 1) is an alkylidene 2-oxindole derivative with antiangiogenic activity, acting as a highly effective multitarget tyrosine kinase inhibitor (mainly against VEGFR2, PDGFRβ, c-Kit, and Flt-3) and it is indicated as a first-line treatment against metastatic renal cell carcinoma or neuroendocrine tumors.[4]

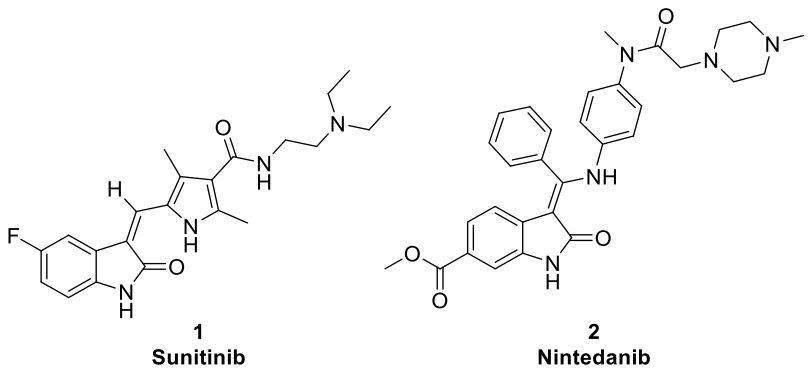

Figure 1. *Structure of the TKIs sunitinib (**1**) and nintedanib (**2**).*

Another structurally similar, potent TKI is nintedanib (**2**, Figure 1), which targets three major pro-angiogenic and pro-fibrotic pathways mediated by the VEGFRs, FGFRs and PDGFRs, Src and Flt-3 kinases. It is clinically approved for the treatment of Idiopathic Pulmonary Fibrosis (IPF) and recent clinical evidences have shown nintedanib having significant efficacy in the treatment of non-small cell lung cancer (NSCLC) and ovarian cancer.[5] Both these small molecules are multi-kinase inhibitors, a seemingly desirable characteristic for drugs in the treatment of both cancer and fibrosis-related diseases; in fact, it has been demonstrated that the use of multi-kinases inhibitors is beneficial in overcoming tumor resistance and increasing therapeutic success as compared to selective kinase inhibitors.[5]

Interestingly, recent studies have highlighted the impact of integrin-mediated signalling in TKI-cancer therapy resistance,[3,6] but how integrins regulate response to this class of drugs remains

debated, despite the role of these receptors (in particular the α_V integrins) and their crosstalk with GFRs have been largely described.[3,6-8] The most likely hypothesis is the mutual cooperation between the two distinct receptor systems in which *(i)* integrins induce ligand-independent activation of GFRs and, on the other hand, *(ii)* growth factors can induce adhesion molecules to propagate adhesion-independent signals.[9] In fact, the signals triggered by either GFRs or integrins might follow parallel and often superimposable pathways, that converge on common downstream effectors (Figure 2a) leading to a therapy-resistant tumor.

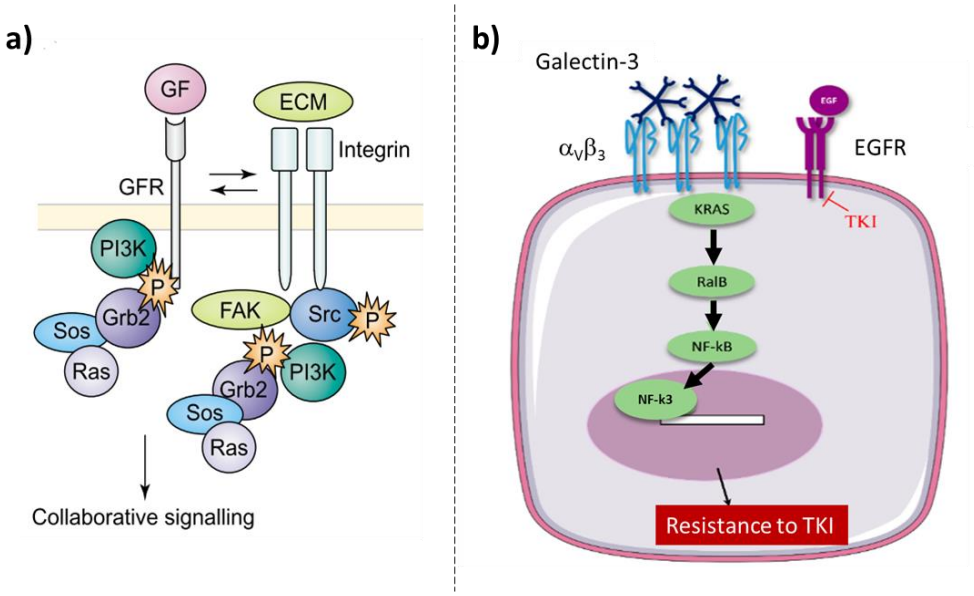

Figure 2. *Scheme of the crosstalk between integrins and GFRs: (**a**) and (**b**) mechanism of $\alpha_V\beta_3$-mediated resistance in tumors treated with EGFR-TKI. Adapted from Refs. 6 and 9.*

For instance, in tumors treated with EGFR-TKI, cells start to overexpress $\alpha_V\beta_3$ integrin, leading to a resistant tumor; in fact, galectin-3 binds to the oligosaccharide moieties of β_3 integrin and promotes integrin/KRAS interaction, independently of integrin-mediated adhesion to ECM proteins. KRAS activates the downstream RalB/NFkB pathway that leads to therapy resistance by promoting a stem cell-like phenotype,[6] as shown in Figure 2b. Furthermore, a crosstalk between $\alpha_V\beta_6$ and EGFR, which regulates bidirectional force transmission and controls breast cancer invasion, have been recently described.[10] Hence, therapeutic strategies targeting integrin/EGFR interaction to prevent the emergence of acquired resistance to EGFR-TKIs have been largely proposed.[3]

The integrin-GFRs crosstalk is important not only in the development of tumor resistance, but also in cancer progression, malignant transformation and metastasis spread. Increasing piece of evidence[3] indicate that cells within the tumor environment upregulate the expression and signalling functions of integrins (mainly $\alpha_V\beta_6$ and $\alpha_V\beta_3$) inducing Epithelial-To-Mesenchymal Transition (EMT). As described in Chapter 2 (Paragraph 2.1.2.), the cancer-related EMT process is characterized by transformation of cancer cells into invasive forms that migrate to other organs, leading to tumor progression and metastasis spread. For these reasons, targeting EMT-related biomolecules is emerging as a novel therapeutic approach for preventing migration and invasion in several cancer types.[3,7] For instance, the combined administration of α_V integrin ligands and sunitinib has been shown to enhance the inhibitory effect of sunitinib on TGFβ1-induced EMT in human non-small cell lung cancer cells.[7]

To conclude, recent evidences show how the crosstalk of signaling pathways between integrins and growth factor receptors is extremely important in the development of tumor resistance and in

inducing EMT process, which aggravates cancer progression and leads to malignant transformation. The development of dual agents aimed at inhibiting both integrins and GFRs simultaneously could be a promising therapeutic approach for tumor- and fibrosis-related diseases.

On this line, our research group has recently developed three novel dual covalent conjugates (**3**, **4** and **5**, Figure 3) comprising the $\alpha_V\beta_3$ integrin targeting cyclopeptidomimetic c(AmpRGD) (depicted in red), the TKI sunitinib moiety (depicted in blue), and three different types of linkers (depicted in black) with the aim to *(i)* exploit the c(AmpRGD) ligand ability to selectively target $\alpha_V\beta_3$ integrin-overexpressing cells; *(ii)* enhance integrin-mediated cell internalization of the construct, *(iii)* possibly interfere with the crosstalk between $\alpha_V\beta_3$ integrin and VEGFR, and (*iv*) address the sunitinib moiety at the respective intracellular TK targets.[4,11,12]

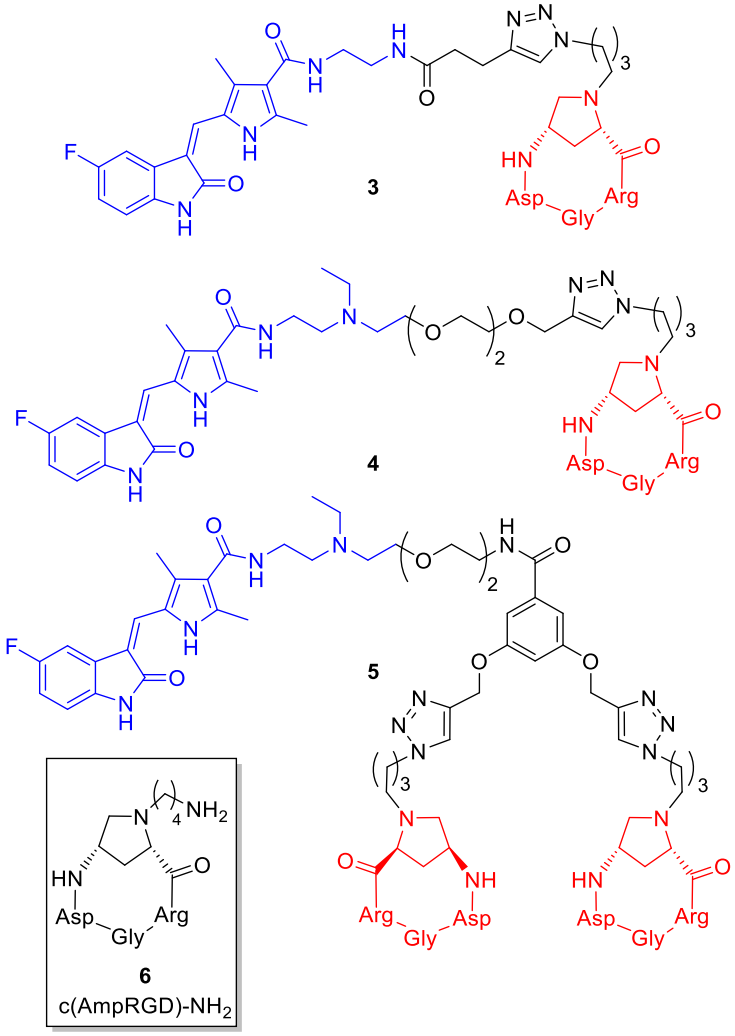

***Figure 3**. Structure of the three covalent conjugates synthesized in the last year by our research group. The $\alpha_V\beta_3$ targeting peptide moiety is represented in red, the linker spacer in black and the sunitinib unit in blue. The free $\alpha_V\beta_3$ ligand c(AmpRGD)-NH_2 (**6**) is displayed in the box.*

In these compounds, conjugation of the integrin-recognizing peptide with the appended drug did not affect the ligand binding competence toward $\alpha_V\beta_3$; meanwhile, the kinase inhibitory activity of the constructs remained comparable to that of sunitinib alone.[12] Conjugates **3**–**5** were studied *in vitro* (human melanoma cell lines M21 and A375, human ovarian cancer cell line IGROV-1) and *in vivo* (nude mice) as inhibitors of tumor angiogenesis and progression. It was proven that cell uptake was mediated by $\alpha_V\beta_3$ integrins, and dimeric compound **5** was better internalized as compared to

congeners **3** and **4**, probably due to its enhanced affinity toward the integrin receptor and favourable physico-chemical properties (e.g. protonation state). It is worth noticing that dimeric compound **5** underwent only partial cell internalization and this behaviour was judged to be beneficial; the authors speculated that a possible synergy action could be operative involving both the extracellular RGD−integrin interaction (provided by the non-internalized fraction) and the sunitinib−VEGFR2 kinase interaction (provided by the amount of internalized compound). Compounds **3** and **4**, though structurally similar, showed a very different uptake profile and overall biological activity, highlighting how the structure of the linker could deeply influence the physical-chemical-biological properties of the resulting conjugates.

Interestingly, a decreased aggressiveness in tumor cell population was observed under chronic treatment with conjugates **3** and **5** as compared to sunitinib alone, opening the way for the use of these selective conjugates as drugs able to overcome the TKI-related tumor resistance. Finally, the *in-vivo* targeting ability together with tumor inhibition of compounds **3** and **5** was demonstrated by experiments on tumor implanted nude mice, indicating a striking antitumor activity of this conjugate versus sunitinib; taken together, these results support the interest of integrin-targeted sunitinib conjugates for the treatment of drug-resistant tumors.

4.2. Aim of the Project

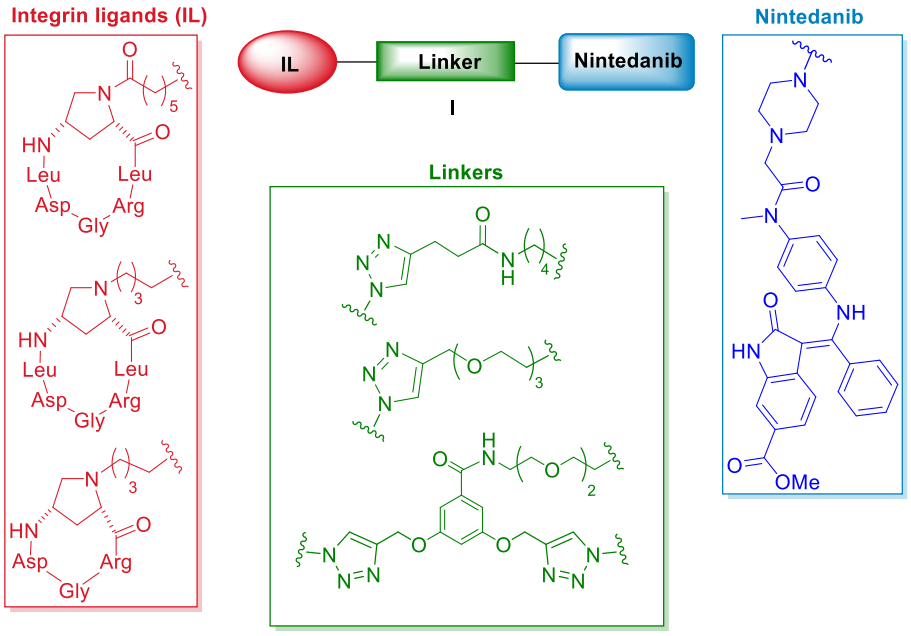

Figure 4. *Structure of the nine different covalent conjugates of general formula* ***I*** *object of this work.*

Based on the promising results of the previously mentioned sunitinib-based conjugates, and conscious that the covalent conjugation of two active ingredients may lead to novel molecular constructs with dual-targeting features and unexplored, yet improved physical-chemical properties, we advanced a new project, aimed at the construction of new covalent conjugates connecting an α_V integrin targeting ligand with the TKI nintedanib.

In particular, a panel of nine different covalent conjugates of type **I** was designed and synthesized (Figure 4), constituted by a nintedanib-like moiety as the TKI ingredient (depicted in blue), which is alternatively linked to three different RGD-based cyclopeptides as integrin targeting units (depicted in red) by means of three different triazole-based uncleavable linkers (depicted in green). While incorporating the same TKI (nintedanib), these nine compounds comprise several points of variability: *(i)* the sequence of the cyclopeptide namely, *c*(AmpLRGDL) *vs c*(AmpRGD), which is responsible for the selective $\alpha_V\beta_6$ *vs* $\alpha_V\beta_3$ integrin targeting ability (vide infra); *(ii)* N^{α} amide *vs* amine appendage within the aminoproline unit; and *(iii)* chemical nature of the triazole-based linkers featuring different lengths, amide/PEG/amide-PEG functionalities, and monomeric *vs* dimeric presentations.

To complete the work, all the synthesized compounds are intended to be tested by Prof. Francesca Bianchini (University of Florence) towards different cancer cell lines (e.g. adenocarcinoma human alveolar basal epithelial cells A549) and/or fibrotic cell models, to evaluate *(i)* whether the competence of the two active units are preserved namely, the ligand binding competence toward α_V integrin overexpressing cells and the TK inhibitory activity in vitro; *(ii)* the ability of these conjugates to interfere with the cross-talk between integrins ($\alpha_V\beta_3$ and/or $\alpha_V\beta_6$) and GFRs, and *(iii)* the possible inhibition of the Epithelial-To-Mesenchymal Transition process (EMT). With these responses in hand, a thorough structure-activity relationship study will be possible in order to elucidate the impact that the diverse structural variations have on the overall biological behavior.

4.3. Results and discussion

4.3.1. Design and retrosynthesis

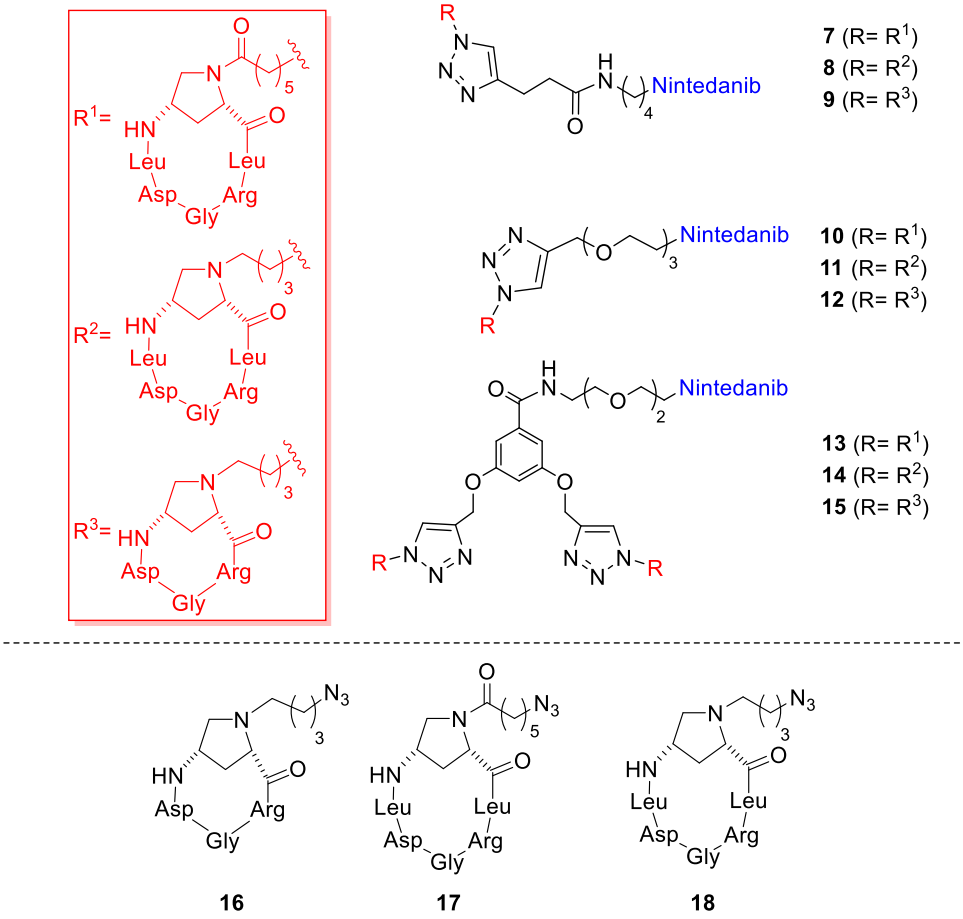

Figure 5. *Structures of the novel designed covalent conjugates* ***7-15*** *(up) and the parent aminoproline-based cyclopeptidomimetics* ***16-18*** *(bottom).*

Inspired by the previous work focused on sunitinib-based covalent conjugates, we designed the nine different novel conjugates **7**-**15** portrayed in Figure 5.

The crystal structure of nintedanib in the receptor site of VEGFR2 showed that the *N*-methyl-piperazinyl moiety of nintedanib is not involved in the receptor recognition[13] and, consequently, the piperazine nucleus was selected as anchoring point for the linker. For the integrin recognizing motif, three different aminoproline-based cyclic peptidomimetics were chosen (Figure 5, bottom): the reported $\alpha_V\beta_3$ integrin ligand c(AmpRGD) **16**,[4,14] the N^{α}-acyl appended $\alpha_V\beta_6$ integrin ligand c(AmpLRGDL) **17**[15] and the N^{α}-alkyl appended $\alpha_V\beta_6$ integrin ligand **18**. In practice, compound **18** is a slightly modified version of **17** where the N^{α}-aminoproline is decorated with a 4-azido-butyl residue instead of a 6-azido-hexanoyl chain. This structural modification was introduced to investigate whether an extra tertiary amine in the whole construct could influence the behaviour of the final conjugates in terms of solubility and cell internalization. Previous studies had in fact suggested that the endosome and/or lysosome escape of similar conjugates could be favoured by a changing in the protonation grade.[11] Finally, three different linkers were planned (depicted in black, Figure 5, up) as having two monomeric types of conjugates (the former with an alkyl linker

and the latter with a PEG spacer) and one dimeric conjugate, with a benzoyl-PEG moiety as linker. The choice of this kind of uncleavable linker were made based on the matured experience of our research group in the previously mentioned sunitinib-RGD conjugates.

Scheme 1. *General retrosynthetic approach, as exemplified to access compound* ***7****.*

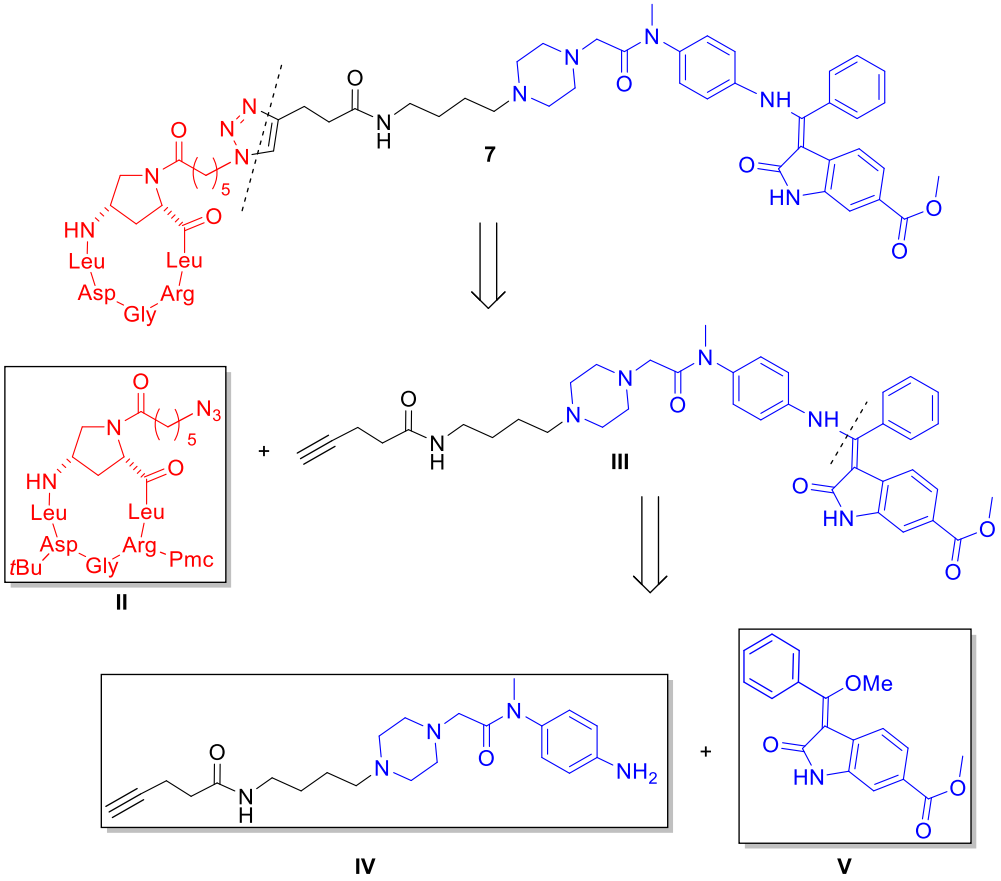

The general retrosynthetic approach is shown in Scheme 1, using compound **7** as a representative example. The triazole ring, product of a copper-catalyzed azide-alkyne click reaction, can be disconnected yielding azide **II** and alkyne **III**. The enamine motif of compound **III** can be the product of a stereospecific conjugated nucleophilic addition,[16] and it can be traced back to aniline **IV** and alkylidene oxindole **V**.

Compounds of type **II**, **IV** and **V** were chosen as the main building blocks for the synthesis of all the covalent conjugates, as *(i)* cyclic peptidomimetics of type **II,** having the terminal azide functionality ready for a copper-catalyzed click reaction, can be easily synthesized from the constitutive amino acid residues, as shown in Chapter 2 (Paragraph 2.3.2.); *(ii)* aniline **IV** can be synthesized by slightly modifying a procedure reported in the literature[16] and (*iii*) the oxindole nucleus **V** can be synthesized according to the published procedure to nintedanib.[16]

4.3.2. Synthesis of the cyclic peptidomimetics

The synthesis of the three different peptide building blocks was accomplished by SPPS followed by in-solution cyclization. The procedure for the synthesis of the aminoproline nucleus **19** (Scheme 2) and the protected cyclopeptide **21** was performed as reported in the literature,[4] while the synthesis of **20** and **22** has been reported in Chapter 2 (Paragraph 2.3.2.).

Scheme 2. *Up, structures of the two aminoproline nuclei* ***19*** *and* ***20*** *and the three protected cyclic peptidomimetics* ***21***, ***22*** *and* ***23****. Bottom, scheme of the synthesis of cyclopeptide* ***23****.*

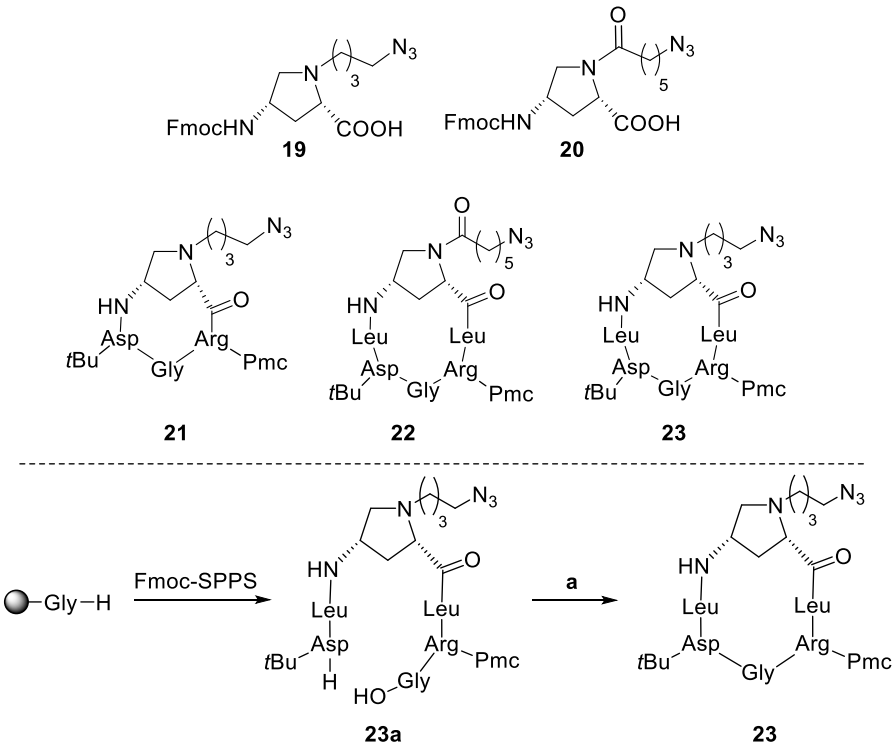

[a]Reagents and conditions: **Fmoc-SPPS**: (i) Fmoc-Arg(Pmc)-OH, Fmoc-Leu-OH, **19**, Fmoc-Leu-OH, Fmoc-Asp(*t*Bu)-OH; HATU, HOAt, collidine, DMF, (ii) piperidine, DMF, (iii) AcOH, TFE, DCM; 90% yield; **a**) HATU, HOAt, collidine, DCM/DMF (15:1), 6h, 50% yield.

For the synthesis of peptide **23**, the linear precursor **23a** was synthesized using the Fmoc-based SPPS protocol starting from the preloaded H-Gly-2-ClTrt resin (Scheme 2). Each amino acid was sequentially added to the growing sequence, alternating coupling steps (HATU, HOAt and collidine) and Fmoc-cleavage procedures (piperidine:DMF). Finally, once the desired sequence was completed, the cleavage from the resin was performed using acidic conditions (AcOH/TFE/DCM) to obtain the linear peptide **23a** in 90% yield. The subsequent in-solution cyclization reaction was carried out using diluted conditions (15:1 DCM/DMF solvent mixture, 1-3 mM) and HATU, HOAt as coupling reagents, giving the protected cyclic peptidomimetic **23** in 50% yield. Compounds **21**, **22** and **23** were used for the final click reaction, which is described in the Paragraph 4.3.5.

4.3.3. Synthesis of the linker-piperazinyl nuclei

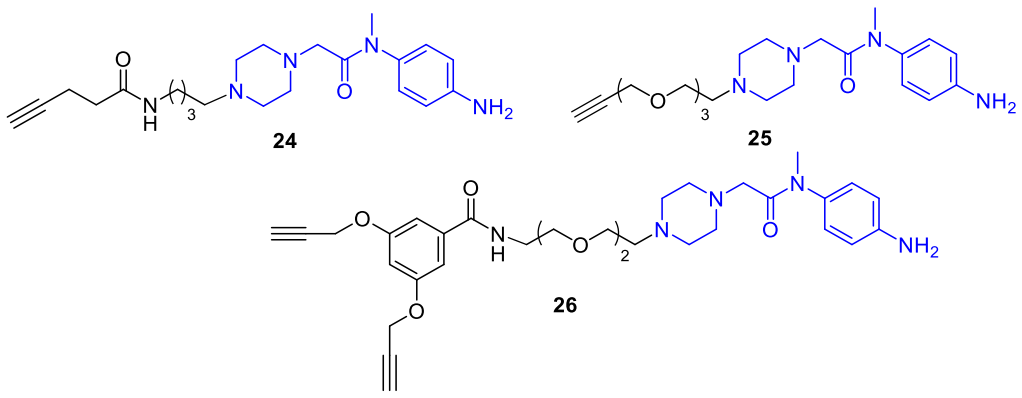

Figure 6. *Structures of the three different linker-piperazinyl nuclei* ***24****-****26****.*

The three building blocks **24**, **25** and **26** (Figure 6) are constituted by the three different linker motifs (depicted in black) and the same piperazinyl nucleus of nintedanib (depicted in blue). Initially, the structure of the "shorter linker" **24** was designed with a slight modification of the structure, that was a three-methylene-long chain between the piperazinyl and the pentinoic acid motifs. However, the planned synthesis, starting from 3-aminopropanol **28** (Scheme 3, Eq. 1), resulted unexpectedly very challenging. Indeed, the coupling reaction between amine **28** and 4-pentynoic acid **27** yielded successfully an amide intermediate, which was subjected to the subsequent tosylation step leading to the mix of products **29** and **30**, probably due to an intramolecular nucleophilic displacement involving a 6-membered cycle. For this reason, the synthesis route was modified by performing tosylation before amidation, as shown in Scheme 3 (Eq. 2); even in this instance, however, the final coupling reaction yielded unexpectedly the same mix of products, with the undesired ester **30** prevailing. Therefore, the structure of the designed linker was slightly modified by introducing an additional methylene group in order to avoid any intramolecular side reaction involving 6-membered cycles.

***Scheme 3**. Failed synthesis routes for the "short linker" **24** (Eq.1 and Eq.2) and synthesis of the linker motif **37** (Eq.3).*[a]

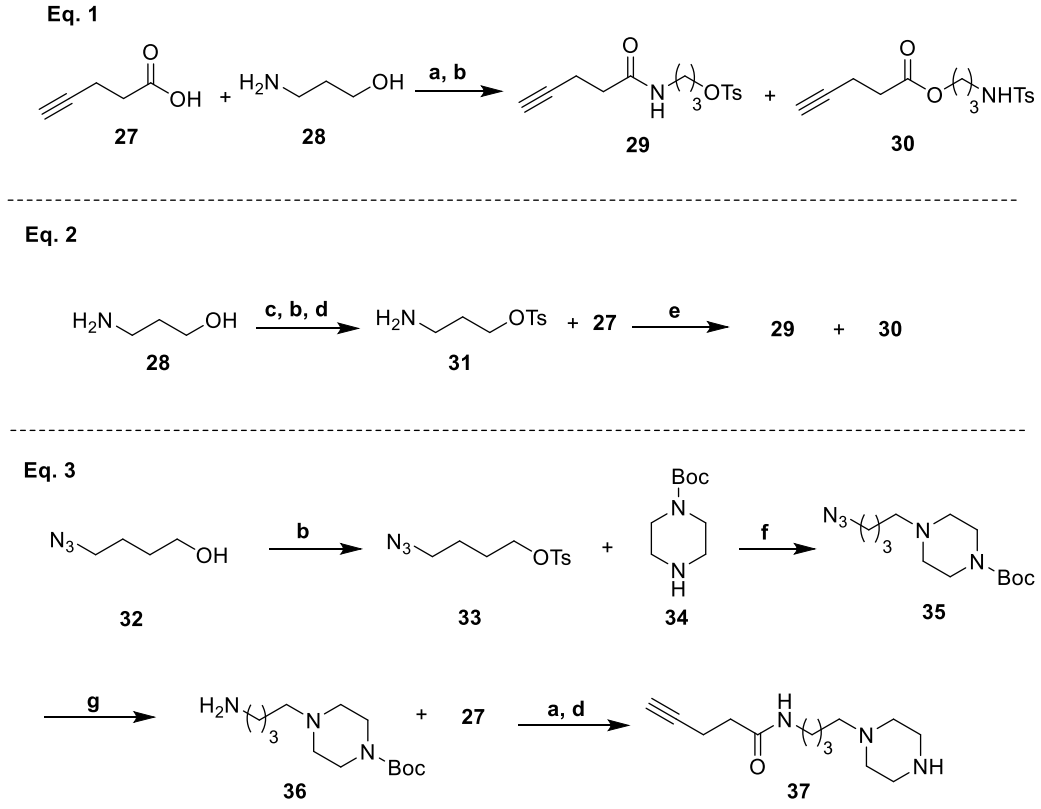

[a]Reagents and conditions: **a**) HATU, TEA, DCM dry, N_2, rt, 2-6h, 70-80% yield; **b**) p-TsCl, TEA, DMAP, DCM dry, rt, 7-15h, 65-72% yield; **c**) di-*tert*-butyl dicarbonate, DMAP, ACN dry, N_2, rt, 3h, 85% yield; **d**) TFA/DCM 1.7:10, 1h, rt, 3h, quant. yield; **e**) pivaloyl chloride, DIPEA, DCM dry, rt, 4h; **f**) Cs_2CO_3, ACN dry, N_2, 60°C, 3 days, 79% yield; **g**) H_2, Pd/C, EtOAc, CH_3COONa, rt, 3h, 91% yield.

The renewed synthesis was planned to start from the 4-azidobutanol **32** (Scheme 3, Eq. 3) instead of 3-aminopropanol **28**. Alcohol **32** was tosylated with 4-toluenesulfonyl chloride and 4-dimethylaminopyridine (DMAP) in basic conditions, giving azide **33** in good yield. A nucleophilic substitution of compound **33** by Boc-piperazine **34** was performed, yielding compound **35** (79% yield), subsequently reduced by palladium-catalyzed hydrogenation, giving primary amine **36** (91%

yield). Finally, a coupling reaction between amine **36** and pentynoic acid **27** and the following Boc-removal in acidic conditions were performed, producing alkyne **37** in good yield.

The syntheses of the other two linker-piperazinyl nuclei **25** and **26** were performed starting from the tosylated compounds **38** and **40**, respectively (Scheme 4), in turn prepared according to literature procedures.[4] Compounds **38** and **40** reacted in a nucleophilic substitution with the Boc-piperazine **34**, giving the piperazinyl-substituted protected intermediates in acceptable yields (67-75%), even if the reaction time was quite long (up to 3 days for the reaction between **34** and **40**). The protected intermediates were then easily deprotected in acidic conditions, yielding alkynes **39** and **41** quantitatively.

Scheme 4. *Synthesis of alkynes **39** and **41**.*[a]

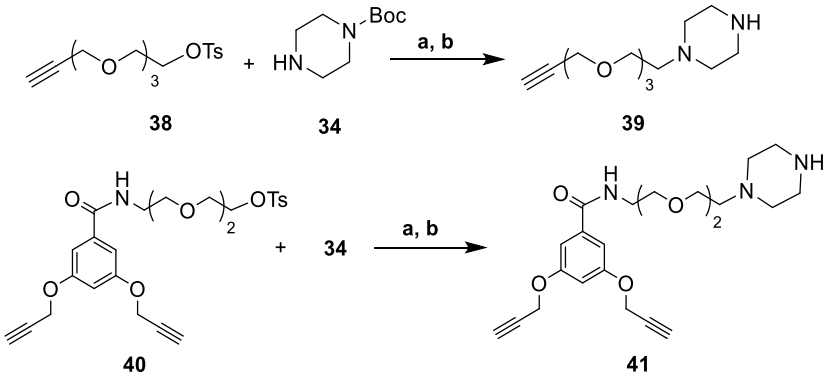

[a]Reagents and conditions: **a**) Cs_2CO_3, ACN dry, N_2, 60 °C, 18h - 3 days, 67-75% yield; **b**) TFA/DCM 1.7:10, rt, 1 h, quant. yield.

The synthesis of the 2-chloro-*N*-methyl-*N*-(4-nitrophenyl)acetamide **44** (Scheme 5) started with the acylation of *p*-nitroaniline **42** with 2-chloroacetic pivalic anhydride, generated by previous activation of chloroacetic acid **43** with pivaloyl chloride. The resulting 2-chloro-*N*-(4-nitrophenyl)acetamide was then methylated with Me_2SO_4, generating the 2-chloro-*N*-methyl-*N*-(4-nitrophenyl)acetamide **44** in a 76% yield.

Piperazines **37**, **39** and **41** were subjected to a nucleophilic substitution with 2-chloroacetamide **44** in presence of K_2CO_3, providing three nitro-compounds **45**-**47** in acceptable yields. In the case of compound **46**, it was important that the conversion was complete, since the starting material **39** and the product **46** resulted inseparable both by direct and reverse phase flash chromatography, probably due to the influence of the three-polyethylene glycol chain.

Finally, the nitro-group within **45**-**47** was selectively reduced with zinc and ammonium chloride to give the three aniline derivatives **48**-**50** in moderate to good yields, which were used in the subsequent nucleophilic addition with the oxindole nucleus.

Scheme 5. *Synthesis of aniline derivatives* ***48-50****.*[a]

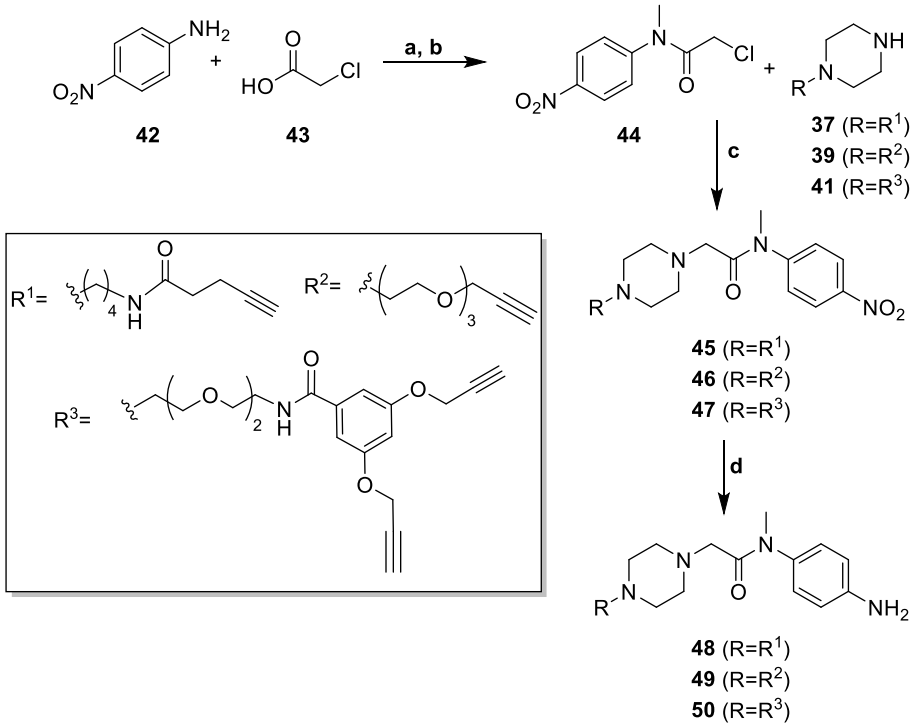

[a]Reagents and conditions: **a**) pivaloyl chloride, DCM dry, N_2, from 0 °C to rt, 5h, 58% yield; **b**) K_2CO_3, Me_2SO_4, acetone, 60 °C, 16h, 69% yield; **c**) K_2CO_3, acetone, rt, 16-35h, 57-73% yield; **d**) Zn, NH_4Cl, 10% water in MeOH, 70 °C, 5-7 h, 65-91% yield.

4.3.4. Synthesis of the oxindole nucleus and Claisen-type reaction

The oxindole nucleus **57** (Scheme 6) was synthesized with a few modifications compared to a reported procedure.[16] A nucleophilic addition between methyl 3-nitrobenzoate **51** and methyl 2-chloroacetate **52** was performed in presence of potassium *tert*-butoxide, leading to a mixture of regioisomers **53** and **53a** in ratio 90:10, which were inseparable by flash chromatography and were used as a mixture in the following reaction.

The reduction of the nitro group was performed by H_2 and Pd/C and, in these conditions, the amino compound derived from the reduction of **53** spontaneously cyclized to give the 2-oxindole **54** with 71% yield, which was easily separated from the by-product **54a**. The optimization of the reaction required a careful selection of the solvent mixture. Acetic acid was necessary for the formation of the cyclized product **54** and, after several attempts, the highest yield of the desired product was obtained with the DCM/AcOH 5:10 mixture. Then, the nitrogen atom of oxindole **54** was protected with acetic anhydride, resulting in the *N*-acetyl-2-oxindole **55**, that was purified by crystallization in methanol. All the attempts to purify the crude by flash chromatography were unsuccessful; in fact, mixtures of undefined by-products were collected, given by the degradation of **55** on silica. Then, compound **55** was reacted in a Claisen-type reaction with the trymethylorthobenzoate **56**, giving the oxindole nucleus **57** as a single stereoisomer in 83% yield. Finally, the stereospecific conjugated nucleophilic addition of anilines **48**-**50** to oxindole **57** consigned the three different linker-nintedanib nuclei **58**-**60** in moderate to good yields as single stereoisomers, which were used in the following click reactions.

Scheme 6. *Synthesis of the oxindole nucleus* ***57*** *and the linker-nintedanib nuclei* ***58-60****.*[a]

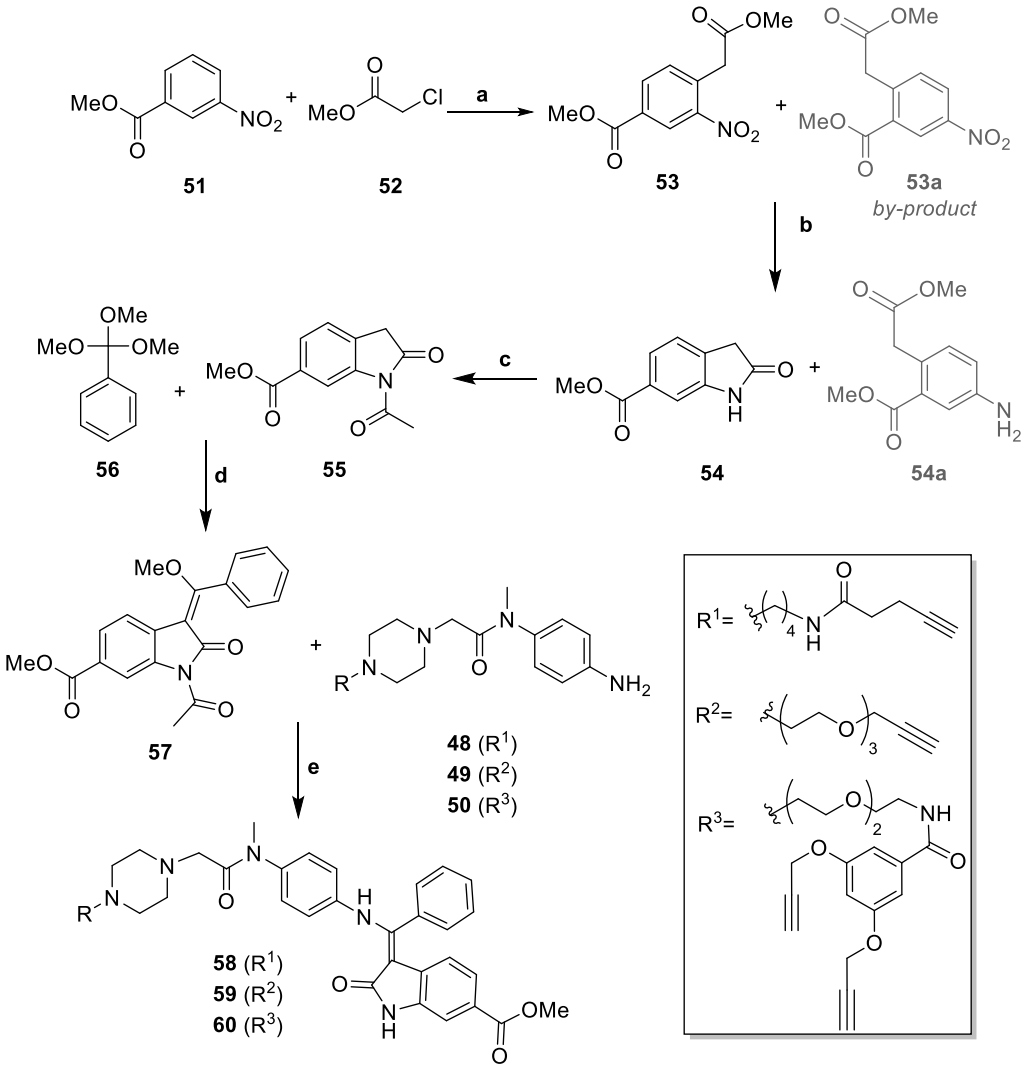

[a]Reagents and conditions: **a**) *t*BuOK, DMF, 0 °C, rt, 10 min, 50% yield; **b**) Pd/C, H_2, DCM/AcOH 5:10, rt, 16h, 71% yield; **c**) Ac_2O, toluene, 120 °C, 6h, 71% yield; **d**) Ac_2O, 120 °C, 4.5 h, 83% yield; **e**) DMF, 80°C, then piperidine, 24 h, 53-71% yield.

4.3.5. Final click reaction and deprotection

Alkyne-terminating compounds **58-60** were individually linked to the azide terminal of cyclic peptidomimetics **21-23** by copper-catalyzed click reactions (Scheme 7). All the protected intermediates were not purified by flash chromatography; the crude mixtures resulting from the click reactions were accurately washed with water to remove the excess of salts, and then subjected to the final deprotection step in acidic conditions, providing the final conjugates **7**-**15**. The combined yields for the two-step click-reaction/deprotection sequence proved moderate to very good, comprised in the range 46-93%.

The nine final covalent conjugates were purified by reverse-phase preparative HPLC and fully characterized by NMR and HRMS techniques.

Compounds **7**-**15** are currently under biological evaluation (in collaboration with Prof. Francesca Bianchini, University of Florence) and the preliminary results of these studies are shown in the following chapter.

Scheme 7. *Final click reaction and deprotection steps for the synthesis of the covalent conjugates* ***7-15****.*[a]

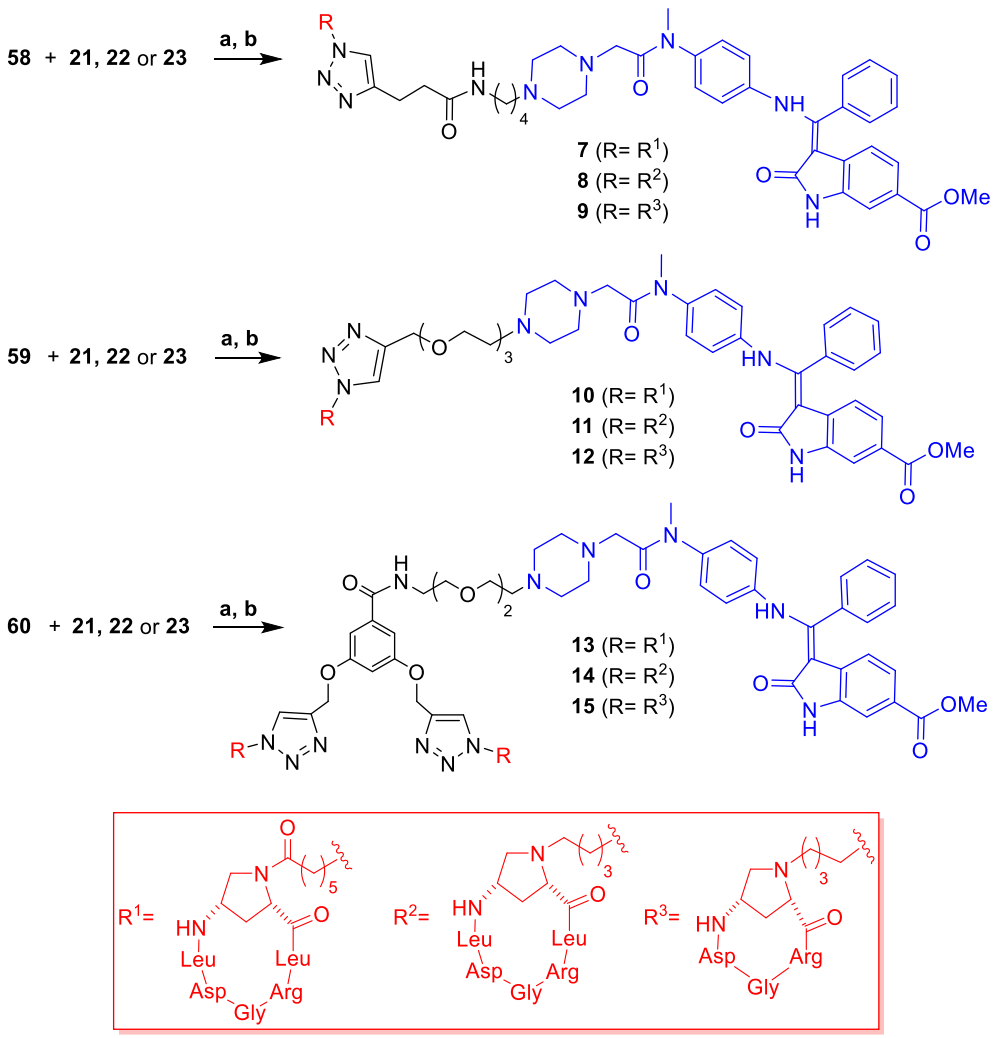

[a]Reagents and conditions: **a**) $Cu(OAc)_2$, sodium ascorbate, DMF/H_2O 3:7, rt, 12-16 h; **b**) TFA/TIS/H_2O 95:2.5:2.5, rt, 1 h; 46-93% (2 steps).

4.3.6. Preliminary biological evaluation

The final covalent conjugates **7**-**15**, together with cyclopeptide ligands **16**-**18** and nintedanib used as reference compounds, are currently under biological investigations towards non-small cell lung cancer cell line A549 (nintedanib has been largely studied towards this cell line),[17] and some preliminary results for the compound series **7**, **10** and **13** are here reported.

Determination of $\alpha_V\beta_6$ integrin expression on A549 cells revealed the presence of this receptor at low density. However, when these cells were grown for 48 hours in the presence of rhTGFβ1 (10ng/ml), the expression of this integrin was sensibly higher. Comparison of the biological activity of the conjugates on A549 cells grown either in the absence or in the presence of TGFβ could therefore give useful indications on the role of $\alpha_V\beta_6$ integrin.

First of all, the inhibition cell adhesion assay to fibronectin (FN), an $\alpha_V\beta_6$ integrin natural ligand, was performed, to study the ability of these compounds to bind $\alpha_V\beta_6$ integrin on the A549 cell surface. The assay was carried out with increasing concentrations of compounds **7**, **10**, **13** and cyclic peptidomimetic **17** (0.5, 1 and 5 μM). As shown in Figure 10 (up), all compounds inhibited cell adhesion in a dose-related manner. The best inhibition percentage was registered with compounds

10 and **7**, that even at 1 µM were able to give more than 50% of adhesion inhibition of the A549 cells previously exposed to TGFβ; on the other hand, quite surprisingly, dimeric conjugate **13** definitely proved the worst ligand of the series, showing that the two integrin ligands in the same molecule not only are not able to bind two receptors contemporarily, but they likely interfere each other during the binding event. The highest values observed with the cells previously exposed to TGFβ confirmed that the inhibition was primarily given by the interaction of the tested compounds with the integrin $\alpha_V\beta_6$, whose concentration significantly increased in comparison to standard A549 cells.

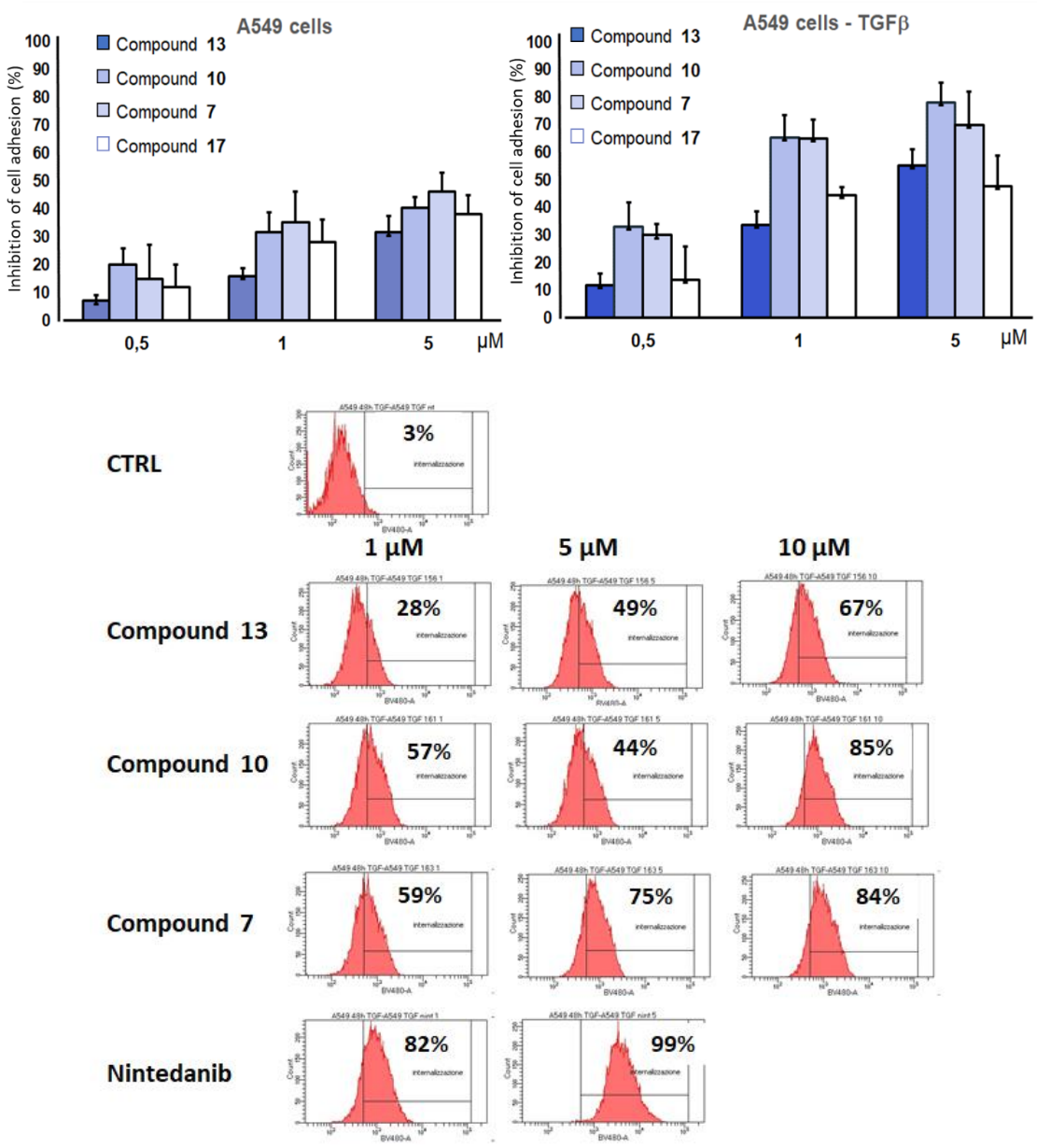

Figure 10. Up, inhibition of A549 cell adhesion to FN in the presence of compounds **7**, **10** and **13**, or c(AmpLRGDL) **17** (2 h). On the left, A549 cells were grown in standard conditions, on the right cells were previously exposed for 48h to TGFβ (10ng/ml). The inhibitory activity was calculated as percentage of cell adhesion to FN in untreated cells and was expressed as means ± SEM. Bottom, fluorescence intensity (FacScan FLT1/BV407ex480em-A) in A549/TGFβ pre-treated cells exposed for 24 h to nintedanib or conjugates **7**, **10** and **13**, at different concentrations (1-10 µM). Percentage intervals indicate fluorescence(BV480-A)-positive cells from three independent experiments.

Also, similarity of the binding competence between monomeric ligands **7** and **10** would point to a similar impact of the amide *vs* PEG linker on binding ability, while the increased binding observed for dual conjugates **7** and **10** vis-à-vis the unconjugated counterpart **17** would indicate a somehow beneficial contribution of the overall construct upon binding to the integrin target.

The cell internalization of nintedanib and the three conjugates **7**, **10** and **13** was investigated by flow cytometry measurements (Figure 10, bottom), taking advantage of the intrinsic fluorescence of the nintedanib moiety. Non-treated (data not shown) and TGFβ pre-treated A549 cells were incubated for 24 h with nintedanib or conjugates **7**, **10** and **13** at different concentrations (1, 5 and 10 μM). Nintedanib was well internalized into the cells already at 1 μM, and better than any other conjugate. The uptake percentage of the conjugates increased when the cells were pre-treated with TGF, indicating a seemingly active role of the $\alpha_V\beta_6$ integrin in the internalization process. Interestingly, compound **7** was in any case better internalized than compounds **10** and **13**, in particular at 5 μM. This reflects the binding ability of this compound with the integrin, measured with the inhibition cell adhesion assay, with a possible favourable impact of the amide linker.

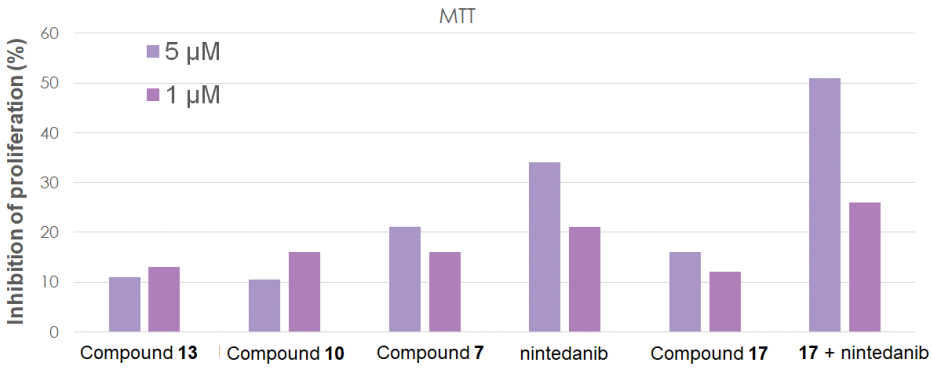

Figure 11. MTT assay of A549/TGFβ pre-treated cells grown in the presence of conjugates **7**, **10** and **13**, ligand **17**, nintedanib, or the combination **17** + nintedanib, at 1 or 5 μM.

The inhibition of cell proliferation was tested by MTT assay, a colorimetric assay for assessing cell metabolic activity (Figure 11). These results confirmed compound **7** to be the most effective of the three conjugates in inhibiting cell proliferation, but it was not as good as nintedanib alone. However, a clear increase of the inhibition was observed when nintedanib was administered in combination with the integrin ligand **17**, pointing to the notion that the combined use of a tyrosine kinase inhibitor and an $\alpha_V\beta_6$ integrin ligand may lead to a potentiated and combined antagonizing activity of these receptors and/or their cross-talk, resulting in a good strategy for a potentiated biological activity. The explanation why the combination of the two active ingredients perform better than the covalent conjugates remains unclear at this stage, and further in-depth studies will be carried out to clarify this point.

4.4. Conclusions and perspectives

Substantial evidences in the literature show that the crosstalk between integrins and Growth Factor Receptors seems to determine drug resistance and sustain the Epithelial-To-Mesenchymal Transition process (EMT). In this chapter, the rational design and the synthesis of nine different covalent conjugates **7**-**15**, embedding both $\alpha_V\beta_6/\alpha_V\beta_3$ integrin ligands and the TKI nintedanib connected by three different types of linkers, have been described. Preliminary in vitro assays in TGFβ-treated A549 cells, in collaboration with Dr. Bianchini at the University of Florence, were carried out for the three conjugate **7**, **10** and **13**. The initial results suggested that conjugates **7** and **10** can inhibit cell adhesion to fibronectin; in addition, conjugate **7** showed good cell internalization and antiproliferative activity even at 1 μM concentration. Interestingly, a clear increase of the proliferation inhibition was observed when the nintedanib was administered in combination with the integrin ligand **17**, confirming that antagonizing both kinase receptors and $\alpha_V\beta_6$ integrin could be a good strategy for the treatment of cancer related diseases, opening the road to innovative treatment for both cancer- and fibrosis-related diseases.

In perspective, the evaluation of biological activity of the whole panel of the synthesized compounds will be useful to verify whether and to what extent the simultaneous antagonism of both TK and α_V integrins will be effective by either the covalent conjugates in this work, the simple combination of the two active units, or next-generation covalent conjugates characterized by scissile linkers.

4.5. Experimental section

4.5.1. General methods and materials

General. See Chapter 2, Paragraph 2.5.2.1.

Materials. H-Gly-2-ClTrt resin, Fmoc-Asp(*t*Bu)-OH; Fmoc-Arg(Pmc)-OH, Fmoc-Leu-OH, 2,4,6-collidine, glacial acetic acid, DIPEA, HATU, HOAt, 4-azidobutanol, 3-aminopropanol were commercially available and were used as such without further purification. N^{α}-(4-azidobutyl)-4-*N*-(Fmoc)aminoproline (**19**), N^{α}-(6-azidohexanoyl)-4-*N*-(Fmoc)aminoproline (**20**), tosyl derivatives **38** and **40** were prepared according to reported procedures.[4,15]

General method for HPLC purification. The final conjugates were purified by reverse phase HPLC (column A, *see general*), with the solvent system H_2O + 0.1% TFA (Solvent A) and ACN (solvent B), using the following method: flow rate 8.0 mL/min; detection at 220 nm, linear gradient from 5% B to 50% B over 23 min, 50% B for 3 min, from 50% B to 5% B over 3 min, room temperature.

Experimental synthetic procedures and characterization data

Synthesis of cyclic peptidomimetic 23

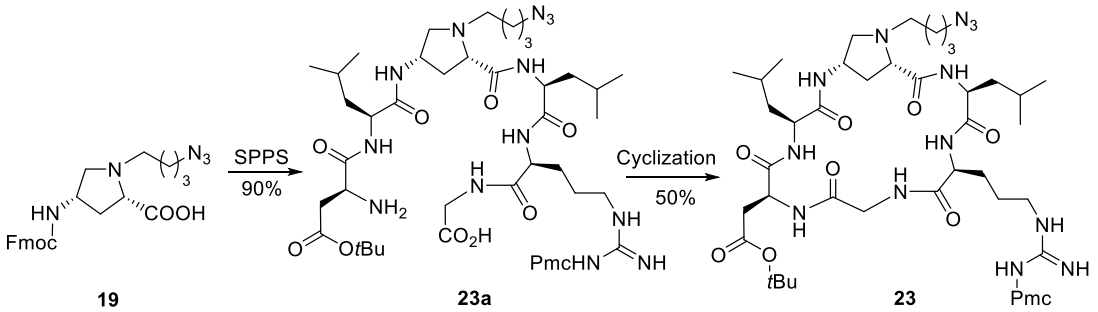

Cyclopeptide **23** was prepared according to the general procedure described in Chapter 2 (Paragraph 2.5.2.1.) for compound **11** by using the aminoproline nucleus **19**. The linear pentapeptide **23a**, precursor of compound **24**, was prepared according to the general SPPS procedure described for linear tetrapeptide **V** (Chapter 2, Paragraph 2.5.2.1.) by using 2-chlorotrityl-Gly-H resin (350.0 mg, 0.203 mmol, 1.0 eq), Fmoc-Arg(Pmc)-OH (188.7 mg, 0.305 mmol, 1.5 eq), Fmoc-Leu-OH (107.8 mg, 0.305 mmol, 1.5 eq), the aminoproline nucleus **19** (137.1 mg, 0.305 mmol, 1.5 eq) and Fmoc-Asp(*t*Bu)-OH (125.5 mg, 0.305 mmol, 1.5 eq). After the resin cleavage, compound **23a** (212 mg, AcOH salt, 90% yield) was recovered as a colourless glassy solid and was used in the following step without further purification (MS (ES^+) *m/z* 1104.7 $[M+H]^+$). The protected cyclopeptide **23** was prepared starting from **23a** (212 mg, 0.0182 mmol, 1 eq) according to the cyclization general procedure describe in Chapter 2 (Paragraph 2.5.2.1.) was obtained as a glassy solid (115.0 mg, TFA salt 50% yield). TLC: EtOAc:MeOH 70:30, R*f* = 0.7. ^{1}H NMR (400 MHz, MeOD): δ 4.71 (m, 1H, H4Amp), 4.48 (m, 3H, αAsp+αLeu), 4.44-4.22 (m, 3H, αArg+H2+αGly), 3.75 (bd, *J* = 16.9 Hz, 1H, αGly), 3.58 (m, 2H, H5Amp), 3,38 (m, 2H, H1'Amp), 3.29-3.12 (m, 4H, H4'+δArg), 2.95 (m, 1H, H3Amp), 2.81 (m, 2H, βAsp), 2.69 (t, *J* = 6.8 Hz, 2H, CH_2 Pmc), 2.59 (s, 3H, CH_3Pmc), 2.58 (s, 3H, CH_3Pmc), 2.13 (m, 3H, CH_3Pmc+H3bAmp), 1.86 (t, *J* = 6.8 Hz, 2H, CH_2Pmc), 1.77-1.59 (m, 12H, βArg+γArg+ γLeu+βLeu+H2'Amp), 1.55 (m, 2H, H3'Amp), 1.47 (s, 9H, *t*Bu), 1.33 (s, 6H, CH_3 Pmc), 0.96 (m, 12H, δLeu). MS (ES^+) *m/z* 1086.7 $[M+H]^+$.

Synthesis of 4-azidobutyl 4-methylbenzenesulfonate 33

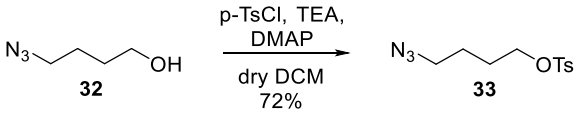

To a solution of 4-azidobutanol **32** (420.0 mg, 3.65 mmol, 1 eq) in dry DCM (10 mL), *p*-TsCl (834.1 mg, 4.38 mmol, 1.2 eq), DMAP (121.0 mg, 0.99 mmol, 0.3 eq) and TEA (509 μL, 4.38 mmol, 1.2 eq) were added. The reaction was kept under stirring for 22 h, then HCl 0.1N (10 mL) was added and the mixture was extracted with DCM (3x). The combined organic layers were dried with $MgSO_4$ and the crude was purified with flash chromatography (Eluent 9:1 DCM:Petroleum Ether), giving compound **33** as a transparent oil (707.0 mg, 72% yield). TLC: Petroleum Ether:EtOAc 70:30, R*f* = 0.8. ^{1}H NMR (400 MHz, $CDCl_3$) 7.81 (d, *J* = 8.5 Hz, 2H, ArH), 7.37 (d, *J* = 8.5 Hz, 2H, ArH), 4.08 (t, *J* = 6.5 Hz, 2H, CH_2), 3.28 (t, *J* = 6.5 Hz, 2H, CH_2), 2.48 (s, 3H, CH_3), 1.59 (m, 2H, CH_2), 1.65 (m, 2H, CH_2). ^{13}C NMR (101 MHz, $CDCl_3$) δ 145.1 (1C, Cq), 133.2 (1C, Cq), 130.1 (2C, CH), 128.1 (2C, CH), 69.9 (1C, CH_2), 50.9 (1C, CH_2), 26.3 (1C, CH_2), 25.2 (1C, CH_2), 21.9 (1C, CH_3). MS (ES^+) *m/z* 270.1 $[M+H]^+$.

Synthesis of 1-Boc-(4-azidobutyl)piperazine 35

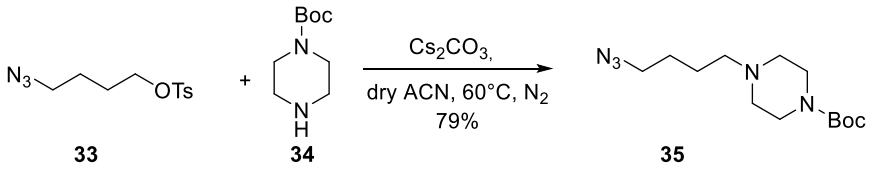

To a solution of compound **33** (113.0 mg, 0.42 mmol, 1 eq) in dry ACN (2 mL) at 60°C, Cs_2CO_3 (163.9 mg, 0.50 mmol, 1.2 eq) and Boc-piperazine **34** (93.8 mg, 0.50 mmol, 1.2 eq) were added. The reaction was kept under stirring for 3 days (adding 2 mL of dry ACN when the solvent was evaporated), then the solvent was removed under reduced pressure. Water (10 mL) was added to the crude and extracted with EtOAc (3x). The combined organic layers were evaporated, and the crude purified with a flash chromatography (eluent: from 100% DCM to 40:60 DCM:EtOAc), giving final compound **35** as a yellowish liquid (94.2 mg, 79% yield). TLC: Petroleum Ether:EtOAc 50:50, R*f* = 0.4. ^{1}H NMR (600 MHz, $CDCl_3$) δ 3.35 (t, *J* = 5.0 Hz, 4H, CH_2NBoc), 3.37 (t, *J* = 6.7 Hz, 2H, CH_2-N_3), 2.29 (m, 6H, CH_2N piperazine), 1.69-1.59 (m, 2H, CH_2CH_2-N_3), 1.52-1.47 (m, 2H, $CH_2CH_2CH_2$-N_3), 1.38 (s, 9H, CH_3 Boc). MS (ES^+) *m/z* 284.2 $[M+H]^+$.

Synthesis of 1-Boc-(4-aminobutyl)piperazine 36

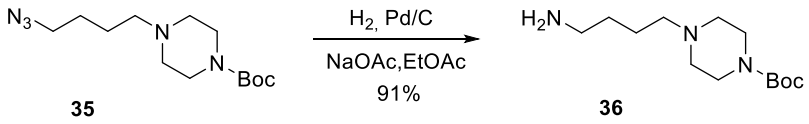

To a solution of azide **35** (240.0 mg, 0.846 mmol, 1 eq) in EtOAc (50 mL), 10 mmol% of sodium acetate and palladium on carbon were added and the reaction was kept stirring under hydrogen atmosphere. After 4 h the reaction mixture was filtered to give amine **36** as a colourless oil (217.9 mg, 91% yield). TLC: Petroleum Ether:EtOAc 50:50 R*f* = 0.05. ^{1}H NMR (600 MHz, $CDCl_3$) δ 3.42 (bt, *J* = 4.8 Hz, 4H, CH_2NBoc), 2.70 (t, *J* = 7.0 Hz, 2H, CH_2NH_2), 2.38-2.32 (m, 6H, CH_2N piperazine), 1.54-1.43 (m, 13H, $CH_2CH_2CH_2$-NH_2+ CH_2CH_2-NH_2+CH_3Boc). ^{13}C NMR (150 MHz, $CDCl_3$) δ 154.9 (1C, Cq), 79.7 (1C, CH), 58.7 (2C, CH_2), 53.2 (1C, CH_2), 43.4 (1C, CH_2), 42.2 (2C, CH_2), 31.8 (3C, CH_3), 28.6 (1C, CH_2), 24.4 (1C, CH_2). MS (ES^+) *m/z* 258.3 $[M+H]^+$.

Synthesis of substituted Boc-piperazine 37a

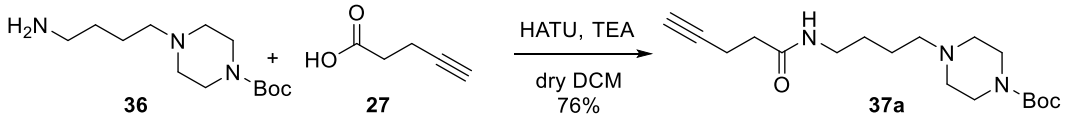

To a solution of amine **36** (199.0 mg, 0.733 mmol, 1.0 eq), 4-pentynoic acid **27** (83.4 mg, 0.85 mmol, 1.1 eq), HATU (323.2 mg, 0.85 mmol, 1.1 eq) in dry DCM (50 mL), NEt_3 was added (237.3 μL, 1.701 mmol, 2.2 eq). The reaction was kept stirring under nitrogen atmosphere. After 3 hours the reaction was quenched by adding $NaHCO_3$ saturated solution (pH = 9) and then extraction with DCM (3x) was performed. The crude was purified by flash chromatography (eluent: 80:20 EtOAc:MeOH), giving compound **37a** as a glassy solid (199.2 mg, 76% yield). TLC: EtOAc:MeOH 80:20 R*f* = 0.6. ^{1}H NMR (600 MHz, $CDCl_3$) δ 6.06 (bs, 1H, NH), 3.42 (bt, *J* = 5.1 Hz, 4H, CH_2-NBoc), 3.27 (m, 2H, OCN-CH_2), 2.51 (td, *J* = 7.2, 2.7 Hz, 2H, Alkyne-CH_2), 2-38-2.34 (m, 8H, CH_2) 1.98 (t, *J* = 2.7 Hz, 1H, CH alkyne), 1.67 (m, 4H, CH_2 piperazine), 1.53 (m, 4H, CH_2), 1.44 (s, 9H, CH_3 Boc). MS (ES^+) *m/z* 338.3 $[M+H]^+$.

Synthesis of substituted piperazine 37

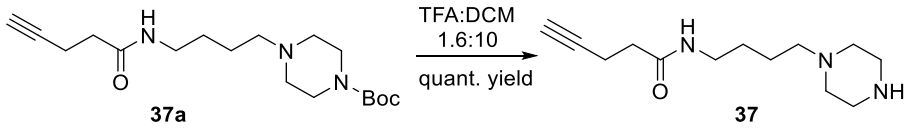

Amine **37** was obtained by deprotection of the corresponding Boc-protected amine **37a** (225.0 mg, 0.874 mmol, 1 eq) using a solution of TFA:DCM 1.6:10 (2.95 mL). The reaction was kept under stirring for 1 h and then quenched by removing of the solvent under reduced pressure. The crude was washed with Et_2O (3x), yielding compound **37** (as double TFA salt) as a yellowish oil (409.0 mg, quantitative yield). ^{1}H NMR (400 MHz, MeOD) δ 3.33-3.25 (m, 4H, CH_2), 2.83 (s, 4H, CH_2), 2.51-2.46 (m, 4H, CH_2), 2.43-2.39 (m, 4H, CH_2), 2.28 (m, 1H, CH alkyne), 1.85-1.79 (m, 4H, CH_2). ^{13}C NMR (101 MHz, MeOD) δ 173.2 (1C, Cq), 82.3 (1C, Cq), 69.2 (1C, CH), 56.5 (2C, CH_2), 40.7 (2C, CH_2), 37.8 (1C, CH2), 37.7 (1C, CH_2), 34.7 (1C, CH_2), 26.2 (1C, CH_2), 19.6 (1C, CH_2), 13.2 (1C, CH_2). MS (ES^+) *m/z* 238.2 $[M+H]^+$.

Synthesis of substituted Boc-piperazine 39a

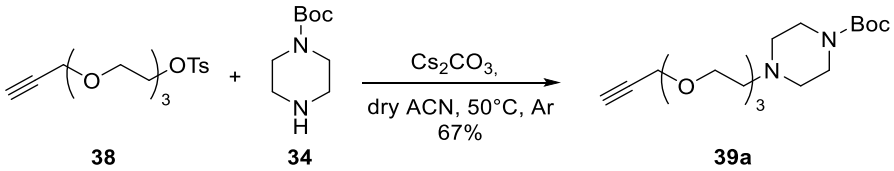

To a round bottom flask containing compound **38** (125.0 mg, 0.37 mmol, 1 eq) in 1 mL of ACN dry, Boc-piperazine **34** (81.6 mg, 0.44 mmol, 1.2 eq) and Cs_2CO_3 (142.7 mg, 0.44 mmol, 1.2 eq) were added. The mixture was left to stir under argon atmosphere at 50 °C for two days. The reaction was quenched by removing the solvent under reduced pressure. Water (10 mL) was added and then extracted with DCM (3x). The crude was purified by flash chromatography (eluent: 95:5 EtOAc:MeOH•NH_3) giving compound **39a** as a yellowish glassy solid (87.7 mg, 67% yield). TLC: EtOAc: MeOH•NH_3 90:10 R*f* = 0.6. ^{1}H NMR (400 MHz, $CDCl_3$) *δ* 4.16 (d, *J* = 2.4 Hz, 2H, CH_2-alkyne), 3.67-3.57 (m, 10H, CH_2), 3.39 (t, *J* = 4.7 Hz, 4H, CH_2NBoc), 2.56 (t, *J* = 5.8 Hz, 2H, OCH_2CH_2N), 2.41 (m, 5H, NCH_2 piperazine + CH alkyne), 1.41 (s, 9H, CH_3 Boc). ^{13}C NMR (100 MHz, $CDCl_3$): *δ* 154.7 (Cq),

79.8 (Cq), 79.7 (Cq), 74.7 (1C, CH), 70.8 (1C, CH_2), 70.6 (1C, CH_2), 70.5 (1C, CH_2), 69.2 (1C, CH_2), 69.0 (1C, CH_2), 58.5 (1C, CH_2), 57.9 (2C, CH_2), 53.5 (2C, CH_2), 28.6 (1C, CH_3). MS (ES^+) *m/z* 357.3 $[M+H]^+$.

Synthesis of substituted piperazine 39

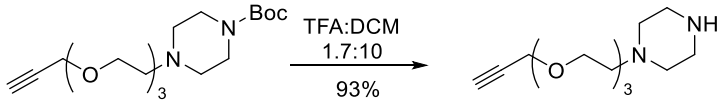

39a **39**

Compound **39a** (169.0 mg, 0.47 mmol, 1 eq) was deprotected as described for compound **37**, using 9 mL of solution of TFA:DCM, to give piperazine **39** as a glassy solid (214.3 mg, 93% yield). ^{1}H NMR (600 MHz, MeOD) δ 4.16 (d, *J* = 2.5 Hz, 2H, alkyne-CH_2), 3.86 (t, *J* = 4.9 Hz, 2H, CH_2), 3.69-3.61 (m, 12H, CH_2), 3.59 (bt, *J* = 5.6 Hz, 2H, CH_2NH), 3.47 (t, *J* = 4.9 Hz, 2H, OCH_2CH_2N), 2.83 (t, *J* = 2.5 Hz, 1H, CH). ^{13}C NMR (151 MHz, $CDCl_3$): δ 79.2 (1C, Cq), 74.8 (1C, CH), 69.9 (1C, CH_2), 69.9 (1C, CH_2), 68.8 (1C, CH_2), 64.0 (1C, CH_2), 57.7 (2C, CH_2), 56.3 (1C, CH_2), 48.7 (2C, CH_2), 40.5 (1C, CH_2). MS (ES^+) *m/z* 257.2 $[M+H]^+$.

Synthesis of substituted Boc-piperazine 41a

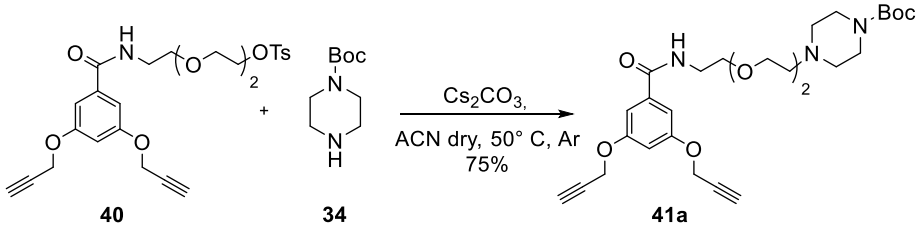

40 **34** **41a**

Compound **41a** was synthesized as described for compound **39a**, starting from tosyl derivative **40** (150.0 mg, 0.29 mmol, 1 eq) and Boc-piperazine **34** (65.2 mg, 0.35 mmol, 1.2 eq). The reaction was left to stir at 50 °C under argon for three days. The solvent was evaporated, water was added (10 mL) and extracted with DCM (3x) The organic layers were collected and concentrated under vacuum, affording a crude residue which was purified by flash chromatography (eluent: EtOAc:MeOH•NH_3 99.2:0.8) to give **41a** (105.2 mg, 75% yield) as a yellowish oil. TLC: EtOAc:MeOH•NH_3 93:7. R*f*= 0.5. ^{1}H NMR (400 MHz, $CDCl_3$) δ 7.07 (bd, *J* = 2.2 Hz, 2H, ArH), 6.74 (t, *J* = 2.2 Hz, 1H, ArH), 4.71 (d, *J* = 2.4 Hz, 4H, $ArOCH_2$), 3.72–3.58 (bm, 12H, OCH_2), 2.57 (m, 4H, CH_2 piperazine), 2.62-2.55 (m, 4H, $OCNCH_2$+CH alkyne), 2.42 (bs, 4H, CH_2 piperazine), 1.46 (s, 9H, CH_3Boc). MS (ES^+) *m/z* 530.3 $[M+H]^+$.

Synthesis of substituted piperazine 41

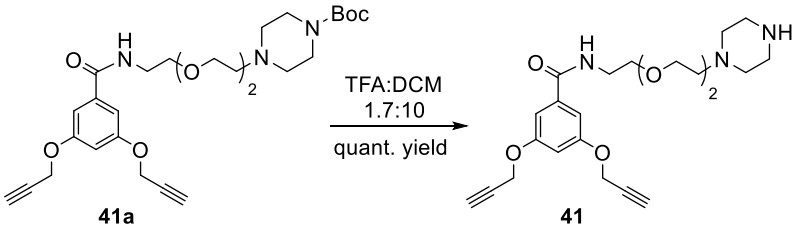

41a **41**

Compound **41a** (89.3 mg, 0.169 mmol, 1.0 eq) was deprotected as described for compound **37**, using 3.5 mL of solution of TFA:DCM, to give piperazine **41** as a glassy solid (91.7 mg, quantitative yield). ^{1}H NMR (400 MHz, $CDCl_3$) δ 7.09 (d, *J* = 2.3 Hz, 2H, ArH), 6.84 (t, *J* = 2.3 Hz, 1H, ArH), 4.80 (d,

J = 2.5 Hz, 4H, $ArOCH_2$), 3.85 (m, 2H, CH_2), 3.70–3.66 (m, 6H, CH_2 piperazine + CH_2), 2.58 (m, 10H, CH_2 piperazine + CH_2), 3.38 (m, 2H, CH_2), 3.02 (t, *J* = 2.5 Hz, 2H, CH alkyne). MS (ES^+) *m/z* 430.3 $[M+H]^+$.

Synthesis of 2-chloro-*N*-(4-nitrophenyl)acetamide 44a

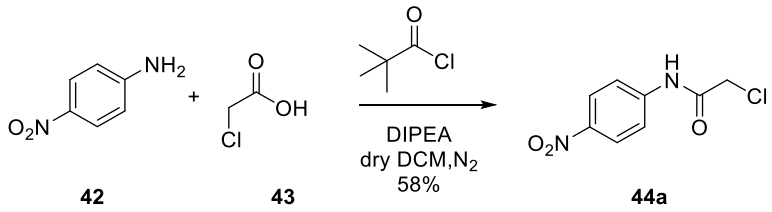

To a solution of 2-chloroacetic acid **43** (1.03 g, 7.38 mmol, 1.7 eq) in dry DCM (10 mL), DIPEA (1.53 mL, 8.69 mmol, 2.0 eq) was added at 0 °C. The mixture was left to stir at 0 °C for 10 min, then pivaloyl chloride (802.00 μL, 6.52 mmol, 1.5 eq) was added dropwise. The reaction was left to stir at room temperature for 1 h, then 4-nitroaniline **42** (600.00 mg, 4.34 mmol, 1.0 eq) was added. After 4 h the solvent was removed under reduced pressure. Then, water (10 mL) was added to the crude and extracted with EtOAc (3x), then dried with $MgSO_4$ and filtered. The solvent was evaporated, and the residue purified by flash chromatography (eluent: 100% DCM), giving compound **44a** (644.30 mg, yield 58%). TLC: 100% DCM, R*f* = 0.3. ^{1}H NMR (400 MHz, $CDCl_3$) δ 8.28 (m, 2H, ArH), 7.79 (m, 2H, ArH), 4.28 (s, 2H, CH_2). MS (ES^+) *m/z* 215.0 $[M+H]^+$.

Synthesis of 2-chloro-*N*-methyl-*N*-(4-nitrophenyl)acetamide 44

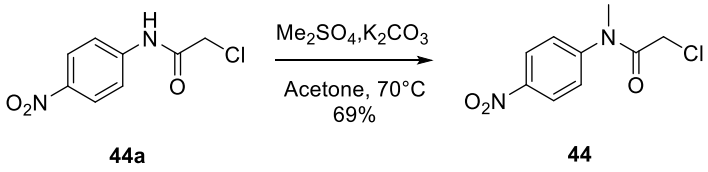

To a solution of compound **44a** (380.2 mg, 1.77 mmol, 1.0 eq.) in acetone (25 mL), K_2CO_3 (406.0 mg, 2.93 mmol, 1.7 eq) was added and the reaction was left to stir at room temperature for 10 min. Then, Me_2SO_4 (278.1 μL, 2.93 mmol, 1.7 eq) was added and stirred at 70 °C for 30 h. During the night the reaction was stirred at room temperature. After completion the reaction was quenched with saturated solution of NH_4Cl and HCl 10% until pH=3, then extracted with EtOAc (3x). The combined organic layers were dried with $MgSO_4$, filtered and the solvent removed under reduced pressure. The crude was purified by flash chromatography (eluent: 50:45:5 Petroleum Ether:DCM:EtOAc), giving compound **44** as light-yellow solid (450.0 mg, yield 69%). TLC: 100% DCM, R*f* = 0.4. ^{1}H NMR (300 MHz, $CDCl_3$) δ 8.33 (m, 2H, ArH), 7.50 (m, 2H, ArH), 3.96 (s, 2H, CH_2), 3.41 (s, 3H, CH_3). MS (ES^+) *m/z* 229.1 $[M+H]^+$.

Synthesis of nitro-derivative 45

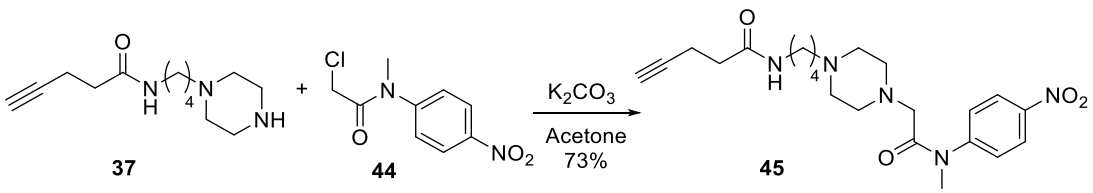

To a solution of amine **37** (409.1 mg, 0.871 mmol, 1.0 eq) and compound **44** (258.7 mg, 1.132 mmol, 1.3 eq) in acetone (20 mL), K_2CO_3 (481.3 mg, 3.482 mmol, 4 eq) was added. The reaction was left under stirring for 22 h, then the solvent was removed under reduced pressure and the residue was dissolved in DCM and filtered by cotton. The crude was purified by flash chromatography (gradient: from 100% EtOAc to 8:2 EtOAc:MeOH•NH_3) giving compound **45** as a yellowish oil (271.4 mg, 73% yield). TLC: 9:1 EtOAc:MeOH•NH_3, R*f* = 0.6. ^{1}H NMR (400 MHz, MeOD) δ 8.29 (m, 2H, ArH), 7.46 (m, 2H, ArH), 6.23 (m, 1H, NH), 3.37 (s, 3H, CH_3), 3.27 (m, 2H, OCN-CH_2), 3.08 (s, 2H, NCH_2CON), 2.57-2.34 (m, 14 H, Alkyne-CH_2 + 4CH_2 piperazine + CH_2-N-Piperazine+CH_2CON), 1.99 (t, *J* = 2.8 Hz, 1H, CH Alkyne), 1.57-1.52 (m, 4H, CH_2) ^{13}C NMR (101 MHz, MeOD) δ 169.3 (1C, Cq), 149.7 (1C, Cq), 127.4 (2C, CH), 125.2 (1C, Cq), 124.9 (2C, CH), 119.0 (1C, Cq), 83.3 (1C, Cq), 69.4 (1C, CH), 60.6 (2C, CH_2), 57.9 (2C, CH_2), 53.0 (1C, CH_2), 39.3 (2C, CH_2), 37.6 (1C, CH2), 35.6 (1C, CH_3), 27.6 (1C, CH_2), 24.3 (1C, CH_2), 15.1 (1C, CH_2). MS (ES$^+$) *m/z* 430.3 $[M+H]^+$.

Synthesis of nitro-derivative 46

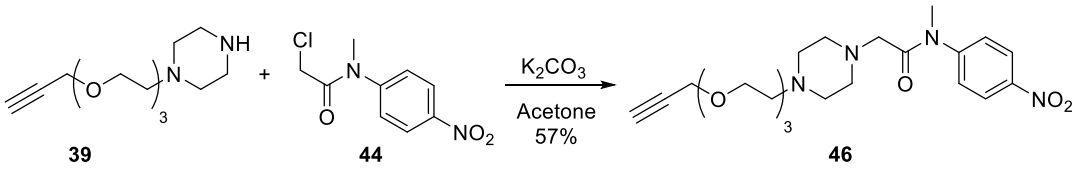

Compound **46** was obtained as described for compound **45**, using amine **39** (214.3 mg, 0.44 mmol, 1.0 eq) and compound **44** (131.3 mg, 0.57 mmol, 1.3 eq). The crude was purified by flash chromatography (gradient: from 100% EtOAc to 9:1 EtOAc:MeOH•NH_3) giving compound **46** as a yellowish oil (113.9 mg, 57% yield). TLC: 9:1 EtOAc:MeOH•NH_3, R*f* = 0.8. ^{1}H NMR (400 MHz, MeOD) *δ* 8.28 (m, 2H, ArH), 7.46 (m, 2H, ArH), 4.21 (d, *J* = 2.5 Hz, 2H, Alkyne-CH_2), 3.72-3.58 (m, 12H, CH_2), 3.37 (s, 3H, CH_3), 3.06 (s, 2H, NCH_2CON), 2.57 (t, *J* = 5.7 Hz, 2H, CH_2), 2.48 (m, 6H, CH_2), 2.45 (t, *J* = 2.5 Hz, 1H, CH alkyne). ^{13}C NMR (100 MHz, $CDCl_3$): 169.4 (1C, Cq), 149.7 (1C, Cq), 127.4 (1C, Cq), 125.0 (2C, CH), 79.8 (2C, CH), 74.7 (1C, Cq), 70.8 (1C, CH), 70.6 (1C, CH_2), 70.5 (1C, CH_2), 69.3 (1C, CH_2), 69.0 (1C, CH_2), 60.7 (1C, CH_2), 58.6 (1C, CH_2), 57.8 (1C, CH_2), 53.5 (1C, CH_2), 53.2 (1C, CH_2), 37.6 (1C, CH_3). MS (ES$^+$) *m/z* 449.4 $[M+H]^+$.

Synthesis of nitro-derivative 47

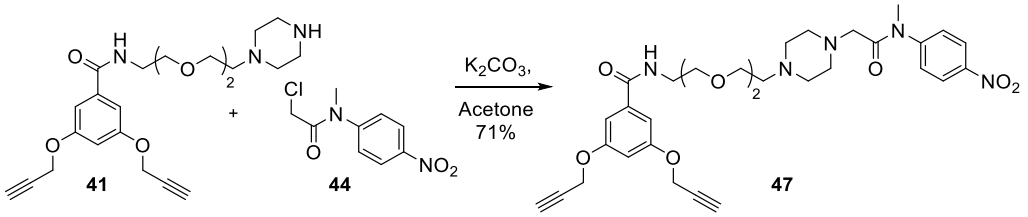

Compound **47** was obtained as described for compound **45**, using amine **41** (196.0 mg, 0.298 mmol, 1.0 eq) and compound **44** (88.7 mg, 0.338 mmol, 1.3 eq). The crude was purified by flash chromatography [linear gradient to elution from 100% EtOAc to 90:10 EtOAc:MeOH•NH_3], giving compound **47** (131.8 mg, yield 71%). TLC: 9:1 EtOAc:MeOH•NH_3, R*f* = 0.6. ^{1}H NMR (400 MHz, MeOD) *δ* 8.32 (m, 2H, ArH), 7.59 (m, 2H, ArH), 7.10 (d, *J* = 2.3 Hz, 2H, ArH), 6.80 (dd, *J* = 2.3, 2.3 Hz, 1H, ArH) 4.79 (d, *J* = 2.3 Hz 4H, ArOCH_2), 3.70-3.53 (m, 10H, CH_2), 3.39-3.54 (bs, 3H, CH_3), 3.12 (bs, 2H, NCH_2CON), 3.00 (t, *J* = 2.4 Hz, 2H, CH alkyne), 2.52 (t, *J* = 5.7 Hz, 2H, CH_2), 2.44 (m, 8H, CH_2 piperazine). MS (ES$^+$) *m/z* 622.6 $[M+H]^+$.

Synthesis of aniline-derivative 48

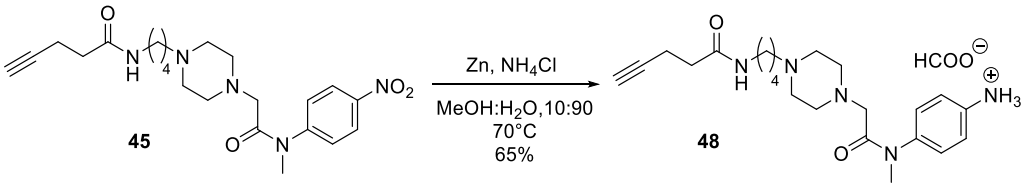

To a solution of nitrobenzene **45** (250 mg, 0.582 mmol, 1 eq) in 24 mL of a solution of H_2O:MeOH 10:90, NH_4Cl (68.5 mg, 1.281 mmol, 2.2 eq) and zinc powder (342.5 mg, 5.238 mmol, 9 eq) were added. The reaction was kept under stirring at 70 °C under reflux for 7 h, then the reaction was filtered on paper and cotton and the solvent was removed under reduced pressure. The crude was purified by flash chromatography (gradient: from 100% EtOAc to 60:40 EtOAc:MeOH•NH_3), giving aniline **48** as a glassy solid (151.9 mg, 65% yield). TLC: 85:15 EtOAc:MeOH•NH_3, R*f* = 0.3. ^{1}H NMR (400 MHz, MeOD) δ 6.99 (m, 2H, ArH), 6.76 (m, 2H, ArH), 3.23 (t, *J* = 6.8 Hz, 2H, CH_2), 3.21 (s, 3H, CH_3), 3.09 (s, 2H, CH_2), 2.93 (m, 4H, CH_2), 2.80 (m, 3H, NH_3+), 2.68 (m, 4H, CH_2), 2.51-2.36 (m, 2H, CH_2), 2.42-2.37 (m, 2H, CH_2), 2.31 (bt, *J* = 2.4 Hz, 1H, CH Alkyne), 1.66 (m, 2H, CH_2), 2.33 (m, 2H, CH_2). ^{13}C NMR (101 MHz, MeOD) δ 174.1 (1C, Cq), 171.2 (1C, Cq), 149.6 (1C, Cq), 133.5 (1C, Cq), 128.9 (2C, CH), 116.7 (2C, CH), 83.6 (1C, Cq), 70.4 (1C, CH_2), 59.5 (1C, CH_2), 58.1 (2C, CH_2), 53.2 (2C, CH_2), 52.2 (1C, CH_2), 39.6 (1C, CH_2), 38.0 (1C, CH_2), 36.0 (1C, CH_3), 27.9 (1C, CH_2), 23.3 (1C, CH_2), 15.7 (1C, CH_2), 15.7 (1C, CH_2). MS (ES$^+$) *m/z* 401.5 $[M+H]^+$.

Synthesis of aniline-derivative 49

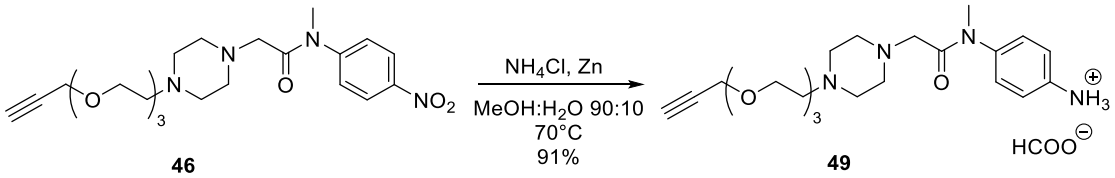

Aniline-derivative **49** was synthesized as described for compound **48**, starting from nitrobenzene **46** (100.0 mg, 0.22 mmol, 1.0 eq). The crude was purified by flash chromatography (gradient: from 100% EtOAc to 60:40 EtOAc:MeOH•NH_3), giving aniline **49** as a glassy solid (82.1 mg, 91% yield). TLC: 85:15 EtOAc:MeOH•NH_3, R*f* = 0.8. ^{1}H NMR (400 MHz, $CDCl_3$) *δ* 6.97 (m, 2H, ArH), 6.75 (m, 2H, ArH), 4.89 (bs, 3H, NH_3^+), 4.19 (d, *J* = 2.4 Hz, 2H, alkyne-CH_2), 3.69-3.58 (m, 10H, CH_2), 3.19 (s, 3H, CH_3), 2.97 (s, 2H, NCH_2CON), 2.88 (t, *J* = 2.4 Hz, 1H, CH alkyne), 2.72-2.60 (m, 6H, CH_2), 2.52 (m, 4H, CH_2). 13C NMR (101 MHz, MeOD) δ 170.3 (1C, Cq), 148.3 (1C, Cq), 132.5 (1C, Cq), 127.8 (2C, CH), 115.5 (2C, CH), 79.5 (1C, CH), 74.9 (1C, Cq), 70.3 (1C, CH_2), 70.1 (1C, CH_2), 68.9 (1C, CH_2), 68.0 (1C, CH_2), 58.9 (1C, CH_2), 57.8 (2C, CH_2), 57.3 (2C, CH_2), 52.8 (1C, CH_2), 52.4 (1C, CH_2), 36.8 (1C, CH_3). MS (ES$^+$) *m/z* 419.3 $[M+H]^+$.

Synthesis of aniline-derivative 50

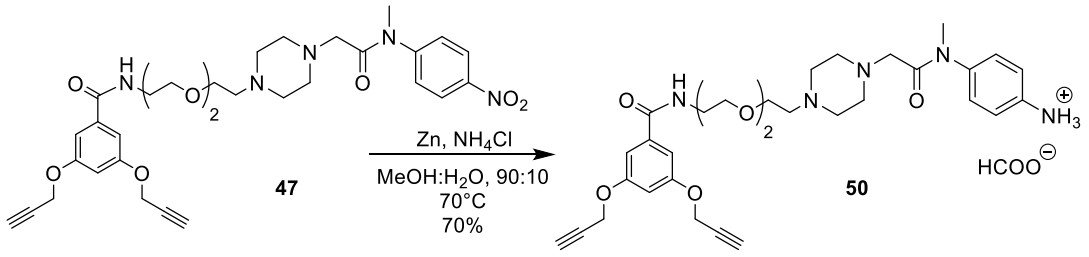

Aniline-derivative **50** was synthesized as described for compound **47**, starting from nitrobenzene **47** (131.0 mg, 0.21 mmol, 1.0 eq). The crude was purified by flash chromatography (gradient: from 100% EtOAc to 80:20 EtOAc:MeOH•NH_3), giving compound **50** (88.5 mg, yield 70%). ^{1}H NMR (400 MHz, MeOD) δ 7.08 (d, *J* = 2.3 Hz, 2H, ArH), 6.96 (m, 2H, ArH), 6.80 (t, *J* = 2.3 Hz, 1H, ArH), 6.75 (m, 2H, ArH), 4.76 (d, *J* = 2.3 Hz, 4H, $ArOCH_2$) 3.67-3.54 (m, 12H, CH_2,), 3.17 (m, 3H, CH_3), 3.02 (t, *J* = 2.3 Hz, 2H, CH alkyne), 2.92 (bs, 2H, CH_2), 2.59-2.39 (m, 10H, CH_2 piperazine+CH_2). MS (ES^+) *m/z* 592.7 $[M+H]^+$.

Synthesis of Methyl 4-(2-methoxy-2-oxoethyl)-3-nitrobenzoate 53

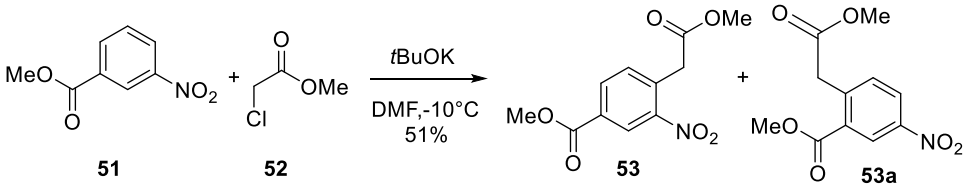

To a suspension of *t*BuOK (1.30 g, 11.6 mmol, 2.1 eq) in DMF (12 mL), a solution of methyl-3-nitrobenzoate **51** (1.00 g, 5.5 mmol, 1.0 eq) and 2-chloroacetic acid **53** (533 μL, 6.1 mmol, 1.1 eq) in DMF (2 mL) was added dropwise and the mixture was left to stir at -10°C. After 10 minutes, the reaction was put in a mixture of ice (100 mL) and aq. HCl 37% (3.5 mL). The mixture was filtered and the purification of the solid by flash chromatography (eluent: 80:20 petroleum ether:EtOAc) gave a mixture 9:1 (determined by NMR spectrum) of compounds **53** (0.72 g, 51% yield) and **53a** as yellowish oil. TLC: Petroleum Ether:EtOAc 6:4, R*f* = 0.8. ^{1}H NMR (300 MHz, $CDCl_3$): δ 8.77 (d, *J* = 1.6 Hz, 1H, ArH), 8.26 (dd, *J* = 7.6, 1.5 Hz, 1H, ArH), 7.48 (d, *J* = 7.8 Hz, 1H, ArH), 4.10 (s, 2H, CH_2), 3.99 (s, 3H, CH_3), 3.73 (s, 3H, CH_3). MS (ES^+) *m/z* 254.1 $[M+H]^+$.

Synthesis of methyl-2-oxoindoline-6-carboxylate 54

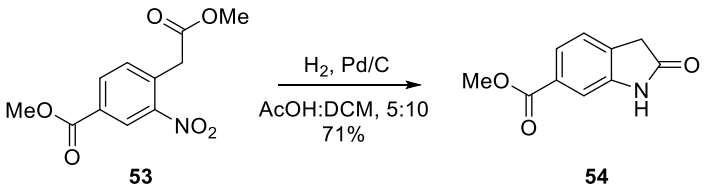

To a solution of compound **53** (354.0 mg, 1.39 mmol, 1.0 eq) in $AcOH_{(gl)}$/DCM (15 mL, 2/1), catalytic Pd/C was added, and three cycles vacuum/H_2 were carried out. The reaction was left to stir at room temperature for 6 h, and then it was filtered by a sintered glass filter. The solvent was removed under reduced pressure and the crude was purified by flash chromatography (gradient: from 50:50

Petroleum Ether:EtOAc to 100% EtOAc), giving compound **54** as pink solid (267.0 mg, 71% yield). TLC: Petroleum Ether:EtOAc 6:4, R*f* = 0.2. ^{1}H NMR (400 MHz, $CDCl_3$): δ 8.54 (bs, 1H, NH), 7.87 (dd, *J* = 7.9, 1.5 Hz, 1H, CH 5-oxindole), 7.66 (bs, 1H, CH 7-oxindole), 7.41 (d, *J* = 7.9 Hz, 1H, CH 4-oxindole), 4.03 (s, 3H, CH_3), 3.71 (s, 2H, CH_2). MS (ES^+) *m/z* 192.1 $[M+H]^+$.

Synthesis of 2-oxindole nucleus 57

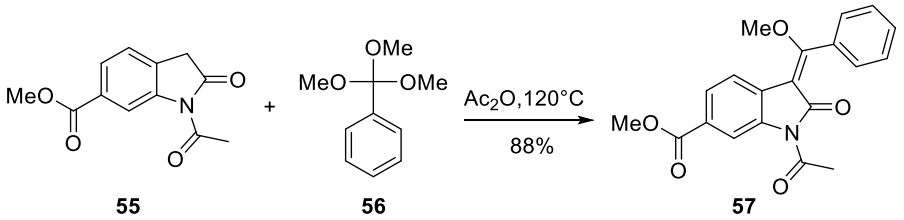

55 **56** **57**

To a solution of *N*-acetyl-oxindole **55** (200.0 mg, 0.84 mmol, 1.0 eq) in Ac_2O (2 mL), trimethyl orthobenzoate **56** (450 μL, 2.52 mmol, 3.0 eq) was added. The mixture was stirred at 120° C under reflux for 4.5 h. After completion the solvent was removed under reduced pressure. The obtained solid was washed with petroleum ether, giving the product **57** as light-yellow solid (260.2 mg, 88% yield). TLC: Petroleum Ether:EtOAc 50:50, R*f* = 0.5. ^{1}H NMR (400 MHz, $CDCl_3$) δ 8.92 (bd, *J* = 1.0 Hz, 1H, CH 7-oxindole), 8.04 (d, *J* = 8.0 Hz, 1H, CH 4-oxindole), 7.97, (dd, *J* = 8.1, 1.5 Hz, 1H, CH 6-onxindole), 7.61, (m, 3H, ArH), 7.42, (m, 2H, ArH) 3.96, (s, 3H, CH_3 ester), 3.79 (s, 3H, CH_3 ether) 1.56 (s, 3H, CH_3 acetyl). MS (ES^+) *m/z* 352.1 $[M+H]^+$.

Synthesis of nintedanib-linker nucleus 58

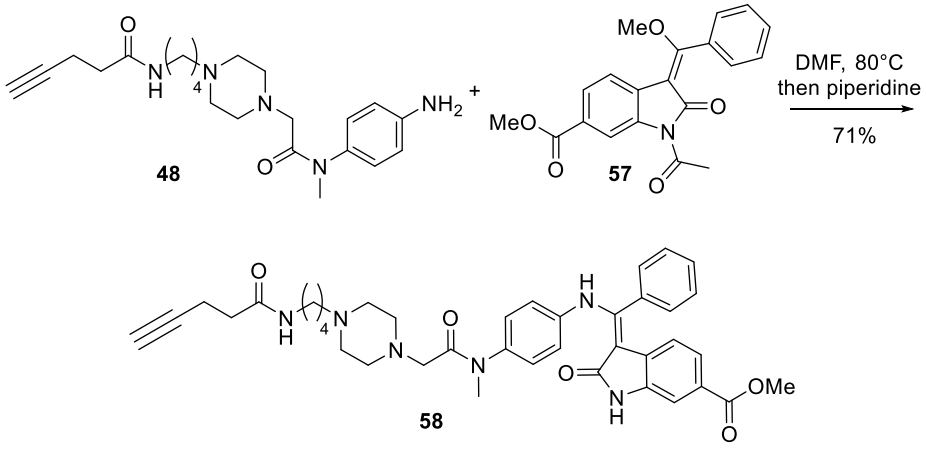

48 **57** **58**

To a solution of aniline **48** (151.9 mg, 0.354 mmol, 1 eq) in DMF (35 mL) at 80 °C under reflux, 2-oxindole **57** (136.7 mg, 0.289 mmol, 1.1 eq) was added. The reaction was left to stir for 30 h, then piperidine (78.1 μL, 0.354 mmol, 1 eq) was added and the system was left to raise to room temperature. After 2 h, the solvent was removed under reduced pressure and the crude was purified by flash chromatography (gradient: from 98:2 EtOAc:MeOH•NH_3 to 95:5), giving compound **58** as a yellowish oil (147.7 mg, 71% yield). TLC: EtOAc:MeOH•NH_3 85:15, R*f* = 0.3. ^{1}H NMR (400 MHz, MeOD) δ 7.64-7.55 (m, 4H, ArH), 7.49 (m, 2H, ArH), 7.29 (m, 1H, ArH), 7.12 (m, 2H, ArH), 6.94 (m, 2H), 5.97 (m, 1H, ArH), 3.87 (s, 3H, CH_3 ester), 3.37 (s, 3H, CH_3 amide), 3.24-3.16 (m, 4H, CH_2), 2.84 (s, 2H, CH_2), 2.52-2.36 (m, 12H, CH_2), 2.29 (t, *J* = 2.3 Hz, 1H, CH alkyne), 1.54 (m, 4H, CH_2). MS (ES^+) *m/z* 677.4 $[M+H]^+$.

Synthesis of nintedanib-linker nucleus 59

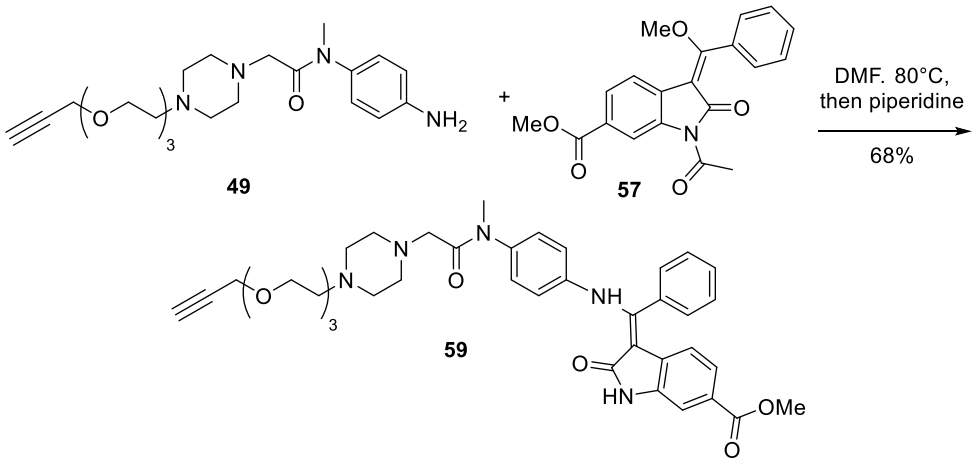

Compound **59** was synthesized as described for compound **64**, starting from aniline **49** (82.1 mg, 0.20 mmol, 1 eq). The crude was purified by flash chromatography (gradient: from 98:2 EtOAc:MeOH•NH_3 to 90:10), giving compound **59** as a yellow oil (90.0 mg, 68% yield). TLC: EtOAc:MeOH•NH_3 8:2, R*f* = 0.8. ^{1}H NMR (400 MHz, $CDCl_3$) δ 7.63-7.52 (m, 4H, ArH), 7.46-7.37 (m, 3H, ArH), 6.99 (m, 2H, ArH), 6.81 (m, 2H, ArH), 6.01 (d, *J* = 8.3 Hz, 1H, ArH), 4.20 (d, *J* = 2.4 Hz, 2H, CH_2-alkyne), 3.87 (s, 3H, CH_3 ester), 3.72-3.61 (m, 12H, CH_2), 3.19 (s, 3H, CH_3N), 2.81 (s, 2H, NCH_2CON), 2.64-2.56 (m, 8H, CH_2), 2.44 (t, *J* = 2.4 Hz, 1H, CH alkyne). ^{13}C NMR (101 MHz, $CDCl_3$) δ 171.1 (1C, Cq), 169.6 (1C, Cq), 167.5 (1C, Cq), 158.5 (1C, Cq), 140.2 (1C, Cq), 138.5 (1C, Cq), 135.6 (1C, Cq), 132.5 (1C, Cq), 130.8 (1C, CH), 129.8 (Cq), 129.3 (2C, CH), 128.7 (2C, CH), 128.1 (1C, CH), 125.3 (2C, CH), 124.1 (2C, CH), 123.0 (1C, CH), 118.4 (1C, CH), 110.5 (1C, Cq), 79.8 (1C, Cq), 77.4 (1C, CH), 74.8 (1C, CH_2), 70.8 (1C, CH_2), 70.6 (1C, CH_2), 70.5 (1C, CH_2), 69.3 (1C, CH_2), 68.9 (1C, CH_2), 59.7 (1C, CH_2), 58.6 (2C, CH_2), 57.8 (2C, CH_2), 53.5 (1C, CH_2), 53.2 (1C, CH_2), 52.1 (1C, CH_3), 37.5 (1C, CH_3). MS (ES^+) *m/z* 696.3 $[M+H]^+$.

Synthesis of nintedanib-linker nucleus 60

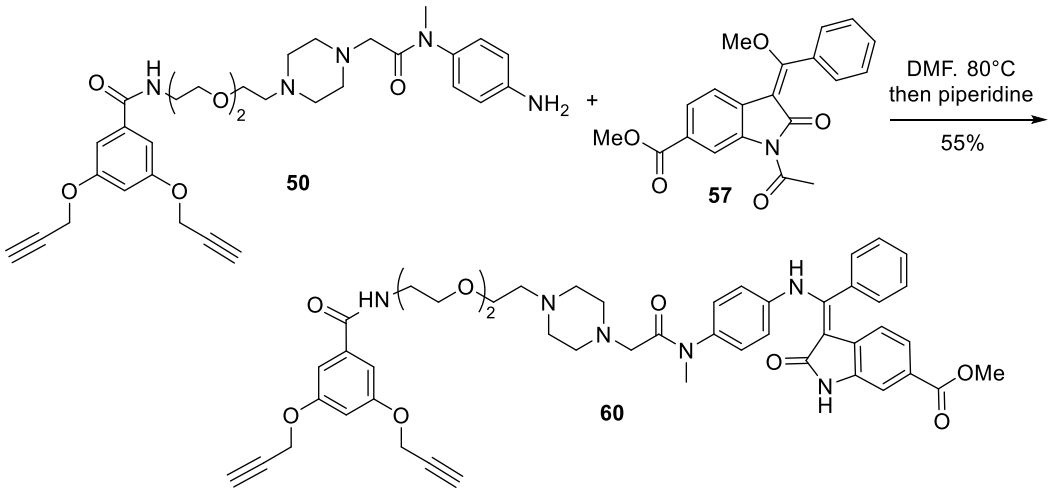

Compound **60** was synthesized as described for compound **57**, starting from aniline **50** (88.5 mg, 0.146 mmol, 1 eq). The crude was purified by flash chromatography (gradient: from 95:5 EtOAc:MeOH•NH_3), giving compound **60** as a yellow oil (67.8 mg, 55% yield). TLC: EtOAc:MeOH•NH_3 95:5, R*f* = 0.2. ^{1}H NMR (400 MHz, MeOD) δ 7.66-7.56 (m, 4H, ArH), 7.51 (m, 2H, ArH), 7.30 (m, 1H, ArH), 7.11 (m, 4H, ArH), 6.95 (m, 2H, ArH), 6.79 (t, *J* = 2.3 Hz, 1H, ArH), 5.97 (d, *J* = 8.5 Hz, 1H, ArH),

4.77 (d, *J* = 2.4 Hz, 4H, $ArOCH_2$), 3.85 (s, 3H, CH_3 ester), 3.67-3.60 (m, 8H, CH_2), 3.56 (t, *J* = 5.6 Hz, 2H, CH_2), 3.17 (bs, 3H, NCH_3), 3.01 (t, *J* = 2.4 Hz, 2H, CH alkyne), 2.81 (bs, 2H, piperazine-CH_2CON), 2.58-2.28 (m, 10H, CH_2 piperazine+CH_2). MS (ES^+) *m/z* 869.4 $[M+H]^+$.

Synthesis of the covalent conjugate 7

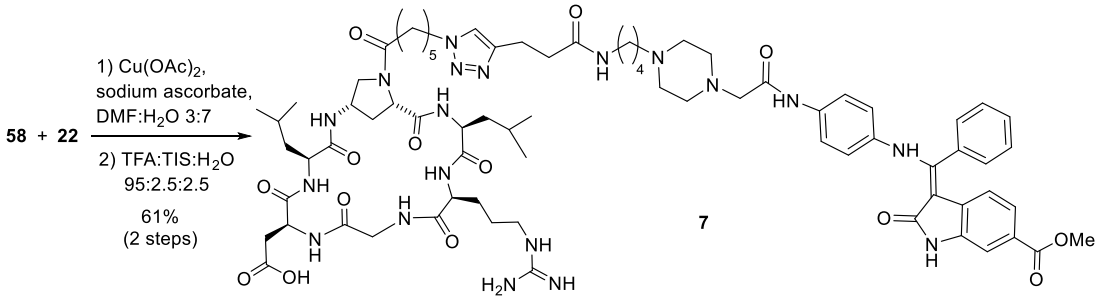

To a solution of compound **58** (7.4 mg, 0.011 mmol, 1 eq) and cyclopeptide **22** (15.0 mg, 0.012 mmol, 1.1 eq) in DMF (1.57 mL), a solution of $Cu(OAc)_2$ (0.64 mg, 0.003 mmol, 0.3 eq) and sodium ascorbate (1.3 mg, 0.007 mmol, 0.6 eq) in water (0.67 mL) was added. The reaction was left under stirring under Argon atmosphere after 3 cycle of argon/vacuum. After 6.5 h, the solvent was removed under reduced pressure and the residue was washed with water (3x) and diethyl ether (3x). The protected intermediate was checked by MS analysis (MS (ES^+)*m/z* 1805.0 $[M+H]^+$), and then it was deprotected using a solution of TFA:TIS:H_2O 95:2.5:2.5 (0.55 mL). The reaction was kept under stirring for 1 h, then the solvent was removed under reduced pressure and the crude was purified by reverse phase HPLC, using the described general method (R_t = 23.0 min) giving the final conjugate **7** (12.3 mg, 61% yield). ^{1}H NMR (400 MHz, MeOD) δ 7.66 (s, 1H, CH triazole), 7.54-7.56 (m, 5H, ArH), 7.52 (m, 2H, ArH), 7.30 (dd, *J* = 8.3, 1.5 Hz, 1H, ArH), 7.16 (m, 2H, ArH), 6.96 (m, 2H, ArH), 6.85 (m, 2H, ArH), 5.97 (d, *J* = 8.3 Hz, 1H, ArH), 4.39-4.31 (m, 6H, αAsp+αLeu+H2Amp+CH_2), 4.21 (bt, *J* = 6.6 Hz, 1H, H4Amp), 4.15-4.07 (m, 2H, αGly+αArg), 3.89 (m, 1H, H5Amp), 3.87 (m, 3H, CH_3), 3.78 (m, 1H, αGly), 3.37 (m, 1H, H5Amp), 3.29-3.17 (m, 10H, δArg+CH_2), 3.12 (m, 4H, CH_2), 3.01 (bt, *J* = 6.9 Hz, 2H, CH_2), 2.92 (dd, *J* = 17.6, 4.6 Hz, 1H, βAsp), 2.88-2.75 (m, 2H, βAsp+H3Amp), 2.56 (m, 2H, CH_2), 2.33 (m, 2H, CH_2), 1.89 (m, 4H, CH_2), 1.79-1.47 (m, 15H, βArg+γArg+γLeu+βLeu+CH_2+H3Amp), 1.31 (m, 4H, CH_2), 0.98 (dd, *J* = 17.9, 6.5 Hz, 6H, δLeu), 0.93 (dd, *J* = 17.9, 6.5 Hz, 6H, δLeu). HRMS(ES+) $C_{74}H_{103}N_{19}O_{14}$ calcd for [M+H]+ 1481.7932, found 1481.7960.

Synthesis of the covalent conjugate 8

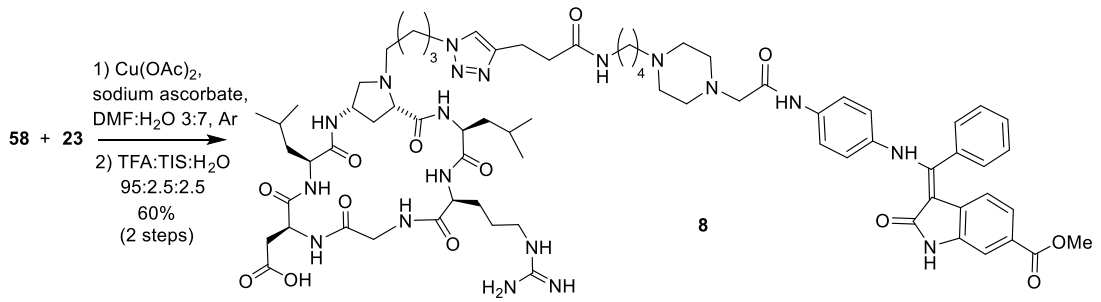

Covalent conjugate **8** was synthesized as described for compound **7**, starting from **58** (7.7 mg, 0.011 mmol, 1 eq) and cyclopeptide **23** (16.5 mg, 0.013 mmol, 1.1 eq). The protected intermediate was checked by MS analysis (MS (ES^+) *m/z* 1762.9 $[M+H]^+$) and then it was deprotected using a solution of TFA:TIS:H_2O 95:2.5:2.5 (0.57 mL). The reaction was kept under stirring for 1 h, then the solvent

was removed under reduced pressure and the crude was purified by reverse phase HPLC, using the described general method (R_t = 22.9 min), giving the final conjugate **8** (13.0 mg, 60% yield). ^{1}H NMR (400 MHz, MeOD) δ 7.77 (s, 1H, CH triazole), 7.67-7.56 (m, 5H, ArH), 7.53 (m, 2H, ArH), 7.30 (dd, *J* = 8.4, 1.9 Hz, 1H, ArH), 7.16 (m, 2H, ArH), 6.97 (m, 2H, ArH), 5.97 (d, *J* = 8.4 Hz, 1H, ArH), 4.67 (m, 1H, H4Amp), 4.46-4.38 (m, 6H, αAsp+αLeu), 4.37-4.32 (m, 2H, H2Amp), 4.29 (d, *J* = 17.1, 1H αGly), 3.86 (s, 3H, CH_3), 3.76 (d, *J* = 17.1, 1H αGly), 3.61 (m, 1H, H5Amp), 3.52 (m, 1H, H5Amp), 3.30-3.09 (m, 15H, βArg+βAsp+CH_2), 3.03-2.84 (m, 8H, H3Amp+CH_2), 2.57 (t, *J* = 7.1 Hz, 2H, CH_2), 2.16 (m, 1H, H3Amp), 2.02-1.81 (m, 3H), 1.80-1.51 (m, 16H, βLeu+γLeu+βArg+γArg+CH_2), 0.98 (dd, *J* = 19.9, 6.4 Hz, 6H, δLeu), 0.93 (dd, *J* = 19.9, 6.4 Hz, 6H, δLeu). HRMS(ES+) $C_{72}H_{101}N_{19}O_{13}$ calcd for [M+H]+ 1440.7826, found 1440.7854.

Synthesis of the covalent conjugate 9

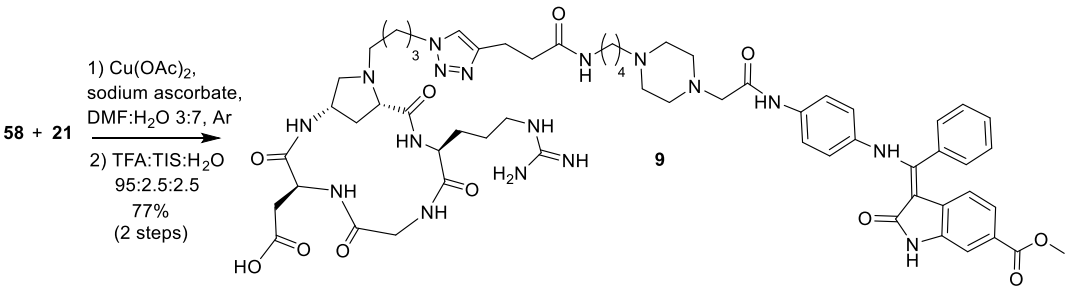

Covalent conjugate **9** was synthesized as described for compound **7**, starting from compound **58** (7.0 mg, 0.010 mmol, 1 eq) and cyclopeptide **21** (12.4 mg, 0.011 mmol, 1.1 eq). The protected intermediate was checked by MS analysis (MS (ES^+) *m/z* 1536.8 $[M+H]^+$) and then it was deprotected using a solution of TFA:TIS:H_2O 95:2.5:2.5 (0.51 mL). The reaction was kept under stirring for 1 h, then the solvent was removed under reduced pressure and the crude was purified by reverse phase HPLC, using the described general method (R_t = 22.0 min), giving the final conjugate **9** (13.5 mg, 77% yield). ^{1}H NMR (400 MHz, MeOD) δ 7.77 (s, 1H, CH triazole), 7.69-7.57 (m, 5H, ArH), 7.53 (m, 2H, ArH), 7.30 (dd, *J* = 8.4, 1.5 Hz, 1H, ArH), 7.17 (m, 2H, ArH), 6.97 (m, 2H, ArH), 5.97 (d, *J* = 8.4 Hz, 1H, ArH), 4.72 (dd, *J* = 6.1 Hz, 1H, αAsp), 4.56 (d, *J* = 11.3 Hz, 1H, H2Amp), 4.41 (t, *J* = 6.9 Hz, 2H, CH_2), 4.31 (m, 1H, H4Amp), 4.25 (m, 1H, αArg), 4.07 (m, 2H, αGly+H5Amp), 3.87 (s, 3H, CH_3), 3.41 (bm, 2H, αGly+H5Amp), 3.30-3.18 (m, 10H, δArg+CH_2), 3.17-3.12 (m, 2H, CH_2), 3.06-2.82 (m, 10H, CH_2+βAsp), 2.69 (d, *J* = 15.1 Hz, 1H, H3Amp), 2.57 (t, *J* = 6.6 Hz, 2H, CH_2), 1.95 (m, 2H, CH_2), 1.84-1.51 (m, 13H, βArg+γArg+H3Amp+CH_2). HRMS(ES+) $C_{60}H_{79}N_{17}O_{11}$ calcd for [M+H]+ 1213.6145, found 1231.61.71.

Synthesis of the covalent conjugate 10

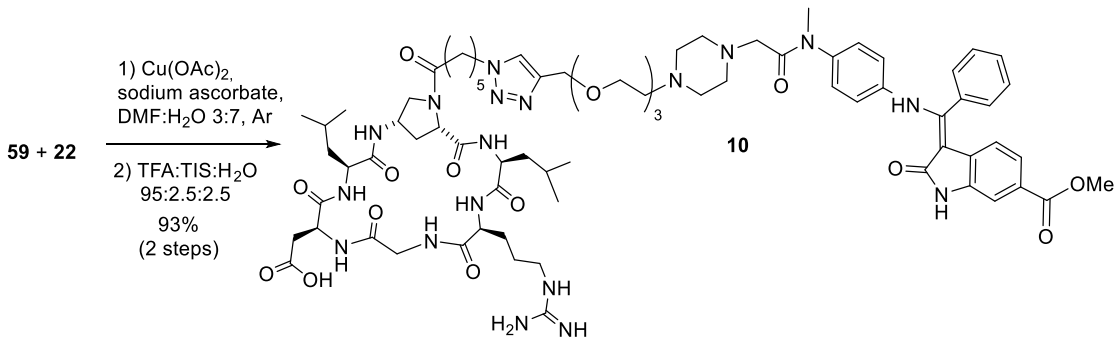

Dual conjugate **10** was synthesized as described for compound **7**, starting from compound **59** (9.1 mg, 0.013 mmol, 1.0 eq) and cyclopeptide **22** (18.0 mg, 0.014 mmol, 1.1 eq). The protected intermediate was checked by MS analysis (MS (ES^+) *m/z* 1823.9 $[M+H]^+$) and then it was deprotected using a solution of TFA:TIS:H_2O 95:2.5:2.5 (0.65 mL). The reaction was kept under stirring for 1 h, then the solvent was removed under reduced pressure and the crude was purified by reverse phase HPLC, using the described general method (R_t = 23.2 min), giving the final conjugates**10** (19.5 mg, 93% yield). ^{1}H NMR (400 MHz, MeOD) δ 8.00 (s, 1H, CH triazole), 7.79-7.57 (m, 5H, ArH), 7.52 (m, 2H, ArH), 7.30 (dd, *J* = 8.4, 1.6 Hz, 1H, ArH), 7.17 (m, 2H, ArH), 6.95 (m, 2H, ArH), 5.97 (d, *J* = 8.4 Hz, 1H, ArH), 4.61 (s, 2H, O-CH_2-triazole), 4.50-4.36 (m, 6H, αAsp+αLeu+CH_2+ H4Amp), 4.21 (m, 1H, αArg), 4.11 (m, 2H, αGly+H2Amp), 3.91-3.78 (m, 7H, CH_2+αGly+ H5Amp+CH_2), 3.66 (m, 10H, CH_2), 3.38 (m, 1H, H5Amp), 3.26-3.15 (m, 8H, αArg+CH_2), 3.12 (m, 2H, CH_2), 2.95 (dd, *J* = 17.5, 4.5 Hz, 1H, βAsp), 2.86-2.76 (m, 3H, βAsp+CH_2), 2.55 (m, 1H, H3Amp), 2.42-2.25 (m, 2H, CH_2), 1.97-1.57 (m, 17H, βArg+γArg+βLeu+ γLeu+CH_2+H3Amp), 1.33 (m, 4H, CH_2), 0.98 (dd, *J* = 18.2, 6.1 Hz, 6H, δLeu), 0.93 (dd, *J* = 18.2, 6.1 Hz, 6H, δLeu). HRMS(ES+) $C_{74}H_{105}N_{18}O_{16}$ calcd for [M+H]+ 1501.7878, found 1501.7937.

Synthesis of the covalent conjugate 11

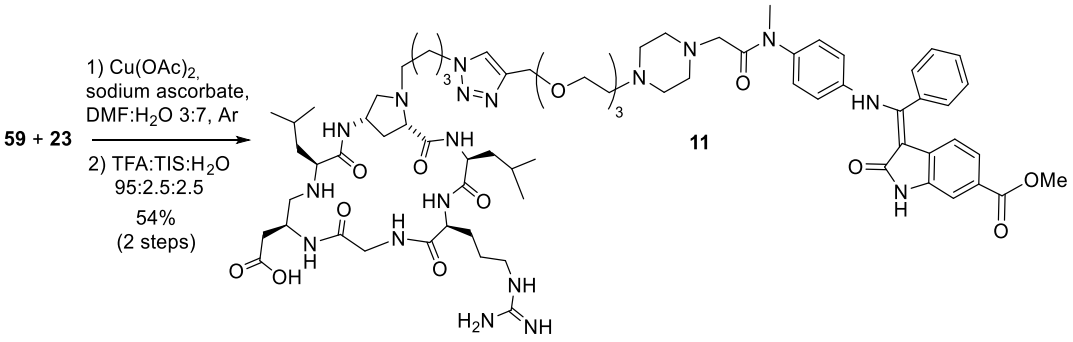

Dual conjugate **11** was synthesized as described for compound **7**, using compound **59** (6.9 mg, 0.009 mmol, 1 eq) and cyclopeptide **23** (14.4 mg, 0.011 mmol, 1.1 eq). The protected intermediate was checked by MS analysis (MS (ES^+) *m/z* 1717.9 $[M+H]^+$) and then it was deprotected using a solution of TFA:TIS:H_2O 95:2.5:2.5 (0.65 mL). The reaction was kept under stirring for 1 h, then the solvent was removed under reduced pressure and the crude was purified by reverse phase HPLC, using the described general method (R_t = 22.5 min), giving the final conjugate **11** (9.7 mg, 54% yield). ^{1}H NMR (400 MHz, $CDCl_3$) δ 8.01 (s, 1H, CH triazole), 7.76-7.57 (m, 4H, ArH), 7.53 (m, 2H, ArH), 7.30 (dd, *J* = 8.3, 1.9 Hz, 1H, ArH), 7.17 (m, 2H, ArH), 6.96 (m, 2H, ArH), 5.97 (d, *J* = 8.3 Hz, 1H, ArH), 4.68 (m, 1H, αAsp), 4.62 (bs, 2H, OCH_2-triazole), 4.57-4.47 (m, 8H, H2 Amp+CH_2+H4 Amp+2αLeu+H5 Amp+αArg), 4.28 (d, *J* = 17.4 Hz, 1H, αGly), 3.86 (bs, 3H, CH_3), 3.82 (m, 2H, CH_2), 3.76 (d, *J* = 17.4 Hz, 1H, αGly), 3.67 (s, 10 H, CH_2), 3.56 (m, 1H, H5b Amp), 3.28-3.15 (m, 11H, 2CH_2+δArg+H4'+CH_3), 3.00-2.79 (m, 7H, βAsp+H3a Amp+CH_2-CON+CH_2), 2.17 (d, *J* = 14.8 Hz, 1H, H3b Amp), 2.03-1.57 (m, 18H, H2'+H3'+βArg+γArg +γLeu+βLeu+2CH_2), 1.00-0.88 (m, 12H, δLeu). HRMS(ES+) $C_{72}H_{103}N_{18}O_{15}$ calcd for [M+H]+ 1458.7772, found 1459.7800.

Synthesis of the covalent conjugate 12

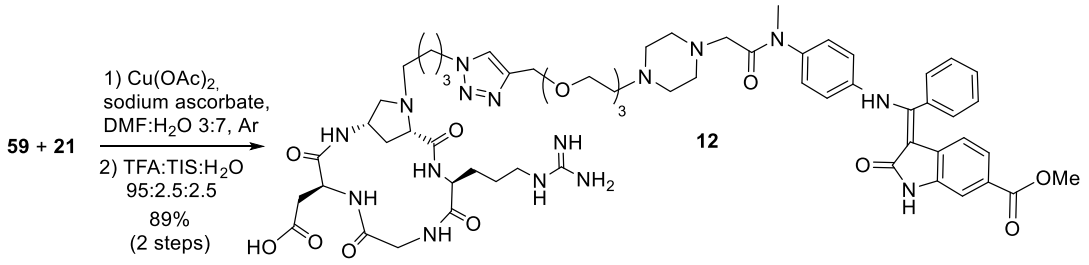

Dual conjugate **12** was synthesized as described for compound **7**, starting from compound **59** (10 mg, 0.01 mmol, 1.0 eq) and cyclopeptide **21** (17.4 mg, 0.02 mmol, 1.1 eq). The protected intermediate was checked by MS analysis (MS (ES^+) *m/z* 1555.8 $[M+H]^+$) and then it was deprotected using a solution of TFA:TIS:H_2O 95:2.5:2.5 (0.75 mL). The reaction was kept under stirring for 1 h, then the solvent was removed under reduced pressure and the crude was purified by reverse phase HPLC, using the described general method (R_t = 22.2 min), giving the final conjugate **12** (19.6 mg, 89% yield). ^{1}H NMR (400 MHz, MeOD) δ 8.00 (s, 1H, CH triazole), 7.66-7.58 (m, 5H, ArH), 7.52 (m, 2H, ArH), 7.31 (dd, *J* = 8.3, 1.6 Hz, 1H, ArH), 7.17 (m, 2H, ArH), 6.92 (m, 2H, ArH), 5.98 (d, *J* = 8.3 Hz, 1H, ArH), 4.72 (bdd, *J* = 6.1, 6.1 Hz, 1H, αAsp), 4.62 (bs, 2H, O-CH_2-triazole), 4.56 (d, *J* = 11.2 Hz, 1H, H2Amp), 4.45 (t, *J* = 6.7 Hz, 2H, CH_2), 4.31 (m, 1H, H4Amp), 4.26 (bt, *J* = 7.3 Hz, 1H, αArg), 4.11-4.04 (m, 2H, αGly + H5Amp), 3.86 (bs, 4H, CH_2), 3.82 (m, 2H, CH_2), 3.67 (m, 10, CH_2), 3.43 (m, 2H, H5Amp+αGly), 3.25 (m, 4H, δArg+CH_2), 3.21 (m, 4H, CH_2), 2.86 (m, 3H, H3Amp+βAsp), 2.70 (d, *J* = 15.1 Hz, 1H, H3Amp), 1.97 (m, 2H, βArg), 1.84-1.61 (m, 8H, δArg+CH_2), 1.31 (m, 4H, CH_2). HRMS(ES+) $C_{60}H_{81}N_{16}O_{13}$ calcd for [M+H]+ 1233.6091, found 1233.6152.

Synthesis of the covalent conjugate 13

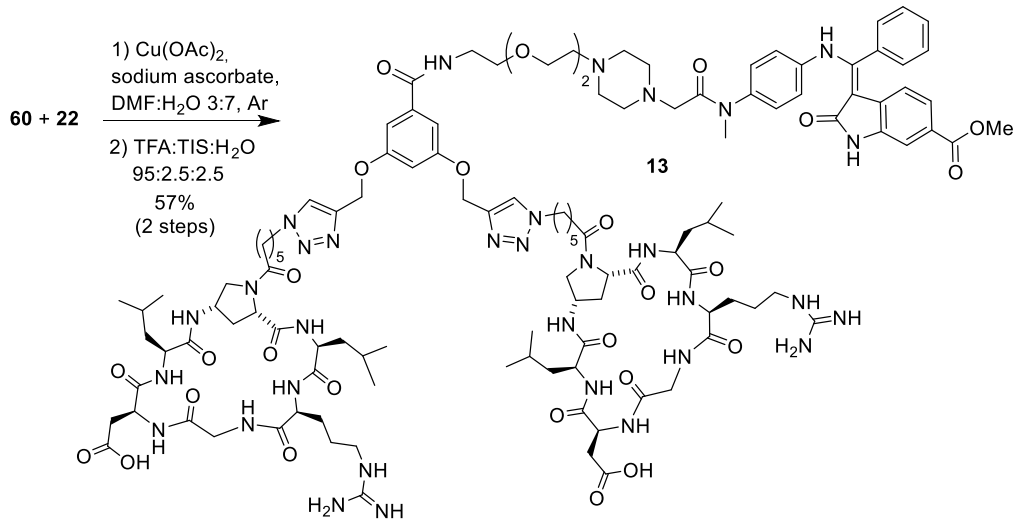

To a solution of compound **60** (10.0 mg, 0.012 mmol, 1 eq) and cyclopeptide **22** (32.8 mg, 0.0265 mmol, 2.3 eq) in DMF (1.69 mL), a solution of $Cu(OAc)_2$ (1.38 mg, 0.007 mmol, 0.6 eq) and sodium ascorbate (2.73 mg, 0.014 mmol, 1.2 eq) in water (0.73 ml) was added. The reaction was left under stirring under argon atmosphere after 3 cycle of argon/vacuum. After 14 h, the solvent was removed under reduced pressure and the residue was washed with water (3x) and diethyl ether (3x). The protected intermediate was checked by MS analysis (MS (ES^+) *m/z* 3124.5 $[M+H]^+$) and then it was deprotected using a solution of TFA:TIS:H_2O 95:2.5:2.5 (0.57 mL). The reaction was kept under stirring for 1 h, then the solvent was removed under reduced pressure and the crude was

purified by reverse phase HPLC, using the descrbied general method (R_t = 23.1 min), giving the final conjugate **13** (16.6 mg, 57% yield). ^{1}H NMR (400 MHz, MeOD) δ 8.10 (bs, 2H, CH triazole), 7.66-7.55 (m, 5H, ArH), 7.50 (m, 2H, ArH), 7.30 (m, 1H, ArH), 7.12 (m, 4H, ArH), 6.90 (m, 2H, ArH), 5.96 (d, *J* = 8.1 Hz, 1H, ArH), 5.20 (bs, 4H, ArO-CH_2-triazole), 4.51-4.36 (m, 10H, αAsp+αLeu+H4Amp+H2Amp), 4.19 (m, 2H, αArg), 4.10 (m, 4H, CH_2), 3.89-3.84 (m, 5H, CH_3+αGly), 3.83-3.75 (m, 4H, αGly+H5Amp), 3.68 (m, 8H, CH_2), 3.58 (m, 2H, CH_2), 3.42 (m, 2H, H5Amp), 3.30-3.13 (m, 10H, δArg+CH_2), 3.98-3.81 (m, 8H, βAsp+CH_2), 2.55 (m, 2H, H3Amp), 2.42-2.20 (m, 4H, CH_2), 1.98-1.83 (m, 10H, H3Amp+CH_2), 1.80-1.54 (m, 22H, βLeu+βArg+γArg+CH_2), 1.36-1.26 (m, 8H, CH_2+γLeu), 0.97 (dd, *J* = 18.4, 6.1 Hz, 12H, δLeu), 0.92 (dd, *J* = 18.4, 6.1 Hz, 12H, δLeu). HRMS(ES+) $C_{119}H_{171}N_{32}O_{27}$ calcd for [M+H]+ 2480.2913, found 2479.29017.

Synthesis of the covalent conjugate 14

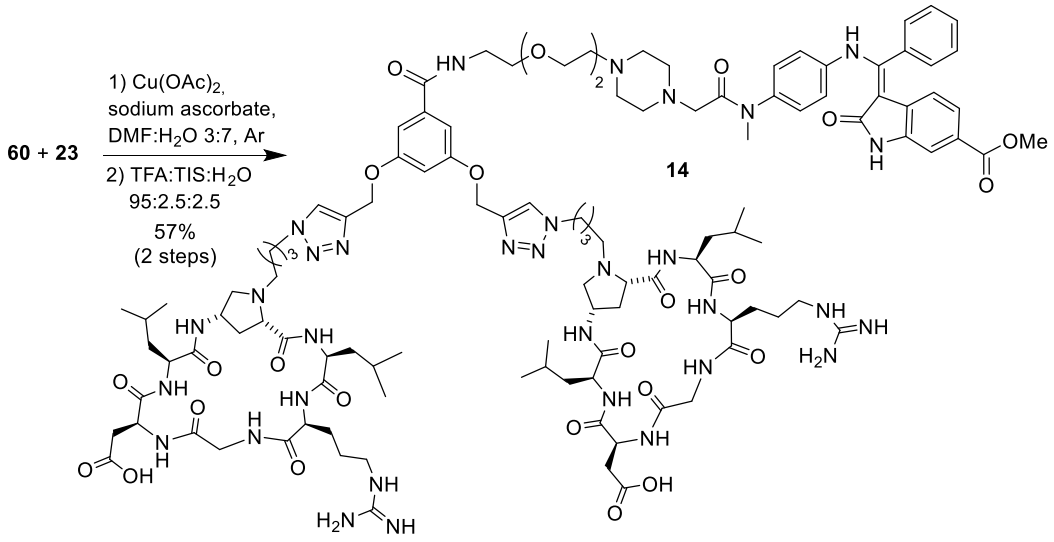

Covalent conjugate **14** was synthesized as described for compound **13** starting from compound **60** (10.0 mg, 0.0115 mmol, 1 eq) and cyclopeptide **23** (33.4 mg, 0.0253 mmol, 2.3 eq).The protected intermediate was checked by MS analysis (MS (ES^+) *m/z* 3040.7 $[M+H]^+$) and it was deprotected using a solution of TFA:TIS:H_2O 95:2.5:2.5 (0.58 mL). The reaction was kept under stirring for 1 h, then the solvent was removed under reduced pressure and the crude was purified by reverse phase HPLC, using the described general method (R_t = 22.1 min), giving the final conjugate **14** (20.1 mg, 56% yield). ^{1}H NMR (400 MHz, MeOD) δ 8.09 (s, 2H, CH triazole), 7.66-7.57 (m, 5H, ArH), 7.51 (m, 2H, ArH), 7.29 (dd, *J* = 8.3, 1.6 Hz, 1H, ArH), 7.12 (m, 4H, ArH), 6.94 (m, 2H, ArH), 5.97 (d, *J* = 8.3 Hz, 1H, ArH), 5.19 (bs, 4H, Ar-OCH_2-traziole), 4.69 (m, 2H, αAsp), 4.50-4.31 (m, 14H, H4Amp+ αLeu+H2Amp+CH_2), 4.28 (d, *J* = 17.5 Hz, 2H, αGly), 3.86 (s, 3H, CH_3), 3.82-3.79 (m, 2H, αArg), 3.76 (d, *J* = 17.5 Hz, 2H, αGly), 3.72-3.63 (m, 8H, CH_2), 3.62-3.51 (m, 4H, H5Amp), 3.29-3.08 (m, 16H, δArg+CH_2), 2.95 (m, 2H, CH_2), 2.85 (m, 4H, βAsp or CH_2), 2.77 (m, 4H, βAsp or CH_2), 2.18 (m, 2H, H3Amp), 2.05-1.94 (m, 4H, CH_2), 1.93-1.84 (m, 2H, H3Amp), 1.80-1.58 (m, 24H, βLeu+βArg+γArg+γLeu+CH_2), 0.98 (dd, *J* = 19.6, 6.4 Hz, 12H, δLeu), 0.92 (dd, *J* = 19.6, 6.4 Hz, 12H, δLeu). HRMS(ES+) $C_{115}H_{167}N_{32}O_{25}$ calcd for [M+H]+ 2396.2702, found 2395.2753.

Synthesis of the covalent conjugate 15

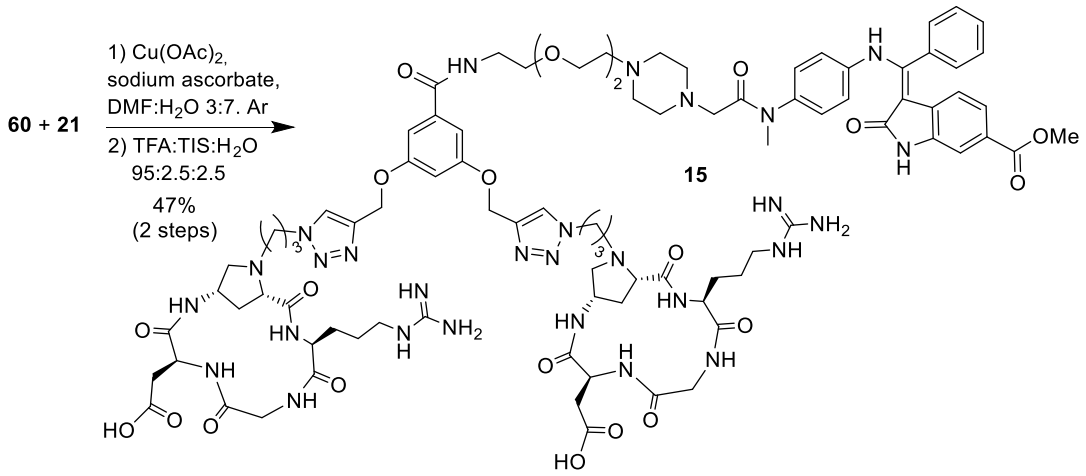

Covalent conjugate **15** was synthesized as described for compound **13**, starting from compound **60** (22.6 mg, 0.026 mmol, 1 eq) and cyclopeptide **21** (64.2 mg, 0.059 mmol, 2.3 eq). The protected intermediate was checked by MS analysis (MS (ES^+) *m/z* 2588.3 $[M+H]^+$) and then 25 mg (0.0099 mmol, 1 eq) were deprotected using a solution of TFA:TIS:H_2O 5:2.5:2.5 (0.49 mL). The reaction was kept under stirring for 1 h, then the solvent was removed under reduced pressure and the crude was purified by reverse phase HPLC, using the described general method with the only exception of using column B with flowrate 3.0 ml/min (R_t = 21.3 min), giving the final conjugate **15** (11.9 mg, 46% yield).^{1}H NMR (400 MHz, MeOD) δ 8.09 (bs, 2H, CH triazole), 7.66-7,57 (m, 5H, ArH), 7.49 (m, 2H, ArH), 7.29 (dd, *J* = 8.3, 1.7 Hz, 1H, ArH), 7.13 (m, 4H, ArH), 6.94 (m, 2H, ArH), 5.95 (d, *J* = 8.3 Hz, 1H, ArH), 5.20 (m, 4H, ArOCH_2-triazole), 4.69 (m, 2H, αAsp), 4.58 (d, *J* = 11.4 Hz, 2H, H2Amp), 4.47 (m, 6H, H4Amp+CH_2), 4.32 (m, 2H, αArg), 4.22 (m, 2H, H5Amp), 4.12-4.05 (m, 2H, αGly), 3.86 (bs, 3H, CH_3), 3.81 (m, 2H, H5Amp), 3.69 (m, 8H, αGly+δArg+CH_2), 3.59 (m, 2H, H5Amp), 3.47-2.40 (m, 2H, αGly), 3.30-3.21 (m, 8H, CH_2), 3.18 (m, 2H, CH_2), 3.14 (m, 2H, H3Amp), 2.98-2.89 (m, 4H, CH_2), 2.87-2.77 (m, 6H, βAsp+CH_2), 2.73-2.66 (m, 2H, H3Amp), 2.04-1.90 (m, 6H, CH_2), 1.85-1.56 (m, 14H, γArg+βArg+CH_2), 1.31 (m, 4H, CH_2). HRMS(ES+) $C_{91}H_{123}N_{28}O_{21}$ calcd for [M+H]+ 1943.9339, found 1942.9329.

4.5.2. HPLC chromatograms

General method for purity determination. The purity of the final compound was determined by reverse phase HPLC (column B), with the solvent system H_2O + 0.1% TFA (Solvent A) and ACN (solvent B), using the following method: flow rate 3.0 mL/min; detection at 220 nm, linear gradient from 5% B to 50% B over 23 min, 50% B for 3 min, from 50% B to 5% B over 3 min, room temperature.

Compound 7

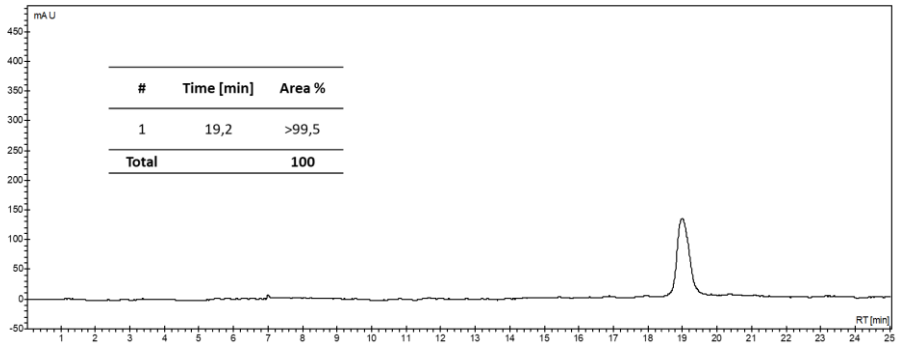

#	Time [min]	Area %
1	19,2	>99,5
Total		**100**

Compound 8

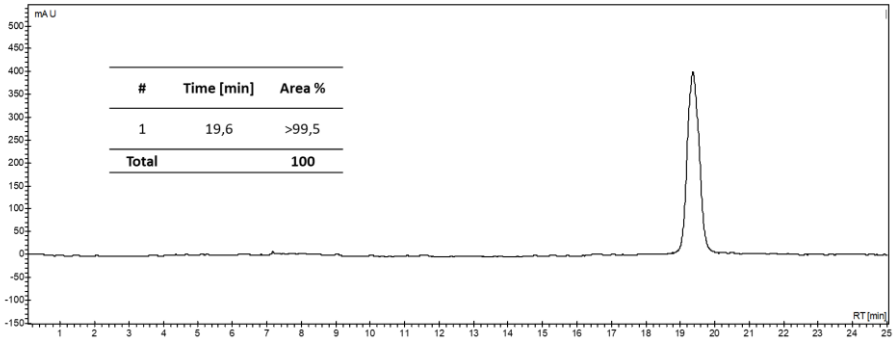

#	Time [min]	Area %
1	19,6	>99,5
Total		**100**

Compound 9

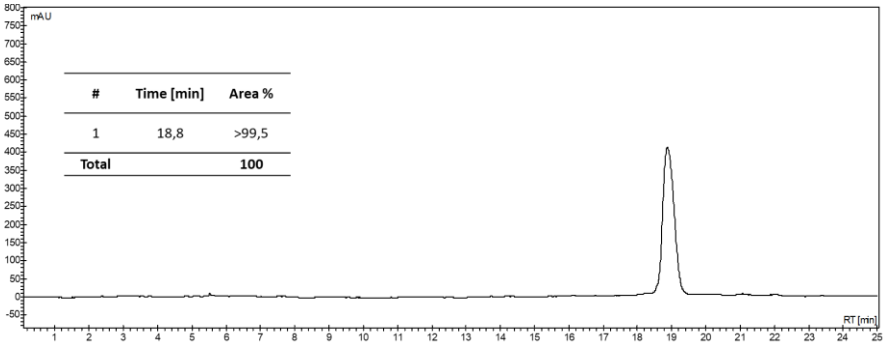

#	Time [min]	Area %
1	18,8	>99,5
Total		**100**

Compound 10

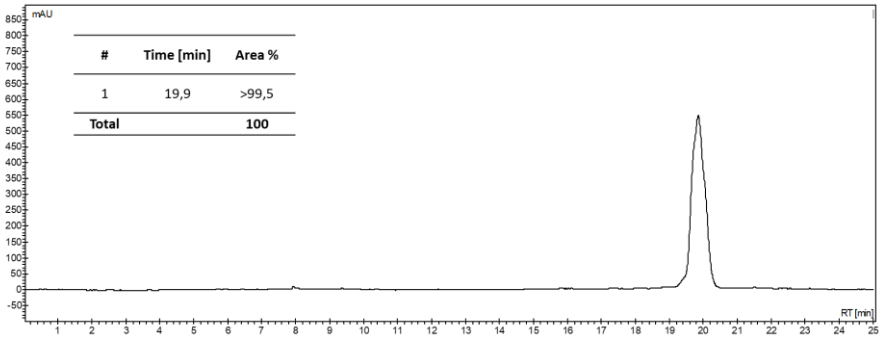

#	Time [min]	Area %
1	19,9	>99,5
Total		**100**

Compound 11

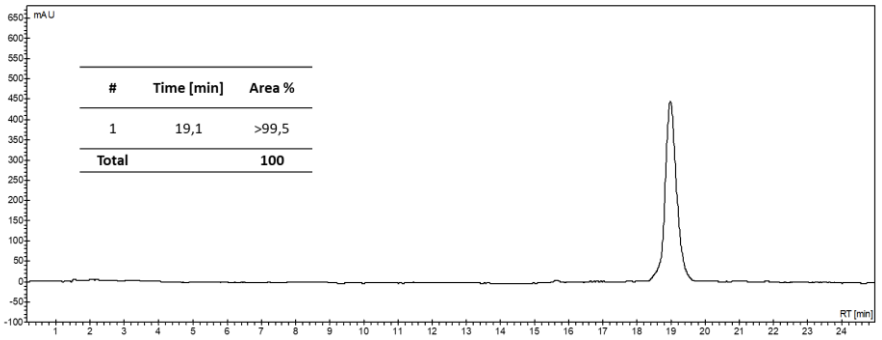

#	Time [min]	Area %
1	19,1	>99,5
Total		**100**

Compound 12

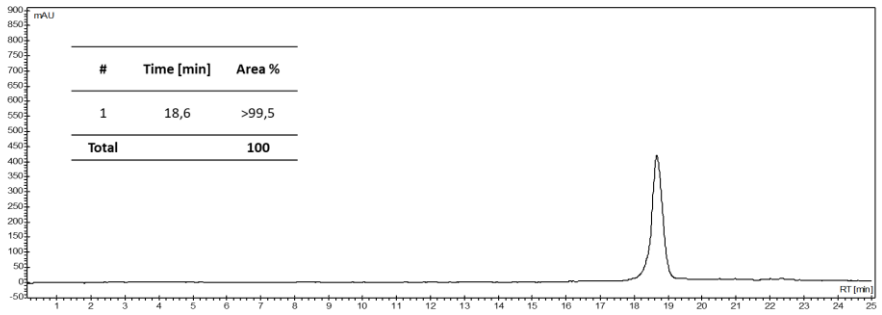

#	Time [min]	Area %
1	18,6	>99,5
Total		**100**

Compound 13

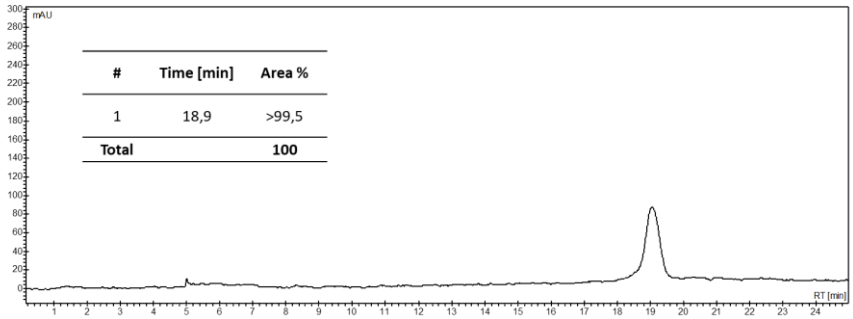

#	Time [min]	Area %
1	18,9	>99,5
Total		**100**

Compound 14

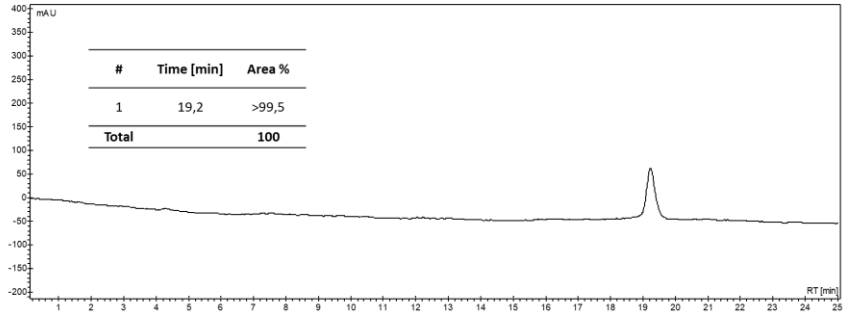

#	Time [min]	Area %
1	19,2	>99,5
Total		**100**

Compound 15

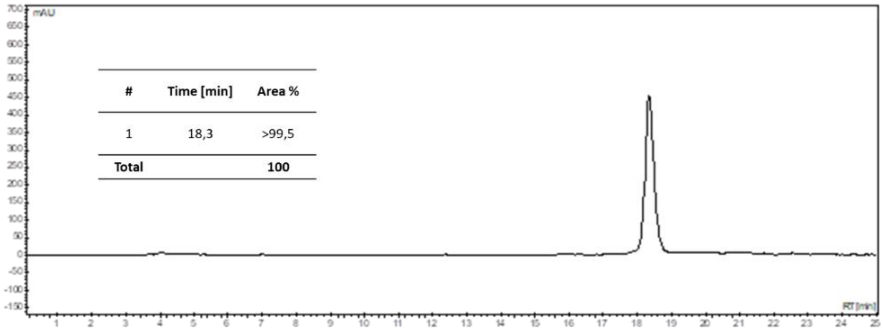

#	Time [min]	Area %
1	18,3	>99,5
Total		**100**

4.6. References

(**1**) Vasan, N.; Baselga, J.; Hyman, D. M. A View on Drug Resistance in Cancer. *Nature* **2019**, *575*, 299–309.
(**2**) Norouzi, S.; Gorgi Valokala, M.; Mosaffa, F.; Zirak, M. R.; Zamani, P.; Behravan, J. Crosstalk in Cancer Resistance and Metastasis. *Crit. Rev. Oncol. Hematol.* **2018**, *132*, 145–153.
(**3**) Javadi, S.; Zhiani, M.; Mousavi, M. A.; Fathi, M. Crosstalk between Epidermal Growth Factor Receptors (EGFR) and Integrins in Resistance to EGFR Tyrosine Kinase Inhibitors (TKIs) in Solid Tumors. *Eur. J. Cell Biol.* **2020**, *99*, 151083.
(**4**) Sartori, A.; Portioli, E.; Battistini, L.; Calorini, L.; Pupi, A.; Vacondio, F.; Arosio, D.; Bianchini, F.; Zanardi, F. Synthesis of Novel c(AmpRGD)–Sunitinib Dual Conjugates as Molecular Tools Targeting the $\alpha_V\beta_3$ Integrin/VEGFR2 Couple and Impairing Tumor-Associated Angiogenesis. *J. Med. Chem.* **2017**, *60*, 248–262.
(**5**) Roth, G. J.; Binder, R.; Colbatzky, F.; Dallinger, C.; Schlenker-Herceg, R.; Hilberg, F.; Wollin, S.-L.; Kaiser, R. Nintedanib: From Discovery to the Clinic. *J. Med. Chem.* **2015**, *58*, 1053–1063.
(**6**) Cruz da Silva, E.; Dontenwill, M.; Choulier, L.; Lehmann, M. Role of Integrins in Resistance to Therapies Targeting Growth Factor Receptors in Cancer. *Cancers* **2019**, *11*, 692.
(**7**) Park, K.-Y.; Kim, J. Cyclic Pentapeptide CRGDfK Enhances the Inhibitory Effect of Sunitinib on TGFβ1-Induced Epithelial-to-Mesenchymal Transition in Human Non-Small Cell Lung Cancer Cells. *PLoS One* **2020**, *15*, e0232917.
(**8**) Wang, C.; Wang, T.; Lv, D.; Li, L.; Yue, J.; Chen, H.-Z.; Xu, L. Acquired Resistance to EGFR TKIs Mediated by TGFβ1/Integrin β_3 Signaling in EGFR-Mutant Lung Cancer. *Mol. Cancer Ther.* **2019**, *18*, 2357–2367.
(**9**) Comoglio, P. M.; Boccaccio, C.; Trusolino, L. Interactions between Growth Factor Receptors and Adhesion Molecules: Breaking the Rules. *Curr. Opin. Cell Biol.* **2003**, *15*, 565–571.
(**10**) Thomas, J. R.; Moore, K. M.; Sproat, C.; Maldonado-Lorca, H. J.; Mo, S.; Haider, S.; Hammond, D.; Thomas, G. J.; Prior, I. A.; Cutillas, P. R.; Jones, L. J.; Marshall, J. F.; Morgan, M. R. Integrin $\alpha_V\beta_6$-EGFR Crosstalk Regulates Bidirectional Force Transmission and Controls Breast Cancer Invasion. *bioRxiv* **2018**, 407908.
(**11**) Bianchini, F.; Portioli, E.; Ferlenghi, F.; Vacondio, F.; Andreucci, E.; Biagioni, A.; Ruzzolini, J.; Peppicelli, S.; Lulli, M.; Calorini, L.; Battistini, L.; Zanardi, F.; Sartori, A. Cell-Targeted c(AmpRGD)-Sunitinib Molecular Conjugates Impair Tumor Growth of Melanoma. *Cancer Lett.* **2019**, *446*, 25–37.
(**12**) Sartori, A.; Corno, C.; De Cesare, M.; Scanziani, E.; Minoli, L.; Battistini, L.; Zanardi, F.; Perego, P. Efficacy of a Selective Binder of $\alpha_V\beta_3$ Integrin Linked to the Tyrosine Kinase Inhibitor Sunitinib in Ovarian Carcinoma Preclinical Models. *Cancers* **2019**, *11*, 531.
(**13**) Wollin, L.; Wex, E.; Pautsch, A.; Schnapp, G.; Hostettler, K. E.; Stowasser, S.; Kolb, M. Mode of Action of Nintedanib in the Treatment of Idiopathic Pulmonary Fibrosis. *Eur. Respir. J.* **2015**, *45*, 1434–1445.
(**14**) Battistini, L.; Burreddu, P.; Carta, P.; Rassu, G.; Auzzas, L.; Curti, C.; Zanardi, F.; Manzoni, L.; Araldi, E. M. V; Scolastico, C.; Casiraghi, G. 4-Aminoproline-Based Arginine-Glycine-Aspartate Integrin Binders with Exposed Ligation Points: Practical in-Solution Synthesis, Conjugation and Binding Affinity Evaluation. *Org. Biomol. Chem.* **2009**, *7*, 4924–4935.
(**15**) Bugatti, K.; Bruno, A.; Arosio, D.; Sartori, A.; Curti, C.; Augustijn, L.; Zanardi, F.; Battistini, L. Shifting Towards $\alpha_V\beta_6$ Integrin Ligands Using Novel Aminoproline-Based Cyclic Peptidomimetics. *Chem. Eur. J.* **2020**, *26*, 13468–13475.
(**16**) Roth, G. J.; Heckel, A.; Colbatzky, F.; Handschuh, S.; Kley, J.; Lehmann-Lintz, T.; Lotz, R.; Tontsch-Grunt, U.; Walter, R.; Hilberg, F. Design, Synthesis, and Evaluation of Indolinones as Triple Angiokinase Inhibitors and the Discovery of a Highly Specific 6-Methoxycarbonyl-Substituted Indolinone (BIBF 1120). *J. Med. Chem.* **2009**, *52*, 4466–4480.

(**17**) Ihara, H.; Mitsuishi, Y.; Kato, M.; Takahashi, F.; Tajima, K.; Hayashi, T.; Hidayat, M.; Winardi, W.; Wirawan, A.; Hayakawa, D.; Kanamori, K.; Matsumoto, N.; Yae, T.; Sato, T.; Sasaki, S.; Takamochi, K.; Suehara, Y.; Ogura, D.; Niwa, S.; Suzuki, K.; Takahashi, K. Nintedanib Inhibits Epithelial-Mesenchymal Transition in A549 Alveolar Epithelial Cells through Regulation of the TGFβ/Smad Pathway. *Respir. Investig.* **2020**, *58*, 275–284.

Chapter 5. Dual conjugates targeting $\alpha_V\beta_6$ and PAR1

5.1. Introduction

Idiopathic Pulmonary Fibrosis (IPF) is a rare, chronic and fibrotic lung disease which affects around 5 million people globally, characterized by an extremely poor prognosis and a median survival after diagnosis around 3-5 years.[1] In this pathology, an excess of conjunctive tissue, more specifically fibroblasts, settles in the lungs damaging their tissues, which consequently cannot operate in the right way. Nowadays, the origin of the IPF is not well known, but it is thought to result from the aberrant wound-healing responses to repetitive lung injury. In fact, the current pattern suggests that, after lung injury, the epithelial damage allows fibrotic cell infiltration in the alveolar *interstitium*, leading to an abnormal excess of matrix synthesis, which is characteristic of pulmonary fibrosis (Figure 1).[2] Failure of epithelial repair (with reduced epithelial proliferation and increased apoptosis) promotes fibrosis and the resulting thicker tissue is responsible for a gradual onset of shortness of breath that can eventually lead to pneumonia or heart failure.

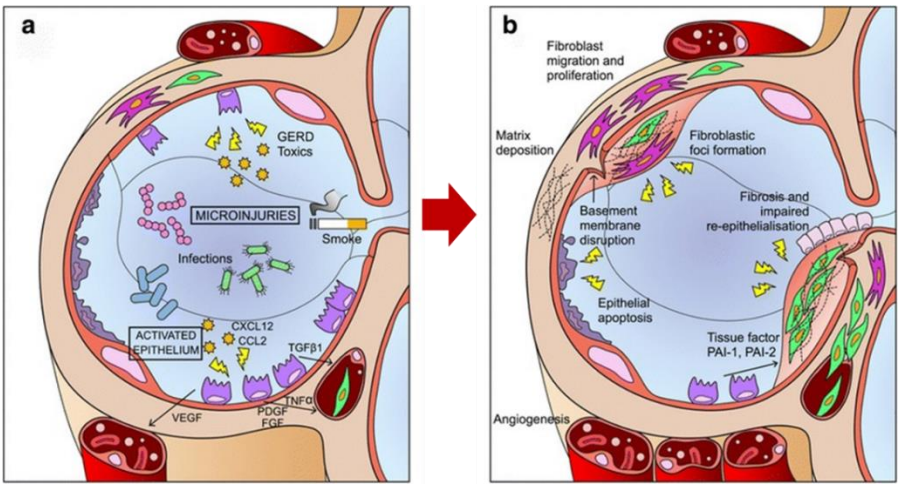

Figure 1. *Schematic view of IPF pathogenesis .Repeated injuries over time lead to maladaptive repair process, characterized by epithelial cells apoptosis, proliferation and epithelium-mesenchymal cross-talk (**a**) and following fibroblasts, myofibroblasts proliferation and accumulation of extracellular matrix (**b**). Adapted from Ref 2.*

Currently, just two drugs have been approved for IPF treatment (pirfenidone and nintedanib), though they only slow disease progression and cause several side-effects. For these reasons, research in the field of IPF is still active and many related targets are currently under investigation.[1,3]

The $\alpha_v\beta_6$ integrin has recently emerged as an attractive therapeutic target in the IPF treatment.[4] As discussed in Chapter 2, this integrin is not expressed in healthy adult epithelia, but it is overexpressed in cancer, tumorigenesis, metastasis and fibrosis. The $\alpha_v\beta_6$ integrin activates cytokine TGFβ, which is a central mediator of fibrogenesis, since it is upregulated, and it mediates fibroblasts phenotype and function. However, due to the pleiotropic and multifunctional nature of TGFβ, its inhibition maybe detrimental, leading to possible and severe side effects.[5]

The involvement of PAR receptors in inflammatory response and coagulation processes, crucial events in IPF, has been widely described.[6,7] In particular, PAR1 plays a key role in the regulation of the thrombotic response (e.g. it is involved in the formation of blood clot in blood vessels to limit the bleeding) by mediating the cooperation between coagulation and inflammatory response, which is extremely important in the development of IPF.[8] However, as described for TGFβ, PAR1 is

pleiotropic, and unselective blockage of its cascade could cause several side effects, especially in the coagulation response.

Interestingly, an axis between $\alpha_V\beta_6$ integrin and PAR1, where PAR1 seems to "help" this integrin in the activation of TGFβ, has been recently described (Figure 2).[9,10]

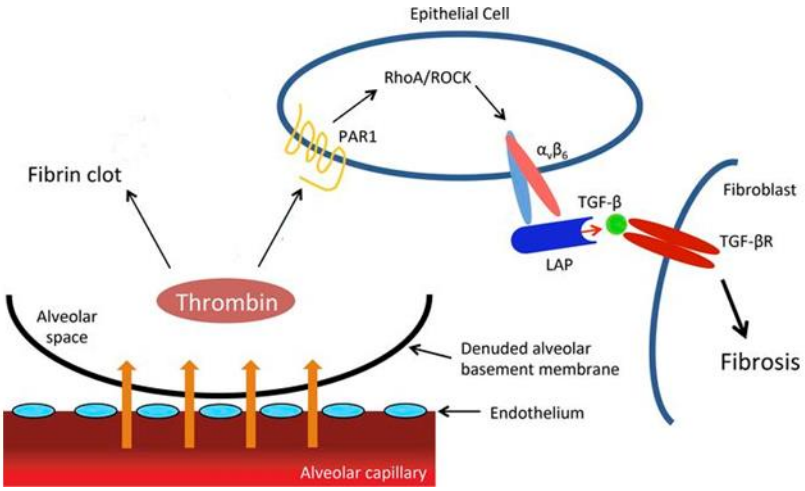

Figure 2. *Scheme of the cross-talk between PAR1 and $\alpha_V\beta_6$. Adapted from Ref 9.*

In fact, as a consequence of lung injury, the alveolar epithelium is damaged, which leads to intra-alveolar activation of the coagulation cascade and generation of active thrombin, which is a PAR1 agonist. In addition to its main "duty", namely proteolytic cleavage of fibrinogen to generate fibrin in the airspaces, thrombin also cleaves and activates proteinase activated receptor 1 (PAR1). It has been shown that activation of PAR1 on alveolar epithelial cells consequently activates the $\alpha_v\beta_6$ integrin[11] (in a RhoA- and Rho kinase-dependent manner), which results in the release of extracellular active TGFβ from the latency-associated peptide (LAP). Consequently, active TGF-β can promote signalling through its receptors to exert profibrotic effects in an autocrine way.

For this reason, the concomitant blockade of both the $\alpha_v\beta_6$ integrin and PAR1 receptors could interrupt this dangerous thrombin/PAR1/$\alpha_v\beta_6$/TGFβ axis, thereby halting the progression from lung injury to fibrosis.

5.2. Aim of the project

Based on the evidence that $\alpha_V\beta_6$ is expressed only in case of pathogenesis and PAR1 is pleiotropic, a selective $\alpha_V\beta_6$ ligand could be used as a targeting unit for the delivery of PAR1 antagonists in the diseased site; for this reason, the synthesis of novel dual covalent conjugates of type **I** (Figure 3) selectively targeting both $\alpha_V\beta_6$ integrin and PAR1 is proposed.

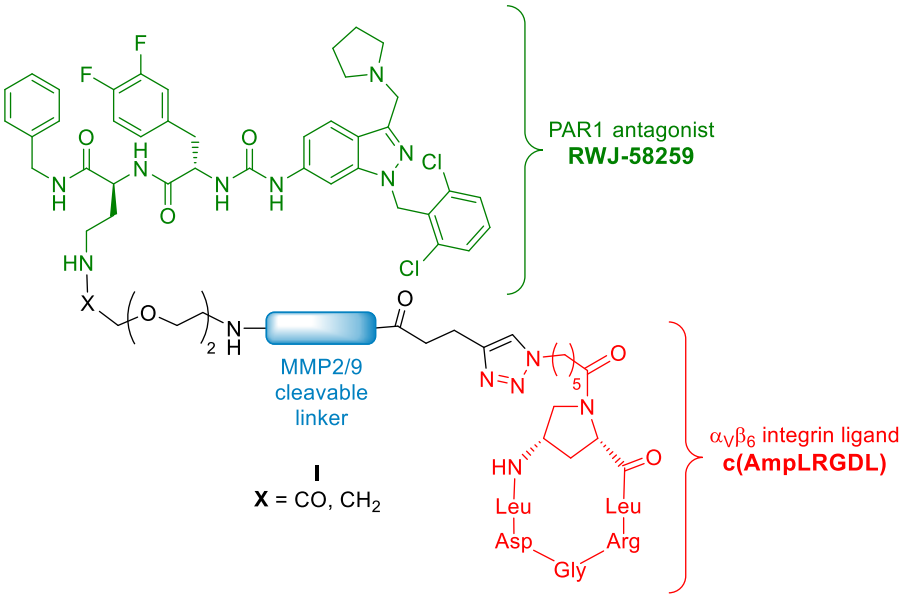

I
X = CO, CH_2

Figure 3. *Structure of the proposed $\alpha_V\beta_6$-PAR1 dual conjugates.*

The reported aminoproline-based cyclopseudopeptide c(AmpLRGDL)[12] recently synthesized in our research group has been chosen as $\alpha_V\beta_6$ integrin ligand prototype (Figure 3, depicted in red); concerning the PAR1 antagonist moiety, the known RWJ-58259 antagonist has been chosen (Figure 3, depicted in green).[13,14] As the connecting unit, a linker selectively cleavable by MMP2/9 (metalloproteases 2 and 9) was designed to be used for the *in situ* delivery of the active PAR1 antagonist, since these metalloproteases are overexpressed in the lung and, in particular, in IPF.[15] In this general scenario, and before synthesizing the projected dual conjugates, it is extremely important to verify whether the functionalization of both the PAR1 antagonist and the $\alpha_V\beta_6$ ligand would impact on their activity/selectivity toward the respective receptors. In other words, it is important to ascertain *(i)* the competence of the cyclopeptide to act as a $\alpha_V\beta_6$ integrin ligand even when connected to the appended linker and *(ii)* the ability of the RWJ-58259 moiety to act as a PAR1 antagonist when released in situ after cleavage of the linker by metalloproteases.

In this context, the aim of the present project is the design and development of the parallel synthesis of both the c(AmpLRGDL)-containing and the RWJ-58259-containing portions of the projected dual conjugates, in order to establish the feasibility of the whole plan. The two novel compounds are intended to be accessed by alternating in-solution/solid phase synthesis procedures; subsequent biological assays are planned to be executed (in collaboration with colleagues at CNR Milan and at the Institut de Recherche en Santé Digestive INSERM, Tolouse) toward $\alpha_V\beta_6$ integrin and PAR1 receptors, respectively.

5.3. Results and discussion

5.3.1. Design of a novel MMP2/9-sensitive covalent PAR1/$\alpha_v\beta_6$ integrin targeted conjugate

As discussed above, the novel proposed dual conjugate **1** (Figure 4) is constituted by the PAR1 antagonist RWJ-58259 (depicted in green), the $\alpha_v\beta_6$ integrin ligand c(AmpLRGDL) (depicted in red), the MMP2/9-sensitive cleavable linker (depicted in blue) and two spacers (depicted in black).

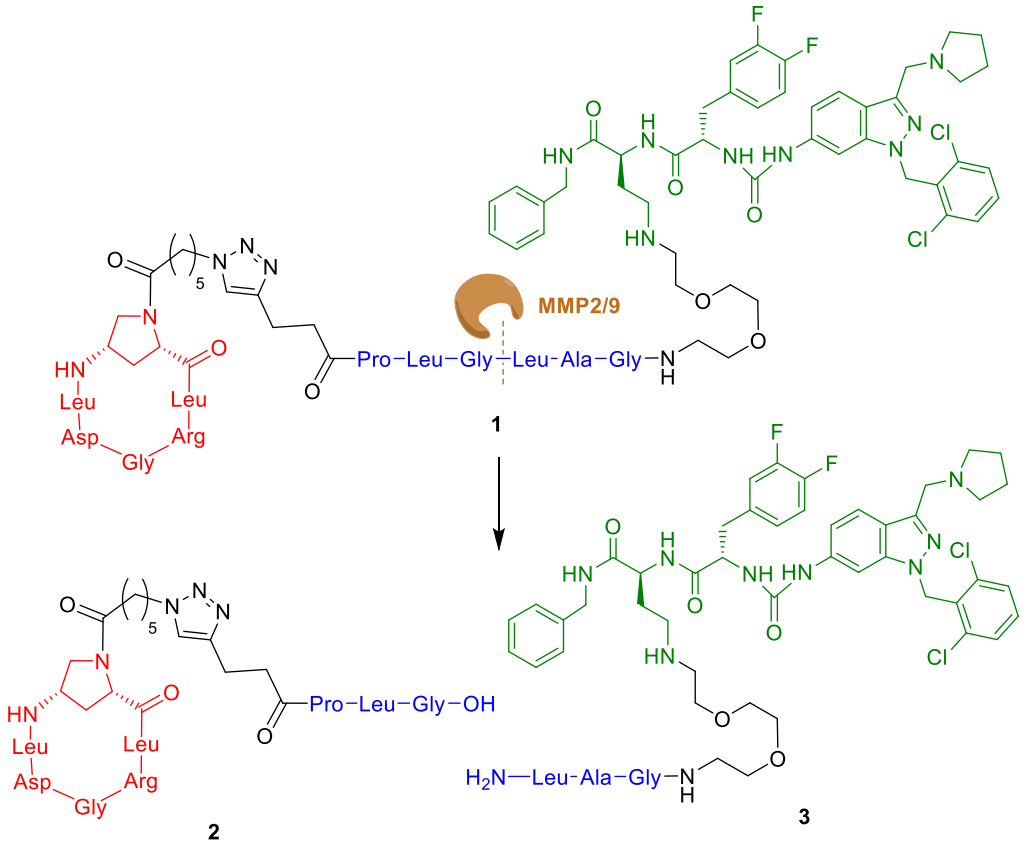

Figure 4. *Structure of the projected covalent conjugate **1** and the in situ delivered active units **2** and **3**.*

Several compounds have been reported in the literature[16] as PAR1 antagonists and one of them (vorapaxar) has recently been approved in the clinics for the reduction of thrombotic and cardiovascular events. However, since the synthesis route to this drug could be very challenging and time-consuming, this small molecule was not considered as a good starting point as PAR1 antagonist prototype. On the contrary, to prove the concept that simultaneous targeting of $\alpha_v\beta_6$ and PAR1 may result beneficial in the IPF treatment, the use of a more accessible PAR1 ligand, namely RWJ-58259 ($IC_{50(PAR1)}$ 150 nM) was judged to be more convenient.[13,14] It has to be underlined that a modified version of RWJ-58259 involving the appended primary amine has been recently reported,[17] suggesting that this amine functionality can be exploited as a useful anchoring point to synthesize the designed dual conjugates likely without perturbing the PAR1 ligand competence.

As for the linker moiety, a MMP2/9-sensitive cleavable linker has been chosen, as these metalloproteases are overexpressed in the lung and, in particular, in IPF.[15] Nowadays, many selectively cleavable linkers have been reported;[18] among them, the sequence PLG~LAG has been

frequently used and many assays and studies have been reported on this subject (in comparison with the negative-control sequence LALGPG),[19] and for this reason it has been chosen for this project.

Finally, two spacers have been selected: *(i)* a PEG2 unit, to likely ensure the right distance between the PAR1 antagonist and the peptidic linker, in order to minimize the steric interference which could negatively impact on the interaction between the ligand and its receptor, and *(ii)* a "pentynoic motif", to make the conjugation between the peptidic linker and the c(AmpLRGDL) ligand possible by a copper-catalyzed click reaction.

As mentioned above, the projected conjugates are supposed to be cleaved *in situ* by MMP2/9, generating compound **2**, the functionalized version of the $\alpha_v\beta_6$ integrin ligand c(AmpLRGDL), and compound **3**, the functionalized version of the PAR1 antagonist RWJ-58259; before synthesizing the whole conjugate, it is important to know whether and how these structural modifications affect the activity toward the respective receptors. For this reason, in the following chapters the synthesis of compounds **2** and **3** will be described.

5.3.2. Synthesis of functionalized cyclopeptide 2

Scheme 1. *Retrosynthetic approach (Eq. 1) and synthesis (Eq. 2) of compound* ***2.***[a]

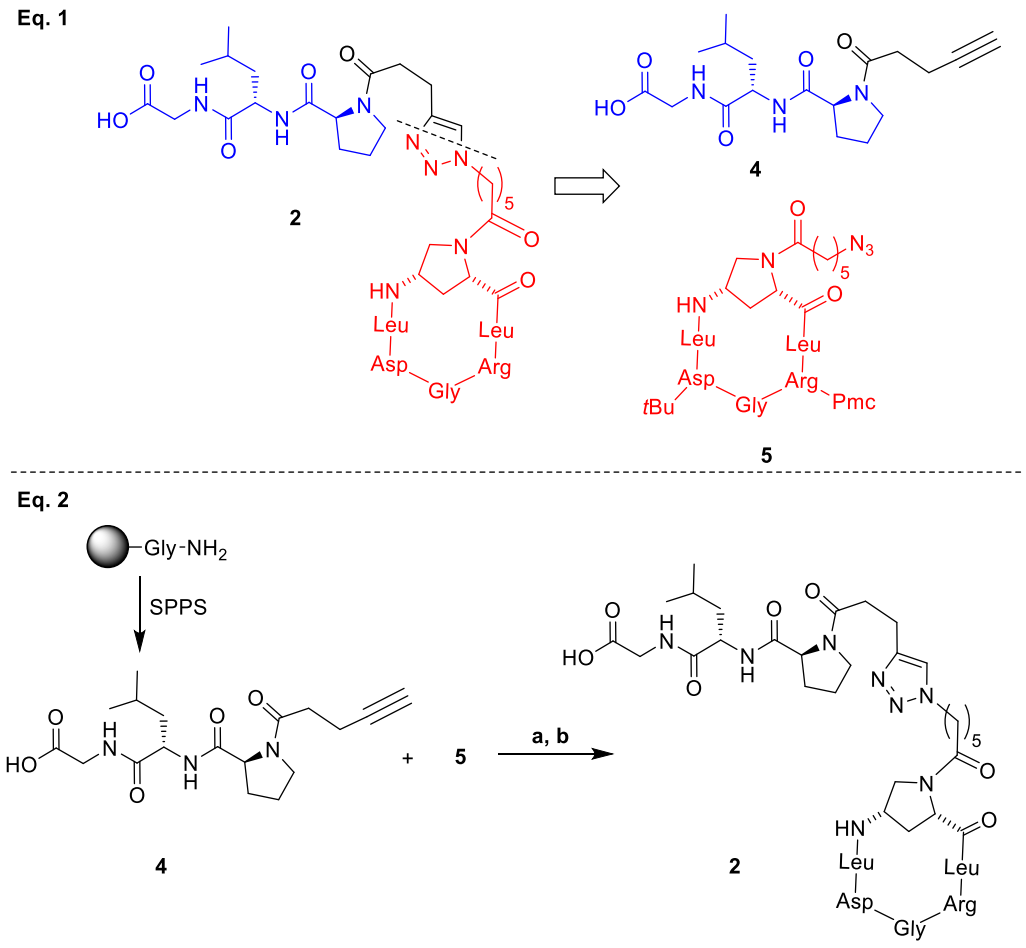

[a]Reagents and conditions: **Fmoc-SPPS**: (i) Fmoc-Leu-OH, Fmoc-Pro-OH, 4-pentynoic acid; HATU, HOAt, collidine, DMF, rt, (ii) piperidine, DMF, rt, (iii) AcOH, TFE, DCM, rt, 94% yield; **a**) $Cu(OAc)_2$, sodium ascorbate, DMF/H_2O 7:3, 6.5h, rt, 80% yield; **b**) TFA/TIS/H_2O (95:2.5:2.5), 1h, rt, 72% yield.

Compound **2** can be the product of a copper-catalyzed click reaction between alkyne **4** (Scheme 1, Eq. 1) and azide **5**; the synthesis of peptide **4** was performed by SPPS, while cyclopeptidomimetic **5** was synthesized as reported in Chapter 2 (Paragraph 2.3.2.).

Linear peptide **4** was synthesized using the Fmoc-based SPPS protocol starting from the preloaded H-Gly-2-ClTrt resin (Scheme 1, Eq. 2); each amino acid was sequentially added to the growing sequence, alternating coupling steps (HATU, HOAt and collidine) and Fmoc cleavage procedures (piperidine/DMF). At the end of the desired sequence, the cleavage from the resin was performed using acid conditions (AcOH/TFE/DCM) to obtain the linear peptide **4** in very good yield (94%). Then, a copper-catalyzed click reaction between compounds **4** and **5** was performed. Initially, this reaction was carried out in acetonitrile; however, after 24 hours only the presence of the two starting materials was observed; thus, the reaction was performed in a solvent mixture of DMF and H_2O (7:3), yielding the protected intermediated (not shown) in good yield (80%). It is extremely important to perform the reaction with a minimum excess of azide **5** (1.1 equivalent), to ensure the complete conversion of alkyne **4**; indeed, purification of the final compound **2** from the residues of the unreactive alkyne **4** resulted very challenging. Finally, "clicked" intermediate was deprotected in acidic conditions, giving the final functionalized cyclopeptidomimetic **2** in a 74% yield.

5.3.3. Synthesis of compound 3, the functionalized version of RWJ-58259

Compound **3** (Scheme 2) can be disconnected at the secondary amine, tracing back to the reported antagonist RWJ-58259 **6** and the PEG-peptide **7**, which in turn can be disconnected at the glycine residue, yielding triethylene glycolamine **8** and the tripeptide **9**.

Scheme 2. *Retrosynthetic approach of compound **3**.*

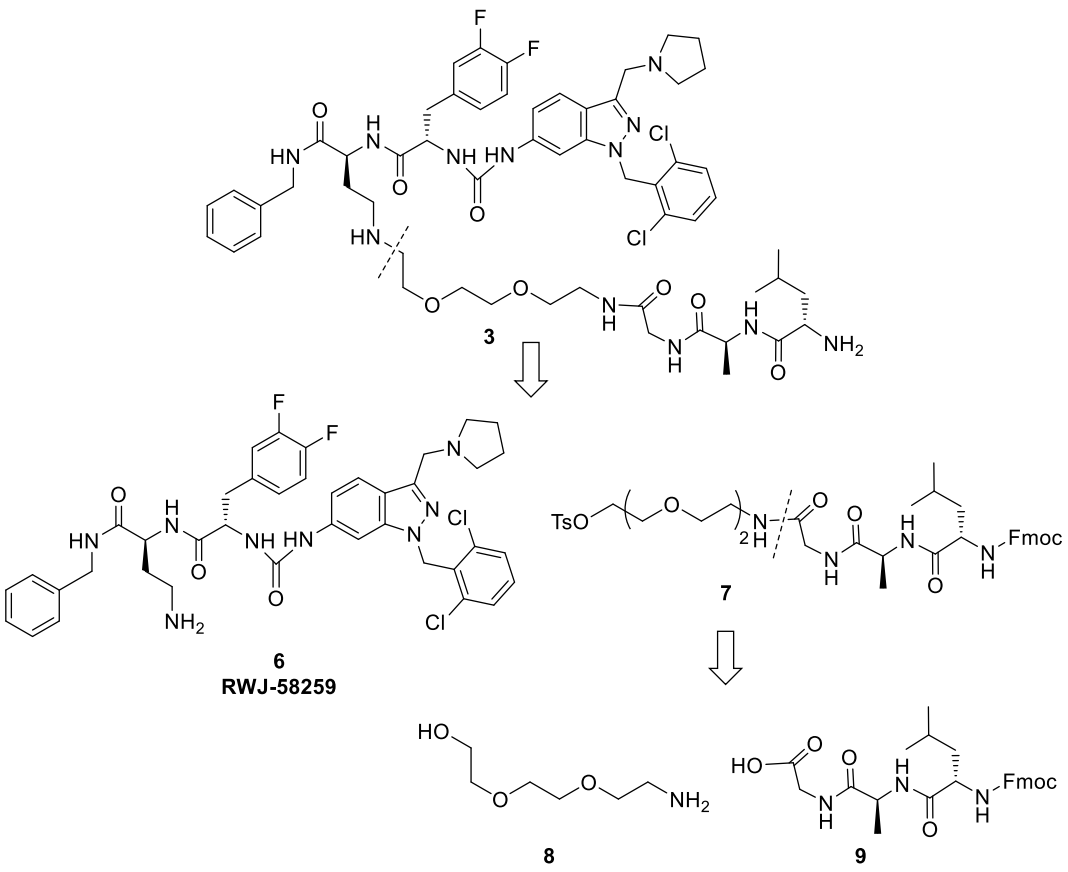

Compound **8** is a commercially available reagent and peptide **9** can be easily synthesized by SPPS, as described for peptidomimetic **4**; the PAR1 antagonist RWJ-58259 **6** was planned to be synthesized as reported in the literature,[17,20] despite the synthesis route resulted unexpectedly very challenging and required to be optimized.

Scheme 3. *Synthesis of compound **6** (Eq.1) and compound **7** (Eq. 2).*[a]

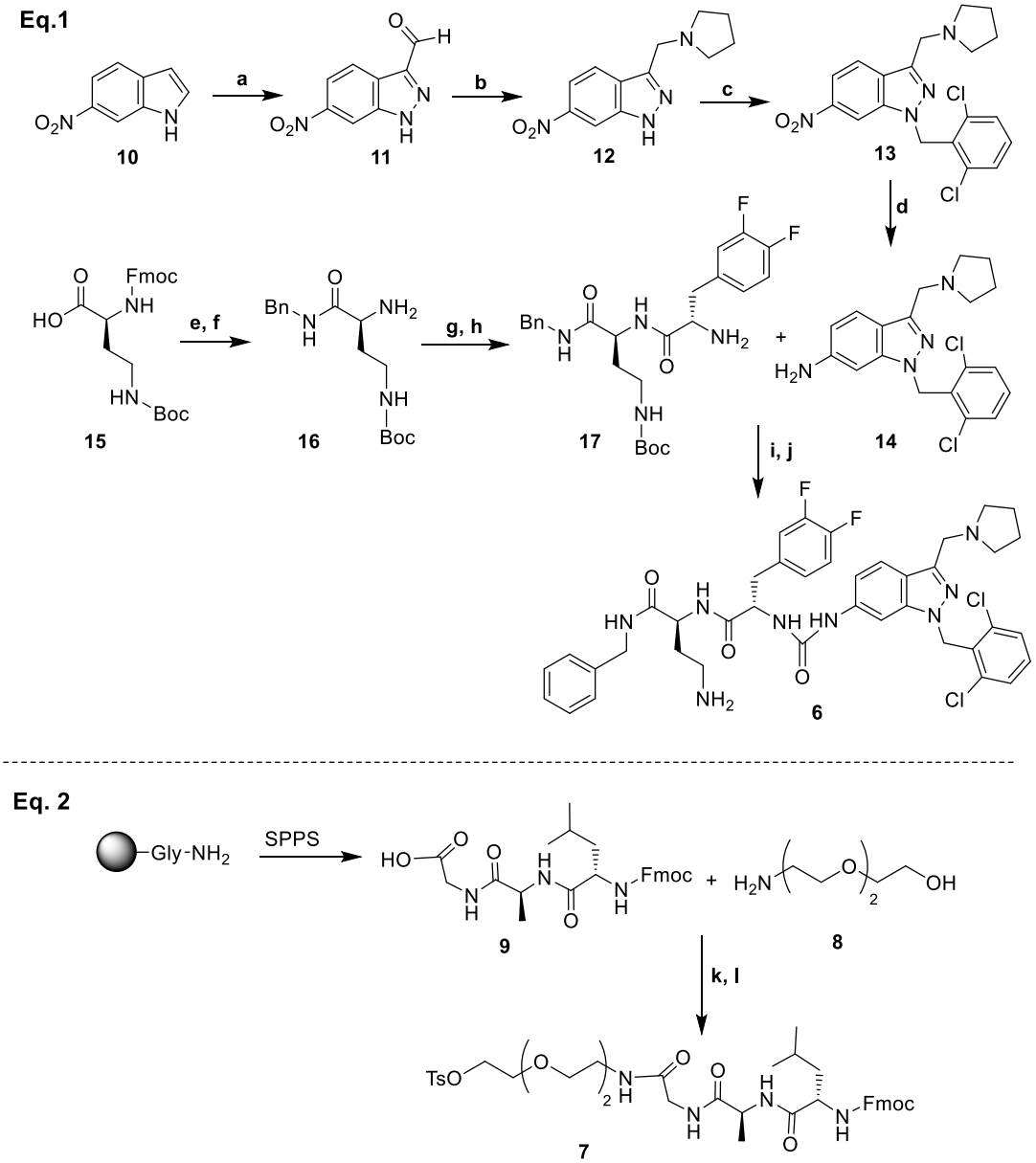

[a]Reagents and conditions: **a**) $NaNO_2$, HCl 6N, H_2O, rt, 4h, quant. yield; **b**) pyrrolidine, $NaBH(OAc)_3$, DCE/DMF/AcOH 90:9:1, rt, 3.5h, 80% yield; **c**) 2,6-dichlorobenzyl bromide, Cs_2CO_3, THF, 50 °C, 6h, 64% yield; **d**) monohydrated hydrazine, $FeCl_3 \cdot 6H_2O$, MeOH, activated charcoal, 100 °C, 2h, 83% yield; **e**) benzylamine, HATU, collidine, rt, 4h, 95% yield; **f**) piperidine, DCM/ACN, rt, 3h, 91% yield; **g**) Fmoc-3,4-difluoroPhe-OH, HATU, HOAt, collidine, rt, 3h, 81% yield; **h**) piperidine, ACN, rt, 2h, 95% yield; **i**) triphosgene, DMAP, DIPEA, dry THF, -5° C to rt, 3h; **j**) HCl in 1,4-dioxane 4N, 1h, rt, 97% yield (two steps); **Fmoc-SPPS**: (i) Fmoc-Ala-OH, Fmoc-Leu-OH; HATU, HOAt, collidine, DMF, rt, (ii) piperidine, DMF, rt, (iii) AcOH, TFE, DCM, rt, 95% yield; (**k**) HATU, HOAt, DIPEA, dry DMF:DCM, rt, 6h, 85% yield; (**l**) *p*-TsCl, DMAP, dry ACN, 50 °C, 25% yield.

Originally, for the synthesis of compound **6** it was planned to use an alternating in-solution/solid phase approach, as described in the literature,[21] to avoid the time-consuming purification steps and rendering the synthesis faster. However, the solid phase synthesis resulted very arduous: in

particular, the final step of the urea formation resulted extremely complicated and the final compound **6** was never observed, despite the numerous attempts. For this reason, the synthesis was finally performed using in-solution reactions (Scheme 3, Eq. 1).

As described in the literature, indazole **11** was synthesized by treating indole **10** with $NaNO_2$ in HCl 6N (quant. yield). Then, compound **11** was subjected to a reductive amination with pyrrolidine in the presence of $NaBH(OAc)_3$, yielding compound **12** in an 80% yield. A nucleophilic substitution between 2,6-dichlorobenzyl bromide and indazole **12** was performed in basic conditions, and the resulting product **13** was subjected to a nitro-selective reduction. Initially, the nitro-reduction was performed with zinc and ammonium chloride, as described in Chapter 4 (Paragraph 4.3.3.); however, the reaction led to many different by-products (likely arisen from polymerization reactions) while the desired amine **14** was not observed. Then, a palladium-catalysed reduction in hydrogen atmosphere was performed in several solvent systems: in these conditions, formation of product **14** was observed but isolation from the numerous by-products resulted very challenging. Next, the reaction was carried out by using monohydrated hydrazine, $FeCl_3$ in MeOH at 65° C; again, no product **14** was observed, but interestingly with this procedure only few by-products were generated. Finally, the reaction was performed exactly as described by Dockendorff et al.,[17] by using monohydrated hydrazine, $FeCl_3 \cdot 6H_2O$, activated charcoal, MeOH in a Schlenk tube, keeping the temperature at 100 °C for 2 hours. This procedure nicely produced the amine product **14** in a very good 85% yield.

Dipeptide **17** was obtained with an alternating in-solution coupling reaction and Fmoc-deprotection, as described in the literature.[21] Then, compounds **17** and **14** were coupled to the final urea formation, leading to the PAR1 antagonist RWJ-58259. Initially, this reaction was performed with 4-nitrophenylchloroformate, as reported in the literature;[21] however, RWJ-58259 was not observed, despite different activation conditions of both starting compounds **17** and **14** were adopted. Additionally, one of the isolated by-products seemed to indicate that the "indazole nucleus" **14** degraded during the reaction, maybe due to the pyrrolidine motif unexpectedly reacting with 4-nitrophenylchloroformate. Given these unsuccessful results, the urea formation was attempted using triphosgene as the coupling reagent, as reported by Dockendorff et al.;[17] indeed, using triphosgene and DMAP, the urea function was successfully implemented. During the execution of this step, we became aware of the fact that it is important not to isolate the Boc-protected intermediate by chromatographic purification, since this compound has a very poor solubility in the commonly used solvents. For this reason, Boc removal was performed directly on the crude protected urea by using HCl and dioxane, yielding the final PAR1 antagonist RWJ-58259 in a high yield (97%). Of note, the reported procedure was implemented in our hands, raising the reaction yield from a modest 58% to a very good 97%, as reported in Table 1, which summarizes the distinct attempts to achieve the urea functionality within **6**.

Then, the synthesis of the pegylated peptide **7** was performed as shown in Scheme 3 (Eq. 2). Firstly, peptide **9** was synthesized by SPPS, as described for compound **4**. A coupling reaction with triethylene glycolamine **8** and peptide **9** was carried out using HATU, HOAt and DIPEA and producing an alcohol intermediate (not shown) in 85% yield, which was next subjected to tosylation by means of *p*-TsCl and DMAP, ultimately giving compound **7** in a poor, yet optimizable 25% yield.

Table 1. *Reagents and conditions for the synthesis of urea* ***6****.*[a]

Entry	Indazole 14	Amine 17	DMAP	Triphosgene	DIPEA	Time	Yield%
1	2.75 eq	1.77 eq	7.05 eq	1.00 eq	---	2 h	58%
2	2.75 eq (HCOOH salt)	1.77 eq	7.05 eq	1.00 eq	---	2 h	10%
3	2.75 eq (HCOOH salt)	1.77 eq	8.00 eq	1.00 eq	1.00 eq	2 h	26%
4	2.75 eq	1.50 eq	7.00 eq	1.00 eq	---	2 h	90%
5	2.60 eq	1.33 eq	5.50 eq	1.00 eq	1.50 eq	3 h	97%

[a]Entry 1 corresponds to the reported procedure. Ref. 17.

The final nucleophilic substitution reaction between amine **6** and tosyl compound **7** was performed in dry ACN in presence of Cs_2CO_3 (as described for a similar tosylated spacer in Chapter 4, Paragraph 4.3.3.), but the reaction unexpectedly led to the Fmoc-deprotection of compound **7** instead of substituted product **3**. This unpredicted result guided us to modify the synthesis route, planning to perform *(i)* the oxidation of alcohol precursor of **7** to an aldehyde intermediate to be exploited in a reductive amination with amine **6**, or alternatively *(ii)* the oxidation of the same alcohol to carboxylic acid to be used in a peptide coupling reaction with amine **6**. These experiments are currently underway, and their outcome will drive us in the synthesis of novel functionalized PAR1 antagonists, hopefully endowed with biological activity similar to the reference antagonist RWJ-58259.

5.4. Conclusions and perspectives

IPF is a chronic and rare disease with poor prognosis and the drugs currently in commerce just slow the disease progression. For these reasons, it is extremely important keeping going to investigate novel targets and therapeutics. One strategy in this direction would imply the perturbation/modulation of the crosstalk between $\alpha_V\beta_6$ and PAR1 *via* the use of a selective dual-conjugated small molecules which could help to elucidate the pathogenesis and to find novel treatments for this aggressive disease. In this work, the design of the novel cleavable covalent conjugate **1** (Figure 4) was implemented, and the synthesis of compound **2**, a functionalized version of a known $\alpha_V\beta_6$ integrin ligand, as well as the synthesis of advanced intermediates **6** and **7** toward amine **3** or amide **3a**, modified functionalized versions of the known PAR1 antagonist, were shown (Figure 5). The optimization of the synthesis route and the synthesized novel compounds will drive us to understand, after suitable in vitro biological evaluation, to what extent the introduced structural modifications could alter the biological activity of the original ligands, with the ultimate goal of synthesizing novel covalent and dual conjugates as investigational probes and potential chemotherapeutics for IPF.

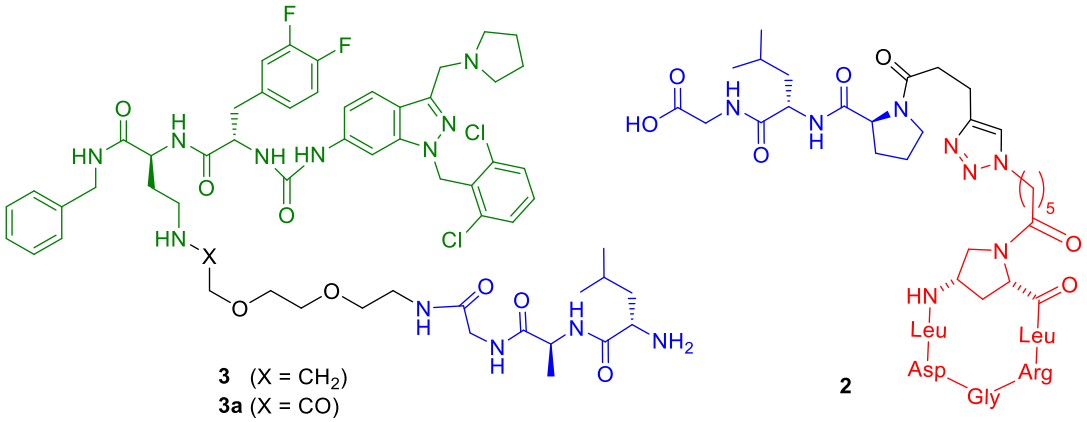

Figure 5. *Structure of compounds **3**, **3a** and **2** targeted in this work.*

5.5. Experimental section

5.5.1. General methods and materials

General. See Chapter 2, Paragraph 2.5.2.1.

Materials. H-Gly-2-ClTrt resin, Fmoc-Ala-OH; Fmoc-Pro-OH, Fmoc-3,4-difluoroPhe-OH, 4-pentynoic acid, 2,4,6-collidine, glacial acetic acid, DIPEA, HATU, HOAt, 4-azidobutanol, 3-aminopropanol, triphosgene, DMAP, 4-toluelsulfonyl chloride, triethylene glycolamine, 6-nitroindole, (S)-4-(Boc-amino)-2-(Fmoc-amino)butyric acid, 2,6-dichlorobenzyl bromide were commercially available and were used as such without further purification. Peptidomimetic **5** was synthesized as reported in Chapter 2, Paragraph 2.5.2.1 (see compound **22**).

Experimental synthetic procedures and characterization data

Synthesis of tripeptide 4

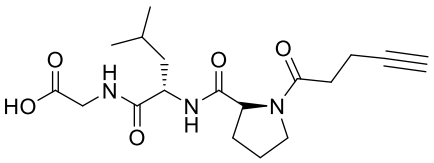

4

Peptide **4** was synthesized according to the general procedure for Solid Phase Synthesis described in Chapter 2 (Paragraph 2.5.2.1.) for compound **11**, using the preloaded 2-chlorotrityl-Gly-H resin (loading 0.63 mmol/g, 435.0 mg, 0.274 mmol, 1 eq), Fmoc-Leu-OH (145.6 mg, 0.411 mmol, 1.5 eq), Fmoc-Pro-OH (138.6 mg, 0.411 mmol, 1.5 eq) and 4-pentinoic acid (40.3 mg, 0.411 mmol, 1.5 eq). After the cleavage from the resin, the linear tripeptide **4** (93.8 mg, 94% yield) was collected as a colourless glassy solid, which was used in the following step without further purification. ^{1}H NMR (400 MHz, MeOD) (*2 atropisomers, 1:0.3, spectrum of the major one*) δ 4.46 (dd, *J* = 10.5, 4.9 Hz, 1H, αLeu), 4.39 (dd, *J* = 8.5, 3.7 Hz, 1H, αPro), 3.94 (d, *J* = 17.9, 1H, αGly), 3.87 (dd, *J* = 17.9 Hz, 1H, αGly), 3.74-3.57 (m, 2H), 2.64 (t, *J* = 7.8 Hz, 2H), 2.48-2.41 (m, 2H), 2.37-2.17 (m, 2H), 2.26 (t, *J* = 2.4 Hz, 1H, CH Alkyne), 2.02 (m, 2H), 1.80-1.54 (m, 3H), 0.96 (d, *J* = 6.8 Hz, 3H, δLeu), 0.92 (d, *J* = 6.0 Hz, 3H, δLeu). MS (ES$^+$) *m/z* 366.3 $[M+H]^+$.

Synthesis of tripeptide 2a

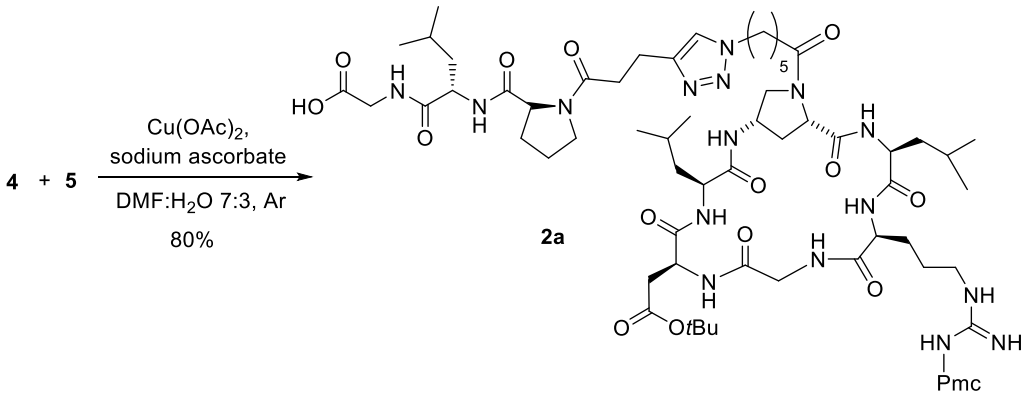

To a solution of compound **4** (3.00 mg, 0.0080 mmol, 1 eq) and cyclopeptide **5** (12.20 mg, 0.0090 mmol, 1.1 eq) in DMF (1.20 mL), a solution of $Cu(OAc)_2$ (0.49 mg, 0.0025 mmol, 0.3 eq) and sodium ascorbate (0.98 mg, 0.0048 mmol, 0.6 eq) in water (0.52 mL) was added. The reaction was left under stirring under argon atmosphere after 3 cycles of argon/vacuum. After 6.5 h, the solvent was removed under reduced pressure and the residue was carefully washed with water (3x). The crude product was purified by reverse phase chromatography (gradient: from 90:10 H_2O+0.1%TFA:ACN to 100% ACN) affording the protected cyclopeptide **2a** as a colourless glassy solid (10.30 mg, TFA salt, 80% yield). TLC: EtOAc:MeOH 80:20+ 0.1% AcOH, R*f* = 0.1. ^{1}H NMR (400 MHz, CD_3OD) δ 7.97 (bs, 1H, CH triazole), 4.54-4.45 (m, 2H), 4.45-4.32 (m, 5H), 4.16 (s, 1H), 4.11-3.98 (m, 2H), 3.94-3.82 (m, 3H), 3.74-3.69 (m, 1H), 3.60-3.49 (m, 2H), 3.44 (m, 1H), 3.28-3.14 (m, 2H), 3.07-3.01 (m, 2H), 2.92 (dd, *J* = 16.4, 4.5 Hz, 1H), 2.84-2.72 (m, 2H), 2.68 (t, *J* = 6.9 Hz, 2H, CH_2 Pmc), 2.56 (s, 3H, CH_3 Pmc), 3.55 (s, 3H, CH_3 Pmc), 2.54-2.48 (m, 1H) 2.44-2.35 (m, 1H), 2.32-2.18 (m, 2H), 2.11 (s, 3H, CH_3 Pmc), 2.06-1.82 (m, 10H), 1.81-1.50 (m, 15H), 1.44 (m, 9H, CH_3 *t*Bu), 1.31 (m, 8H, CH_3 Pmc), 1.01-1.08 (m, 18 H, Hδ Leu). MS (ES$^+$) *m/z* 1494.1 $[M+H]^+$.

Synthesis of tripeptide 2

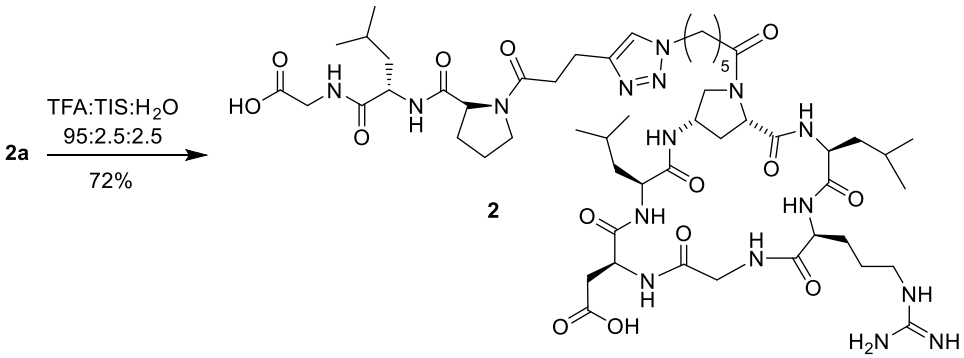

Cyclopeptide **2** (10.30 mg, 0.006 mmol, 1 eq) was deprotected using a solution of TFA:TIS:H_2O 95:2.5:2.5 (457.0 μL). The reaction was kept under stirring for 1 h, then the solvent was removed under reduced pressure. The crude was carefully washed with Et_2O and then purified by reverse phase chromatography (eluent: from 80:20 H_2O+0.1%TFA:ACN to 20:80 80:20 H_2O+0.1%TFA: ACN), giving the final conjugate **2** (7.4 mg, TFA salt 72% yield). ^{1}H NMR (400 MHz, MeOD) δ 7.85 (s, 1H, CH triazole), 4.48- 4.37 (m, 5H), 4.36-4.32 (m, 2H), 4.12 (m, 1H), 4.05 – 4.00 (m, 1H), 3.91-2.81 (m, 2H), 3.76 (d, *J* = 17.7 Hz, 1H, αGly), 3.53 (m, 1H), 3.45 (m, 1H), 3.24-3.13 (m, 2H), 3.04-2.97 (m, 1H), 2.94 (dd, *J* = 17.1, 4.2 Hz, 1H), 2.85-2.75 (m, 2H) 2.74-2.68 (m, 1H), 2.67 (m, 1H), 2.55-2.37 (m, 2H), 2.32 – 2.18 (m, 2H), 1.99-1.80 (m, 12H), 1.76-1.55 (m, 12H), 1.28 (m, 3H), 0.98 – 0.84 (m, 18H, δ Leu). MS (ES$^+$) *m/z* 1172.0 $[M+H]^+$.

Synthesis of 6-nitro-1*H*-indazole-3-carbaldehyde 11

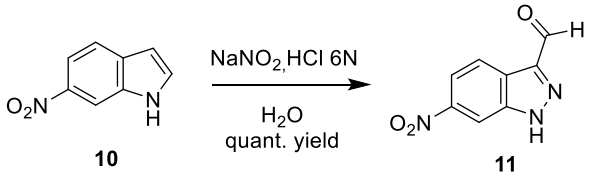

To a solution of $NaNO_2$ (2.13 g, 30.8 mmol, 10 eq) in H_2O (50.0 mL), 6-nitroindole **10** (0.5 g, 3.1 mmol, 1 eq) was added and the resulting yellow suspension was vigorously stirred for 5 minutes. Then, 6N aq HCl (4.6 mL) was added dropwise over a period of 15 minutes and the resulting

suspension was left to stir for 4 hours. Then, the reaction was filtered on Büchner and the precipitate was washed with water (5x). The resulting brown solid was dissolved in EtOAc and the solvent was evaporated under reduced pressure, yielding compound **11** as a brownish solid (0.77 g, quantitative yield). TLC: Petroleum Ether:EtOAc 7:3, R*f* = 0.4. ^{1}H NMR (400 MHz, DMSO) δ 14.79 (s, 1H, NH), 10.25 (s, 1H, CHO), 8.61 (s, CH 7-indazole), 8.33 (d, *J* = 8.8 Hz, 1H, CH 4-indazole), 8.17 (bd, *J* = 8.8 Hz, 1H, CH 5-indazole). MS (ES$^+$) *m/z* 192.1 $[M+H]^+$.

Synthesis of compound 12

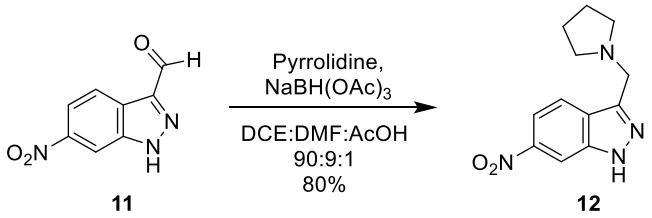

Aldehyde **11** (935.9 mg, 4.89 mmol, 1 eq) was dissolved in a solution of DCE:DMF:AcOH 90:9:1 (240.0 mL) and pyrrolidine (2.0 mL, 24.48 mmol, 5 eq) was added, and the solution instantly turns from translucid to red. $NaBH(OAc)_3$ (6.2 g, 29.38 mmol, 6 eq) is added in 3 portions at 5 minutes intervals and the resultant suspension was left stirring for 3.5 hours. Then the solvent was removed under reduced pressure and water was added, and the residue was extracted with EtOAc:H_2O saturated with Na_2CO_3 (3x). The collected organic layers were concentrated under reduced pressure and the crude was purified by flash chromatography (eluent: from 100% DCM to 85:15 DCM/MeOH•NH_3), yielding product **12** as brownish glassy solid (504.0 mg, 80% yield). TLC:DCM:MeOH•NH_3) 95:5, R*f* = 0.4. ^{1}H NMR (400 MHz, $CDCl_3$) δ 8.29 (m, 1H, CH 7-indazole), 7.89 (m, 2H, CH 4,5-indazole), 4.12 (s, 2H, CH_2), 2.71 (m, 4H, CH_2 pyrrolidine), 1.82 (m, 4H, CH_2 pyrrolidine). MS (ES$^+$) *m/z* 247.3 $[M+H]^+$.

Synthesis of compound 13

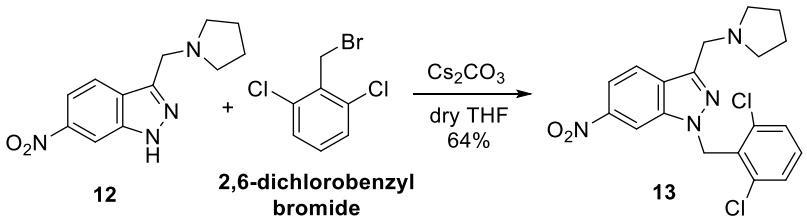

To a solution of indazole **12** (504.0 mg, 2.05 mmol, 1 eq) in dry THF (24.0 mL), Cs_2CO_3 (534.3 mg, 1.64 mmol, 0.8 eq) and 2,6-dichlorobenzilbromide (491.8 mg, 2.05 mmol, 1 eq) were added. The reaction was kept stirring at room temperature for 6 hours, then Cs_2CO_3 (134.0 mg, 0.41 mmol, 0.2 eq) was added and the reaction was kept stirring for additional 17 hours at room temperature, 2 hours at 40 °C and 4 hours at 55°C. The reaction mixture was concentrated by removing the solvent under reduced pressure. Then, water (10 mL) was added and extracted with EtOAc (3x). The collected organic layers were concentrated under reduced pressure and the crude was purified by flash chromatography (eluent: from 100% EtOAc to 90:10 EtOAc:MeOH), yielding the *N*-substituted product **13** as yellow solid (530.0 mg, 64%). TLC: EtOAc:MeOH•NH_3 98:2, R*f* = 0.5. ^{1}H NMR (400 MHz, $CDCl_3$) δ 8.24 (s, 1H, ArH), 7.89 (d, *J* = 8.7 Hz, 2H, ArH), 7.32-7.28 (d, *J* = 7.8 Hz, 2H, ArH), 7.19 (t, *J* = 8.16 Hz, 1H, ArH), 5.77 (s, 2H, CH_2), 3.92 (s, 2H, CH_2), 2.49 (s, 4H, CH_2 pyrrolidine), 1.69 (m, 4H, CH_2 pyrrolidine). MS (ES$^+$) *m/z* 405.1 $[M+H]^+$.

Synthesis of compound 14

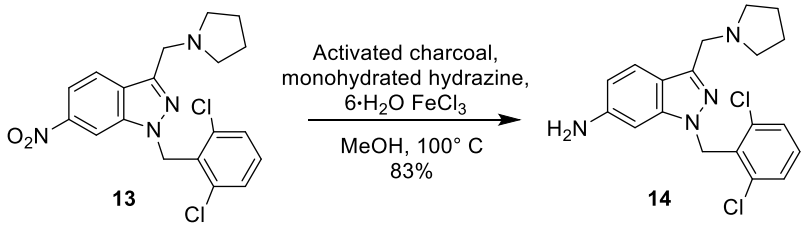

To a solution of nitro derivate **13** (200.0 mg, 0.49 mmol, 1 eq) in dry MeOH (50.0 mL) in a dried pressure tube reactor, activated charcoal (25% mmol), monohydrated hydrazine (384.8 µL, 7.89 mmol, 16 eq) and iron (III) chloride hexahydrate (33.3 mg, 0.12 mmol, 0.25 eq) were added. The reaction mixture was degassed and conditioned with nitrogen. The reactor was then closed and kept under stirring at 100 °C for 2 hours. Then, the reaction was allowed to return at room temperature and the solution was filtered. The collected organic layers were concentrated under reduced pressure. The crude was purified by flash chromatography (eluent: from 95:5 DCM:MeOH to 80:20), yielding aniline derivate **14** as a white solid (153.7 mg, 83% yield). TLC: DCM:MeOH 9:1, R*f* = 0.3. ^{1}H NMR (400 MHz, MeOD) δ 7.52 (d, *J* = 8.4 Hz, 1H, CH 4-indazole), 7.43 (dd, *J* = 8.0, 1.12 Hz, 2H, ArH), 7.33 (dd, *J* = 8.8, 7.2 Hz, 1H, ArH), 6.72 (d, *J* = 1.76 Hz, 1H, CH 7-indazole), 6.68 (dd, *J* = 8.6 ,1.76 Hz, 1H, CH 5-indazole), 5.64 (s, 2H, CH_2), 4.09 (bs, 2H, CH_2), 2.86 (m, 4H, CH_2 pyrrolidine), 1.83 (m, 4H, CH_2 pyrrolidine).

Synthesis of compound 16a

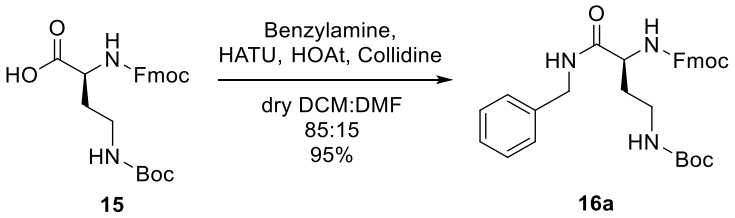

To a solution of acid **15** (500.0 mg, 1.14 mmol, 1 eq) in a mixture DCM:DMF 85:15 dry (67 mL), HBTU (430.4 mg, 1.14 mmol, 1 eq), HOAt (154.5 mg, 1.14 mmol, 1 eq) and collidine (150 µL, 1.14 mmol, 1 eq) were added. The mixture was left to stir for 3 min, then benzylamine (133.8 µL, 1.25 mmol, 1.1 eq) was added. The reaction was kept stirring for 4 hours, then water (10 mL) was added and it was extracted with DCM (2x). The collected organic layers were dried over Na_2SO_4, filtered and the solvent was evaporated under reduced pressure. The crude was purified by flash chromatography (eluent: from 80:20 EtOAc:Petroleum Ether, to 100% EtOAc, then to 60:40 EtOAc:MeOH), yielding product **16a** as white solid (573.0 mg, 95% yield). TLC: EtOAc:Petroleum Ether 8:2, R*f* = 0.8. ^{1}H NMR (400 MHz, MeOD) δ 7.79 (d, *J* = 7.3 Hz, 2H, ArH Fmoc), 7.67 (d, *J* = 7.2 Hz, 2H, ArH Fmoc), 7.38 (t, *J* = 7.4 Hz, 2H, ArH Fmoc), 7.33-7.17 (m, 7H, ArH), 4.46-4.32 (m, 4H, CH_2+CH_2 Fmoc), 4.21 (t, *J* = 6.7 Hz, 1H, CH Fmoc), 4.13 (dd, *J* = 9.6, 4.9 Hz, 1H, CHα), 3.20-2.99 (m, 2H, CH_2), 1.99-1.86 (m, 1H, CH_2β), 1.82-1.67 (m, 1H, CH_2β), 1.42 (s, 9H, CH_3 Boc). MS (ES$^+$) *m/z* 530.6 $[M+H]^+$.

Synthesis of compound 16

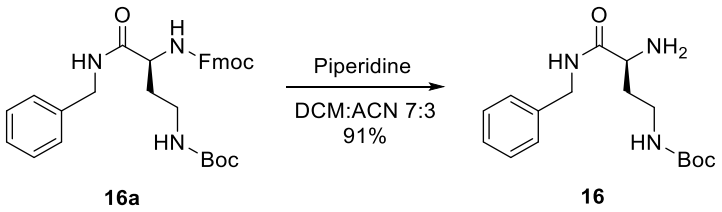

To a solution of compound **16a** (416.0 mg, 0.79 mmol, 1 eq) in ACN:DCM 70:30 (28.0 mL) piperidine (168.0 µL, 1.69 mmol, 2.15 eq) was added. The reaction was kept stirring for 3 hours, then the solvent was removed under reduced pressure and the resulted crude material was purified by flash chromatography (eluent: from 100% EtOAc to 95:15 EtOAc:MeOH•NH_3), yielding product **16** as white solid (219.4 mg, 91% yield). TLC: EtOAc:MeOH•NH_3, R*f* = 0.5. ^{1}H NMR (600 MHz, MeOD) δ 7.33-7.28 (m, 4H, ArH), 7.26-7.22 (m, 1H, ArH), 4.39 (m, 2H, CH_2), 3.36-3.33 (m, 1H, CHα), 3.19-3.08 (m, 2H, CH_2), 1.87-1.79 (m, 1H, CH_2β), 1.62 (m, CH_2β), 1.40 (s, 9H, CH_3 Boc). MS (ES$^+$) *m/z* 308.2 $[M+H]^+$.

Synthesis of compound 17a

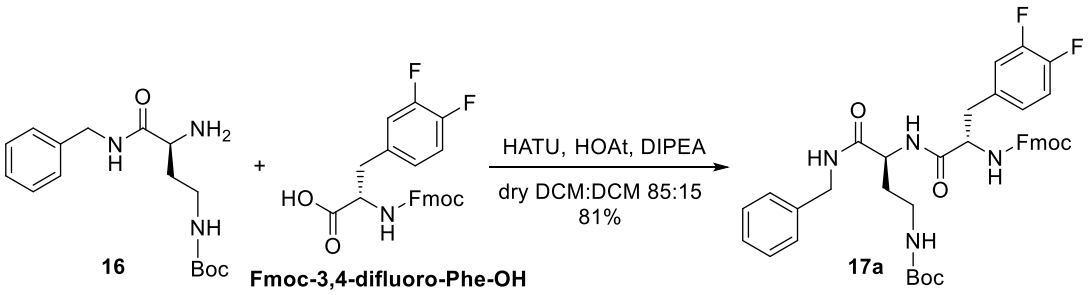

Compound **17** was synthesized as described for compound **16a**, using Fmoc-3,4-difluoro-Phe-OH **I** (273.9 mg, 0.65 mmol, 1 eq) and amine **16** (219.4 mg, 0.71 mmol, 1.1 eq). The reaction was kept stirring for 3 hours, then the solvent was removed under reduced pressure. Then, water (10 mL) was added and the mixture was extracted with DCM (2x). The collected organic layers were filtered on Büchner. The solid residue was collected with DCM and the solvent was removed under reduced pressure. The crude was purified by flash chromatography (eluent: from 80:20 EtOAc:Petroleum Ether to 100% EtOAc, then to 80:20 EtOAc:MeOH), yielding product **17a** as white solid (375.0 mg, 81% yield). TLC: EtOAc:MeOH 9:1, R*f* = 0.8. ^{1}H NMR (400 MHz, MeOD) δ 7.79 (d, *J* = 7.6 Hz, 2H, ArH Fmoc), 7.57 (dd, *J* = 7.4, 7.4 Hz, 2H, ArH Fmoc), 7.38 (dd, *J* = 7.4, 7.4 Hz, 2H, ArH Fmoc), 7.32-7.23 (m, 6H, ArH), 7.23-7.12 (m, 2H, ArH), 7.08 (m, 1H, ArH), 7.02-6.95 (m, 1H, ArH), 4.41-4.29 (m, 5H), 4.23 (m, 1H), 4.15 (t, *J* = 6.7 Hz, 1H, CH Fmoc), 3.17–2.94 (m, 3H), 2.86 (m, 1H), 2.04-1.89 (m, 1H), 1.84-1.71 (m, 1H), 1.40 (bs, 9H, Boc).MS (ES$^+$) *m/z* 713.5 $[M+H]^+$.

Synthesis of compound 17

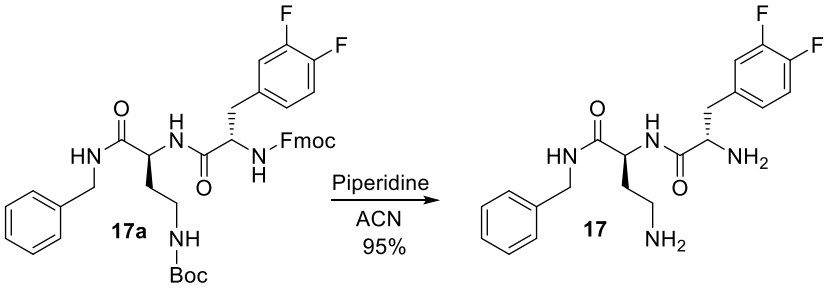

Compound **17a** (375.4 mg, 0.52 mmol, 1 eq) was deprotected with a solution at 5% of piperidine in ACN (52.5 mL). The reaction was kept stirring for 1 hour and 40 minutes, then it was concentrated under reduced pressure and the resulting crude was purified by flash chromatography (eluent: from 100% EtOAc to 90:10 EtOAc:MeOH), yielding product **17** as white solid (243.9 mg, 95% yield). TLC: DCM:MeOH•NH_3 95:5, R*f* = 0.7. ^{1}H NMR (400 MHz, MeOD) δ 7.34-7.21 (m, 5H, ArH), 7.17-7.06 (m, 2H, ArH), 7.01-6.95 (m, 1H, ArH), 4.41-4.31 (m, 3H), 3.60 (dd, *J* = 6.1, 6.1 Hz, 1H), 3.06-2.90 (m, 3H), 2.83 (dd, *J* = 13.9, 7.6 Hz, 1H), 1.98-1.86 (m, 1H), 1.81-1.69 (m, 1H), 1.43 (s, 9H, CH_3 Boc). MS (ES$^+$) *m/z* 491.3 $[M+H]^+$.

Synthesis of compound 6

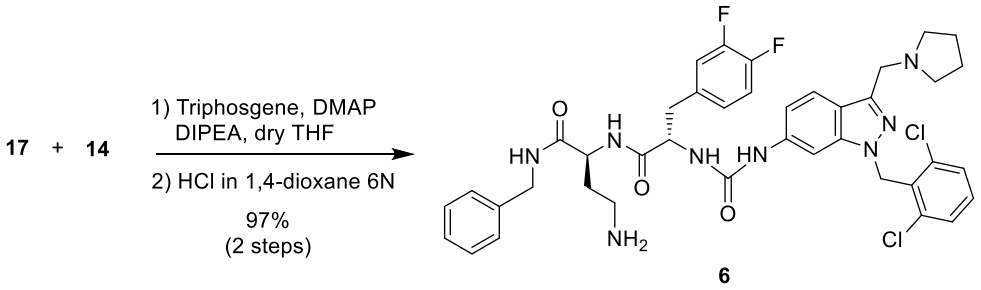

To a solution of compound **14** (65.0 mg, 0.17 mmol 2.6 eq) in THF dry (22.0 mL) at -5° C DMAP, (45.2 mg, 0.37 mmol, 5.5 eq) and triphosgene (19.8 mg, 0.07 mmol, 1 eq) were added. The reaction was kept stirring for 8 minutes at -5°C, then a solution of **17** (43.0 mg, 0.088 mmol, 1.3 eq) and DIPEA (17.4 µL, 0.10 mmol 1.5 eq) in THF (5.0 mL) was added, and the system was put under nitrogen atmosphere. The reaction was kept stirring for 1 hour at -5°C, then for 2 hours at room temperature. The reaction was concentrated by removing the solvent under reduced pressure. The resulted brownish crude material was washed with Et_2O (3x), Et_2O:DCM 70:30 (3x) and EtOAc (3x). Then, the residue was subjected to deprotection using a solution of HCl and 1,4-Dioxane 4N (5.0 mL). The reaction was kept stirring for 50 minutes at room temperature, then the solvent was removed under reduced pressure. The resulted crude was neutralized with MeOH•NH_3, then it was concentrated under reduced pressure and purified with flash chromatography (eluent: from 95:5 DCM:MeOH•NH_3 to 82:18), yielding product **6** as a white solid (51.3 mg, 97%). ^{1}H NMR (400 MHz, MeOD) δ 7.94 (bd, *J* = 1.6 Hz, 1H, ArH), 7.71 (bd, *J* = 8.6 Hz, 1H, ArH), 7.44 (dd, *J* = 8.0 Hz, 1.0 Hz, 2H, ArH), 7.35 (m, 1H, ArH), 7.29-7.19 (m, 5H, ArH), 7.19-7.12 (m, 2H, ArH), 7.12 - 7.06 (m, 1H, ArH), 7.04 (dd, *J* = 8.8, 1.6 Hz, 1H, ArH), 5.61 (bs, 2H, CH_2), 4.55-4.45 (m, 4H), 4.42-4.33 (m, 2H), 4.12 (s, 2H, CH_2), 3.15 (m, 1H), 3.07-2.93 (m, 3H), 2.83 (m, 4H, CH_2 pyrrolidine), 2.28-2.16 (m, 1H), 2.07-1.92 (m, 1H), 1.84 (m, 4H, CH_2 pyrrolidine). MS (ES$^+$) *m/z* 791.5 $[M+H]^+$.

Synthesis of peptide 9

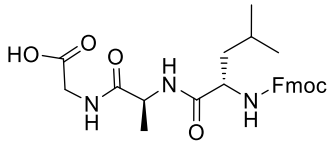

9

The linear tripeptide **9** was prepared according to the general procedure for Solid Phase Synthesis described in Chapter 2 (Paragraph 2.5.2.1.) for compound **11**, by using 2-chlorotrityl-Gly-H resin (loading 0.52mmol/g, 400.0 mg, 0.208 mmol, 1 eq), Fmoc-Ala-OH (97.0 mg, 0.312, 1.5 eq) and Fmoc-Leu-OH (113.0 mg, 0.312 mmol, 1.5 eq). After the resin cleavage, compound **6** (95.0 mg, 95%) was recovered as a colourless glassy solid and was used in the following step without further purification. ^{1}H NMR (600 MHz, DMSO-d_6) δ 8.13 (t, *J* = 5.8 Hz, 1H, NH Gly), 7.89 (d, *J* = 7.6 Hz, 2H, ArH), 7.72 (t, *J* = 7.4 Hz, 2H, ArH), 7.50 (d, *J* = 8.4 Hz, 1H, NH Ala), 7.41 (t, *J* = 7.4 Hz, 2H, ArH), 7.32 (m, 2H, ArH), 4.35-4.28 (m, 2H, CH_2 Fmoc), 4.26-4.21 (m, 2H, CH Fmoc+αAla), 4.06 (dd, *J* = 11.3, 6.7 Hz, 1H, α Leu), 3.79 (d, *J* = 17.6, 5.8 Hz, 1H, αGly), 3.72 (d, *J* = 17.6, 5.8 Hz, 1H, αGly), 3.32 (bs, 1H, COOH), 1.67-1.56 (m, 1H, γLeu), 1.51-1.36 (m, 2H, β Leu), 1.21 (d, *J* = 7.1 Hz, 3H, β Ala), 0.84 (d, *J* = 6.7 Hz, 3H, δ Leu), 0.81 (d, *J* = 6.7 Hz, 3H, δ Leu). MS (ES$^+$) *m/z* 482.3 $[M+H]^+$.

Synthesis of PEG-tripeptide 7a

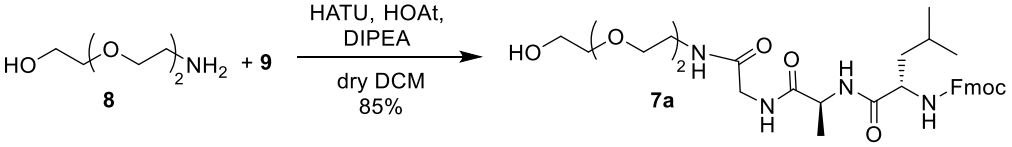

Peptide **9** (50.0 mg, 0.10 mmol, 1 eq) was dissolved in dry DMF (0.7 mL) and dry DCM (0.3 mL). HATU (51.0 mg, 0.13 mmol, 1.3 eq), HOAt (18.0 mg, 0.13 mmol, 1.3 eq) and DIPEA (19.0 μL, 0.11 mmol, 1.1 eq) were then added to the stirring solution. After 15 minutes triglycolamine **8** (15.0 μL, 0.11 mmol, 1.1 eq) was added to the solution. The reaction was let stirring under N_2 atmosphere for 8 hours. At the end of the reaction, the product was concentrated under reduced pressure to give a yellow oil. The crude was purified by reverse phase flash chromatography (eluent: from 100% EtOAc to 90:10 EtOAc:MeOH+1% AcOH), yielding compound **7a** as a yellowish oil (42.0 mg, 85% yield). TLC: EtOAc:MeOH 9:1+0.1% AcOH, R*f* = 0.3. ^{1}H NMR (600 MHz, MeOD) δ 7.76 (d, *J* = 7.6 Hz, 2H, ArH Fmoc), 7.64 (t, *J* = 7.0 Hz, 2H ArH Fmoc), 7.36 (t, *J* = 7.5 Hz, 2H, ArH Fmoc), 7.28 (td, *J* = 7.5, 1.2 Hz, 2H, ArH Fmoc), 4.39 (m, 1H, CH Fmoc), 4.32 (m, 1H, CH Fmoc), 4.26 (q, *J* = 7.0 Hz, 1H, αAla), 4.18 (m, 1H, CH Fmoc), 4.10 (t, *J* = 7.5 Hz, 1H, αLeu), 3.89 (d, *J* = 16.8 Hz, 1H, αGly), 3.72 (d, *J* = 16.8 Hz, 1H, αGly), 3.61 (m, 2H), 3.55 (m, 4H), 3.49 (m, 4H), 3.32 (m, 2H), 1.70-1.62 (m, 1H, γLeu), 1.54 (dd, *J* = 7.5, 7.5 Hz, 2H, βLeu), 1.36-1.32 (m, 3H, βAla), 0.93 (d, *J* = 6.6 Hz, 3H, δ Leu), 0.90 (d, *J* = 6.6 Hz, 3H, δ Leu). MS (ES$^+$) *m/z* 613.4 $[M+H]^+$.

Synthesis of tosyl derivative 7

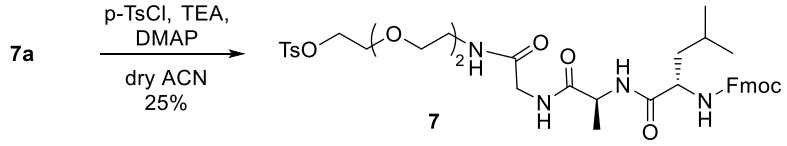

To a solution of compound **7a** (122.0 mg, 0.199 mmol, 1 eq) and DIPEA (69.3 µL, 0.398 mmol, 2 eq) in dry ACN (1.3 mL), DMAP (4.9 mg, 0.039 mmol, 0.2 eq), *p*-TsCl (75.9 mg, 0.398 mmol, 2 eq) and catalytic amount of Na_2SO_4 were added. The reaction was left to stir under N_2 atmosphere at 50 °C for 24 hours. The reaction was concentrated by removing the solvent under reduced pressure. Then water (5 mL) was added and extracted with EtOAc (3x). The combined organic layers were concentrated under low pressure and the crude was purified by reverse phase chromatography (eluent: from 80:20 H_2O+0.1%TFA:ACN to 10:90), yielding compound **7** as a yellowish oil (11.5 mg, 25%). TLC: EtOAc:MeOH 9:1, R*f* = 0.6. ^{1}H NMR (400 MHz, MeOD) δ 7.73 (m, 4H, ArH), 7.61 (m, 2H, ArH), 7.38-7.30 (m, 4H, ArH), 7.25 (m, 2H, ArH), 4.36 (m, 1H, CH Fmoc), 4.28 (m, 1H, CH Fmoc), 4.22 (q, *J* = 7.1 Hz, 1H αAla), 4.14 (m, 1H, CH Fmoc), 4.07 (m, 1H, αLeu), 4.04 (m, 2H, CH_2) 3.88 (d, *J* = 16.8 Hz, 1H, αGly), 3.67 (d, *J* = 16.8 Hz, 1H, αGly), 3.54 (m, 2H), 3.43 (m, 6H), 3.27 (m, 2H) 2.37 (s, 1H, CH_3), 1.63 (m, 1H, γLeu), 1.51 (dd, *J* = 7.3, 7.3 Hz, 2H, βLeu), 1.32 (d, *J* = 7.1 Hz, 3H, βAla), 0.90 (dd, *J* = 6.3 Hz, 3H, δLeu), 0.90 (dd, *J* = 6.3 Hz, 3H, δLeu). MS (ES$^+$) *m/z* 767.3 $[M+H]^+$.

5.6. References

(**1**) Kolb, M.; Bonella, F.; Wollin, L. Therapeutic Targets in Idiopathic Pulmonary Fibrosis. *Respir. Med.* **2017**, *131*, 49–57.
(**2**) Sgalla, G.; Iovene, B.; Calvello, M.; Ori, M.; Varone, F.; Richeldi, L. Idiopathic Pulmonary Fibrosis: Pathogenesis and Management. *Respiratory Research* **2018**, *19*, 32.
(**3**) Ballester, B.; Milara, J.; Cortijo, J. Idiopathic Pulmonary Fibrosis and Lung Cancer: Mechanisms and Molecular Targets. *Int. J. Mol. Sci.* **2019**, *20*, 593.
(**4**) Goodwin, A.; Jenkins, G. Role of Integrin-Mediated TGFβ Activation in the Pathogenesis of Pulmonary Fibrosis. *Biochem. Soc. Trans.* **2009**, *37*, 849–854.
(**5**) Biernacka, A.; Dobaczewski, M.; Frangogiannis, N. G. TGFβ Signaling in Fibrosis. *Growth Factors* **2011**, *29*, 196–202.
(**6**) Heuberger, D. M.; Schuepbach, R. A. Protease-Activated Receptors (PARs): Mechanisms of Action and Potential Therapeutic Modulators in PAR-Driven Inflammatory Diseases. *Thrombosis J.* **2019**, *17*, 4.
(**7**) José, R. J.; Williams, A. E.; Chambers, R. C. Proteinase-Activated Receptors in Fibroproliferative Lung Disease. *Thorax* **2014**, *69*, 190–192.
(**8**) Lin, C.; von der Thüsen, J.; Daalhuisen, J.; ten Brink, M.; Crestani, B.; van der Poll, T.; Borensztajn, K.; Spek, C. A. Protease-Activated Receptor (PAR)-2 Is Required for PAR-1 Signalling in Pulmonary Fibrosis. *J. Cell. Mol. Med.* **2015**, *19*, 1346–1356.
(**9**) Shea, B. S.; Probst, C. K.; Brazee, P. L.; Rotile, N. J.; Blasi, F.; Weinreb, P. H.; Black, K. E.; Sosnovik, D. E.; Van Cott, E. M.; Violette, S. M.; Caravan, P.; Tager, A. M. Uncoupling of the Profibrotic and Hemostatic Effects of Thrombin in Lung Fibrosis. *JCI Insight* **2017**, *2*, e86608.
(**10**) Tatler, A. L.; Jenkins, G. TGFβ Activation and Lung Fibrosis. *Proc. Am. Thorac. Soc.* **2012**, *9*, 130–136.
(**11**) Jenkins, R. G. Ligation of Protease-Activated Receptor 1 Enhances $\alpha_v\beta_6$ Integrin-Dependent TGFβ Activation and Promotes Acute Lung Injury. *J. Clin. Invest.* **2006**, *116*, 1606–1614.
(**12**) Bugatti, K.; Bruno, A.; Arosio, D.; Sartori, A.; Curti, C.; Augustijn, L.; Zanardi, F.; Battistini, L. Shifting Towards $\alpha_v\beta_6$ Integrin Ligands Using Novel Aminoproline-Based Cyclic Peptidomimetics. *Chem. Eur. J.* **2020**, *26*, 13468–13475.
(**13**) Chackalamannil, S. Thrombin Receptor (Protease Activated Receptor-1) Antagonists as Potent Antithrombotic Agents with Strong Antiplatelet Effects. *J. Med. Chem.* **2006**, *49*, 5389–5403.
(**14**) Andrade-Gordon, P.; Maryanoff, B. E.; Derian, C. K.; Zhang, H.-C.; Addo, M. F.; Darrow, A. L.; Eckardt, A. J.; Hoekstra, W. J.; McComsey, D. F.; Oksenberg, D.; Reynolds, E. E.; Santulli, R. J.; Scarborough, R. M.; Smith, C. E.; White, K. B. Design, Synthesis, and Biological Characterization of a Peptide-Mimetic Antagonist for a Tethered-Ligand Receptor. *Proc. Natl. Acad. Sci.* **1999**, *96*, 12257–12262.
(**15**) Pardo, A.; Cabrera, S.; Maldonado, M.; Selman, M. Role of Matrix Metalloproteinases in the Pathogenesis of Idiopathic Pulmonary Fibrosis. *Respiratory Research* **2016**, *17*, 23-33.
(**16**) Severino, B.; Santagada, V.; Perissutti, E.; Fiorino, F.; Frecentese, F.; De Angelis, F.; Esposito, A.; Caliendo, G. Recent Advances in Synthesis of PAR Ligands as Therapeutic Strategy for Inflammatory Diseases. *Mini-Reviews Med. Chem.* **2009**, *9*, 653–663.
(**17**) Gandhi, D. M.; Majewski, M. W.; Rosas, R.; Kentala, K.; Foster, T. J.; Greve, E.; Dockendorff, C. Characterization of Protease-Activated Receptor (PAR) Ligands: Parmodulins Are Reversible Allosteric Inhibitors of PAR1-Driven Calcium Mobilization in Endothelial Cells. *Bioorg. Med. Chem.* **2018**, *26*, 2514–2529.
(**18**) Vartak, D. G.; Gemeinhart, R. A. Matrix Metalloproteases: Underutilized Targets for Drug Delivery. *J. Drug Target.* **2007**, *15*, 1–20.
(**19**) Olson, E. S.; Aguilera, T. A.; Jiang, T.; Ellies, L. G.; Nguyen, Q. T.; Wong, E. H.; Gross, L. A.; Tsien, R. Y. In Vivo Characterization of Activatable Cell Penetrating Peptides for Targeting Protease Activity in Cancer. *Integr. Biol.* **2009**, *1*, 382–393.

(**20**) Robinson, E.; Knight, E.; Smoktunowicz, N.; Chambers, R. C.; Inglis, G. G.; Chudasama, V.; Caddick, S. Identification of an Active Metabolite of PAR-1 Antagonist RWJ-58259 and Synthesis of Analogues to Enhance Its Metabolic Stability. *Org. Biomol. Chem.* **2016**, *14*, 3198–3201.
(**21**) Zhang, H.; Derian, C. K.; Andrade-Gordon, P.; Hoekstra, W. J.; McComsey, D. F.; White, K. B.; Poulter, B. L.; Addo, M. F.; Cheung, W.; Damiano, B. P.; Oksenberg, D.; Reynolds, E. E.; Pandey, A.; Scarborough, R. M.; Maryanoff, B. E. Discovery and Optimization of a Novel Series of Thrombin Receptor (PAR-1) Antagonists: Potent, Selective Peptide Mimetics Based on Indole and Indazole Templates. *J. Med. Chem.* **2001**, *44*, 1021–1024.

Final remarks

Peptides and peptidomimetics represent an interesting class of potential drugs, as they usually exhibit high specificity and affinity for their biological targets and they are well tolerated by living organisms. Besides their role *per se*, peptidomimetics have also been extensively studied as active targeting components of Small Molecule-Drug Conjugates (SMDCs), since their exquisite target specificity may be exploited to carry appended cytotoxic payloads to the diseased sites thus improving the pharmacological profile of several chemotherapeutics.

The work described in this PhD dissertation has the ambition to widen knowledge in the field of new small-molecule peptidomimetics to be used either as $\alpha_V\beta_3$-/$\alpha_V\beta_6$-targeting integrin ligands, or PAR2 modulators. In addition, their covalent integration with active components, be they antiangiogenic or antinflammatory agents, resulted in the fabrication of novel covalent conjugates.

In particular, Chapter 2 focused on the design and synthesis of a panel of new cyclic peptidomimetics targeting the $\alpha_V\beta_6$ integrin. Among the eighteen synthesized compounds, four of them gave promising results, with $IC_{50(\alpha V\beta 6)}$ values in the low nanomolar range (4.6-58.5 nM, solid phase receptor binding assay) and selectivity indexes (reported as the ratio between $IC_{50(\alpha V\beta 3)}$ and $IC_{50(\alpha V\beta 6)}$) in the range 243-628.

Chapter 3, concerning the work done during my period abroad at the University of Erlangen-Nürnberg (in the research group of Prof. Dr. Gmeiner), focused on the development of novel peptidomimetics as ligands of Proteinase-Activated Receptor 2 (PAR2). Twenty novel peptidomimetics were synthesized, and the best performing PAR2 agonist among them showed IC_{50} (tested by IP-One-HEK assay) in the nanomolar range.

Chapter 4 dealt with the synthesis of nine novel covalent conjugates to be used as potential antitumor and antifibrotic agents. The projected conjugates are constituted by an analogue of the kinase inhibitor nintedanib, which is linked to an RGD-based integrin-targeting cyclopeptidomimetic by means of a robust linker moiety. Preliminary results towards TGFβ-treated melanoma tumor cells seem to confirm that antagonizing both kinase receptor and $\alpha_V\beta_6$ integrin could be a good strategy to address cancer-related diseases.

Finally, Chapter 5 concerns the design of MMP2/MMP9-cleavable conjugates addressing both PAR1 and $\alpha_V\beta_6$ receptors, since the cross-talk between these two receptors has emerged as a possible target for the treatment of Idiopathic Pulmonary Fibrosis (IPF). The opening move of this project was the parallel synthesis of the two separated active modules, i.e. the $\alpha_V\beta_6$ integrin ligand and the PAR1 agonist, intended to be first evaluated in *in-vitro* assays towards the corresponding receptors, with the aim to prove that the independent moieties maintain their biological activity upon proteolytic release.

In conclusion, the work described in this PhD dissertation emphasizes the importance of peptidomimetics both as ligands *per se* and as components in SMDCs. Hopefully, the promising results here obtained will drive the research in finding novel peptidomimetic-based compounds to be used as biological tools for comprehension and treatment of oncology-, fibrosis-, and inflammation-related diseases.

Acknowledgments

I would like to thank my supervisor, Prof. Lucia Battistini, for all the time she spent in teaching, supporting and helping me. There is nothing better than having a mentor who fully understands you. I could not desire a better supervisor.

I would like also to thank Prof. Franca Zanardi, Prof. Andrea Sartori and Prof. Claudio Curti, for all the time and knowledge they shared with me, never denying my requests for help.

I am grateful to Prof. Peter Gmeiner (University of Erlangen-Nürnberg, Germany), for giving me the opportunity to attend a precious experience aboard. Thank also to Dr. Jürgen Einsiedel for all the knowledge he shared with me.

I wish to thank Prof. Tolomelli (University of Bologna) and Prof. Trabocchi (University of Florence) for their painstaking revision work.

During my PhD I followed several students, which helped me to achieve the results I presented in this dissertation: thank to Cecilia Mora, Lisa Augustijn, Stefano Cremonesi, Alexia Ripak, Margherita Restori and Gabriele Petese.

Grazie alla mia famiglia, che mi ha sempre accompagnato durante tutto questo percorso, senza mai negarmi alcun aiuto. Grazie alle mie sorelle, mio supporto costante, per aver sempre creduto in me, più di quanto io abbia mai fatto. Grazie ai miei cognati, perché siete sempre entusiasti qualsiasi cosa io faccia: la vostra energia mi è stata indispensabile durante tutti questi anni.

Grazie agli amici che hanno addolcito questo percorso, ognuno alla sua maniera, ma comunque sempre in modo eccezionale.

“If it's ka it'll come like a wind, and your plans will stand before it
no more than a barn before a cyclone.”

[Stephen King – Wizard and Glass]